The Institute of Paper Chemistry

Appleton, Wisconsin

Doctor's Dissertation

The Occurrence and Light Induced Formation of *ortho*-Quinonoid Structures in High Yield Pulp Lignins

Stuart E. Lebo, Jr.

January, 1988

THE OCCURRENCE AND LIGHT INDUCED FORMATION OF ortho-QUINONOID STRUCTURES IN HIGH YIELD PULP LIGNINS

A thesis submitted by

Stuart E. Lebo, Jr.

B.A. 1981, Shippensburg State University

M.S. 1983, Lawrence University

in partial fulfillment of the requirements
of The Institute of Paper Chemistry
for the degree of Doctor of Philosophy
from Lawrence University
Appleton, Wisconsin

January, 1988

TABLE OF CONTENTS

ABSTRACT

"Yellowing" upon exposure to light is a major problem associated with the use of high yield pulps, both bleached and unbleached. Because of this problem, the use of high yield pulps as substitutes for fully bleached chemical pulps has been severely limited. Although various model studies have indicated that colored quinonoid lignin structures are formed when such pulps are exposed to light, the light induced formation of these structures *in situ* has not been extensively studied. The occurrence and light induced formation of quinonoid lignin structures, particularly *ortho*-quinonoid lignin structures, is the subject of this investigation. Specifically, work was aimed at determining if such structures occur and/or are photochemically generated in white spruce refiner mechanical pulp sheets, and, if photochemically generated, what the quantum yield of their formation is.

Diffuse reflectance UV-visible, diffuse reflectance Fourier transform infrared, and solid state ^{31}P NMR spectroscopy were the major investigative tools used to follow the formation of quinonoid lignin structures during light induced yellowing. These methods were also the major investigative tools for determining if unirradiated pulp contained these structures. The results obtained when irradiated white spruce refiner mechanical pulp (RMP) sheets were examined before and after reaction with sodium dithionite, sulfur dioxide, and trimethyl phosphite showed that approximately five *ortho*-quinonoid lignin structures per 100 C_9 lignin units were formed when 160 g/m^2 white spruce sheets were irradiated for 10 hours with simulated sunlight. These results were confirmed by comparison with simple model quinones and with sheets formed from an *ortho*-quinone enhanced white spruce pulp. In subsequent studies with "monochromatic" UV light, the quantum yield for the 312.5 nm light induced formation of such structures in 160 g/m^2 sheets was determined to be 8.0×10^{-2} moles of *ortho*-quinonoid lignin structures per mole of absorbed photons.

The results obtained when unirradiated white spruce refiner mechanical pulp (RMP) sheets were examined showed that this pulp also contained ortho-quinonoid lignin structures. As in the analysis of the irradiated pulp, these results were confirmed by comparison with simple models and with a white spruce pulp enhanced with ortho-quinonoid lignin structures. Quantitative analysis of this unirradiated refiner mechanical pulp indicated that it contained approximately six ortho-quinonoid lignin structures per 100 C_9 lignin units.

In both the irradiated and unirradiated cases, ortho-quinonoid lignin structures are major contributors to these pulps. Based on Kubelka-Munk measurements, the contribution of these structures to the absorbance of the unirradiated pulp was estimated to be 47% at 415 nm, 73% at 457 nm, and 75% at 520 nm. While the nature of the other major contributor was not determined, it was shown that this product has an absorption maximum at 395 nm and that this product is not easily reduced by sodium dithionite, sulfur dioxide or trimethyl phosphite. It was also shown that the rate at which this product is formed depends on the wavelength of the light incident upon the pulp with the maximum rate occurring around 312.5 nm.

Thus, it was shown that ortho-quinonoid lignin structures are present in high yield pulps. Their presence is partly responsible for the low brightnesses of these pulps. It was also shown that more of these structures are formed when high yield pulps are exposed to light. They are not, however, the only colored structures formed.

INTRODUCTION

PERSPECTIVE

Increasing wood costs and predicted wood shortages have continued to stimulate interest in the production and use of high yield mechanical pulps. Annual production of mechanical pulps worldwide has been estimated to be 30 million tons/acre and growing.[1] This estimate includes both stone groundwood and refiner mechanical pulps.

Because of their inferior strength and brightness properties, mechanical pulps have historically been used in lower valued papers, particularly newsprint. Recent developments in mechanical pulping and bleaching technology have, however, moved high yield pulps from filler pulp status to that of higher quality pulps.[2] Despite these gains, a major problem still associated with the use of such pulps, both bleached and unbleached, is that they "yellow" upon exposure to light. This light induced yellowing results in undesirable increases in pulp color and decreases in pulp brightness. Because of this problem, the use of mechanical pulps as substitutes for bleached chemical pulps is still severely limited.

The photochemical and chemical reactions involved in the light induced yellowing of mechanical pulps, while of great economic interest, are not completely understood. Previous work with model compounds, isolated wood lignins, and various groundwood pulps has suggested that *para*- and/or *ortho*-quinonoid lignin structures are formed during the yellowing process. It is well known that such structures are highly colored and their formation would account for at least part of the color developed when these pulps are exposed to sunlight.

On the basis of the abovementioned studies, it has further been suggested that quinonoid structures may contribute to the "natural" color of wood and wood pulps. In many cases, this color must be eliminated by bleaching and further limits the use of such pulps to grades where color is not important.[2] Thus, it can be seen that the study of such structures *in situ* is of both theoretical and practical interest.

LITERATURE SURVEY

The Occurrence of Quinonoid Lignin Structures

The occurrence of both *para*- and *ortho*-quinonoid lignin structures has been postulated by a number of researchers. Freudenberg,[3,4] for instance, found quinonoid structures in synthetic "dehydropolymerizate" lignins (DHP lignins). These DHP lignins, which were formed by the action of enzymes on coniferyl alcohol, were thought to be similar in structure to the lignin present in wood. On the basis of Freudenberg's findings, Luner[5] and Chudakov and Samsanova[6] investigated the formation of such structures in wood pulps and isolated wood lignins and concluded that quinonoid lignin structures were, indeed, formed in wood during the biosynthesis of lignin. Luner[5] further suggested that quinonoid groups could also be formed after biosynthesis by a free radical attack on lignin by oxygen, as shown in Fig. 1.

On the basis of the results obtained in experiments with appropriate lignin model compounds, Pew and Connors[7] also concluded that phenyl-substituted benzoquinone groups are formed during the biosynthesis of lignin. Pew and Connors also studied the reactions of wood pulps with several different reducing agents. On the basis of the results obtained in these studies, they further concluded that such structures, along with coniferaldehyde type lignin structures, are the

major contributors to the "natural" color of wood and wood pulps. In later studies, Connors et al.[8] actually isolated ortho- and para-quinone products from the reaction mixtures obtained in the enzymatic dehydrogenation of lignin model phenols.

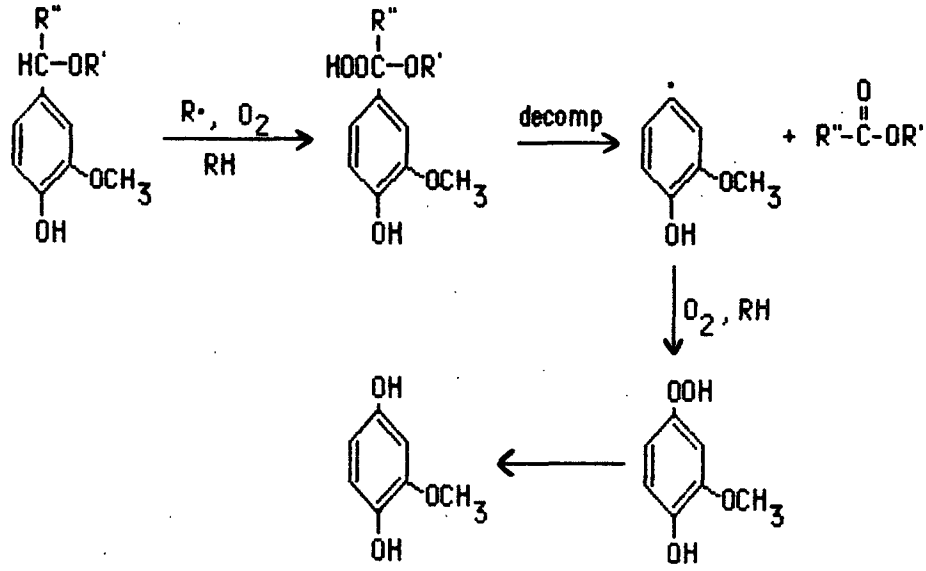

Figure 1. Luner's[5] proposed mechanism for the formation of quinone precursors by free radical attack on lignin.

In a thorough investigation of the effects of reductive and oxidative bleaching reagents on the absorption spectra of lignin in groundwood pulps, Polcin and Rapson[9,10] also found that white spruce groundwood pulp contained a relatively high number of α,β-unsaturated aldehyde and simple quinonoid lignin structures. While no numbers were given, these workers found that such structures contribute significantly to the color of such pulps. In later studies, Falkehag et al.[11] and Imsgard et al.[12] used the complexing ability of reduced quinonoid structures to study the structure of the chromophores present in kraft and spruce milled wood lignins. On the basis of the results of these studies it was concluded that both kraft and spruce milled wood lignin contained small amounts

of ortho-quinonoid structures. In the case of spruce milled wood lignin, this amount was estimated to be ≈ 0.7%. According to these workers, this amount of ortho-quinonoid structures accounted for 35-60% of the light absorption of spruce milled wood lignin at 457 nm.

The presence of both ortho- and para-quinonoid structures in wood and pulp systems has also been suggested by Gierer and his coworkers.[13] The basic chromophore systems in lignin suggested by these workers are shown in Fig. 2. As this figure shows, included in this list are ortho-quinonoid (III) and para-quinonoid (IV) lignin structures.

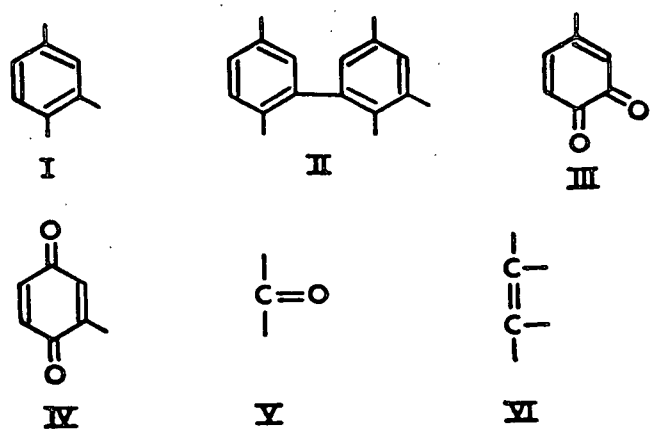

Figure 2. Basic elements of the chromophore systems in lignin as proposed by Gierer.[13]

More recently, the presence of quinonoid lignin structures in wood and wood pulps has been suggested by Hon,[14] who like many of the above workers, has suggested that these groups are one of the preponderant chromophoric groups in high yield wood pulps. Their presence has also been suggested by Cole and Sarkanen,[15] who claimed that the pulp bleaching action of thiol compounds is partly due to the reaction of such compounds with quinonoid lignin structures.

The Light Induced Formation of Quinonoid Lignin Structures

In a series of studies concerning the yellowing of wood by light, Leary[16-18] found that the methoxyl content of wood surfaces decreased upon exposure to light from bare carbon arc lamp. He also found that esterification or alkylation of wood retarded the yellowing process and that the light induced yellowing of lignin-rich materials, such as wood or wood pulp, required molecular oxygen. On the basis of these observations, Leary concluded that the yellowing of lignified materials begins by the oxidation of free phenolic hydroxyl groups in lignin. While no direct evidence was given, he also concluded that the most likely products of these oxidation reactions are para- and ortho-quinonoid lignin structures.

In good agreement with Leary's work, Andrews and DesRosiers[19] and Singh[20] found that the brightness stability of groundwood pulp was significantly increased by benzoylation, etherification or esterification of the free phenolic groups in the lignin. These workers attributed the observed increase in the brightness stability of these pulps to a blocking of reactive phenolic units which, when unblocked, reacted to form colored quinonoid compounds via phenolic free radical intermediates. This conclusion was supported by the fact that blocking of the free phenolic groups in the lignin present in groundwood pulps also prevent the reaction of such groups with Fremy's salt, potassium nitrodisulfonate. As shown in Fig. 3, this reagent converts lignin model compound units into reddish colored ortho-quinonoid compounds via phenoxy free radical intermediates.[21-23]

In later studies, Lin and Kringstad[24-28] examined the photochemical reactions of lignin model compounds in solution and found demethylation combined with the formation of ortho-quinonoid structures and side chain displacement

probably combined with the formation of para-quinonoid structures. As suggested by the above workers, the reactions involved in the formation of these products were shown to involve phenoxy free radical intermediates. On the basis of the results obtained in these studies, Lin and Kringstad suggested that similar free radical reactions were likely to occur in the photoinduced oxidation of lignin in wood or wood pulp; a finding that was supported by the fact that milled wood lignin solutions also discolored upon irradiation. In later model compound studies, Gierer and Lin[29] examined the direct photochemical cleavage of phenacyl aryl ether linkages and proposed the formation of polymeric chromophoric groups via ortho-quinone intermediates. These results suggested, for the first time, that phenolic lignin units may not be necessary for color development.

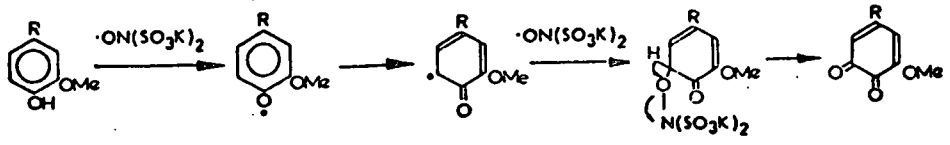

Figure 3. Mechanism for the reaction of Fremy's salt, $GN(SO_3K)_2$, with free phenolic compounds.[21]

More recently, the light induced formation of para- and/or ortho-quinonoid lignin structures has been postulated by Gellerstedt et al.,[30-32] Gratzl,[33] Hirashima and Sumimoto,[34] Lonsky,[35] and by Heitner and Min.[36] A detailed model study was also conducted by Forsskahl,[37] who, like Gierer and Lin,[29] claims that quinonoid lignin structures are intermediates in the yellowing process and may not be present as final products.

Thus, it can be seen that a number of different workers have claimed that quinonoid lignin structures are formed during the irradiation of wood and high yield pulps. It should be noted, however, that while some of these claims are based on the results obtained in pulp studies, most of them are based on the

results of studies of lignin model compounds in solution. Very little work has been done to determine if quinonoid lignin structures are formed *in situ* during the light induced yellowing process.

Proposed Mechanisms for the Light Induced Formation of Quinonoid Lignin Structures

Mechanistic models for the reactions involved in the light induced formation of quinonoid lignin structures have been proposed. All of these models are based on the following general observations.

1. Yellowing of high yield pulps is induced by the UV component of sunlight (i.e., light of wavelengths = 290-390 nm).[16,38-40]
2. Yellowing involves molecular oxygen.[17,24,27,28,32]
3. UV light irradiated wood surfaces show a decrease in methoxyl content.[16-18,40,41]
4. Blocking of phenolic lignin units retards the yellowing reaction.[17,19,20,29,35,42]
5. Free radicals are formed during the yellowing of lignin rich materials.[17,27,35]

For instance, Leary[17] proposed the simple mechanistic model shown in Fig. 4. In this model, UV light is absorbed by an unknown lignin chromophore, A. The excited state form of A, A*, then abstracts a hydrogen atom from a neighboring phenolic unit in the lignin macromolecule to form two free radicals, AH- and (II). The phenolic free radical, II, then reacts with molecular oxygen to form colored products, presumably quinonoid lignin structures.

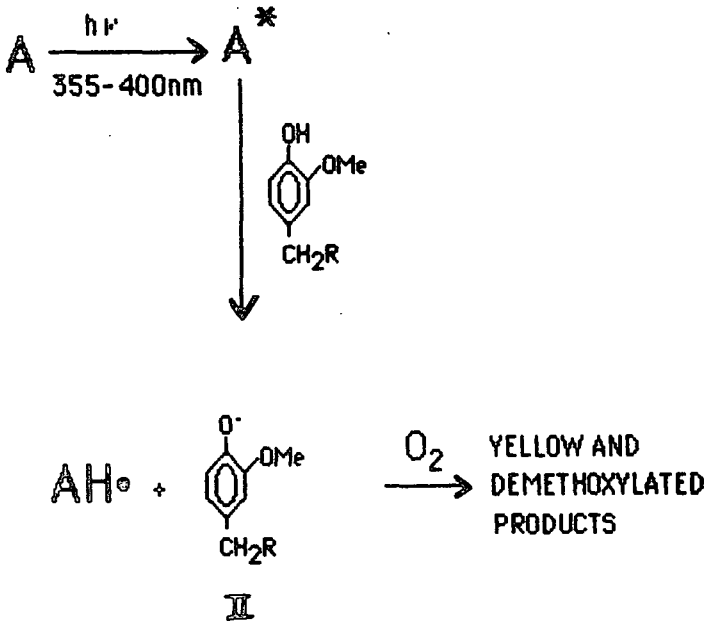

Figure 4. Mechanism of yellowing initially proposed by Leary.[17]

On the basis of the results obtained in later studies of appropriate lignin model compounds, Lin and Kringstad[28] proposed the more detailed mechanistic models shown in Fig. 5 and 6. According to these models, light is absorbed by α-carbonyl groups in lignin. This absorption leads to the formation of excited state α-carbonyl structures which can abstract hydrogen atoms from neighboring phenolic structures. The phenoxy free radicals thus generated, react further to form both ortho- and para-quinonoid lignin structures. Similar mechanistic models were proposed by Gellerstedt and Pettersson[31] and by Lonsky.[35] In Lonsky's mechanistic model, the ketyl radical formed from the α-carbonyl structure acts as a hydrogen donor by transferring its hydrogen atom to a reactive acceptor (Fig. 7). The original α-carbonyl group is reformed in the process, and thus, these groups act as photosensitizers in these reactions. The role of α-carbonyl groups as photosensitizers has also been suggested by Brunow and Sivonen.[43]

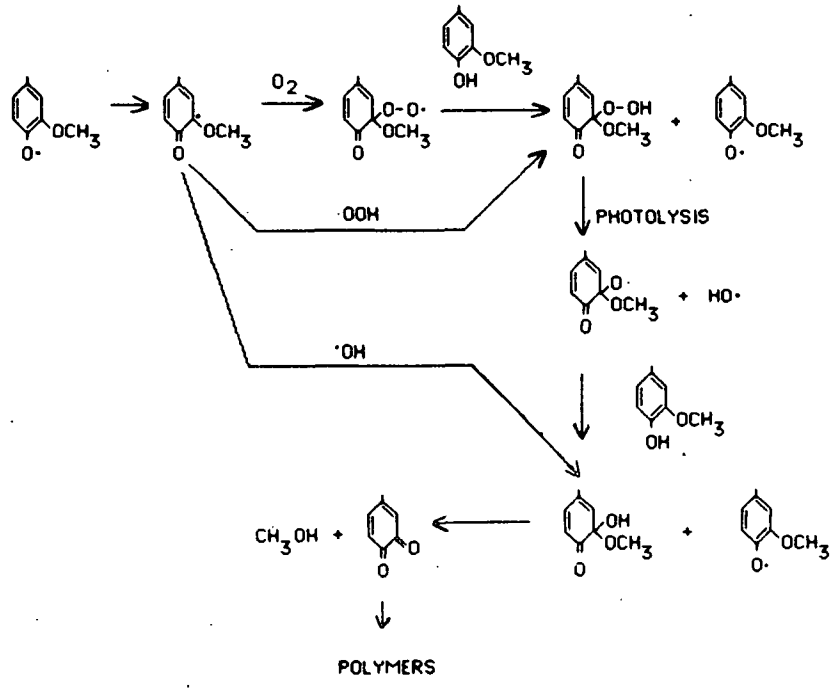

Figure 5. Possible mechanism proposed by Lin and Kringstad[28] for the photo-induced demethylation and formation of ortho-quinonoid structures.

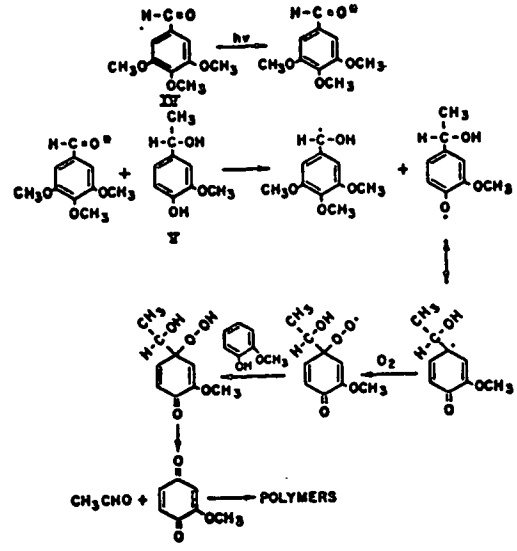

Figure 6. Possible mechanism proposed by Lin and Kringstad[28] for the photo-induced side chain displacement of α-carbinol structures.

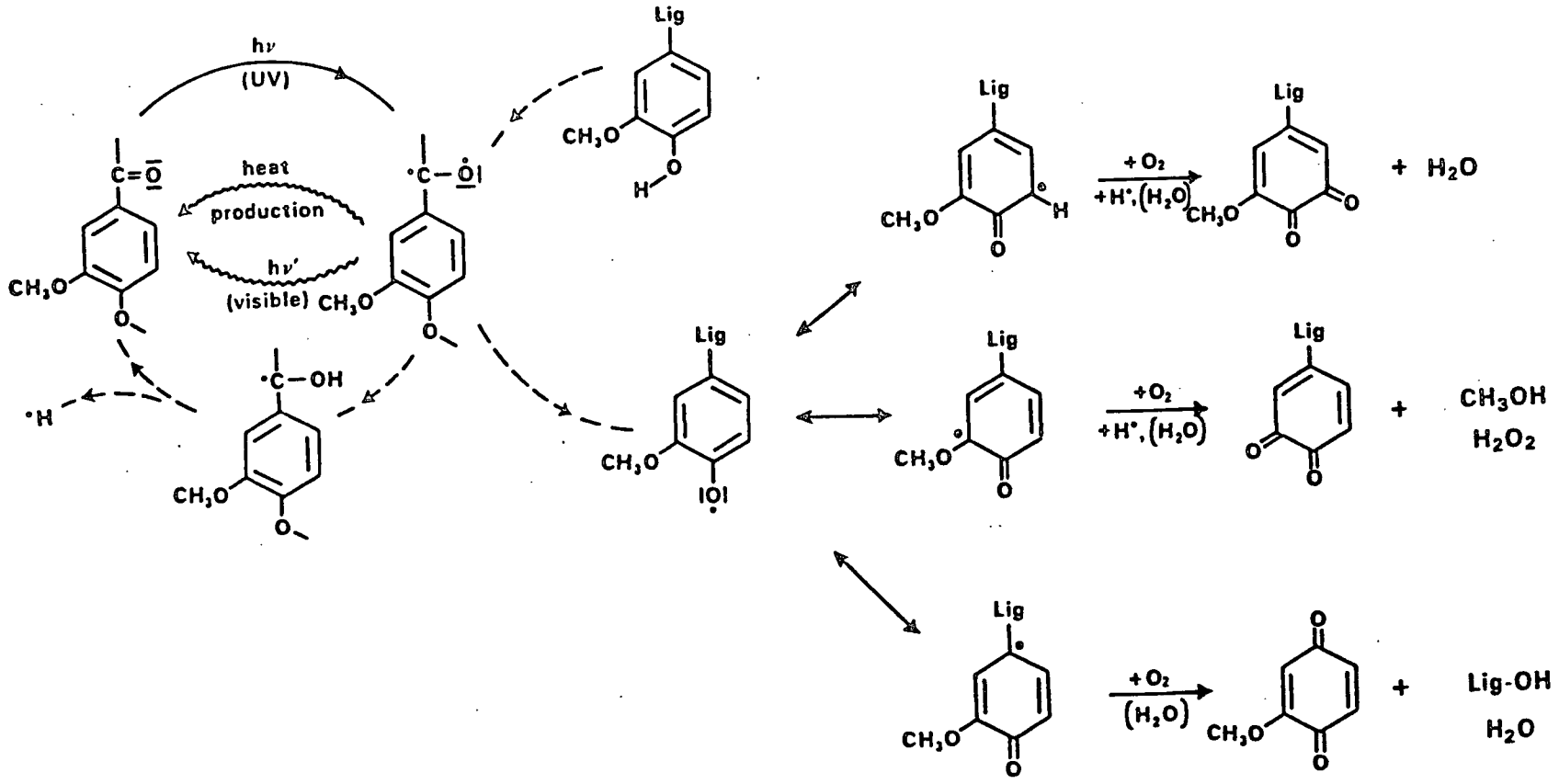

Figure 7. Mechanism for the light induced formation of quinonoid lignin structures proposed by Lonsky.[35]

In addition to models which predict the formation of phenolic free radicals by direct hydrogen abstraction, models involving the formation of such radicals through the interaction of phenolics with photochemically generated singlet oxygen have also been proposed.[30,32,36,37,44-46] On the basis of the results of model studies, the formation of singlet oxygen by energy transfer from excited state carbonyl[32,36,43-46] and ring conjugated C=C double bond structures[30,37] has been suggested. The reactions involved in these models are shown schematically in Fig. 8 and 9, respectively. Once formed, singlet oxygen reacts with neighboring phenolic units to form phenoxy radicals which subsequently react with ground state triplet oxygen to form yellow products. In the case of ring conjugated C=C double bond structures, reactions which lead to the cleavage of the C=C bond are also possible. In these reactions, additional α-carbonyl groups are formed. These α-carbonyl groups can then enter into the sequence of reactions described above.

In an attempt to extend the results obtained in model studies to pulp, Lonsky and Ogryzlo[47] studied the reactions of singlet oxygen with thermomechanical pulp (TMP). In these studies, the formation of singlet oxygen during the UV light irradiation of handsheets formed from this pulp was examined. The direct reaction of these sheets with singlet oxygen was found. Thus, while it is still open to debate, these results suggest that, while singlet oxygen may be important in model systems, it is not important in the yellowing of high yield pulps.

Another mechanistic model which has been proposed to explain the reactions involved in the yellowing of high yield pulps involves the photochemical cleavage of phenacyl aryl ether lignin linkages.[29,48] As shown in Fig. 10 and 11, cleavages of α-carbonyl β-O-4 and noncarbonyl α-O-4 ether linkages occur directly from the excited states in primary photochemical processes. In both

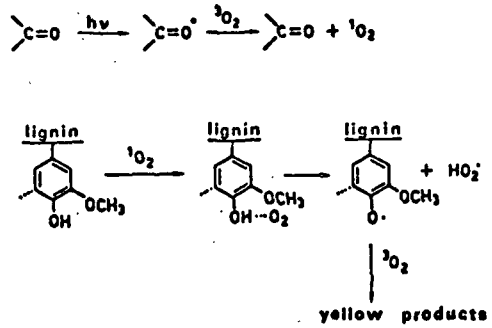

Figure 8. Proposed mechanism for the formation of singlet oxygen by energy transfer from an excited state carbonyl group and subsequent formation of phenoxy radicals by reaction of phenolics with singlet oxygen.[43]

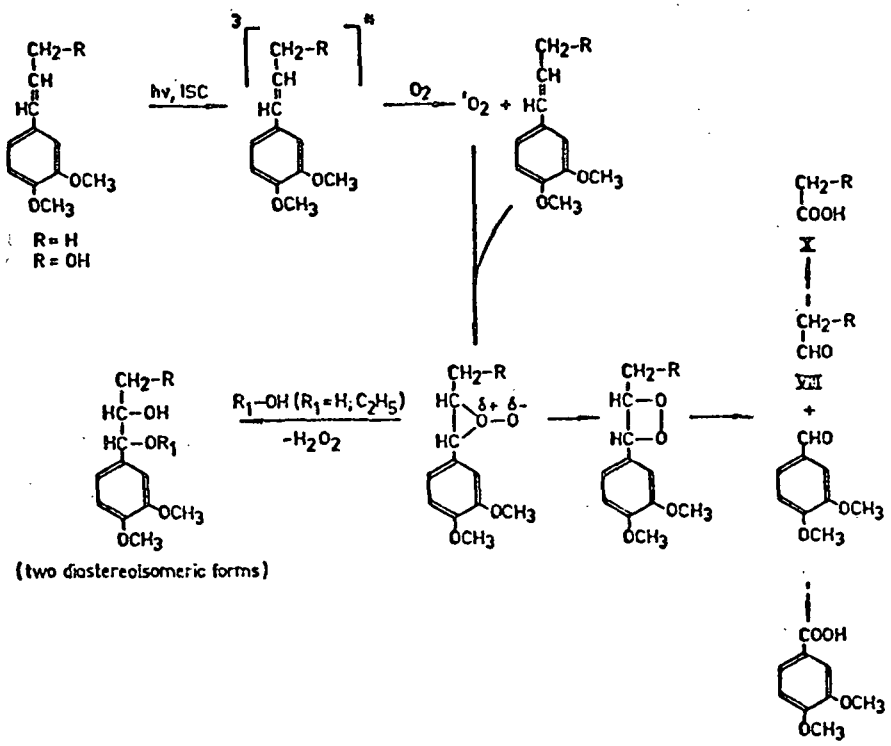

Figure 9. Proposed mechanism for the formation of singlet oxygen by energy transfer from an excited state C=C group and subsequent formation of α-carbonyl groups by reaction of C=C groups with singlet oxygen.[30]

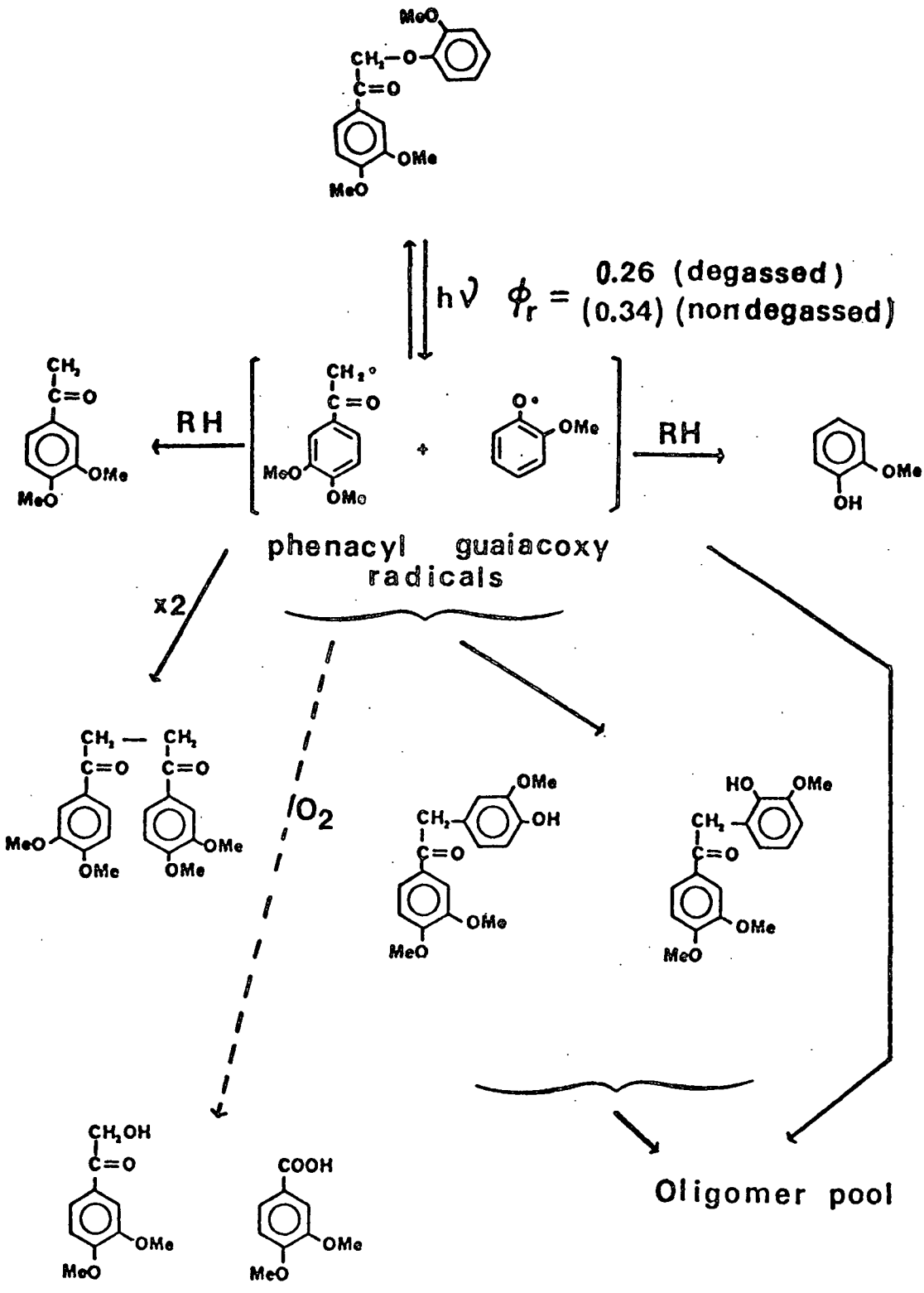

Figure 10. Mechanism proposed by Castellan[48] for the photodegradation of α-carbonyl β-O-4 lignin model dimers.

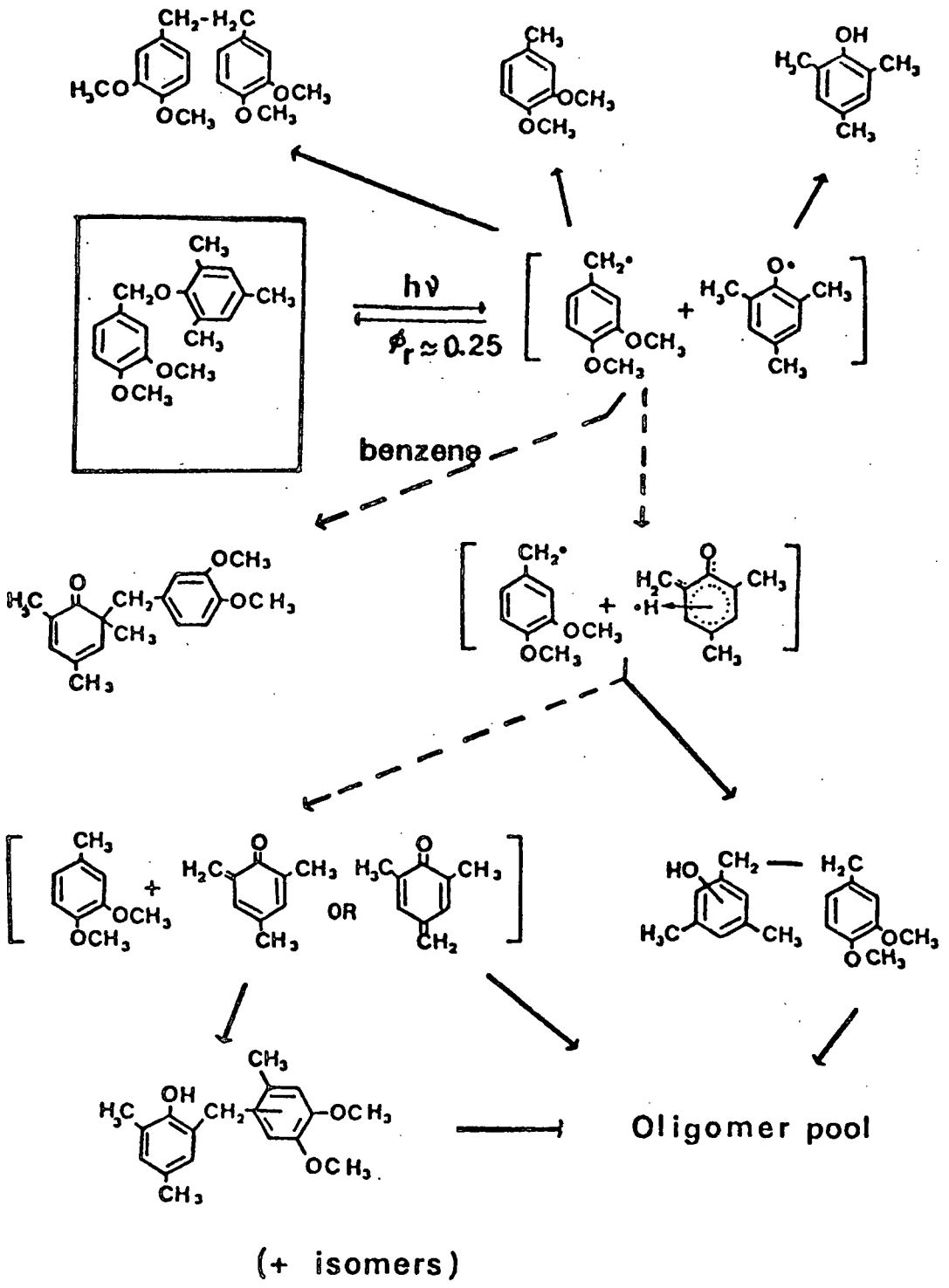

Figure 11. Mechanism proposed by Castellan[48] for the photodegradation of non-carbonyl α-O-4 dimer structures.

reactions, photochemical cleavage of β-O-4 or α-O-4 ether bonds give rise, directly, to phenoxy free radicals. In reactions similar to those described above, these phenoxy free radicals subsequently go on to form colored products including quinones.

Properties and Reactions of Quinonoid Lignin Structures

Spectroscopic Properties

Quinones are cyclic conjugated diketones which have two absorption bands occurring in the UV-visible region of the spectrum. The absorption spectra of quinones, and diones in general, exhibit intense maxima due to $\pi-\pi^*$ transitions and weak longer wavelength maxima due to "forbidden" $n-\pi^*$ transitions.[49] The extensive conjugation present in ortho-quinones leads to a number of $\pi-\pi^*$ bands which tail into the visible, and interactions between the two vicinal carbonyl groups allow two $n-\pi^*$ transitions to occur in diones. The shorter wavelength $n-\pi^*$ transition occurs in the 270-300 nm range and is often buried under the intense $\pi-\pi^*$ absorption of conjugated diones. The longer wavelength $n-\pi^*$ occurs in the 330-540 nm range. This longer wavelength $n-\pi^*$ transition is of interest from a color standpoint and because the $n-\pi^*$ state is believed to be the reactive state in most photoreactions of diones.[49-52]

In the infrared region of the spectrum, model quinones exhibit strong C=O stretching bands in the 1656-1675 cm^{-1} range.[53-55] In work with isolated kraft lignin which had been oxidized with sodium meta-periodate,[56] Furman[57] found the C=O stretching band of the quinones in this lignin occurred at 1663 cm^{-1}. Heitner[58] found the C=O stretching band of what he claimed to be the quinones present in irradiated pulp occurred around 1650 cm^{-1}, while Polcin and Rapson[9,10] claim that the C=O stretching band of quinones in pulp occurs, along with other C=O lignin groups, at approximately 1670 cm^{-1}.

In general, C=O containing compounds also exhibit strong Raman scattering in the 1650-1820 cm^{-1} range.[59-60] Unfortunately, Raman spectroscopic studies of quinones, even in solution, have not been widespread. In theory, however, the C=O stretching bands of quinones should, in general, also occur in this range.

Reactions

In studies of the brightening of lignin in pulp with sodium dithionite, Hosoya et al.,[61] treated lignosulfonates, lignin model compounds and spruce groundwood with aqueous sodium dithionite, aqueous sodium bisulfite and sulfurous acid. On the basis of the results obtained in this study, it was concluded that model quinones and quinonoid lignin groups were easily reduced to the corresponding colorless phenolic compounds by these reagents. Later, Hosoya et al.[62] studied the decoloration of para-quinonoid model compounds with these same agents and found that simple para-quinonoid models were all decolored by these reagents. None of these reagents, however, completely decolored polymers of the simple model compound, 2-methoxy-para-quinone. In addition to these reports, Marton and Adler[63] have also suggested that sulfur dioxide reduced quinonoid groups in lignins to phenolic type species, and Nadein et al.[64] have used sodium dithionite to estimate the number of ortho-quinonoid groups present in oxidized kraft lignins.

In terms of the quinonoid lignin structures present in pulp systems, Polcin and Rapson[9,10] studied the effects of dithionite on the absorption spectra of lignin in groundwood pulps and found that this reagent reduced such structures to colorless phenolic products. Consistent with these results, Pew and Connors[7] found that sodium dithionite and sulfur dioxide also reduced quinonoid lignin structures in groundwood pulp to colorless phenolic products.

In their work with reducing reagents, Pew and Connors[7] also found that groundwood pulp was significantly brightened by reaction with trimethyl phosphite, $P(OCH_3)_3$. The reason for the observed increase in pulp brightness was not specified. In model systems, however, trimethyl phosphite reacts very quickly and nearly quantitatively with ortho-quinones and other α-β-diketones.[65-95] Under dry N_2, the products formed in these reactions are colorless 1:1 (quinone: trimethyl phosphite) adducts. For instance, the 1:1 adduct shown in Fig. 12 is formed when trimethyl phosphite is reacted with ortho-phenanthrenequinone. These 1:1 adducts, also known as oxyphosphoranes, are quite stable when kept under dry N_2. They react rapidly, however, with water or oxygen.[70-73,75,79,81-94] As shown in Fig. 13, cyclic phosphate triesters (I), cyclic phosphate diesters (II) and noncyclic alkyl ethers of ortho-quinol phosphates (III) can be formed when oxyphosphoranes react with water.

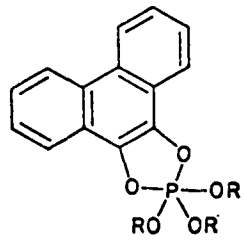

Figure 12. 1:1 Adduct formed when trimethyl phosphite is reacted with ortho-phenanthrenequinone.

In addition to forming 1:1 adducts with ortho-quinones, trimethyl phosphite has also been shown to form colorless 1:1 adducts with para-quinones.[83,93-97] Yields in these reactions are also near quantitative, but the 1:1 adducts formed from para-quinones are always noncyclic alkyl ethers of para-quinol phosphates. For example, trimethyl phosphite reacts with para-benzoquinone to form the 1:1 adduct shown in Fig. 14. When compared to the 1:1 adducts formed from ortho-quinones, these adducts are relatively stable toward water and oxygen.

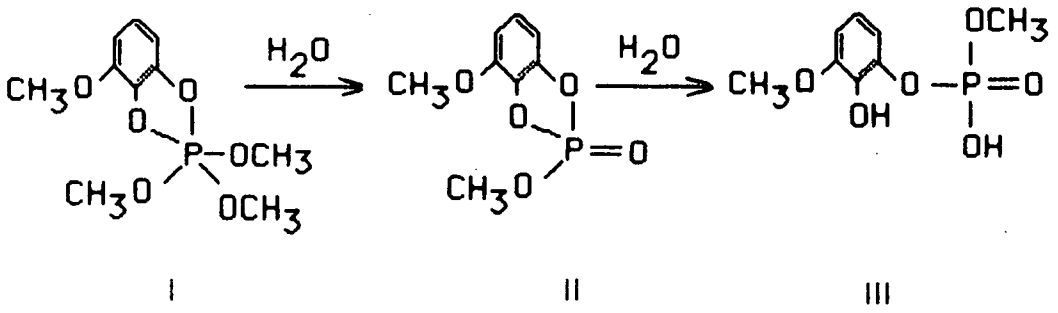

I II III

Figure 13. Possible reactions of oxyphosphoranes with water.

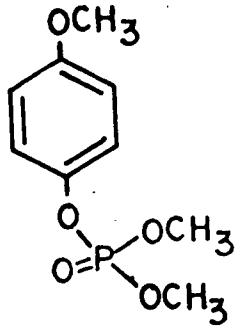

Figure 14. 1:1 Adduct formed when trimethyl phosphite was reacted with para-benzoquinone.[92]

One study which is of particular interest here is the study conducted by Medvecz.[98] In this study, the reactions of trimethyl phosphite with ortho- and para-quinone models related to the yellowing of high yield pulps were examined. The ortho-quinone quinone model examined was 3-methoxy-ortho-benzoquinone. When this model was reacted with trimethyl phosphite, in dichloromethane, the 1:1 adduct shown in Fig. 15 was obtained in nearly quantitative yield. When this 1:1 adduct was reacted with 3/4 mole equivalent of water, the hydrolysis product shown in Fig. 16 was obtained. Figures 15 and 16 also show the specific ^{31}P NMR chemical shifts of these products and of these types of products in general.

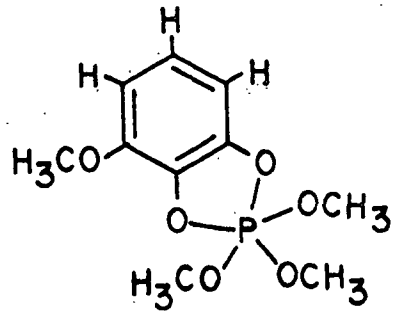

-45.76 ppm

-(45-60 ppm)

Figure 15. 1:1 Adduct formed when 3-methoxy-ortho-benzoquinone was reacted with trimethyl phosphite.[98]

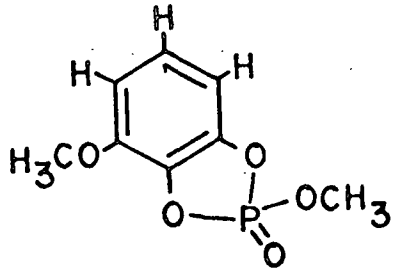

-11.1 ppm
(12-15 ppm)

Figure 16. Hydrolysis product formed when the 1:1 adduct shown in Fig. 15 was reacted with 3/4 mole equivalent of water.[98]

The para-quinone model studied by Medvecz was 2-methoxy-para-benzoquinone. When this model was reacted with trimethyl phosphite, in dichloromethane, the 1:1 adduct shown in Fig. 17 was obtained in near quantitative yield. Figure 17 also shows the ^{31}P NMR shift of this adduct and of these types of adducts in general. When this 1:1 adduct was reacted with water, no reaction was observed.

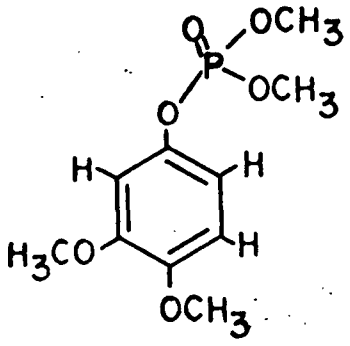

-2.6 ppm
-(4-6 ppm)

Figure 17. 1:1 Adduct formed when 2-methoxy-para-benzoquinone was reacted with trimethyl phosphite.[98]

A Brief Review of the Theory of Reflectance Spectroscopy

When light is incident upon the surface of an infinitely thick specimen such as an opaque sheet of pulp, part of the light is absorbed by the specimen and part of the light is scattered (i.e., reflected). The amount of light absorbed is dependent on the wavelength of the light incident upon the pulp sheet and on the chemical composition of the pulp. Light scattering results from the heterogeneous structure of the pulp sheet and of the individual fibers which make up this sheet. In general, light scattering occurs wherever there is a change in the index of refraction of the fibrous medium. The complicated interface system of fibrous material and air causes light to be scattered from pulp sheets and the mechanisms of this scattering are those of simple Fresnel reflection at interfaces, refraction and diffraction.[99]

One of the most widely used theories for quantitatively describing the relationships between the observable quantities of reflectance and transmittance and the fundamental parameters related to the absorption and scattering of visible light in a turbid medium is that of Kubelka and Munk.[100-102] Modifications of

this theory have been developed for pulp and paper by Steele,[103] Judd,[104-106] Campbell and Benny,[107] and Van den Akker.[99,108] The explicit assumptions and restrictions of this theory are as follows.[109]

1. The theory assumes that the mechanism of scattering is no different at the boundaries than in the body of the medium. In the case of pulp sheets, the scattering is caused by discontinuous indices of refraction. The medium in which the scattering centers are immersed is air. Hence there is no scattering when the light enters the sheet, and consequently this assumption does not pose a problem.

2. The theory assumes that the scattering and absorption coefficients are constant throughout the medium. As far as pulp sheets are concerned, this assumption appears to be valid for most cases. The scattering coefficient is certainly not constant over the cross section of a fiber, since scattering occurs at the outer walls and at the lumen. In a typical sheet, however, there will be enough fibers within a differential element of basis weight, dW, such that the scattering can be considered constant across this differential element. In very thin papers where the thickness is made up of very few fibers, however, it seems that this theory would begin to fail.

3. The theory assumes that the light within the medium is perfectly diffuse (i.e., propagating in all directions with equal intensity). In a medium with a large number of scattering centers, such as paper, this is a reasonable assumption.

4. In theory, the incident light must also be diffuse.

5. The equations developed in this theory apply only to one wavelength at a time.

The equations for calculating the absorption and scattering coefficients of a given sample can be derived from the basic equation developed by Kubelka and Munk[100-102] and modified for paper by Van den Akker.[99,108]

$$\int_{R_b}^{R} \frac{dr}{r^2 - [2(s + k)r]/s + 1} = s \int_{0}^{W} dW \qquad (1)$$

where W = basis weight of sample (g/cm^2)

R_b = reflectance of the surface lying under the sample sheet

R = reflectance from the top surface of the sample sheet

s = specific scattering coefficient (cm^2/g)

k = specific absorption coefficient (cm^2/g)

r = reflectance of a portion of the sample under a hypothetical infinitesimal layer of the material with a backing reflectance, R_b.

For the solution of this equation, consider the two following cases pertinent to this study.

Case 1: The sample sheet has infinite basis weight (i.e., $W = \infty$). In this case $R = R_b = R_\infty$ and Eq. (1) takes the form

$$\frac{k}{s} = \frac{(1 - R_\infty)^2}{2 R_\infty} \qquad (2)$$

Case 2: The sample sheet has a basis weight which is low enough that the reflectance of the sheet is influenced by the backing material. If the backing material is completely black so that its reflectance $R_b = 0$, Eq. (1) gives

$$R_o = \frac{\exp\,[sW(1/R_\infty - R_\infty)] - 1}{(1/R_\infty)\,\exp\,[sW(1/R_\infty - R_\infty)] - R_\infty} \tag{3}$$

$$s = \frac{R_\infty}{W(1 - R_\infty^2)} \frac{\ln(1 - R_\infty R_o)R_\infty}{(R_\infty - R_o)} \tag{4}$$

where R_o is the reflectance of the sheet examined with the black backing. This method is known as the "method of black backing."

Once scattering coefficients, s, have been calculated by means of Eq. (4), the absorption coefficients, k, are obtained by substituting these scattering coefficients into Eq. (2). This is the method which was used in this work.

In conclusion, it should be noted that because of the high absorption power of lignin in the UV range, the light reflectance of lignin rich materials is affected.[110] This phenomena, which has also been observed in other highly absorbing materials such as highly colored papers,[111,112] causes some decrease of determined absorption coefficients from the theoretical absolute absorption coefficients. This deviation from theoretical values has been assumed to be related to incomplete diffusion of light in the scattering process, so that the portion of reflected light is higher than it should be according to Kubelka-Munk theory.[113,114] Heterogeneity in the structure of the scattering material has also been suggested as a possible explanation.[115] Because of this deviation, analyses of absorption coefficients of mechanical pulp sheets were limited to the visible and far UV range in this study, and the results of these analyses were used for qualitative or semiquantitative comparisons only.

THESIS OBJECTIVES

The objectives of this study were, first, to determine if quinonoid lignin structures, and more specifically ortho-quinonoid lignin structures, occur and/or are photochemically generated in white spruce refiner mechanical pulp. If such structures do occur and/or are photochemically generated in this pulp, then the contribution of these structures to the "color" of these pulps and the quantum yield of their light induced formation will be determined. The second objective of this study was to examine the effects of incident wavelength and incident light flux on the overall rate of light induced yellowing (i.e., "color" development). In accomplishing these objectives it was necessary to quantitatively determine the number of ortho-quinonoid lignin structures present in irradiated and unirradiated pulp sheets and to develop a method for measuring the overall rate of light induced yellowing.

Satisfying these objectives will provide a better understanding of the photochemical and chemical reactions which occur when high yield pulp sheets are exposed to light. This understanding should lead to new insights into the problem of brightness stability and, thereby, aid in the development of practical stabilization methods.

EXPERIMENTAL APPROACH

In broad form the approach taken to achieve the abovementioned thesis objectives is given below. This approach can be divided into two parts, paralleling the two thesis objectives. Since these objectives involved investigating the photoinduced formation of quinonoid lignin structures *in situ*, the majority of the work was done using a white spruce refiner mechanical pulp and pulp sheets. Work with model compounds was performed where appropriate or useful.

DETERMINATION OF THE EFFECTS OF WAVELENGTH AND INCIDENT LIGHT FLUX ON THE OVERALL RATE OF LIGHT INDUCED YELLOWING

The first step in this determination involved assembling an apparatus which produced high intensity monochromatic UV light of known incident flux. Once this equipment was assembled, handsheet samples of the white spruce pulp were irradiated, under controlled conditions, with narrow band width light in the 290-390 nm wavelength range. This particular range of light was examined because it is the range of light in natural sunlight which induces yellowing. From spectroscopic analyses of these various samples before and after irradiation, the overall rate of yellowing was evaluated as a function of wavelength. Similar methods were used to evaluate the effect of incident light flux on the rate of yellowing.

DETERMINATION OF THE OCCURRENCE AND LIGHT INDUCED FORMATION OF QUINONOID LIGNIN STRUCTURES

The qualitative determination of quinonoid lignin structures *in situ* involved spectroscopic and chemical analysis of irradiated and unirradiated pulp and pulp sheets before and after reaction with sodium dithionite, sulfur

dioxide, and trimethyl phosphite. These reagents were examined because they are known to react almost quantitatively with quinones. Trimethyl phosphite also forms 1:1 adducts with both ortho- and para-quinonoid lignin structures, and these adducts are structurally different and easily distinguishable through ^{31}P NMR spectroscopy.

EXPERIMENTAL

PREPARATION OF STARTING MATERIALS

Preparation of White Spruce Refiner Mechanical Pulp

The refiner mechanical pulp used in this study was prepared from white spruce (Picea glauca) chips pretreated by soaking for 24 hours in 0.1% EDTA at pH 6.5. The chips were washed and converted into pulp by passing them through a Sprout Waldron Model 105-A laboratory disk refiner. Plate gaps for the five passes were 0.040-inch, 0.008-inch, 0.002-inch, 0.002-inch, and 0.002-inch. The pulp was then centrifuged to remove excess water.

Extraction of White Spruce RMP

The refiner groundwood pulp was ethanol/benzene-hot water extracted according to the procedures described in TAPPI Standard T 264 om-82. Following extraction, the pulp was separated into 500 g batches and stored by freezing in plastic bags.

Evaluation of White Spruce RMP Properties

The physical and optical properties of the pulp were evaluated using handsheets prepared according to TAPPI Standards T 205 om-80 and T 218 os-75, respectively. Evaluations of the physical and optical properties of these sheets was conducted by the Physical Test Lab and Brightness Lab, respectively, at The Institute of Paper Chemistry. The metal ion content of the pulp (iron, copper, and manganese) was determined by inductively coupled plasma emission spectroscopy at VHG Labs, Inc. (180 Zachary Road, No. 5, Manchester, NH 03103). The results of these determinations are summarized in Table 1.

Table 1. Physical and optical properties of laboratory prepared white spruce refiner mechanical pulp.

Pulp Property	Measured Value (mean ± 95% confidence interval)
CSF	110
Density (o.d.; g/cm^3)	0.403
Tensile index (nm/g)	28.9 ± 1.02
Breaking length (km)	3.24 ± 0.11
Burst index ($kPam^2/g$)	1.32 ± 0.13
Tear index (mnm^2/g)	5.04 ± 0.089
TAPPI opacity (%)	93.9
TAPPI brightness (%)	59.83
Metal ion content (ppm, o.d. basis)	
Iron	39.4
Copper	3.1
Manganese	1.3

Determination of Klason Lignin and Methoxyl Content of White Spruce RMP

The Klason lignin content of the extracted refiner groundwood pulp was determined to be 26.9%. The methoxyl content of the pulp was determined to be 5.07% (Zeisel method) by Chem-Lig International, Inc. (320 Ross Avenue, Schofield, WI 54476).

Preparation of White Spruce Acid-Chlorite Holocellulose

The acid-chlorite holocellulose used in this study was prepared from extracted white spruce pulp as follows. Approximately 50.0 g of air dry pulp was soaked for 4 hours in 1.0 L of distilled water. A solution of 25 mL glacial acetic acid, 75 g of sodium chlorite (technical grade) and 1.0 L of distilled

water was added to the pulp slurry and the resulting mixture was placed in a water bath in a hood at 70°C. After one hour at temperature, an additional 25 mL of glacial acetic and 75 g of acid chlorite were added to the mixture. The above step was repeated for two more treatments (4 treatments total), after which the holocellulose was washed with distilled water until the filtrate was neutral and colorless and then three times with 250 mL portions of methanol. The product was then air dried and stored, in the dark, under nitrogen. Using the same procedure used for the pulp, the Klason lignin content of the resulting white spruce holocellulose was determined to be 1.5% (o.d. basis).

Preparation of ortho-Quinone Enhanced Pulp by Oxidation of White Spruce RMP with Fremy's Salt

Using a standard British disintegrator, extractives free pulp was disintegrated for 2 minutes at 0.6% consistency (o.d. basis). The pulp was then diluted to 0.3% consistency with a 3×10^{-3}M solution of Fremy's salt $[ON(SO_3K)_2]$ in 0.10M KH_2PO_4 (pH = 6.5). The resulting mixture was stirred for 30 minutes at room temperature, filtered, and washed with 500 mL of distilled water per 3 g of o.d. pulp. The washed pulp was then diluted to 0.30% consistency with distilled water and the slurry was stirred for an additional 30 minutes. The pulp was again filtered and washed with an additional 500 mL of distilled water per 3 g of o.d. pulp. Samples of this pulp were subsequently used to form handsheets as described below.

Preparation of Handsheets

All 60 g/m^2 handsheets used in this study were prepared from extractive free pulp using the procedures described in TAPPI Standard T 205 om-80 (Forming Handsheets for Physical Tests of Pulp). The reason for using this method was that handsheets of uniform formation were desired. Distilled water was used in these

preparations. The basis weights of the resulting sheets were in the range of 55-60 g/m^2. All 160 g/m^2 handsheets used in this study were prepared from extractive free pulp using the procedures described in TAPPI Standard T 218 os-75 (Forming Handsheets for Reflectance Tests of Pulps). Distilled water was also used in these preparations.

Other Materials Used in this Study

The sources of the other materials used in this study were as follows. The quinone models, 3-methoxy-ortho-benzoquinone and 2-methoxy-para-benzoquinone, were graciously donated by Pat Medvecz and were prepared as described in his Independent Study at The Institute of Paper Chemistry.[98] The quinone models, 3,5-di-tert-butyl-ortho-benzoquinone and 2,6-di-tert-butyl-para-benzoquinone, were purchased from Aldrich Chemical Company. The spruce glucomannan was a generous gift from Norm Thompson. The ivory nut sample was a gift from Ingegerd Uhlin, who used this material in her thesis work at The Institute of Paper Chemistry[116] (see Appendix IX for discussion).

INSTRUMENTAL METHODS

Diffuse Reflectance UV-Visible Spectroscopy

Reflectivity (R_∞) spectra were recorded from handsheets on a Perkin-Elmer Model 320 Spectrophotometer equipped with a Hitachi Model 210-5575 Integrating Sphere accessory (6.0 cm diameter). Pressed $BaSO_4$ disks were used as a reference material. Background corrections were made for this standard using the background correction feature of the Model 320's microprocessor. Data storage and manipulation were accomplished by interfacing the spectrophotometer to an Apple III microcomputer. Subtractions and Kubelka-Munk calculations were computed using a program written for the Apple III (Appendix I).

Diffuse Reflectance Fourier Transform Infrared (FTIR) Spectroscopy

Diffuse reflectance FTIR spectra were recorded on a Nicolet 7199C Fourier Transform Infrared Spectrometer. The spectrophotometer was equipped with a Harrick diffuse reflectance attachment. Spectra of the lignin present in pulp samples were obtained by subtraction of the spectrum of the white spruce acid-chlorite holocellulose described above. All subtractions and integrations were carried out using the software and dedicated computers of this instrument. In these subtractions, the 3000-2800 cm^{-1} C-H stretching band of the carbohydrate portion of these samples were used for normalization. The details of the procedure used in normalization of these spectra are given by Berben et al.[117]

In the experiments described in this thesis, it was assumed that the change in the total number of aromatic lignin units present in the various pulp samples was not significant. In other words, it was assumed that the number of nonaromatic, ortho-quinonoid lignin structures formed from aromatic lignin units was relatively low in comparison to the total number of aromatic lignin units.[11,12,57]

On the basis of this assumption, the areas under the 1665 cm^{-1} C=O stretching band of the lignin present in these various samples was further normalized. In this normalization, the area under the 1510 cm^{-1} aromatic C=C stretching band of the lignin present in each sample described in this paper was evaluated. The 95% confidence interval of this value was determined to be 12.00 ± 0.59 cm^{-1}. Since the variation in this value was less than 5%, the assumption that the reactions studied in this work did not significantly change the total number of aromatic C_9 lignin units present in the pulp samples appeared to be valid. Based on this finding, the normalized areas under the 1665 cm^{-1} C=O stretching bands of the lignin present in these samples were calculated as follows:

normalized area under 1665 cm^{-1} C=O band = [area under 1665 cm^{-1} C=O band] [NF]

where [NF] = normalization factor = $\frac{\text{measured area under 1510 } cm^{-1} \text{ C=C band}}{\text{average area under 1510 } cm^{-1} \text{ C=C band}}$

Typical values for these factors ranged from 0.9 to 1.1.

Raman Spectroscopy

Raman spectra were recorded as handsheets on a Jobin Yvon Ramanor Model HG2 S Raman Spectrometer using 514.5 nm excitation from a Spectra Physics Series 2000 Model 2025 Argon ion laser. These handsheet samples were submerged in water during analysis in order to reduce the fluorescence of these samples. Solution spectra were recorded in dichloromethane or benzene.

Solid State ^{31}P Nuclear Magnetic Resonance (NMR) Spectroscopy

Solid state ^{31}P NMR spectra were recorded using magic angle spinning. These spectra and their corresponding deconvolutions were recorded by Dr. Gary Turner at Spectral Data Services (818 Pioneer, Champaign, IL 61820). In order to maintain an inert environment, sample preparation and analysis were conducted under a dry N_2 environment.

SEM-EDS Analyses

SEM-EDS (scanning electron microscopy-energy dispersive spectrometry) analyses were conducted by the EM Lab at The Institute of Paper Chemistry. Prior to analysis, sheet samples were sectioned under liquid nitrogen and carbon coated.

IRRADIATION PROCEDURES

Irradiation of Handsheets with Simulated Sunlight

Irradiations with simulated sunlight were conducted using an ORIEL Corporation 1000 Watt Solar Simulator operating at the desired output. This

unit was equipped with an air mass one filter and had a 5 x 5 inch output beam. The spectral characteristics of this unit are shown in Fig. 18. After allowing the lamp of this unit to warm up for 30 minutes, sample sheets were positioned on black backing 50 cm from the output lens of the source and irradiated. In order to cool the samples, air was blown over them during the irradiation. The solar simulator unit was located in a humidity (50%) and temperature (21°C) controlled lab.

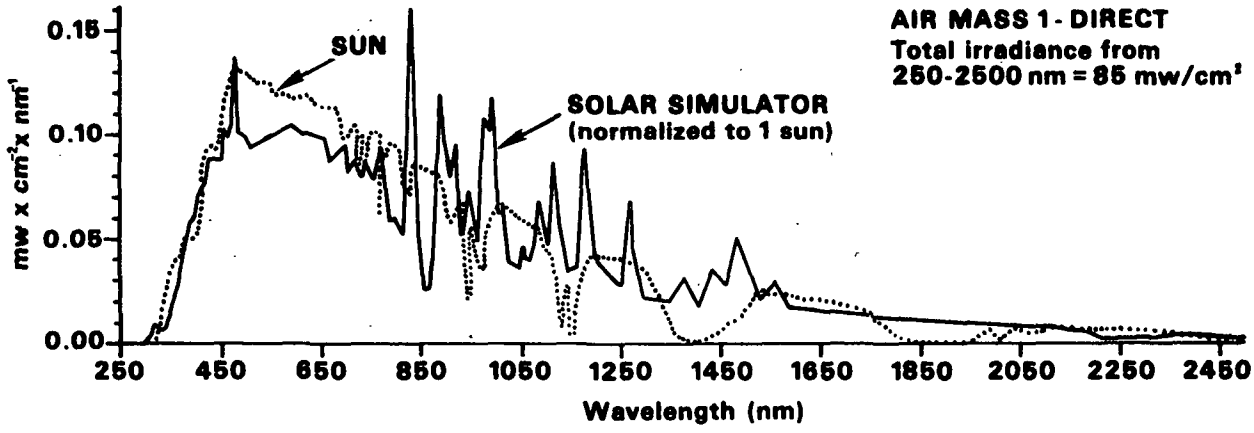

Figure 18. Spectral characteristics of solar simulator used in this study.

Irradiation of Handsheets with Monochromatic UV Light

Equipment

Irradiations with monochromatic UV light were conducted using the optical apparatus shown in Fig. 19. The apparatus consisted of a Schoeffel LH 151 N arc lamp housing equipped with a Hanovia 1000 Watt xenon arc lamp. The lamp was powered by a Christie SCX 1200-121 d.c. power supply. A secondary focusing lens (ORIEL Corporation) was used to focus an image of the arc onto the entrance slit of an ORIEL Corporation Model 7240 grating monochromator equipped with

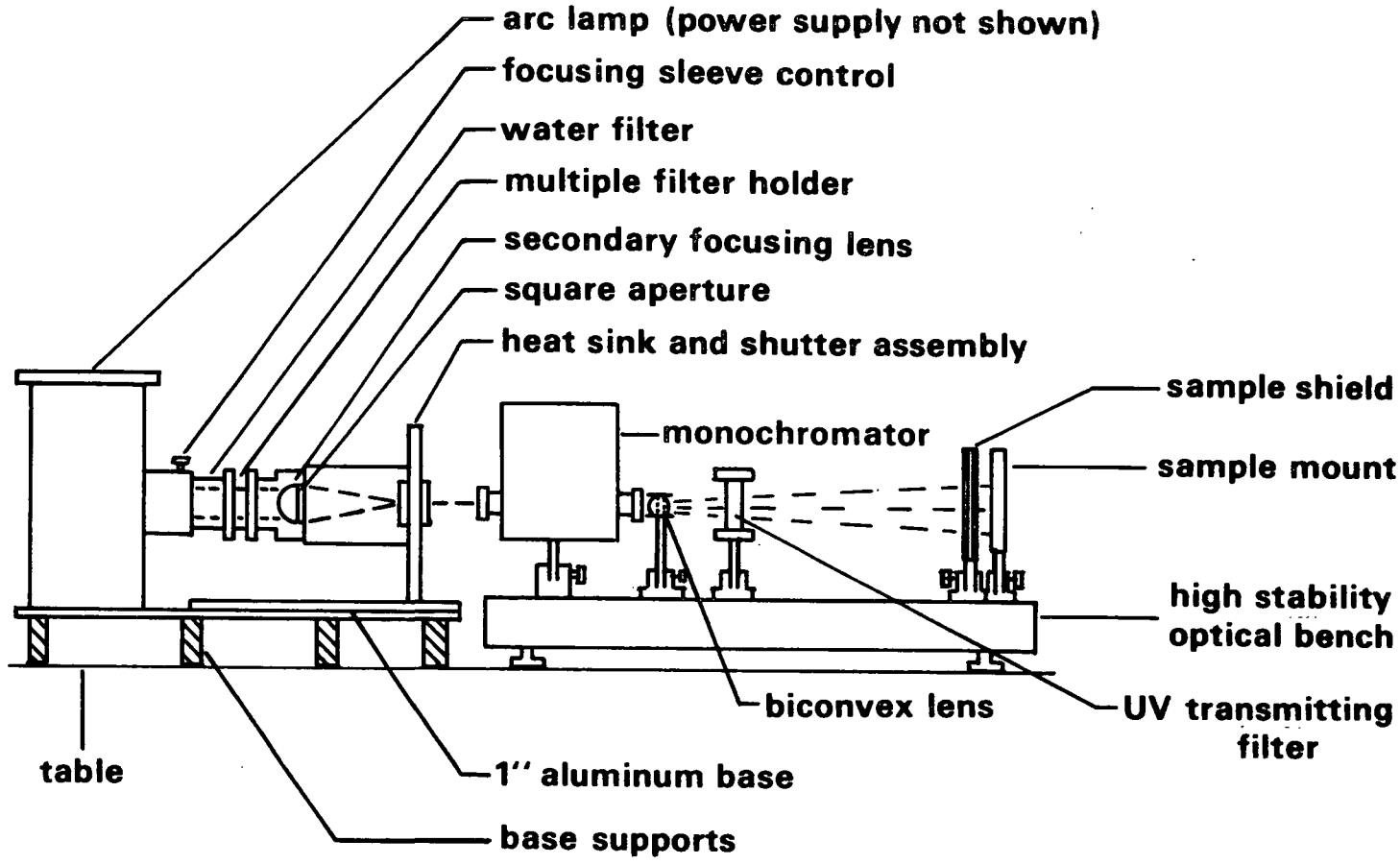

Figure 19. High intensity monochromatic UV light source used in this study.

variable slits. Heat load on the monochromator was reduced by use of a water filter and by a heat sink, both supplied by ORIEL Corporation. The output from the monochromator was focused onto the sample with an additional focusing lens. The amount of stray light reaching the sample was minimized by use of an order sorting filter supplied by ORIEL and a home built "black box" sample shield not shown in Fig. 19.

Measurements of incident light flux, in photons/cm^2 sec, were made with an ORIEL photomultiplier detection system. This system consisted of a Model 7060 photomultiplier head equipped with a photomultiplier tube suitable for use in the 200-700 nm region. The head was powered by an ORIEL Model 7070 photomultiplier readout/power supply unit. The extreme sensitivity of this unit necessitated the use of two attenuation devices; an ORIEL Model 7179 UV grade optical diffuser and an ORIEL Model 5073 neutral density filter (4.0 density). The attenuation factors of these devices were determined experimentally and found to be in good agreement with those provided by ORIEL (Appendix II). Measured photomultiplier currents were converted into incident light fluxes using the radiant power sensitivity curve of this photomultiplier head determined as described in Appendix III.

Procedures

The procedure used in the irradiation of handsheet samples was as follows. The lamp and photomultiplier units were started and allowed to warm up for at least 30 minutes (bias on the photomultiplier was set at 600 volts). During this time the monochromator was turned to the desired wavelength, and the slits of the monochromator were set at the desired widths and heights. In these experiments, slit width was set so as to produce light with a band width of 5 nm. Slit heights were set so as to produce an area of illumination of 2.82 cm^2.

This was the minimum area needed to record reflectance measurements. When the lamp was warmed up, its output was adjusted to give the desired incident light flux, as measured using the photomultiplier system. These adjustments were made through the power supply voltage setting. The photomultiplier unit was then removed and replaced with the sample holder.

Sample handsheets were selected and cut into six smaller samples. The dimensions of these six samples were approximately 5 x 3 cm. The samples were stacked to form a thick pad and the R_∞ spectrum of the resulting pad was recorded and stored on disk. This same pad was subsequently placed in the sample holder shown in Fig. 19 and irradiated for the desired length of time. In order to keep the flux of the light incident upon the sample as constant as possible, periodic checks of incident light flux were made with the photomultiplier system (approximately every half hour), and the variations in the light fluxes in these experiments were less than 5%.

When the desired time period was over, the sample was removed and the incident light flux was again recorded. In order to avoid any possible changes which may occur, the R_∞ spectrum of the irradiated sample was recorded within 5 minutes and stored on disk. The sample was then either replaced and irradiated further (i.e., the kinetics studies), dried for further analysis (i.e., reaction studies, FTIR, etc.) or stored by freezing.

Determination of the Effect of Wavelength on the Relative Rate of Yellowing

Thin handsheets (basis weight, W, approximately 24 g/m^2) were prepared from the test pulp using the procedures described in TAPPI T 205 om-80, except that the amount of slurry added to the handsheet mold was reduced to an amount which gave sheets of the target basis weight. Five "thin" samples were selected from

these sheets. Five "thick" handsheet samples (basis weight approximately 150 g/m^2) were also selected from thick sheets prepared as described above.

The R_o and R_∞ spectra of each of the thin and thick sheet samples, respectively, were recorded in the 290-390 nm region of the spectra. Each of these spectra was, in turn, the computer average of five scans obtained using the CAT feature of the Spec 320. Using the Apple III, the five resulting R_o and R_∞ spectra were then averaged into single R_o and R_∞ spectra. The resulting R_o and R_∞ spectra were used to calculate specific absorption (k_λ) and specific scattering (s_λ) coefficients for the unirradiated test pulp in the wavelength range of interest (i.e., 290-390 nm).

From the k_λ values thus obtained, the incident light flux at each incident wavelength examined [$I_{o(\lambda)}$] was adjusted so that the absorbed light flux, approximated as $I_{o(\lambda)}[1-\exp(-k_\lambda W)]$, was kept as nearly as possible the same at all wavelengths examined. In making these calculations it was assumed that the Beer-Lambert law, $I_{abs}/I_o = 1 - \exp(-kW)$, can be used as a first approximation of the light flux absorbed by these samples, and that k_λ in the range from 290-390 nm did not change significantly during the irradiation procedure. A summary of these experiments is given in Table 2. The irradiation time in all experiments was 90 minutes.

IMPREGNATION OF WHITE SPRUCE RMP SHEETS WITH MODEL QUINONE COMPOUNDS

Selected handsheet samples (basis weight approximately 150 g/m^2) were impregnated with the four following model quinone compounds; 3-methoxy-ortho-benzoquinone, 2-methoxy-para-benzoquinone, 3,5-di-tert-butyl-ortho-benzoquinone and 2,6-di-tert-butyl-para-benzoquinone. Approximately 0.1 g of the first quinone model was dissolved in 10 mL of dichloromethane. Whole handsheets were

then submerged in this solution for 1 minute after which the same was turned over. After one additional minute the sample sheet was removed from the solution, hand pressed between two blotters and air dried. Using fresh handsheets, the procedure was then repeated with the other three model quinones. A control sheet was also prepared using pure dichloromethane. The R_∞ spectra of the dry impregnated sheets were then recorded and stored on disk. If desired, the amount of quinone impregnated into the sheet was determined by weight difference before and after impregnation.

Table 2. Summary of the experiments conducted to determine the effect of incident wavelength on the rate of yellowing.

Incident Wavelength (nm)	k_λ (cm^2/g)	Incident Light Flux (photons/cm^2 sec)	Absorbed Light Flux (photons/cm^2 sec)
295.0	778.81	5.36×10^{13}	5.29×10^{13}
300.0	780.43	5.35×10^{13}	5.28×10^{13}
305.0	773.13	5.39×10^{13}	5.28×10^{13}
310.0	766.58	5.45×10^{13}	5.37×10^{13}
312.5	759.64	5.50×10^{13}	5.40×10^{13}
315.0	769.90	5.42×10^{13}	5.40×10^{13}
320.0	738.44	5.50×10^{13}	5.40×10^{13}
325.0	769.50	5.43×10^{13}	5.40×10^{13}
330.0	705.28	5.92×10^{13}	5.79×10^{13}
335.0	740.27	6.08×10^{13}	5.83×10^{13}
340.0	748.51	6.06×10^{13}	5.83×10^{13}
350.0	737.85	6.15×10^{13}	6.03×10^{13}
360.0	668.32	6.25×10^{13}	6.09×10^{13}
380.0	539.22	7.00×10^{13}	6.63×10^{13}

REACTION OF WHITE SPRUCE RMP SAMPLES WITH SULFUR DIOXIDE AND SODIUM DITHIONITE

Reaction of Pulp Samples with Gaseous Sulfur Dioxide

Thick sheet samples of nonirradiated, irradiated, and Fremy's salt treated pulp were dried under vacuum over P_2O_5 for 48 hours. The R_∞ spectra of these samples were recorded and the samples were redried for 24 hours. The dried sheets were transferred under dry N_2 to a clean desiccator containing a small amount of dry silica gel and the desiccator were evacuated. The desiccator was then filled with dry SO_2 gas and the samples were allowed to react with the gas for 5 days (i.e., until the red color of the Fremy's salt treated sample almost disappeared). The SO_2 gas was evacuated from the system using a vacuum pump (8 hours) and the samples were immediately analyzed by diffuse reflectance UV-visible spectroscopy.

Wiley milled samples (20 mesh) of the above pulps were treated with SO_2 gas in a similar manner and the resulting samples were analyzed by diffuse reflectance FTIR. In order to obtain complete elimination of the red color of the pulp oxidized with Fremy's salt, the reaction time in these experiments was 7 days.

Reaction of Pulp Samples with Aqueous Sulfur Dioxide

After recording R_∞ spectra, thick sheet samples of nonirradiated, irradiated, and Fremy's salt treated pulp were placed in a 5.5 cm diameter Buchner funnel. The samples were wetted with distilled water and sealed in place by pulling a vacuum on the sample. Approximately 500 mL of aqueous sulfur dioxide (pH = 2.5) was slowly filtered through the sample. Filtering time was approximately 30 minutes. These conditions were sufficient enough to totally eliminate the red color of the pulp oxidized with Fremy's salt. The samples were next washed with

distilled water until the filtrate was neutral. The sheet samples were dried in the dark under controlled conditions and then reanalyzed by diffuse reflectance UV-visible spectroscopy. Control sheets were prepared by repeating the above procedure with distilled water only.

Wiley milled (20 mesh) samples of the above pulps were treated with aqueous SO_2 by stirring the pulp (approximately 0.2 g o.d. basis) in aqueous sulfur dioxide (pH = 2.5) for 30 minutes. As above, these conditions were sufficient enough to totally eliminate the red color of the pulp oxidized with Fremy's salt. The samples were then washed until the filtrate was neutral, and the resulting samples were dried over P_2O_5 under vacuum for 48 hours. The samples were then analyzed by diffuse reflectance FTIR. Cellulosic filter paper was used to retain the milled pulp on the filter.

Reaction of Pulp Samples with Aqueous Sodium Dithionite

Sheet samples of nonirradiated, irradiated and Fremy's salt treated pulp were treated with aqueous $Na_2S_2O_4$ using a procedure similar to the one described for the aqueous SO_2 samples. The R_∞ spectra of the samples were recorded. A fresh 0.1M solution of aqueous $Na_2S_2O_4$ in 0.025M KH_2PO_4 (pH 6) was prepared under N_2 using deoxygenated water. While still under an N_2 atmosphere, approximately 500 mL of this solution was slowly filtered through sample sheets. As in the above experiments, these conditions were sufficient enough to totally eliminate the red color of the pulp oxidized with Fremy's salt. Filtering time was about 30 minutes. The samples were then washed with 1.0 L of distilled water and dried over P_2O_2 under vacuum for 48 hours. The UV-visible reflectance spectra of the dry sheets were then recorded. Control sheets were prepared by repeating the above experiments with 0.025M KH_2PO_4.

Wiley milled (20 mesh) samples of the above pulps were treated with aqueous $Na_2S_2O_4$ as follows. Approximately 0.2 g (o.d. basis) samples of each pulp were sealed under vacuum in 125 mL hypo-vials. Ten milliliters of 0.03M $Na_2S_2O_4$ in 0.025M KH_2PO_4 (pH 6) were added to each sample and allowed to react for 3 hours under vacuum. Two temperatures were examined; 20 and 60°C. After the reaction, the samples were washed with 1.5 L of distilled water and dried. The dried samples were then analyzed by diffuse reflectance FTIR.

REACTION OF WHITE SPRUCE RMP SAMPLES WITH TRIMETHYL PHOSPHITE

The sheet samples used in the diffuse reflectance UV-visible analysis were treated with trimethyl phosphite using the following procedure. While under dry, oxygen-free N_2, dried sheet samples (approximately 0.275 g) of unirradiated, irradiated (4 hours) and Fremy's salt treated pulp were placed in separate glass weighing bottles containing 9 mL of anhydrous dichloromethane. The samples were soaked for 15 minutes after which 1.0 mL of trimethyl phosphite (Aldrich Gold Label) was added. The weighing bottles were capped and kept under N_2 for 30 hours. While still under N_2, the circular samples were placed in a 5.5 cm diameter Buchner funnel and washed with 500 mL of anhydrous dichloromethane and 1.0 L of anhydrous diethyl ether. The samples were then dried and placed under vacuum for 48 hours prior to analysis. The purpose of this was to remove any residual phosphite present in these samples.

The Wiley milled pulp samples used in diffuse reflectance FTIR and ^{31}P NMR analyses were prepared by a slightly different procedure. While under N_2, Wiley milled (20 mesh; approximately 0.25 g) samples of each pulp were placed in 10 mL hypo-vials containing 4.5 mL of anhydrous dichloromethane. The samples were soaked for 15 minutes after which 0.5 mL of trimethyl phosphite was added. The

contents were then sealed under N_2. In order to maximize yields, the samples were allowed to react, with occasional stirring, for 7 days. The reacted samples were then washed as described above, evacuated for 48 hours and stored under N_2 until the desired analysis could be performed.

Preparation of SEM-EDS Sheet Samples

Sheets of a very high basis weight were used to prepare SEM-EDS samples. These sheets had a basis weight of 160 g/m^2 and were formed according to the basic procedures described in TAPPI Standard T 205 om-80. These sheets were then exposed to 20 hours of simulated sunlight and reacted with trimethyl phosphite for 7 days as described above. The reacted samples were then sectioned under liquid nitrogen, carbon coated, and analyzed by the EM Lab at The Institute of Paper Chemistry.

EVALUATION OF Δk_λ SPECTRA

The Δk_λ spectra presented in this thesis were determined as follows. The s_λ spectrum of the white spruce pulp used in the work was evaluated using the method of "black backing" described in detail by Polcin and Rapson[118] (Fig. 20). This spectrum was evaluated from measurements of R_o and R_∞ in the 350-700 nm range. Foote[119] has shown that the scattering coefficient of dyed papers decreases with increasing absorption, the effect being small at low levels of dyeing, but pronounced at higher values of the absorption coefficient. Thus, the drop in this spectrum in the 350-400 nm region was considered real and was attributed to the high absorption of the lignin present in the pulp. Once the s_λ spectrum of the pulps was determined, the k_γ spectrum of the pulp was evaluated (Fig. 21). The k_λ spectra of subsequently irradiated or reacted sheet samples were then obtained from R_∞ measurements and from the s_λ spectrum of the pulp shown in Fig. 20, and Δk_λ spectra were calculated using the Apple III.

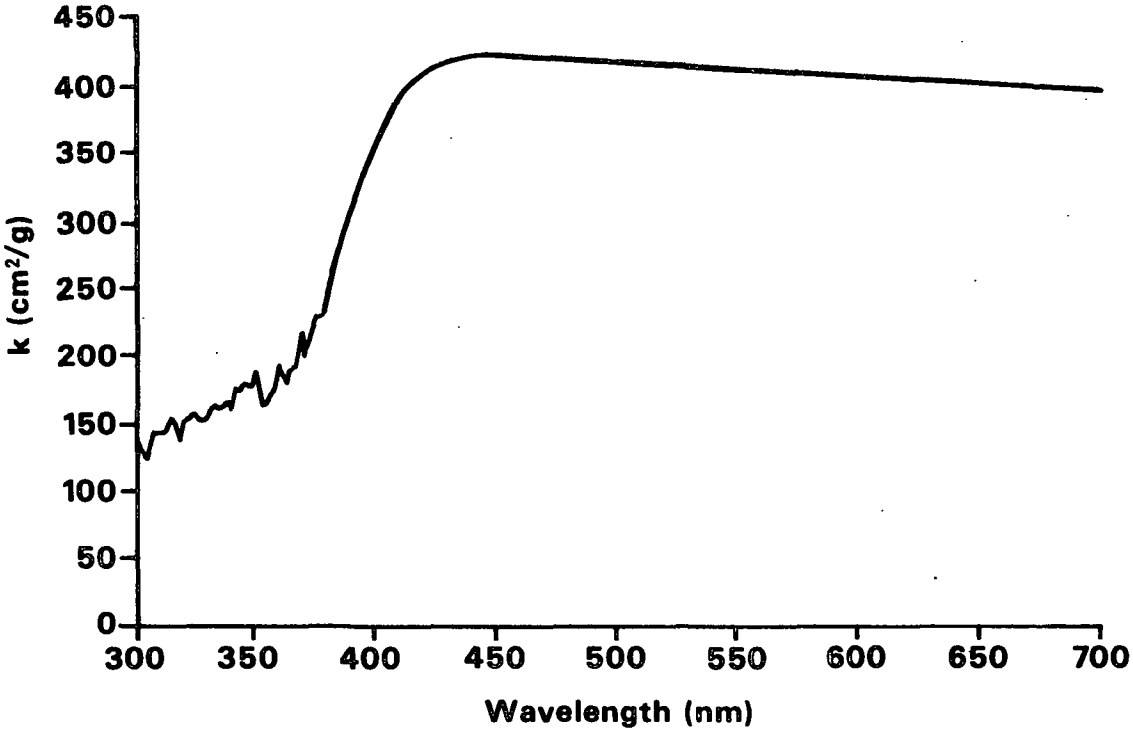

Figure 20. s_λ spectrum obtained from white spruce pulp sheets using the method of "black" backing described by Polcin and Rapson.[118]

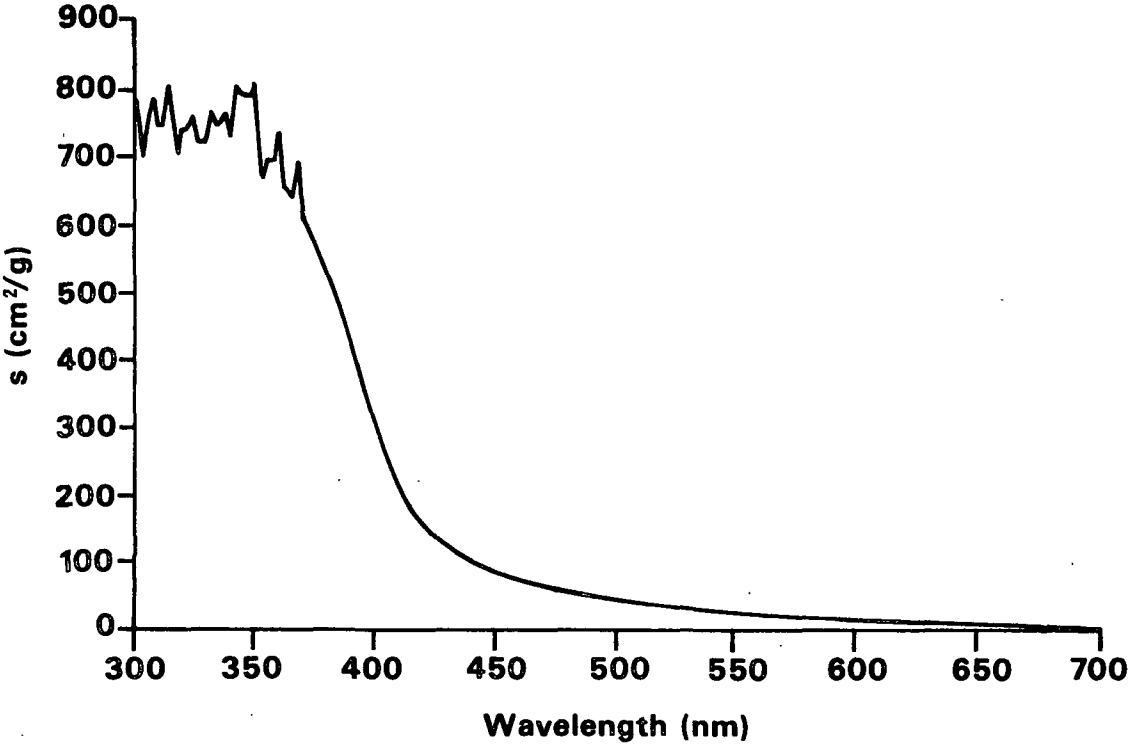

Figure 21. k_λ spectrum obtained from white spruce pulp sheets using the method of "black" backing described by Polcin and Rapson.[118]

RESULTS AND DISCUSSION

The results obtained in this study can be divided into two major sections; one dealing with the results obtained in a photochemical study of the light induced yellowing of high yield white spruce pulp and another dealing with the results obtained in a chemical study of photoyellowed samples of this pulp. The section dealing with the results obtained in the photochemical study is presented first. After this, the second section dealing with the results obtained in a chemical study of photoyellowed samples of this pulp is presented.

THE LIGHT INDUCED YELLOWING OF WHITE SPRUCE REFINER MECHANICAL PULP: PHOTOCHEMICAL ASPECTS

Starting Material

DTPA pretreated white spruce (Picea glauca) wood chips were chosen as the starting material for this study. This choice was based on the desire to have a pulp which was of high purity, but which was also representative of a typical commercial high yield pulp. A laboratory scale disk refiner was used to convert the chips into a refiner mechanical pulp. Following extraction with alcohol-benzene and hot water, this white spruce pulp was used in the experiments described in the following section of this report. This pulp was also used as the substrate in the preparation of the white spruce holocellulose and ortho-quinone enhanced pulp samples described in later sections.

Determination of the Effect of Incident Wavelength on the Rate of 290-390 nm UV Light Induced Yellowing

The wavelength of the absorbed light is an important variable unique to photochemical systems.[120] In studying photochemical reactions, knowledge of the effect of wavelength on the rate of a reaction can yield important information about the overall reaction mechanism. A critical precaution in such studies,

however, is to keep the flux of light absorbed as nearly as possible the same at all wavelengths examined, particularly if one is studying the products of secondary reactions.[120] Thus, it is important that studies of this type be made with light of known wavelength distribution, and the fraction of the incident light absorbed by the sample should be reasonably well known.[120] A third constraint which must be met in experiments of this type is that a good method for measuring the rate of the reaction must exist.

In this study, the first of the constraints noted above was met by using narrow band width light of known wavelength distribution and of known photon flux. This light was provided by the high intensity monochromatic light source described in the Experimental section of this report.

The second constraint noted above was met by irradiating sheet samples in such a manner that the total number of photons absorbed by the pulp was kept approximately constant over the incident wavelength range examined (i.e., 290-390 nm). A detailed discussion of the procedures used in meeting this second constraint was presented in the Experimental section of this paper and, therefore, will not be repeated here.

Because the nature and distribution of the product or products formed during the yellowing reaction are not well known, no absolute method for measuring the rate of light induced yellowing was available. Therefore, the third constraint noted above was met using a rate method based on measurements of Δk_λ. In developing this method, two key assumptions were made. The first assumption was that the Kubelka-Munk specific absorption coefficient, k_λ, was proportional to the number of chromophores present in a given pulp sample. The second assumption was that, under the relatively mild irradiation conditions employed in this

study (i.e., relatively short exposure times, narrow band width light at relatively low light fluxes and controlled temperature and humidity), no changes occurred in the scattering properties of the samples.

Before beginning these studies, however, the validity of these assumptions was tested. The first assumption noted above was tested by impregnating handsheets with varying amounts of 3,5-di-tert-butyl-ortho-benzoquinone. This substance was selected because it was considered to be a fair model for the types of structures postulated to be formed during the photoyellowing process. On the basis of the absorption properties of the model in solution, measurements of $(k/s)_\lambda$ were made at 430 nm. When the $(k/s)_{430\ nm}$ values of these sheets were plotted as a function of the weight fraction of absorbed model, a linear relationship was observed (Fig. 22). Assuming that the scattering coefficient, $s_{430\ nm}$, of these sheet samples was not significantly affected by the impregnation process, these results show that the measured value of $k_{430\ nm}$ is proportional to the weight fraction (i.e., amount) of colored bodies present in these sheets. Thus, if similar quinonoid structures are generated on the surface of fibers during the yellowing reaction, then they should exhibit similar behavior.

In order to test the second experimental assumption noted above, the Kubelka-Munk scattering coefficients, s_λ, of sheet samples were determined before and after irradiation with 310 and 350 nm light. The selection of light of these two wavelengths, while somewhat arbitrary, was based on a desire to examine two wavelengths within the range of interest (i.e., 290-390 nm). As expected, the Δs_λ spectra obtained when the s_λ spectrum of the unirradiated pulp was subtracted from the s_λ spectra of the irradiated pulps showed that irradiation with relatively low intensity UV light does not change the scattering properties of the pulp in the 350-700 nm range (Fig. 23 and 24). Procedurally,

this finding was important because it meant that the k_λ coefficients of irradiated sheet samples could be calculated from the already determined s_λ coefficients of the unirradiated pulp and the measured $R_\infty(\lambda)$ values of the irradiated pulp.[118]

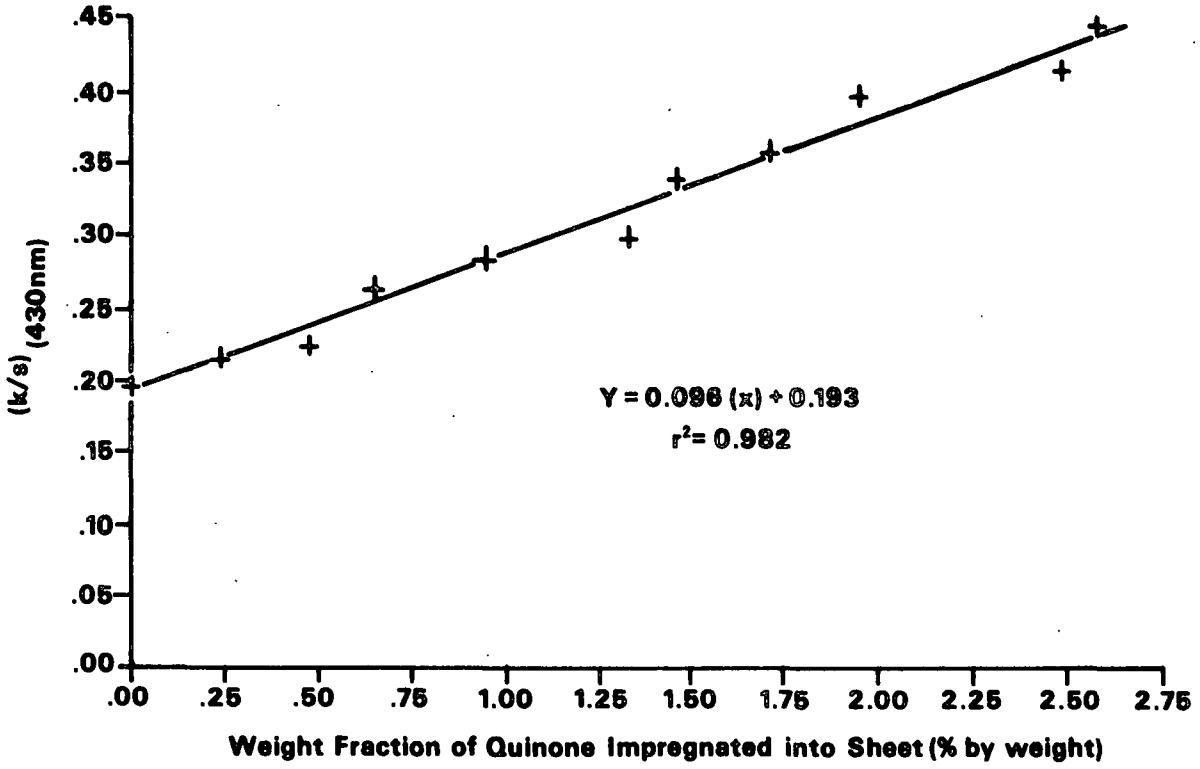

Figure 22. Plot of $(k/s)_{430\ nm}$ versus the weight fraction of quinone impregnated into 160 g/m^2 white spruce pulp sheets.

The k_λ coefficients obtained in this manner were important because they served as the basis of the method developed to evaluate the rate of light induced yellowing. In this method, the k_λ spectra of sheet samples were recorded before and after irradiation with essentially monochromatic light of known wavelength distribution and incident light flux. For each incident wavelength examined, a Δk_λ spectrum was prepared. The Apple III was then used to evaluate the area under the absorption band observed in each of these spectra.

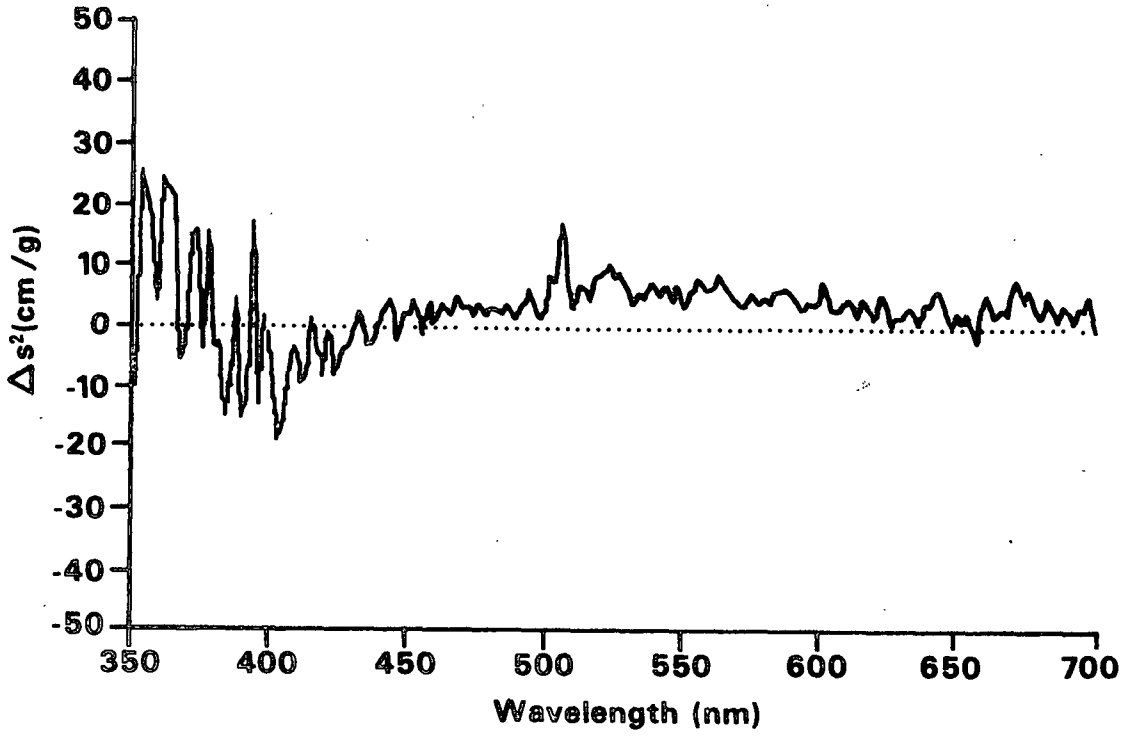

Figure 23. Δs_λ spectrum obtained when the s_λ spectrum of an unirradiated pulp sheet was subtracted from the s_λ spectrum of the same pulp sheet after irradiation with 310 nm UV light (irradiation time = 90 min).

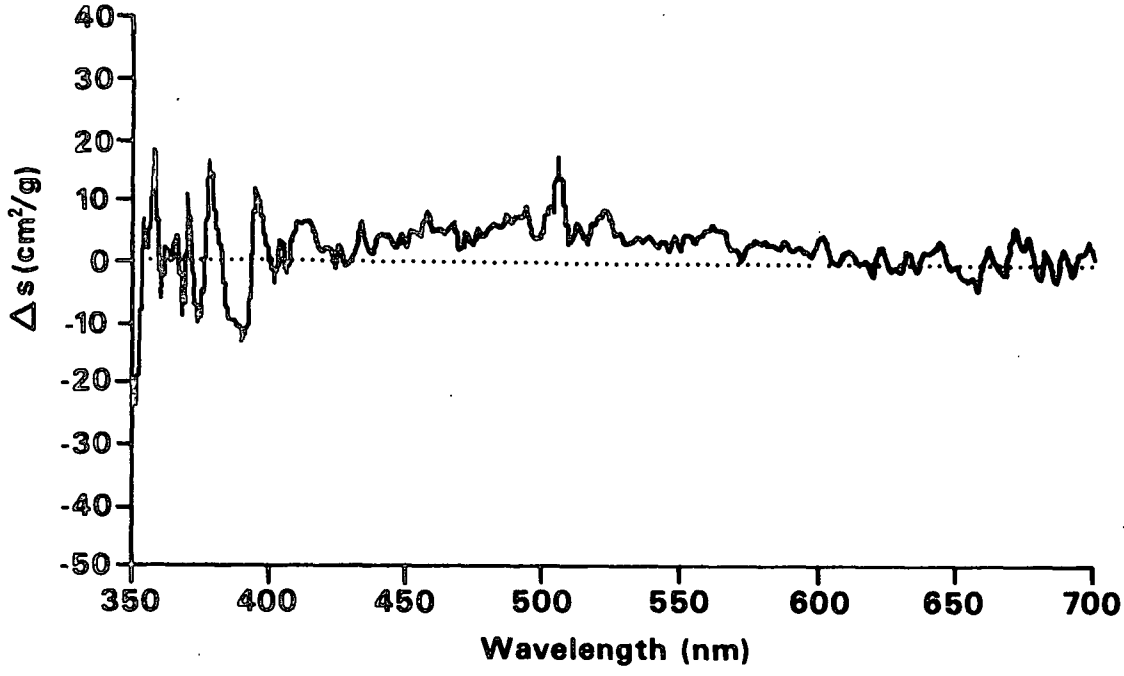

Figure 24. Δs_λ spectra obtained when the s_λ spectrum of an unirradiated pulp sheet was subtracted from the s_λ spectrum of the same pulp sheet after irradiation with 350 nm UV light (irradiation time = 90 min).

The areas thus determined were used, along with $\Delta k_{\lambda(max)}$, as measures of the overall rate of light induced yellowing.

It should be noted at this point that because yellowing is primarily a surface reaction,[121] the absorption coefficient throughout irradiated sheets is not a constant. Since one of the assumptions on which this theory is based is that the absorption and scattering coefficients are constant throughout the medium being examined, the use of the Δk_{λ} method of analysis described above was considered as somewhat limited. However, since the nature of the products generated during the yellowing process is not completely understood and since for a given sample the distribution of color products within the sheet should not change significantly with irradiation time (at least at short irradiation times), this method was considered to be the best method available at this time. It was also felt that the results obtained from such an analysis, while not quantitatively exact, would still be mechanistically useful.

The results obtained in these experiments are shown in Fig. 25 and 26. Figure 25 shows the plot obtained when the areas under the adsorption bands observed in the 350-700 nm range of the Δk_{λ} spectra were plotted as a function of the wavelength of the light incident upon the sheet, and Fig. 26 shows the plot obtained when $\Delta k_{\lambda(400\ nm)}$ [i.e., $\Delta k_{\lambda(max)}$] was plotted as a function of the wavelength of the light incident upon the sheet. The actual Δk_{λ} spectra from which these values were obtained are shown in Appendix IV. The values shown in Fig. 25 and 26 actually represent the average of four runs. Each run was in turn the computer average of five separate measurements. The average error in these values was 5-6%.

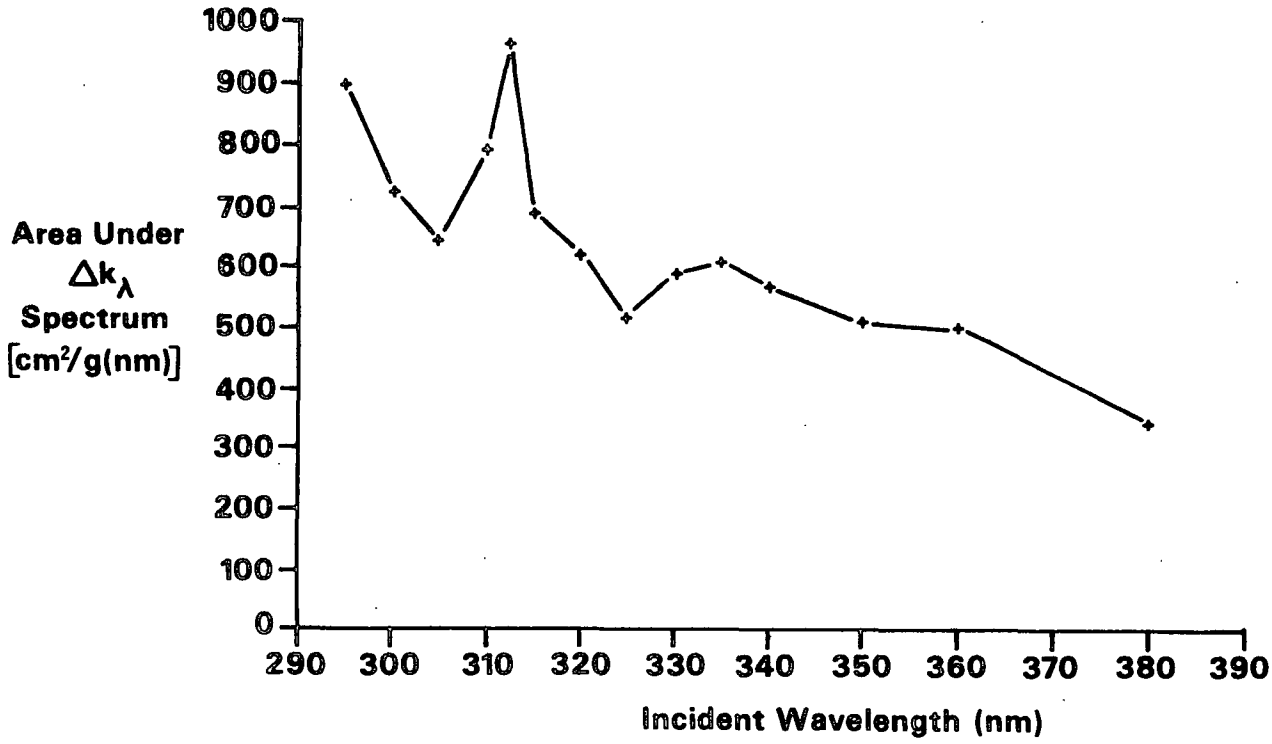

Figure 25. Plot obtained when the areas under the absorption bands observed in the Δk_λ curves of 290-390 nm irradiated pulp sheets were plotted as a function of the wavelength of the light incident upon the sample.

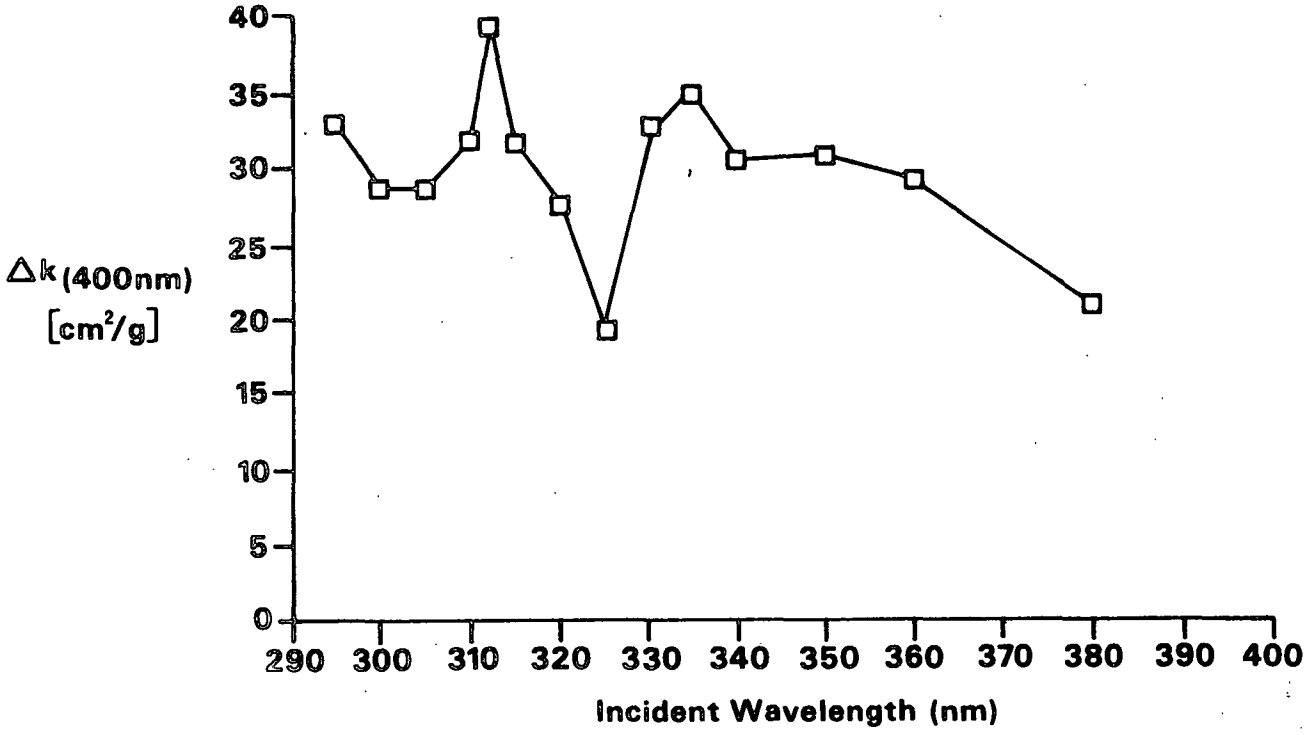

Figure 26. Plot obtained when $\Delta k_{\lambda(400\ nm)}$ [i.e., $\Delta k_{\lambda(max)}$] was plotted as a function of the wavelength of the light incident upon sample sheets.

The plots presented in Fig. 25 and 26 clearly show that while light of all wavelengths within the 290-390 nm range induces chromophore formation (i.e., induces yellowing), the total number of chromophores formed upon irradiation depends on the wavelength of the light incident upon the pulp sheet. Within the range examined, there are two distinct wavelength bands, one from approximately 310-315 nm and another from approximately 325-340 nm, where the rate of light induced yellowing is accelerated. The overall maximum rate of light induced yellowing, as measured by either the areas under the Δk curves obtained in these experiments or by the change in k_λ at 400 nm [i.e., $k_{\lambda(max)}$], occurs at an incident wavelength of 312.5 nm. Since the total number of photons absorbed by these samples was approximately the same for each wavelength examined, these results presented here also indicate that the yield of chromophores per quantum of absorbed energy is greatest at an incident wavelength of 312.5 nm.

From a mechanistic standpoint, the above results suggest that the first step in the light induced yellowing of this pulp is the absorption of light by specific chromophores in the pulp (i.e., those which absorb most strongly within the two bands noted above). The nature of these chromophores was not directly investigated, but a review of the literature indicated that these chromophores are most likely etherified and nonetherified guaiacyl structures containing carbonyl groups in the α position (λ_{max} = 280-320 nm and 330-350 nm, respectively).[57,122-124] It is also possible, however, that the chromophores absorbing in the 325-340 nm range are etherified and/or nonetherified coniferaldehyde type lignin structures (λ_{max} = 340-360 nm).[57,122-124]

Regardless of what types of chromophores absorb within these wavelength bands, the observation that there are two of them indicates that at least two distinct photochemical reactions are occurring. Both reactions ultimately

result in the formation of chromophores, but one reaction is initiated by an excited state species formed from chromophores which absorb in the 310-315 nm range of the spectrum and the second reaction is initiated by a reactive excited state species formed from chromophores which absorb in the 325-340 nm range. While it is only speculative, the fact that the Δk_λ spectra obtained in these experiments were qualitatively similar suggest that the overall reaction sequences initiated by these different excited state species may lead to the formation of the same reaction products.

Determination of the Rates of Sunlight and 312.5 nm UV Light Induced Yellowing

Using a modified version of the Δk_λ method described above, the rates of sunlight and 312.5 nm UV light induced yellowing were experimentally evaluated. The basis for using sunlight in these studies is that it is the light to which pulps are most commonly exposed. The use of 312.5 nm UV light was based on the results presented above (i.e., because the yield of chromophores per quantum of absorbed energy is greatest at this wavelength). In order to minimize any changes that could have occurred during the relatively long times required to obtain entire k_λ spectra, measurements of k_λ were made at three wavelengths within the 350-700 nm range only. In the sunlight studies, measurements of k_λ were made at 415, 457, and 520 nm, and in the 312.5 nm UV light studies measurements of k_λ were made at 400, 457, and 520 nm. These particular wavelengths were selected for use because they are the wavelengths around which $\Delta k_{\lambda(max)}$ occurred, TAPPI brightness is measured and ortho-quinonoid models absorb, respectively. As in the experiments described above, it was assumed in these experiments that the scattering properties of the sheet samples were not significantly changed by irradiation with sunlight of 312.5 nm UV light.

Determination of the Rate of Sunlight Induced Yellowing

When the k_λ coefficients of sample handsheets at 415, 457, and 520 nm were evaluated as a function of irradiation time, the results presented in Table 3 were obtained. The k_λ coefficients presented in Table 3 actually represent the average k_λ coefficients obtained from eight different sample sheets. Confidence intervals for these values were ± 1% at the 95% level.

Table 3. Measured k_λ at 415, 457, and 520 nm as a function of the time of irradiation with simulated sunlight.

Irradiation Time (hours)	k_λ (cm^2/g)[a] 415 nm	457 nm	520 nm
0.0	141.36	46.86	20.24
0.5	164.69	63.83	30.08
1.0	170.15	67.11	30.87
2.0	180.18	72.12	33.38
3.0	193.44	78.52	34.91
4.0	203.43	82.27	36.13
5.0	216.13	93.22	37.95
6.0	228.54	106.10	39.32
8.0	259.19	113.98	43.57
10.0	279.37	122.10	45.98
12.0	295.18	133.93	48.55
14.0	323.97	144.04	52.05

[a] s_λ values at 415, 457, and 520 nm were 404.35, 420.12, and 421.82 cm^2 g, respectively.

When simple zero kinetic analyses of the 415, 457, and 520 nm data were conducted, the plots shown in Fig. 27-29 were obtained. As these figures show, the

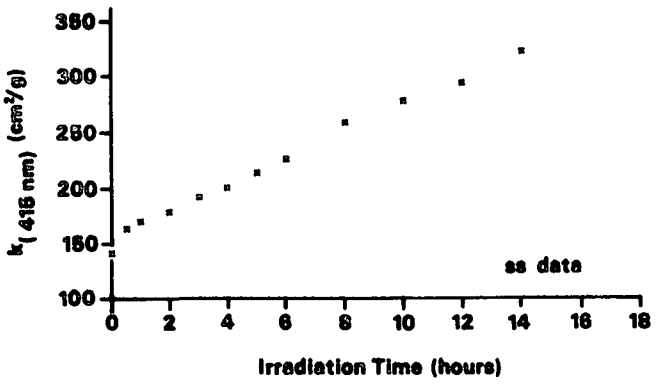

Figure 27. Simple zero order kinetics plot of $k_{(415\ nm)}$ solar simulator data.

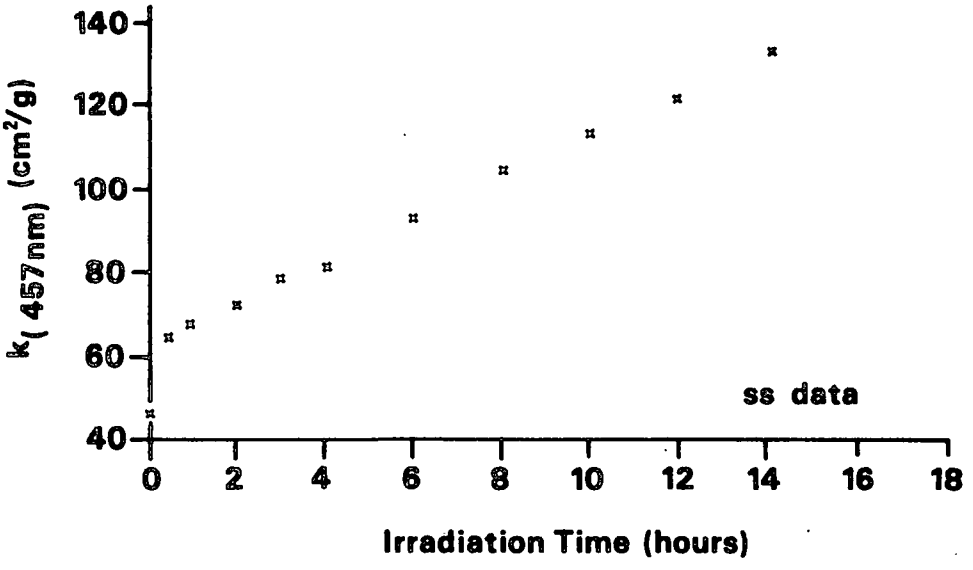

Figure 28. Simple zero order kinetics plot of $k_{(457\ nm)}$ solar simulator data.

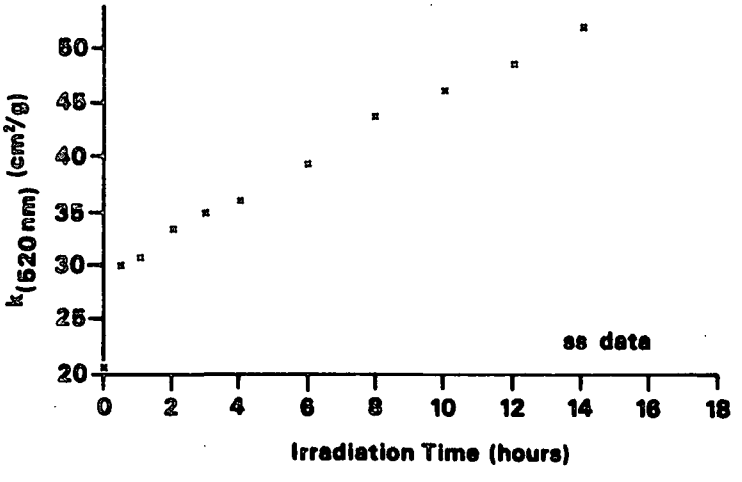

Figure 29. Simple zero order kinetics plot of $k_{(520\ nm)}$ solar simulator data.

rate of sunlight induced yellowing, as measured by k_λ at 415, 457, or 520 nm, appears to follow simple zero order kinetics in the range from 0.5 to 14 hours. In the range from 0 to 0.5 hour, however, the rate of yellowing, as measured by k_λ at 415, 457, or 520 nm, is very fast and deviates from the simple zero order kinetics followed in the later phase. Like the results presented above, this result suggests there are at least two reactions occurring during the yellowing process and that colored products are formed in both of these reactions. Consistent with the results of Whiting et al.,[125] the rate of color formation in at least one of these two reactions follow simple zero order kinetics. The rate of color formation in the second reaction is relatively fast and this reaction appears to be complete within the first 30 minutes of exposure. Thus, this reaction must involve highly reactive structures in the pulp. While it is only speculative, one possibility may be that these structures are coniferaldehyde type structures. Another possibility, which is consistent with the work of Castellan,[48] is that these structures are α-carbonyl β-O-4 and noncarbonyl α-O-4 type lignin structures. Even if it is one of these types of structures, the lack of kinetic data within the initial 30 minutes of irradiation limits making any firm conclusions about the specific reaction order.

An alternate explanation for the two phase kinetic behavior observed in Fig. 27-29 is a "topochemical" one. In other words, the initial (i.e., fast) phase of the kinetics plots shown in Fig. 27-29 result from light induced reactions of lignin structures located on the surface of light (and oxygen) exposed fibers. These light induced reactions lead to rapid yellowing of the fiber, and hence sheet surface. When these "surface" structures have photochemically reacted and the surface of the sheet has yellowed, the kinetics of the reaction start are no longer chemically controlled, but are instead controlled by the rate of diffusion of UV light (or possibly oxygen) into the interior of the fibers.

Determination of the Rate of 312.5 nm UV Light Induced Yellowing

Using the same method described above, the rate of 312.5 nm UV light induced yellowing was evaluated. As was noted earlier, the use of this particular wavelength of light was based on the finding that the yield of chromophores per quantum of absorbed energy is greatest at this wavelength. In order to further maximize chromophore formation, the incident flux of the 312.5 nm light used in these experiments, 4.54×10^{13} photons/cm^2sec, was close to the maximum achievable incident flux. On the basis of the solar simulator results, the time range studied in these experiments was from 0 to 4 hours (i.e., the time range needed to reach the linear portions of the kinetic plots).

The results obtained when the k_λ coefficients of sample handsheets at 400, 457, and 520 nm were determined as a function of irradiation time are presented in Table 4. As this table shows, the initial k_λ coefficients of these sheets at 457 and 520 nm were greater than those of the sheets used in the solar simulator experiments described above. The increase in these coefficients at these wavelengths was attributed to unavoidable reversion of the sheets during storage and was not considered a serious limitation.

Table 4. Measured k_λ at 400, 457, and 520 nm as a function of the time of irradiation with 312.5 nm UV light.

Irradiation Time (hours)	k_λ (cm^2/g)[a] 400 nm	457 nm	520 nm
0.0	249.33	55.84	26.46
0.5	272.72	57.68	27.75
1.0	278.63	59.77	28.34
1.5	283.99	61.11	28.82
2.0	287.51	61.75	29.37
3.0	293.35	64.50	30.32
4.0	300.54	66.36	31.13

[a] s_λ values at 400, 457, and 520 nm were 358.20, 420.12, and 421.82 cm^2 g, respectively.

When simple zero order kinetic analyses of the 400, 457, and 520 nm data were conducted, the plots presented in Fig. 30-32 were obtained. As in the analyses of the sunlight data, the rate of 312.5 nm UV light induced yellowing, as measured by k_λ at 400, 457, or 520 nm, appears to follow simple zero order kinetics in the range from 0.5 to 4 hours. In the range from 0 to 0.5 hour, the rate of 312.5 nm UV light induced yellowing is very fast and deviates from simple zero order kinetics. This finding again suggested that at least two reactions were occurring during the yellowing process or that there was a "topochemical" factor involved in the yellowing process. Thus, in the case of white spruce refiner mechanical pulp the kinetics of sunlight and 312.5 nm UV light induced yellowing appear to be qualitatively similar.

Determination of the Effect of Incident Light Flux on the Rate of 312.5 nm UV Light Induced Yellowing

The flux dependence of the rate of a photochemical reaction can help to establish whether a given reaction product is formed in a primary photochemical process (i.e., in a reaction directly involving an excited state molecule) or in a secondary reaction (i.e., in a dark reaction).[120] For instance, the rates of primary photochemical processes are proportional to the absorbed light intensity (I_a). This proportionality follows from the fact that only one quantum of light is absorbed to initiate a primary photochemical process. Rates of products formed in secondary reactions usually show some other than first-power dependence on I_a.[120] In this study, the effect of incident light flux on the relative rate of photoyellowing was examined using the k_λ method of analysis described above. Three additional incident light fluxes, 3.04×10^{13} photons/cm^2 sec (Flux B), 1.87×10^{13} photons/cm^2 sec (Flux C) and 9.60×10^{12} photons/cm^2 sec (Flux D), were examined (Flux A = 4.54×10^{13} photons/cm^2 sec).

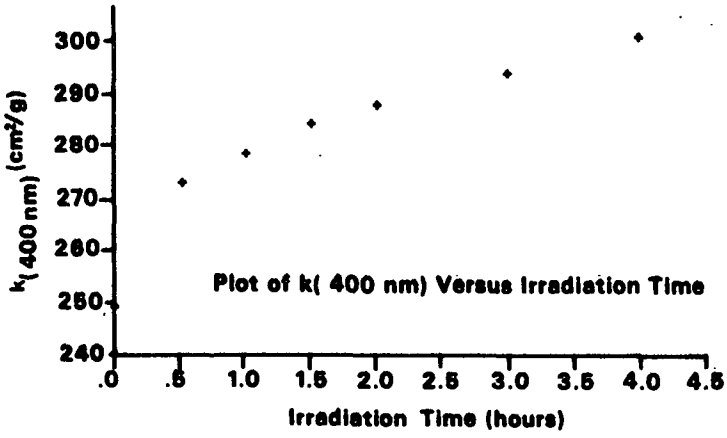

Figure 30. Simple zero order kinetics plot of $k_{(400\ nm)}$ 312.5 nm UV light data.

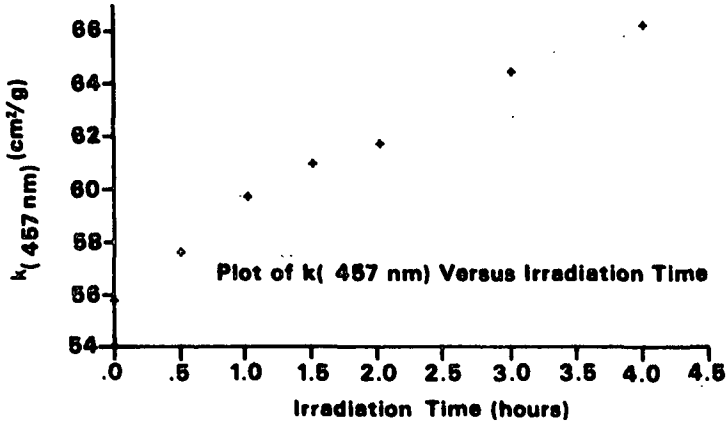

Figure 31. Simple zero order kinetics plot of $k_{(457\ nm)}$ 312.5 nm UV light data.

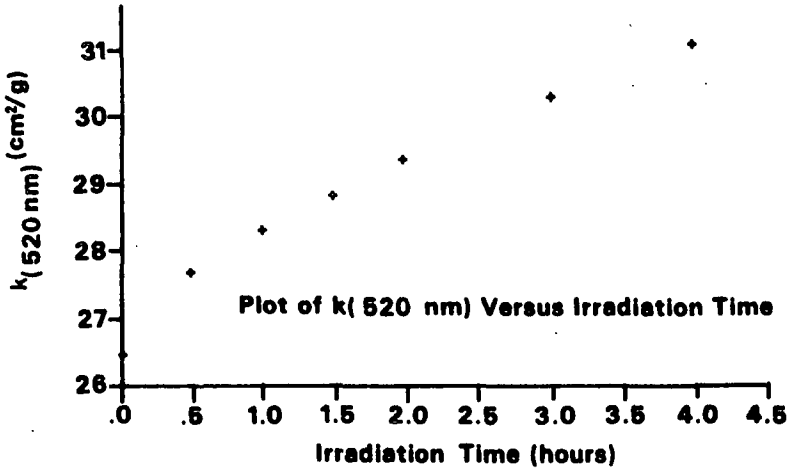

Figure 32. Simple zero order kinetics plot of $k_{(520\ nm)}$ 312.5 nm UV light data.

The results obtained in these experiments are presented graphically in Fig. 33-35. As these figures show, the kinetics of yellowing at the three additional incident light fluxes examined here were very similar to those described above (i.e., they appear to have two distinct phases). The rate of chromophore formation in the zero order phase of the yellowing reaction (i.e., in the range from 0.5 to 4 hours) was determined for each incident flux from the slopes of the linear portions of these curves (obtained by regression analysis), and the results of these determinations are presented in Table 5. The results presented in this table show that regardless of the measuring wavelength, the rate of photoinduced chromophore formation increased with increasing incident light flux. While it is only speculative, it also appeared that the rate of chromophore formation in the initial phase of the yellowing reaction (i.e., in the 0 to 0.5 hour range) increased with increasing incident light flux.

When the logarithms of these rates were plotted against the logarithms of the incident light flux the results shown in Fig. 36-38 were obtained. As these plots show, the rate of photoinduced chromophore formation at 400 nm was proportional to $[I_a]^{0.82}$, although the fit of these data was marginal (90% confidence interval = 0.36). The rate of photoinduced chromophore formation at 457 nm was proportional to $[I_a]^{0.76}$, and the fit of these data was quite good (90% confidence interval = 0.098). The rate of photoinduced chromophore formation at 520 nm was proportional to $[I_a]^{0.72}$, and the fit of these data was also quite good (90% confidence interval = 0.094). The rate constants obtained from the y-intercepts of these plots were 7.43×10^{-14} $(cm^4/g \cdot photon)^{0.82}$, 20.2×10^{-14} $(cm^4/g \cdot photon)^{0.76}$ and 40.2×10^{-14} $(cm^4/g \cdot photon)^{0.72}$ for the 400, 457, and 520 nm data, respectively. Thus, for the linear portion of the kinetics plots shown in Fig. 33-35 (i.e., in the 0.5-4.0 hours range), the rate of 312.5 nm UV light

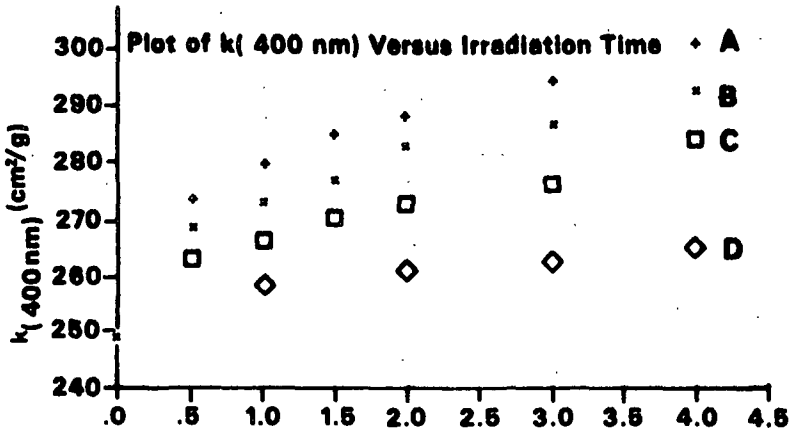

Figure 33. Simple zero order kinetics plots of $k_{(400\ nm)}$ 312.5 nm UV light data at various incident light fluxes.

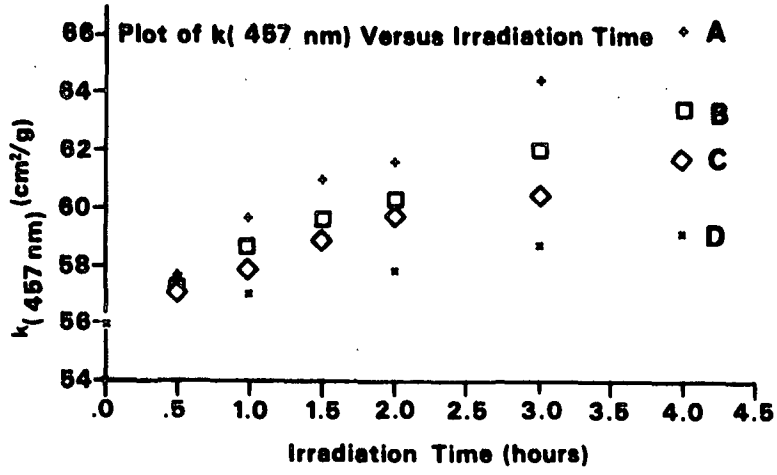

Figure 34. Simple zero order kinetics plots of $k_{(457\ nm)}$ 312.5 nm UV light data at various incident light fluxes.

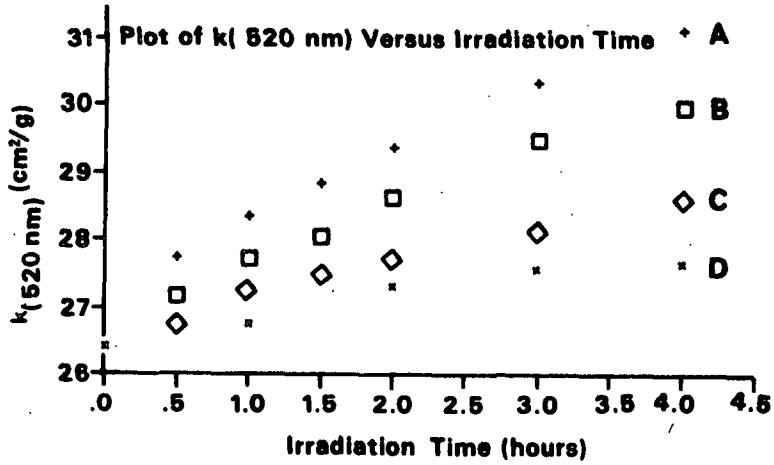

Figure 35. Simple zero order kinetics plots of $k_{(520\ nm)}$ 312.5 nm UV light data at various incident light fluxes.

induced chromophore formation at 400, 457, and 520 nm can be expressed as

$$dk_{(400\ nm)}/dt = 7.43 \times 10^{-14}\ [I_a]^{0.82}$$

$$dk_{(457\ nm)}/dt = 2.02 \times 10^{-13}\ [I_a]^{0.76}$$

$$dk_{(520\ nm)}/dt = 4.02 \times 10^{-13}\ [I_a]^{0.72}$$

where the units on the rate constants are as given above.

Table 5. Rates of photoinduced color formation, dk_λ/dt, at 400, 457, and 520 nm evaluated from the linear portion of the curves shown in Fig. 33-35.

Incident Light Flux (photons/cm^2 sec)	k_λ/dt (cm^2/g hour)[a] 400 nm	457 nm	520 nm
9.60×10^{12}	2.11	0.72	0.33
1.87×10^{13}	5.67	1.32	0.51
3.04×10^{13}	6.66	1.67	0.81
4.54×10^{13}	7.62	2.40	0.96

[a]Obtained from regression analysis of linear portion of curves.

CHEMICAL STUDY OF IRRADIATED WHITE SPRUCE REFINER GROUNDWOOD PULP

If the reaction mechanisms described in the beginning section of this paper are correct, then at least part of the "yellow" color of irradiated white spruce pulp results directly, and/or indirectly, from the UV light induced formation of quinonoid lignin structures. Alternatively, if the light induced formation of such groups could be demonstrated, then this would indicate that the proposed reaction mechanisms presented earlier are possible.

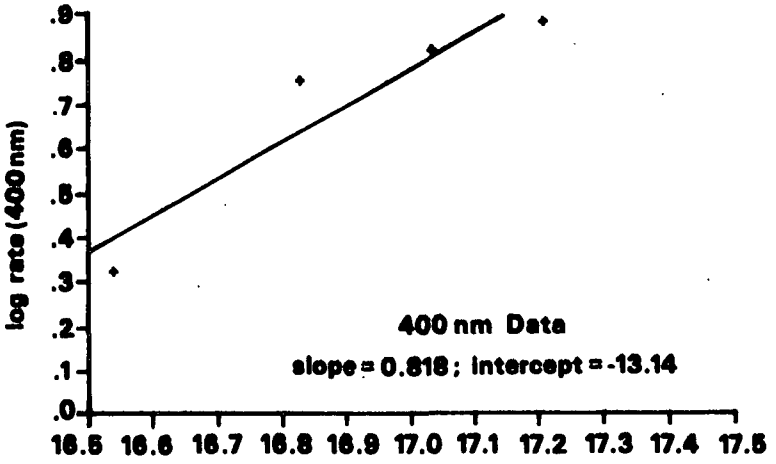

Figure 36. Plot of logarithm of rate at 400 nm versus logarithm of incident light flux.

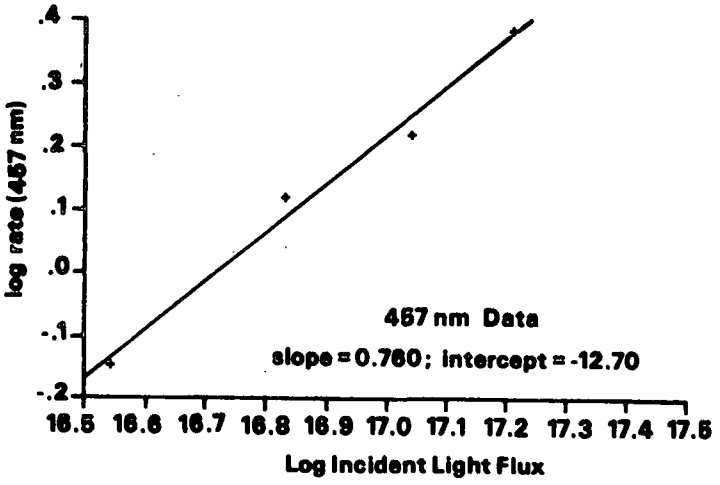

Figure 37. Plot of logarithm of rate at 457 nm versus logarithm of incident light flux.

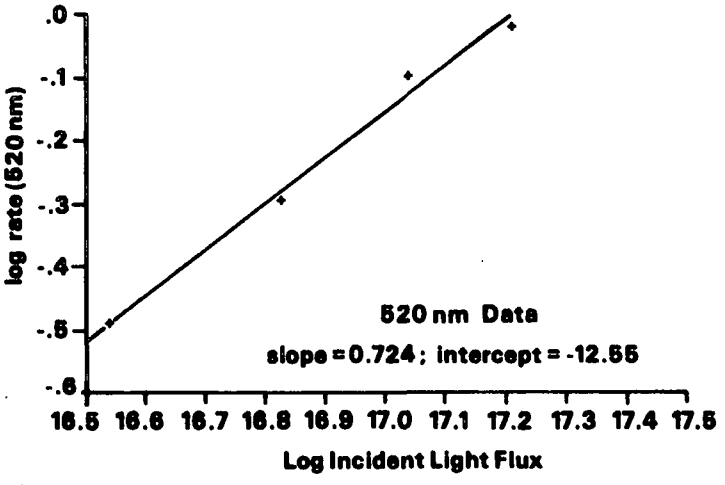

Figure 38. Plot of logarithm of rate at 520 nm versus logarithm of incident light flux.

In this study described below, the UV light induced formation of quinonoid lignin structures was studied using a number of spectroscopic methods including diffuse reflectance UV-visible, diffuse reflectance FTIR, Raman and ^{31}P NMR spectroscopy. The results of these studies were then compared to the results obtained in similar analyses of four quinone model compounds and one ortho-quinone enhanced pulp. The reactions of irradiated pulp with gaseous sulfur dioxide, aqueous sulfur dioxide, aqueous sodium dithionite, and trimethyl phosphite were also studied, and the results of these studies were compared to those obtained in similar studies of the model quinonoid systems.

Selection of Model Quinonoid Systems

The following ortho- and para-quinonoid model compounds were selected for use in this study: 3-methoxy-ortho-benzoquinone (I), 2-methoxy-para-benzoquinone (II), 3,5-di-tert-butyl-ortho-benzoquinone (III), and 2,6-di-tert-butyl-para-benzoquinone (IV). The first two of these models were selected because of their similarity to the quinonoid structures expected to be present in irradiated pulp (Fig. 7). The latter two were selected because they should provide information about the effects of substituents.

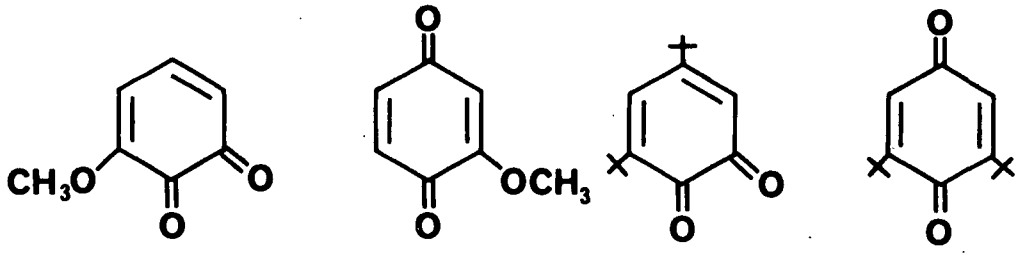

I II III IV

The use of the 3-methoxy-ortho-benzoquinone model rather than an unsubstituted ortho-benzoquinone model was based on the relative instability of ortho-benzoquinone and on the fact that it appeared that there was no significant loss of methoxyl groups during the yellowing of the experimental white spruce pulp

(Table 6). Thus, at least some of the ortho-quinonoid lignin structures formed during the photoinduced yellowing of this pulp could be of the 3-methoxy type. These results also suggest that the light induced demethoxylation of lignin observed by Leary[16-17] may have resulted from exposure to UV light present in the output from the 2 kW carbon arc lamp used by Leary but not present in the simulated sunlight used here (i.e., UV light in the 200-290 nm wavelength range).

Table 6. Methoxyl contents of unirradiated, sunlight irradiated and 312.5 nm UV light irradiated white spruce pulps.

Sample	Incident Light Flux or Lamp Output[a]	Irradiation Time (hours)	Methoxyl Content (%)
Unirradiated pulp	--	--	5.07
Sunlight irradiated pulp	990	20	5.22
312.5 nm irradiated pulp-1	4.60×10^{13}	36	4.93
312.5 nm irradiated pulp-1	5.09×10^{13}	48	5.05

[a]Lamp output in watts and incident light flux in photons/cm^2 sec for sunlight irradiated and 312.5 nm irradiated pulps, respectively.

In addition to the above model compounds, an ortho-quinone enhanced pulp was also used in this study. This pulp was prepared by oxidation with Fremy's salt, potassium nitroso-disulfonate. As noted earlier, this reagent has been shown to selectively oxidize uncondensed phenolic groups in the lignin present in high yield pulps to stable 3-methoxy-ortho-quinonoid lignin structures.[19-23] Because the ortho-quinonoid structures generated in this reaction are actually part of the lignin macromolecule, it was felt that this pulp would be an ideal system for studying the properties and reactivity of such structures in situ.

Diffuse Reflectance UV-Visible Spectroscopic Analysis of Model Quinones

Because of the "solid" nature of pulp materials, the analysis of the UV-visible absorption properties of such materials using conventional absorption spectroscopy is not practical. However, one method which is of great use in the study of solid materials is diffuse reflectance spectroscopy. In this type of spectroscopy, both UV-visible and FTIR, the amount of light reflected from a given solid sample is measured. From these measurements, information about the absorption properties of solid samples can then be derived.

When this method of UV-visible analysis was used to study sheet samples impregnated with the quinone models shown above, some useful information about the absorption properties of these models was obtained. More information was obtained, however, when the reflectance spectrum of an untreated sheet was subtracted from these spectra (Fig. 39 and 40). As Fig. 39 shows, the ΔR_∞ spectra for the impregnation of white spruce sheets with the para-quinone models II and IV each had a single "absorption" band. The wavelength minima of the bands of model II and IV occurred at 430 and 470 nm, respectively. The use of quotes in referring to these absorption bands is based on the fact that the spectra presented in Fig. 39 and 40 were quite different from the true absorption bands of these models in solution (Appendix V). For instance, the wavelength maximum of the π-π^* band of model II, in solution, occurred at approximately 355 nm. The wavelength maximum of the band observed in Fig. 39 occurred at a significantly longer wavelength, approximately 430 nm. In the case of model IV, two absorption bands, a π-π^* band [$\lambda_{(max)} < 350$ nm] and a "forbidden" n-π^* band [$\lambda_{(max)}$ approximately 445 nm], were observed in solution. A single "absorption" band, however, was observed in Fig. 40, and the wavelength maximum of this band occurred at approximately 470 nm.

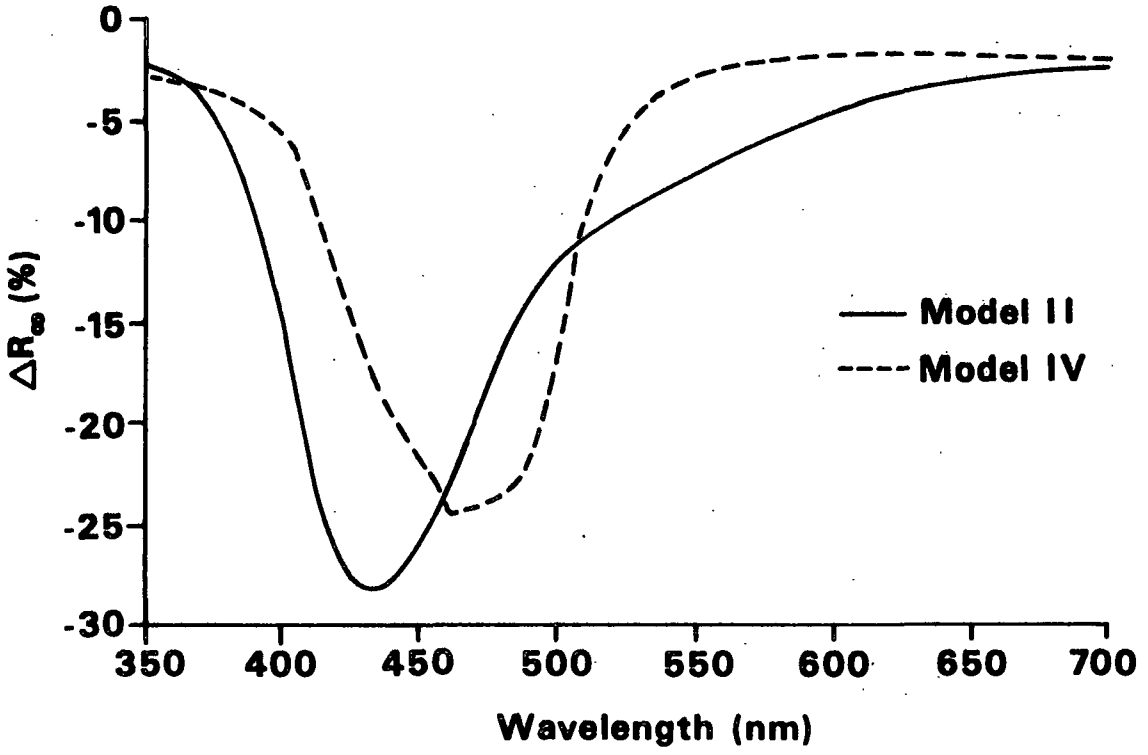

Figure 39. ΔR_∞ spectra obtained upon impregnation of white spruce RMP sheets with the para-quinone models II and IV.

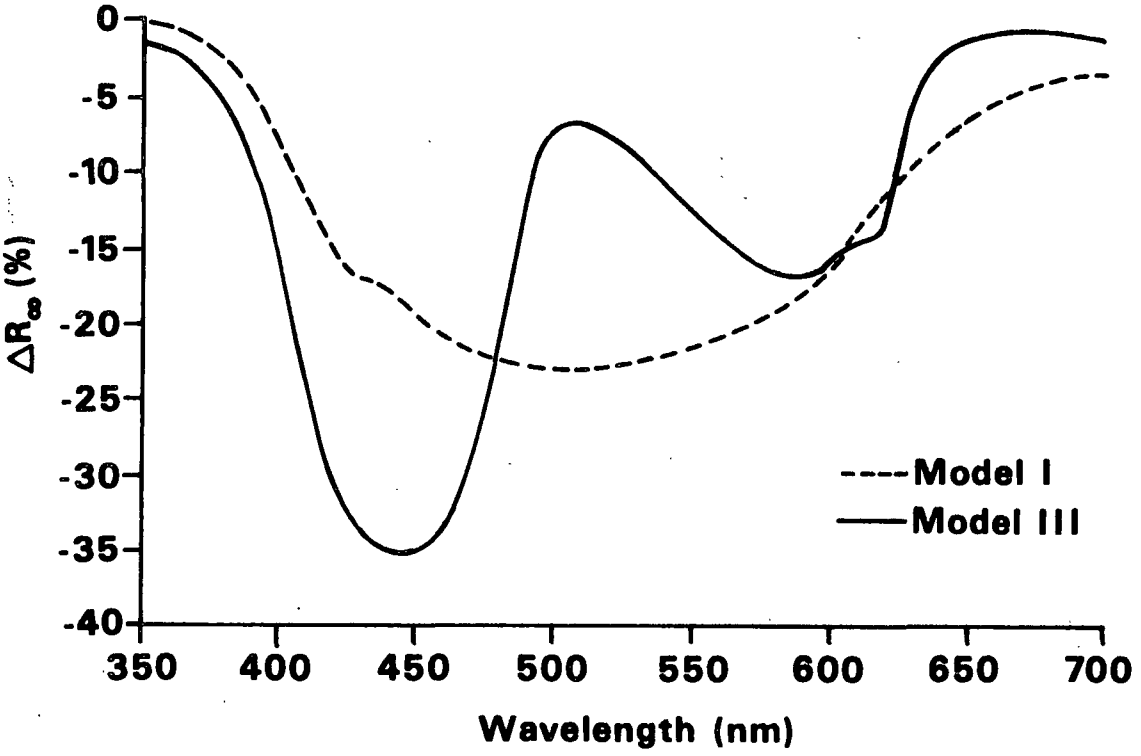

Figure 40. ΔR_∞ spectra obtained upon impregnation of white spruce RMP sheets with the ortho-quinone models I and III.

Significant differences were also observed between the ΔR_∞ and solution spectra of the ortho-quinone models I and III. For instance, model III, in solution, had two absorption bands; an intense $\pi-\pi^*$ band [$\lambda_{(max)}$ approximately 400 nm] and a weak $n-\pi^*$ band [$\lambda_{(max)}$ approximately 560 nm]. The ΔR_∞ spectra obtained for the impregnation of this model also had two "absorption" bands, but the wavelength maxima of these bands occurred at significantly longer wavelengths than those observed in solution ($\pi-\pi^*$ at approximately 445 nm and $n-\pi^*$ at approximately 590 nm). The intensities of the $\pi-\pi^*$ and $n-\pi^*$ bands in these spectra were also different.

In the case of model I, its solution spectrum had a broad $\pi-\pi^*$ band in the UV and this band had a strong shoulder in the visible region of the spectrum which was attributed to a partially hidden $n-\pi^*$ band. The wavelength maximum of the $\pi-\pi^*$ band occurred at approximately 360 nm. In comparison, the ΔR_∞ spectrum for the impregnation of this model had a single broad "absorption" band which had a wavelength maximum at approximately 520 nm.

Using Kubelka-Munk theory, the $(1/s)_\lambda$ spectra of the above sheets were prepared, and $\Delta(k/s)_\lambda$ spectra were calculated (Fig. 41 and 42). Assuming that the impregnation process did not change the scattering properties of these sheets, these $\Delta(k/s)_\lambda$ spectra should more closely approximate the true absorption spectra of these models as solids. As Fig. 41 shows, the $\Delta(k/s)_\lambda$ spectra for the impregnation of the para-quinone models II and IV had one and two absorption bands, respectively. The wavelength maximum of the absorption band of model II occurred at approximately 380 nm, and this band had a tail which extended into visible range. In the case of model IV, the wavelength maxima of the two observed absorption bands were approximately 350 nm (strong) and 460 nm (weak).

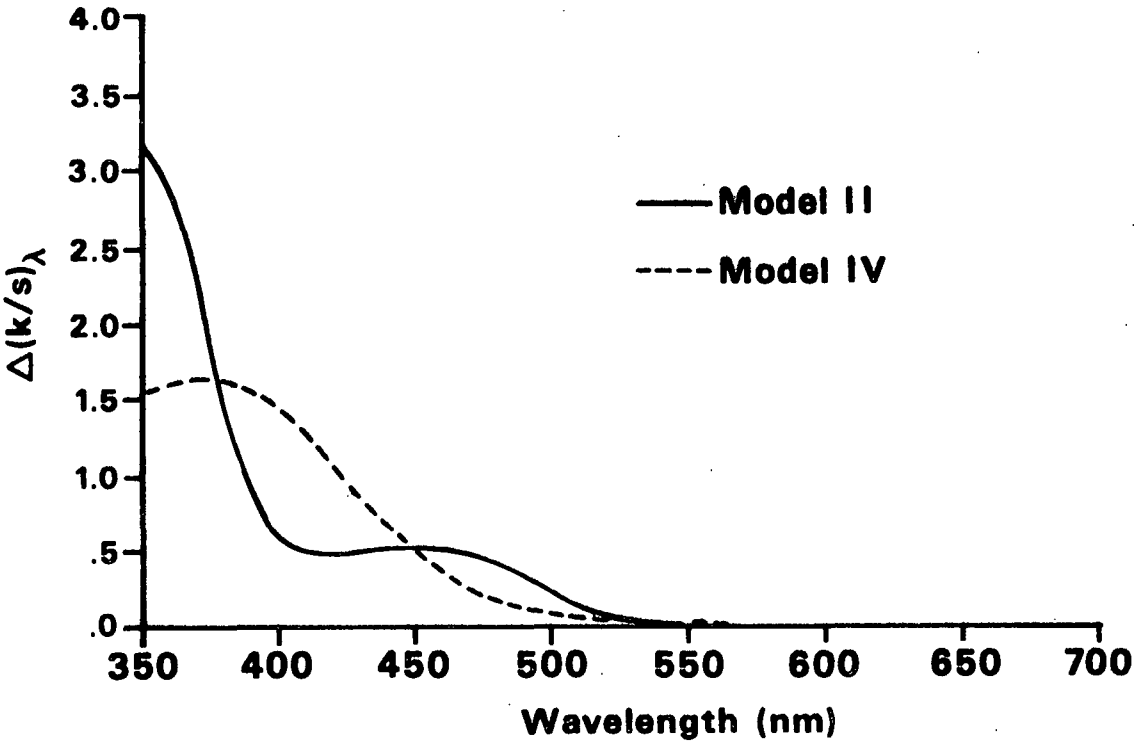

Figure 41. $\Delta(k/s)_\lambda$ spectra obtained upon impregnation of white spruce RMP sheets with the para-quinone models II and IV.

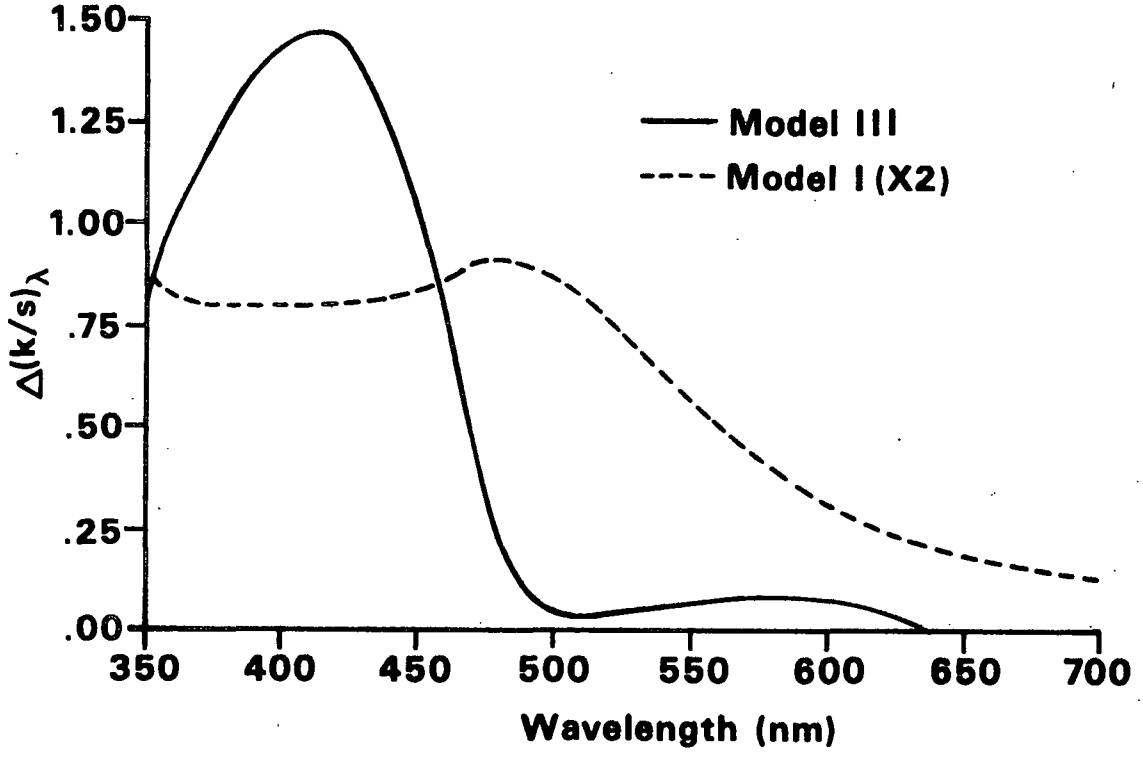

Figure 42. $\Delta(k/s)_\lambda$ spectra obtained upon impregnation of white sprue RMP sheets with the ortho-quinone models I and III.

Thus, with the exception of a slight red shift in wavelength maxima, the $\Delta(k/s)_\lambda$ spectra for the impregnation of these models, as expected, were similar to their corresponding solution spectra. On the basis of this result, the absorption band observed in the $\Delta(k/s)_\lambda$ spectra for the impregnation of model III was attributed to a $\pi-\pi^*$ electronic transition in the solid state and the absorption bands observed in the $\Delta(k/s)_\lambda$ spectrum for the impregnation of model IV were attributed to $\pi-\pi^*$ and $n-\pi^*$ electronic transitions in the solid state.

The $\Delta(k/s)_\lambda$ spectra for the impregnation of the ortho-quinone models I and III had one and two absorption bands, respectively. The wavelength maxima of the absorption bands of model III occurred at approximately 410 nm (strong) and 590 nm (weak). On the basis of the solution spectrum of this model, these absorption bands were attributed to $\pi-\pi^*$ and $n-\pi^*$ electron transitions in the solid state. The wavelength maxima of the broad absorption band of model I occurred at approximately 490 nm, and this band had a tail which extended into the far visible region of the spectrum. For reasons which were not clear, the $\Delta(k/s)_\lambda$ spectrum for the impregnation of this model was different from its solution spectrum. One possible reason for the difference observed in its solution and solid state spectra may have been charge-transfer interactions.[57,126] Such interactions can have significant effects on the intensity and wavelength maxima of both the $\pi-\pi^*$ and $n-\pi^*$ absorption bands of quinones.

Overall, the results presented above indicate that, with the exception of model I, the absorption spectra of the quinone model compounds, in solution, were quite similar to their corresponding solid state $\Delta(k/s)_\lambda$ spectra. In all cases, however, the wavelength maximum of both the $\pi-\pi^*$ and the $n-\pi^*$ absorption bands of these models occurred at longer wavelengths in the solid state than in solution. It should be noted, however, that the position and intensity of the

absorption bands of quinones, in general, are solvent dependent. In this case, the above conclusion is based on solution spectra obtained in methanol.

Diffuse Reflectance UV-Visible Spectroscopic Analysis of Pulp Oxidized with Fremy's Salt

When the ortho-quinone enhanced pulp prepared by oxidation of white spruce RMP with Fremy's salt was analyzed by diffuse reflectance UV-visible spectroscopy, the ΔR_∞ spectrum obtained was qualitatively similar to the ΔR_∞ spectrum of the pulp sheet upon impregnation with 3-methoxy-ortho-benzoquinone (Fig. 43). The $\Delta(k/s)_\lambda$ spectrum for the Fremy's salt oxidation of this pulp was also very similar to the $\Delta(k/s)_\lambda$ spectrum obtained from the impregnated pulp sheet (Fig. 44). On the basis of the results presented above, the absorption band observed in Fig. 44 was attributed to π-π^* transitions in the ortho-quinonoid lignin structures formed in this pulp during oxidation with Fremy's salt.

Diffuse Reflectance Fourier Transform Infrared Analysis of Quinone Model Systems

Further evidence for the formation of ortho-quinonoid lignin structures in pulp oxidized with Fremy's salt was obtained using diffuse reflectance Fourier transform infrared (FTIR) spectroscopy. As stated earlier, model quinones, quinones in isolated kraft lignins and quinones in groundwood pulps have all been shown to exhibit absorption bands in the 1656-1690 cm^{-1} region of the infrared spectrum.[10,11,53-58] The diffuse reflectance FTIR spectrum of the quinone models used in this study had strong absorption bands at 1662 cm^{-1} (I), 1664 cm^{-1} (II), 1650 cm^{-1} (III) and 1650 cm^{-1} (IV). The 1650 cm^{-1} bands of the latter two models were broad and had strong shoulders around 1660 cm^{-1}.

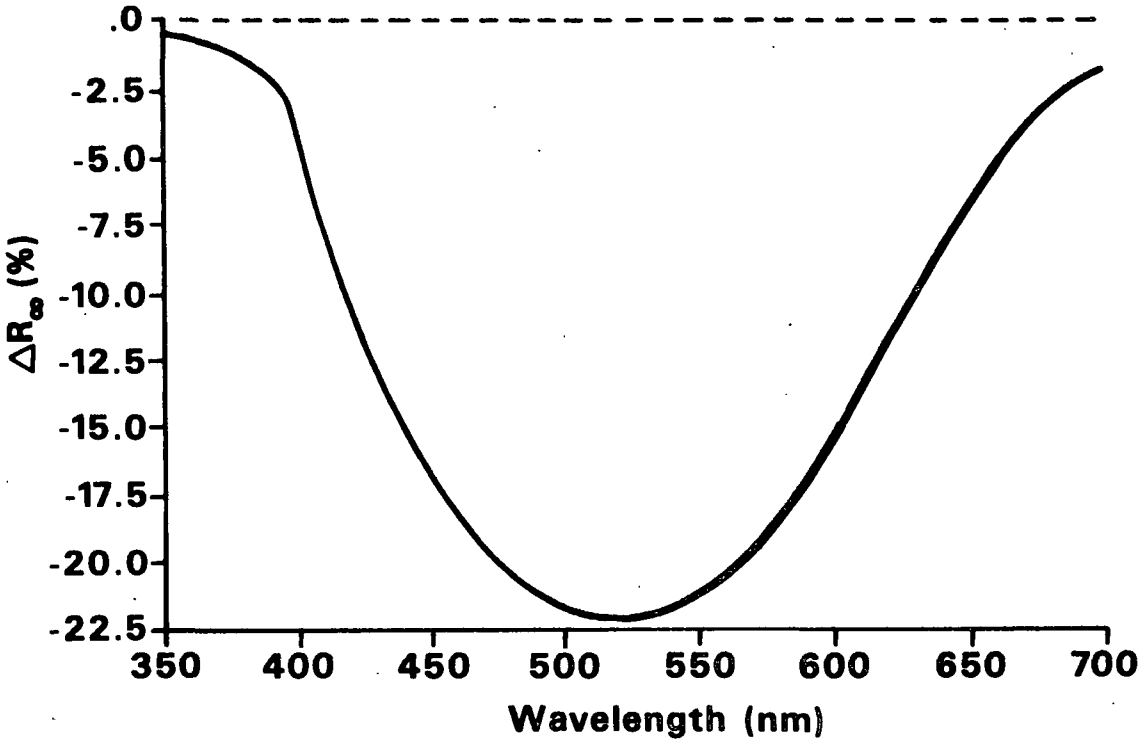

Figure 43. ΔR_∞ spectrum obtained upon oxidation of white spruce refiner mechanical pulp with Fremy's salt.

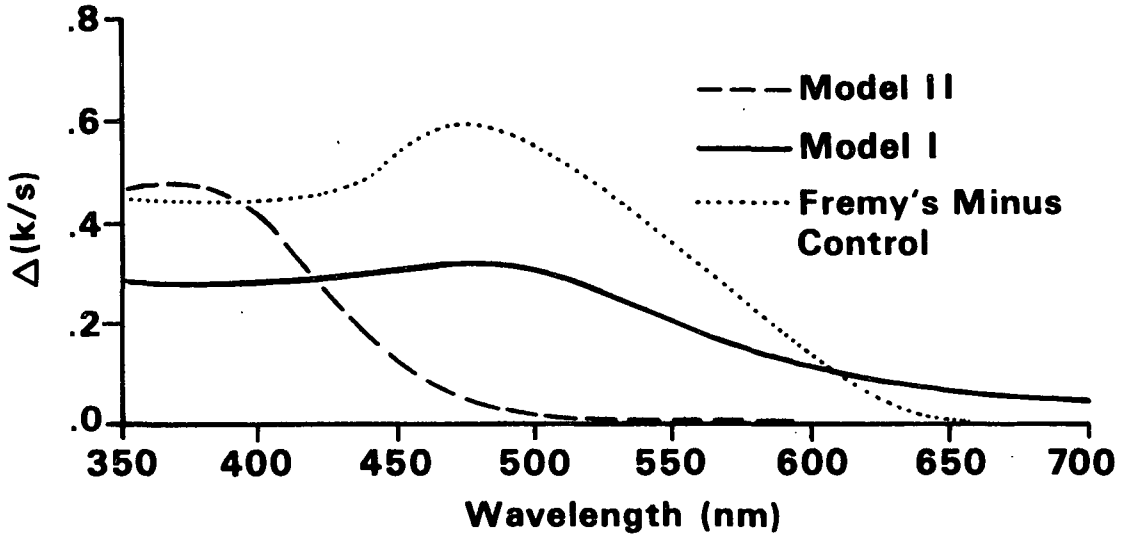

Figure 44. $\Delta(k/s)_\lambda$ spectra obtained upon oxidation of white spruce refiner mechanical pulp with Fremy's salt and upon impregnation of white spruce sheet samples with the quinone models I and II (II x 1/3).

When the Fremy's salt pulp was analyzed, its diffuse reflectance FTIR spectrum had a sharp absorption band at 1665 cm^{-1}. When the diffuse reflectance FTIR spectrum of a white spruce holocellulose (Klason lignin approximately 1.5%) was subtracted from this spectrum, this 1665 cm^{-1} band did not disappear (Fig. 45). This result clearly showed that the absorption band observed at 1665 cm^{-1} was associated with the lignin component of the Fremy's salt pulp. Because untreated white spruce pulp has been shown to have some absorbance in this region,[10,11] it could only be tentatively concluded here that this absorbance was due entirely to the ortho-quinonoid lignin structures formed when the pulp was oxidized with Fremy's salt. While more will be said about this point later, it should be stated here that the strong absorbance of this sample in the 1665 cm^{-1} region of the spectrum was considered to be consistent with the formation of such structures.

Raman Spectroscopic Analysis of Model Quinone Systems

Even further support for the formation of ortho-quinonoid lignin structures in pulp oxidized with Fremy's salt was obtained using Raman spectroscopy. Figure 46 shows the Raman spectra of quinone models I, II, III, and IV in solution in the region from 1500-1800 cm^{-1}. As this figure shows, the two ortho-quinone models, I and III, had strong C=C stretching bands at about 1560 cm^{-1} and weak C=O stretching bands at approximately 1670 cm^{-1}. The two para-quinone models, II and IV had weak C=C stretching bands at approximately 1560 cm^{-1} and strong C=O stretching bands at approximately 1670 cm^{-1}. When sheets impregnated with fairly high amounts of models I or II were analyzed, they gave the Raman spectra shown in Fig. 47(I) and 48(I). For comparison purposes, the Raman spectrum of an untreated pulp sheet was also obtained [Fig. 47(II) and 48(II)].

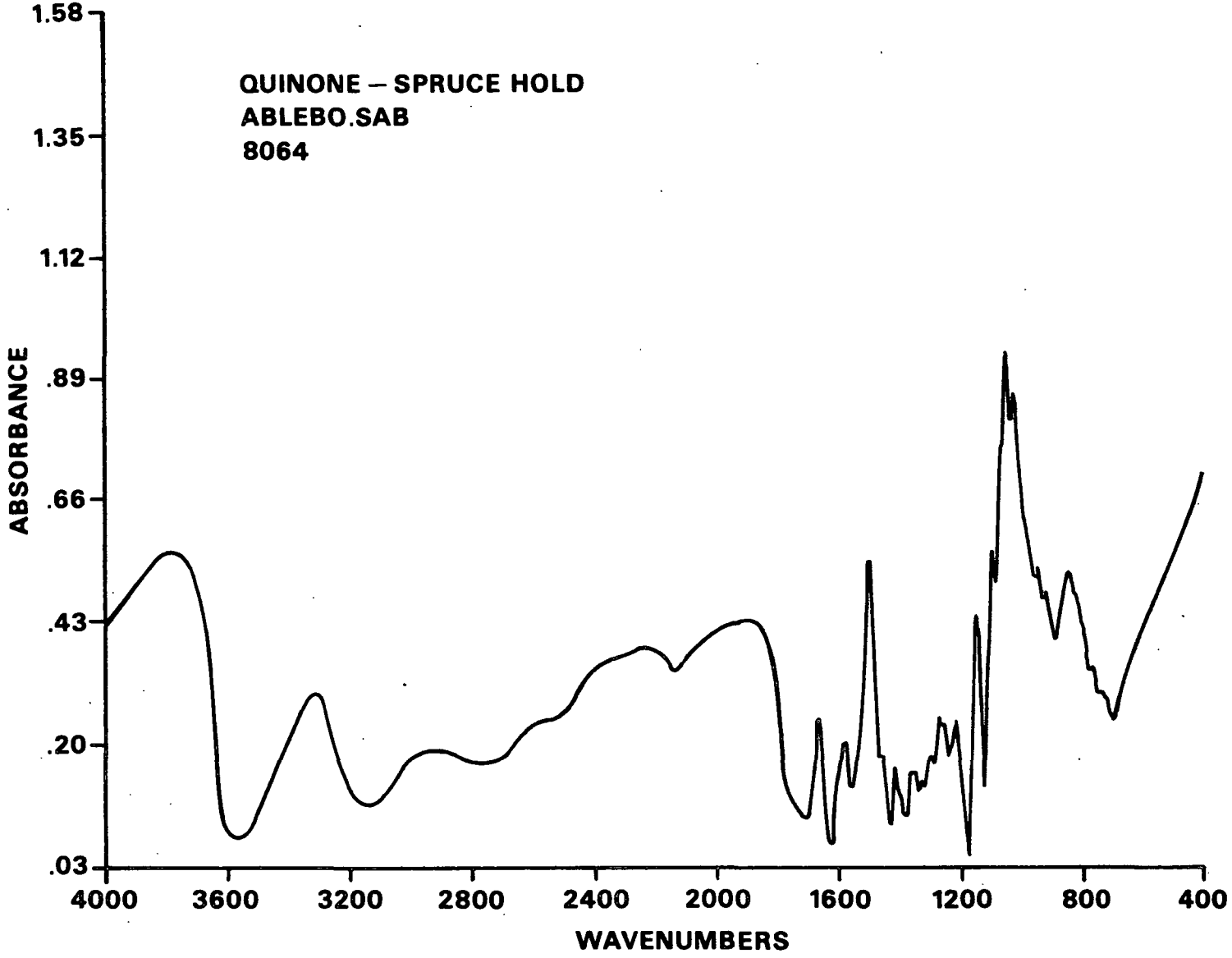

Figure 45. Difference spectrum obtained by subtracting the diffuse reflectance FTIR spectrum of a white spruce holocellulose from the diffuse reflectance FTIR spectrum of white spruce pulp oxidized with Fremy's salt (original spectra shown in Appendix VII).

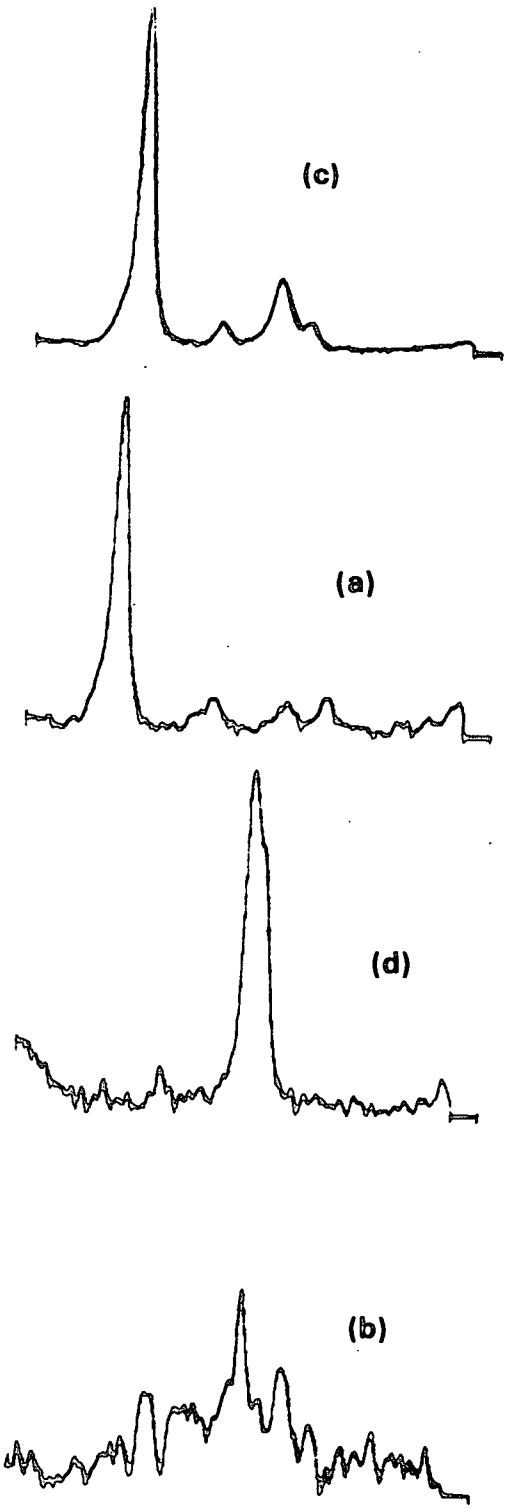

Figure 46. Raman spectra of quinone models I(a), II(b), III(c) and IV(d) in solution (models I, III, and IV in dichloromethane; model II in benzene with benzene subtracted out). Range = 1500 cm^{-1} and 1800 cm^{-1}.

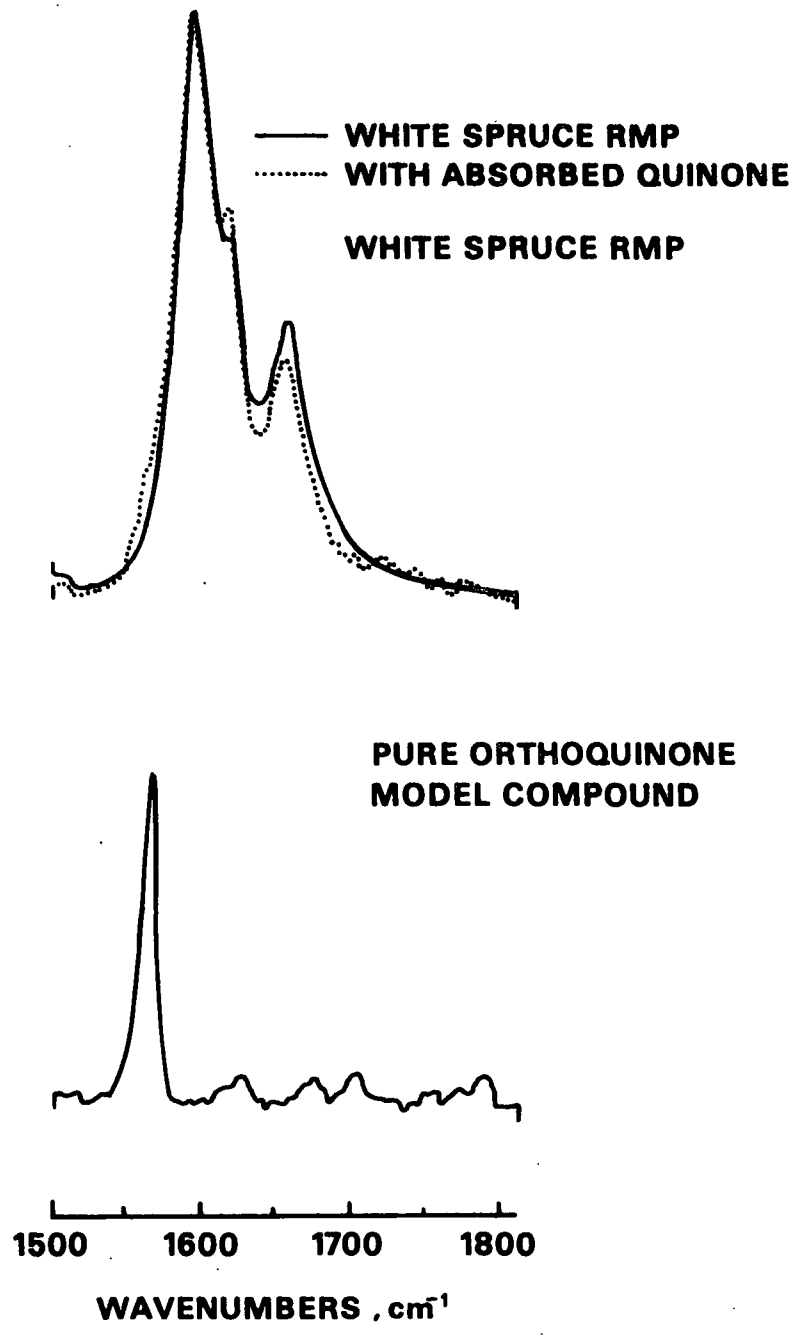

Figure 47. Raman spectra of a sheet formed from white spruce RMP and of a sheet formed from white spruce RMP sheet and impregnated with 3-methoxy-ortho-quinone (lower spectrum is model I).

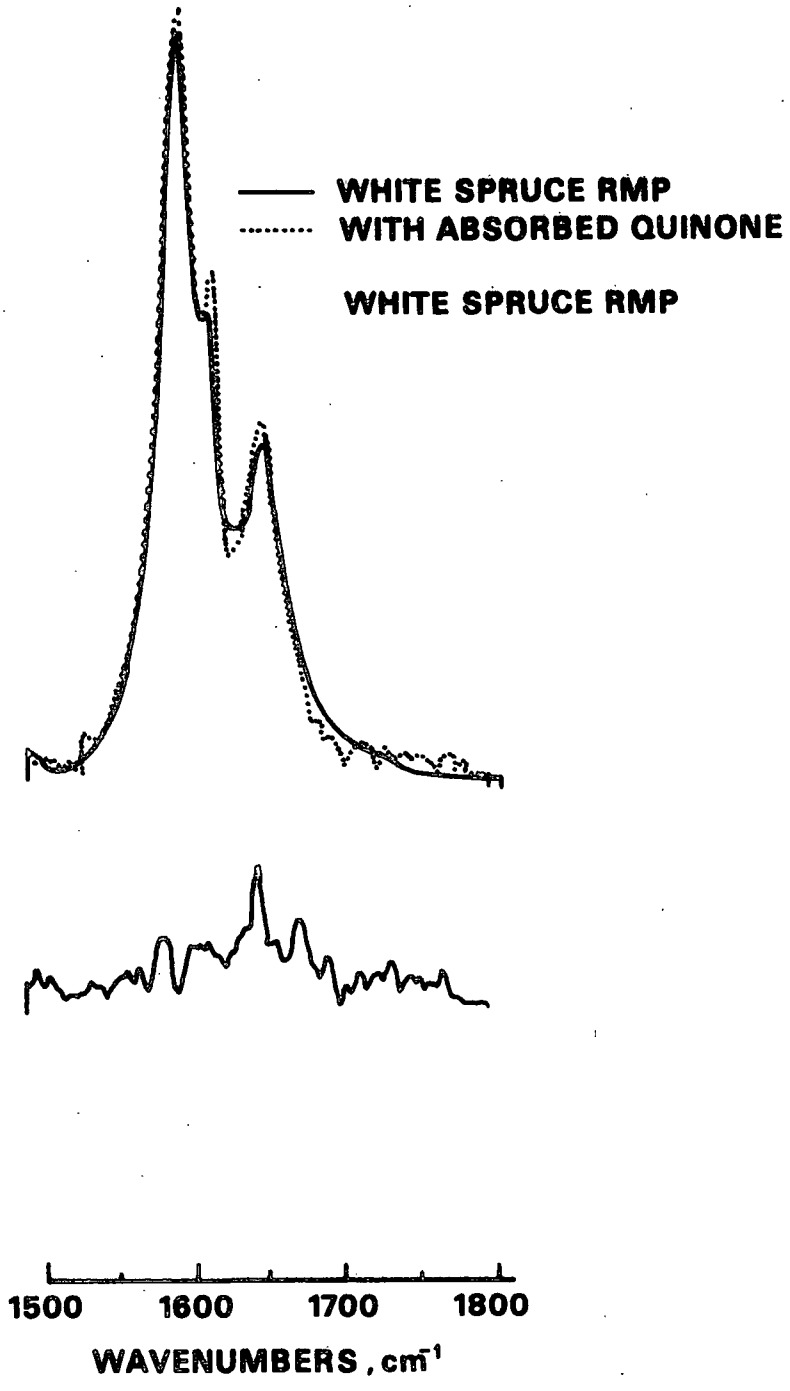

Figure 48. Raman spectra of a sheet formed from white spruce RMP and of a sheet formed from white spruce RMP and impregnated with 2-methoxy-para-quinone (lower spectrum is model II).

As Fig. 47 shows, the spectrum of the pulp impregnated with model I had an observable shoulder in the 1560-1570 cm^{-1} range. This is the range in which the C=C stretching bands of the ortho-quinone models occurred in solution. However, no evidence of any C=O stretching band could be seen. The spectrum of the pulp sheet impregnated with model III showed little change (Fig. 48). On the basis of these results, it appears that, even at relatively high concentrations, the C=C stretching band of ortho-quinone type structures is the only band which, in the presence of pulp, is strong enough to be detected by Raman. Thus, it is unlikely that this method could be used for para-quinones, but if ortho-quinonoid lignin structures are formed in the Fremy's salt pulp, then the Raman spectrum of this pulp should also have an observable shoulder in the 1550-1570 cm^{-1} region of the spectrum.

When the pulp oxidized with Fremy's salt was analyzed by Raman spectroscopy, it gave, as expected, a spectrum with an observable shoulder in the 1550-1570 cm^{-1} region (Fig. 49). A second shoulder was also observed in the 1780-1800 cm^{-1} range. On the basis of the results described above, the appearance of the prominent shoulder in the 1550-1570 cm^{-1} range was attributed to the C=C stretching band of the ortho-quinonoid lignin structures formed in this pulp during oxidation. The nature of the second shoulder was not clear. It could possibly be due to some type of C=O stretching activity.

It should also be noted that a visible light induced bleaching of the Fremy's salt sheet occurred during its analyses. A similar bleaching effect was also observed when the sheet sample impregnated with 3-methoxy-1,2-benzoquinone was analyzed. The extent of the bleaching, however, was not as great. This type of light induced bleaching has been observed before[17,49,127,128] and is not uncharacteristic of quinones.[49-52] Because of this, short analysis times and

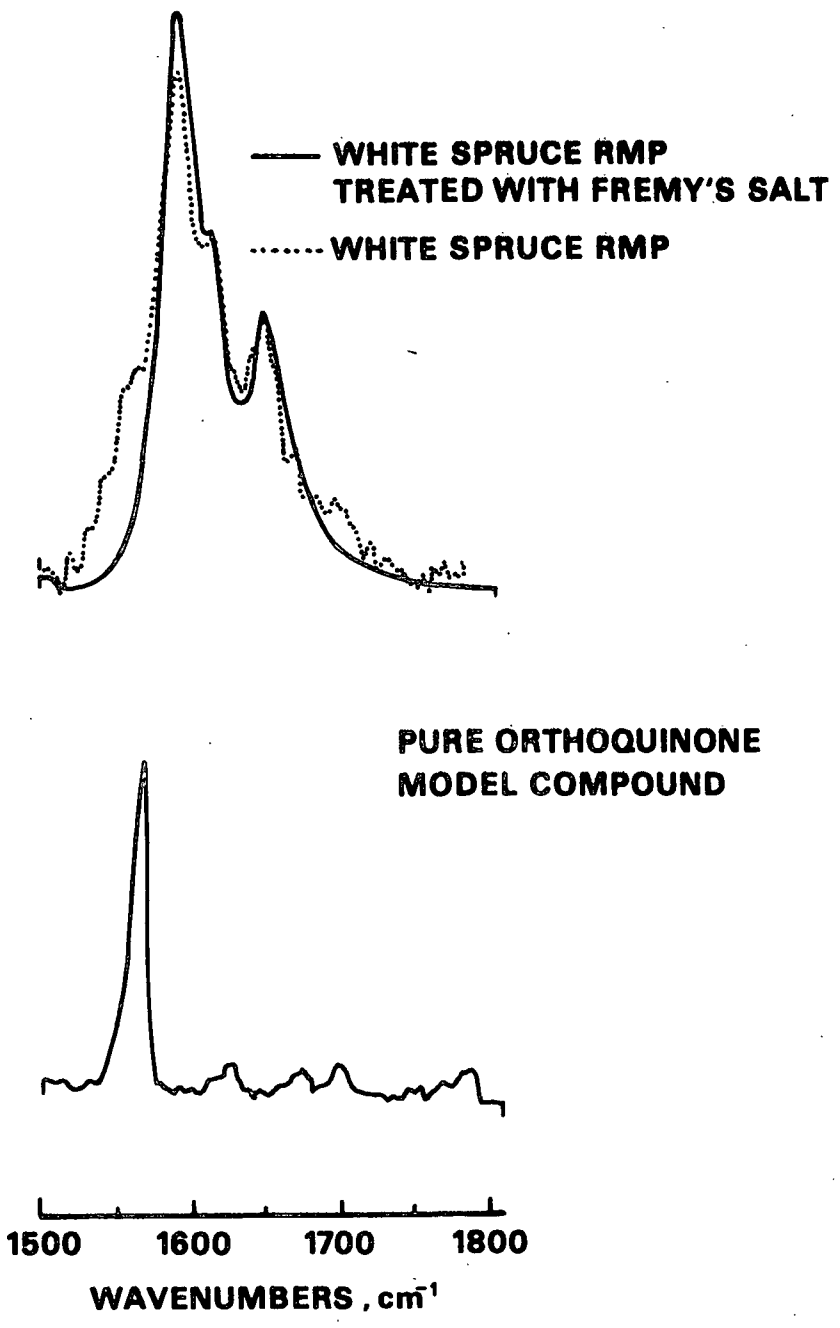

Figure 49. Raman spectra of a sheet formed from white spruce RMP sheet and of a sheet formed from white spruce RMP oxidized with Fremy's salt (lower spectrum is model I).

low laser outputs were required to obtain these spectra. Despite this "bleaching" limitation, however, the results obtained from these analyses support the conclusion that ortho-quinonoid lignin structures are formed when white spruce pulp is oxidized with Fremy's salt.

Reaction of Model Quinone Systems with Sulfur Dioxide and Sodium Dithionite

Using the pulp oxidized with Fremy's salt as a model system, the reactions of ortho-quinonoid lignin structures with gaseous sulfur dioxide, aqueous sulfur dioxide and aqueous sodium dithionite were investigated. These particular reagents were selected because model studies had shown that they reduce ortho-quinones to colorless phenolic structures.[61-64] Model compounds I and III were also rapidly decolored by these reagents. On the basis of these results, it was expected that similar reactions would occur between these reagents and the ortho-quinonoid structures present in the pulp oxidized with Fremy's salt.

When samples of the pulp oxidized with Fremy's salt were reacted with any one of the above agents, the reddish color of these samples was significantly diminished. The shapes of the ΔR_∞ spectra obtained for the reaction of these samples were qualitatively similar to those shown in Fig. 40 and 43 (Fig. 50) and, the reversed magnitude of these curves was consistent with the observed brightening. The $\Delta(k/s)_\lambda$ spectra obtained for the reaction of these samples were, in the visible region of the spectrum, qualitatively similar to the $\Delta(k/s)_\lambda$ spectrum for the Fremy's salt oxidation of the white spruce pulp shown in Fig. 44 (Fig. 51). In the UV region of the spectrum, only the spectrum of the sodium dithionite sample was similar to the spectrum shown in Fig. 44 (Fig. 52). The spectra of the sulfur dioxide samples had an additional absorption band [$\lambda_{(max)} \approx 350$ nm] in this region which was very strong. This result

suggests that dithionite is a more selective reducing agent for ortho-quinonoid lignin structures than is sulfur dioxide.

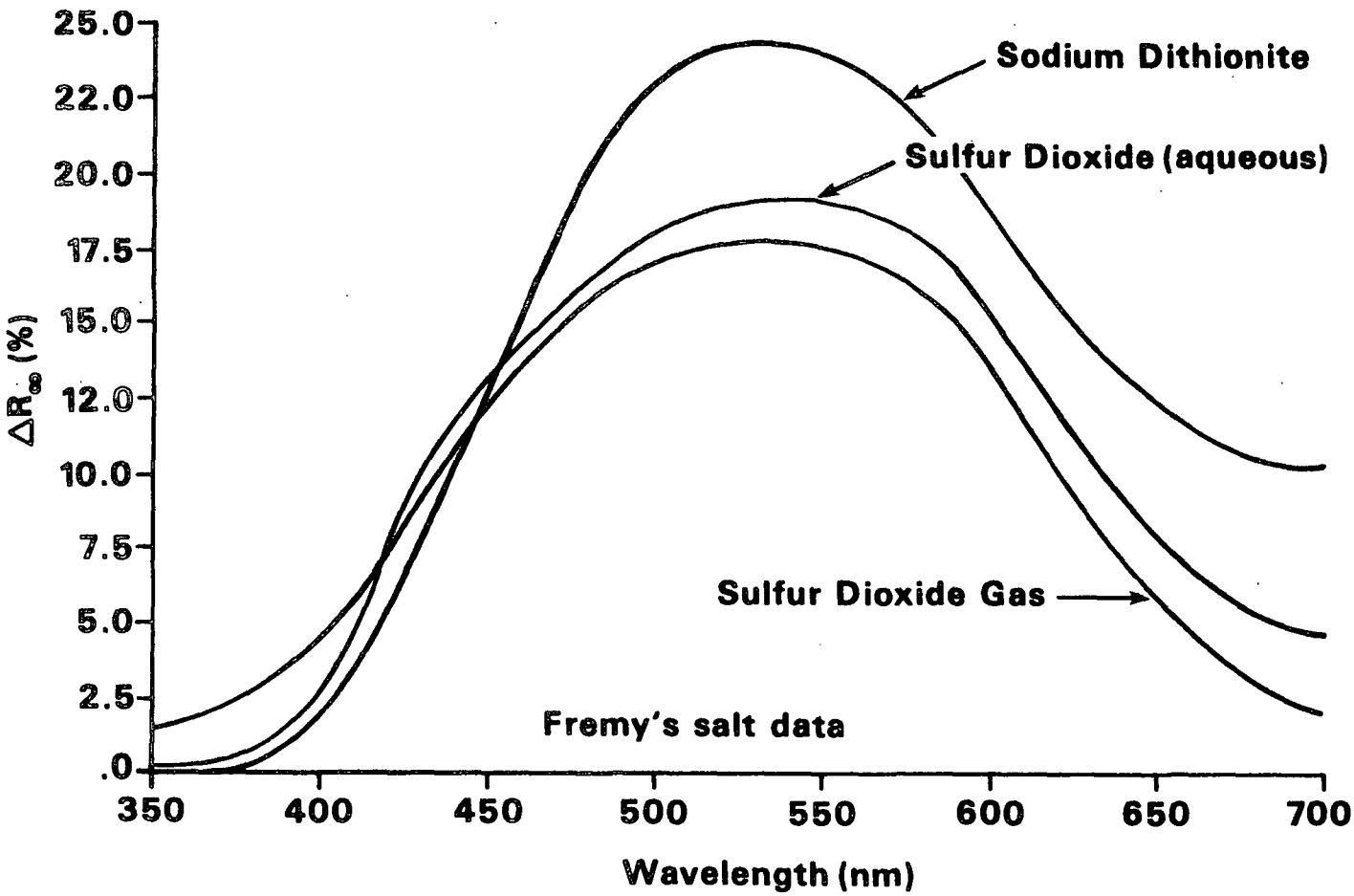

Figure 50. ΔR_∞ spectra obtained upon reaction of sheet samples formed from pulp oxidized with Fremy's salt with sulfur dioxide and sodium dithionite.

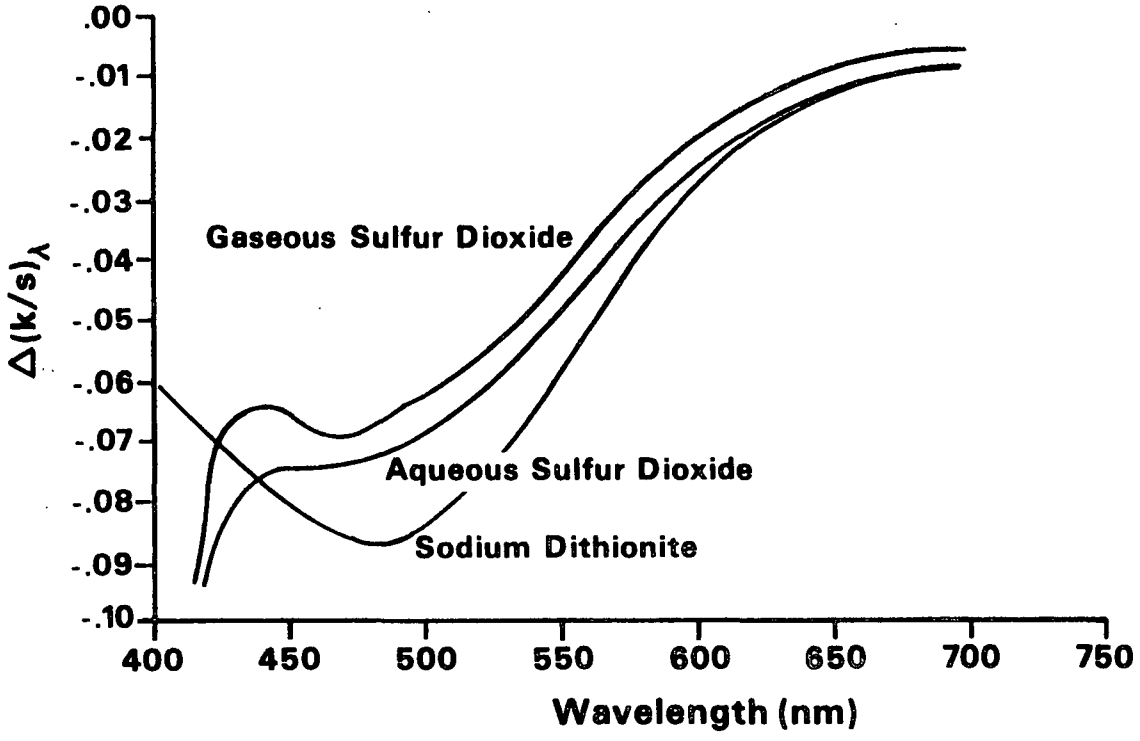

Figure 51. $\Delta(k/s)_\lambda$ spectra obtained upon reaction of sheet samples formed from pulp oxidized with Fremy's salt with sulfur dioxide and sodium dithionite (visible region).

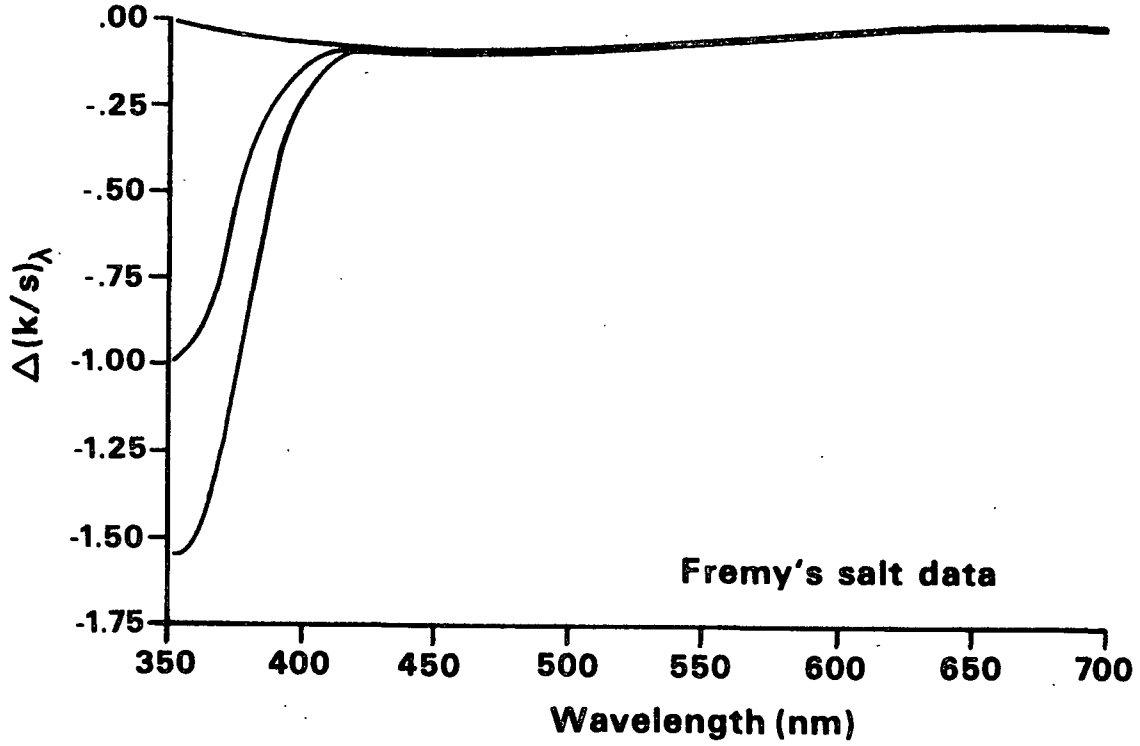

Figure 52. $\Delta(k/s)_\lambda$ spectra obtained upon reaction of sheet samples formed from pulp oxidized with Fremy's salt with sulfur dioxide and sodium dithionite (far UV-visible region).

Overall, the similarity of the spectra in Fig. 51 and 44 in the visible region show that, as expected, all three of these reagents with the ortho-quinonoid groups present in the pulp oxidized with Fremy's salt. The overall magnitudes of the changes observed in these spectra followed the order $SO_{2(g)} < SO_{2(aq)} < S_2O_4^{=}(aq)$. Sulfur dioxide, both gaseous and aqueous, also reacts with structures in the pulp which absorb in the UV region. While the nature of these structures was not determined, work by others[63,129,130] suggests that these structures may be of the coniferaldehyde type.

The results obtained in a subsequent diffuse reflectance FTIR analysis of these samples also supported this conclusion. In this analysis, difference spectroscopy was used to obtain spectra of the "lignin" present in each of the above samples. From these difference spectra, measurements of the areas under the 1665 cm^{-1} C=O and 1510 cm^{-1} aromatic C=C stretching bands present in these spectra were made. Using the procedures described in the Experimental section of this work, normalized areas under the 1665 cm^{-1} C=O stretching bands of these samples were then calculated. In making these calculations of normalized area, it was assumed that the number of reactive ortho-quinonoid lignin structures present in these samples was low in comparison to the total number of aromatic C_9 lignin units. In order to test this assumption, the areas under the 151 cm^{-1} C=C stretching bands of twenty different samples were measured. If the assumption made above is correct, then these areas should be, within reasonable limits, equal. As expected, the deviation in the average area under these bands was less than 5% at the 95% confidence level. Thus, the assumption that the number of reactive ortho-quinonoid lignin structures present in these samples was low in comparison to the total number of aromatic C_9 lignin units is valid, and the use of the 1510 cm^{-1} aromatic C=C stretching band in normalization is justified.

When the normalized areas under the 1665 cm^{-1} absorption bands of the samples described above were determined, the results shown in Table 7 were obtained. As Table 7 shows, the spectrum obtained from lignin present in the unirradiated pulp had a significant C=O stretching band at 1665 cm^{-1}. On the basis of the results obtained by other workers,[10,11,131,132] this band was attributed to pre-existing C=O containing structures in high yield pulp lignins including natural quinonoid lignin structures.[10,11]

Table 7. Normalized area under the 1665 cm^{-1} band of unirradiated pulp, pulp oxidized with Fremy's salt and pulp oxidized with Fremy's salt and reduced with the three reagents examined here.

Pulp Sample Analyzed	Area Under 1665 cm^{-1} Band (cm^{-1})[a]
Unirradiated	5.73 ± 0.12[b]
Fremy's salt oxidized	7.06
Fremy's salt oxidized/aqueous SO_2 reduced	5.34
Fremy's salt oxidized/gaseous SO_2 reduced	5.50
Fremy's salt oxidized/aqueous sodium dithionite reduced (20°C)	5.22
Fremy's salt oxidized/aqueous sodium dithionite reduced (60°C)	4.98

[a]Normalized using average area of 1510 cm^{-1} aromatic C=C stretching band of lignin.
[b]Mean value ± 90% confidence interval.

Upon oxidation with Fremy's salt, the normalized area under the 1665 cm^{-1} band of the lignin present in the white spruce pulp increased. This increase was considered to be consistent with the formation of ortho-quinonoid lignin structures during the oxidation process. Verification of this result was attempted through difference spectroscopy. It should be noted, however, that

the use of this method of analysis for pulp and paper can be complicated by normalization difficulties and questions about the depth to which the infrared beam penetrates the fibers during the analysis. Because of these difficulties, the quality of the spectra obtained from this method can be poor and spectral artifacts are not uncommon. It did appear, however, that consistent with the above results, the difference spectrum obtained upon oxidation of the test pulp with Fremy's salt had a C=O stretching band at approximately 1665 cm^{-1} (Fig. 53). This band was fairly broad and asymmetric.

The results presented in Table 7 also showed that when the pulp oxidized with Fremy's salt was reacted with any of the three reagents noted above, the area under the 1665 cm^{-1} band of the lignin present in this pulp decreased. The amount by which this area decreased was dependent on the reagent used and followed the order: $SO_{2(g)} < SO_{2(aq)} \leq Na_2SO_{4(aq)}$. In all three cases, however, the area remaining under the 1665 cm^{-1} band of the lignin present in this pulp was significantly less than that of the 1665 cm^{-1} band of the lignin present in the unreacted pulp. This finding was tentatively attributed to the reactions of these reagents with the preexisting quinonoid lignin structures alluded to above.

On the basis of the observations described above, it was concluded that white spruce RMP contains a number of quinonoid lignin structures and Fremy's salt oxidation of this pulp increases this number. It was also concluded that these quinonoid structures, whether preexisting or created, react with all three of the reagents examined here.

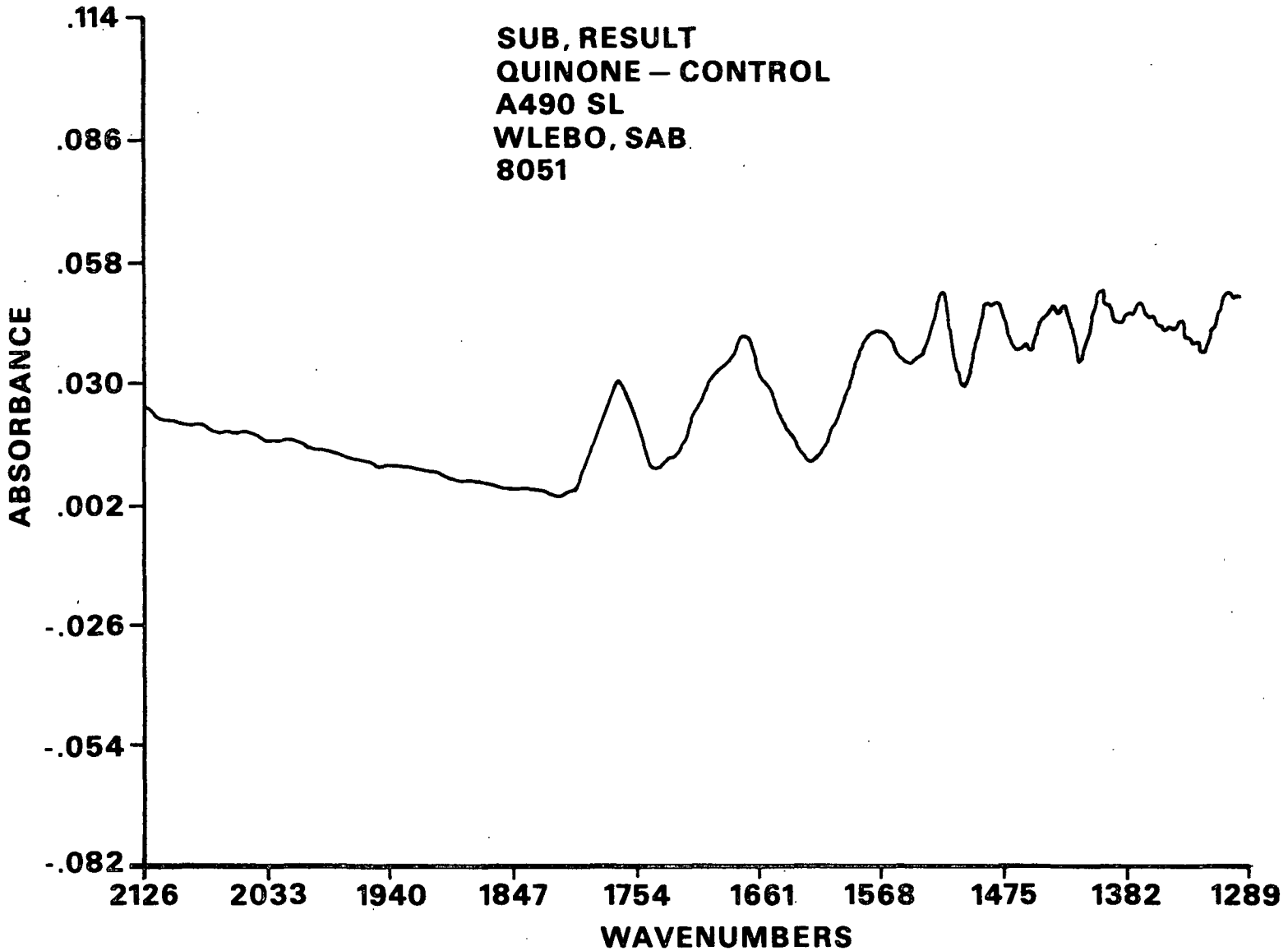

Figure 53. Difference spectrum obtained by subtracting the diffuse reflectance FTIR spectrum of white spruce pulp from the diffuse reflectance FTIR spectrum of white spruce pulp oxidized with Fremy's salt (original spectra shown in Appendix VII).

Reaction of Model Quinone Systems with Trimethyl Phosphite (TMPh)

The reactions of trimethyl phosphite, $P(OCH_3)_3$, with model ortho- and para-quinones have been well documented.[65-98] As noted earlier, these reactions involve the rapid formation of 1:1 adducts which, in most cases, are colorless, and the yields for these reactions are in many cases near quantitative. Upon reaction with trimethyl phosphite, the red color of the pulp oxidized with Fremy's salt almost completely disappeared. The ΔR_∞ spectrum obtained from the reaction of this pulp had one broad band, and the wavelength maximum of this band occurred at 510 nm (Fig. 54). The shape of this band was qualitatively similar to that of the band observed in the ΔR_∞ spectra obtained from the oxidation of white spruce pulp with Fremy's salt and from impregnation of white spruce pulp with 3-methoxy-ortho-benzoquinone. The wavelength maximum of this band, however, occurred at a slightly shorter wavelength than did those of these two earlier pulps.

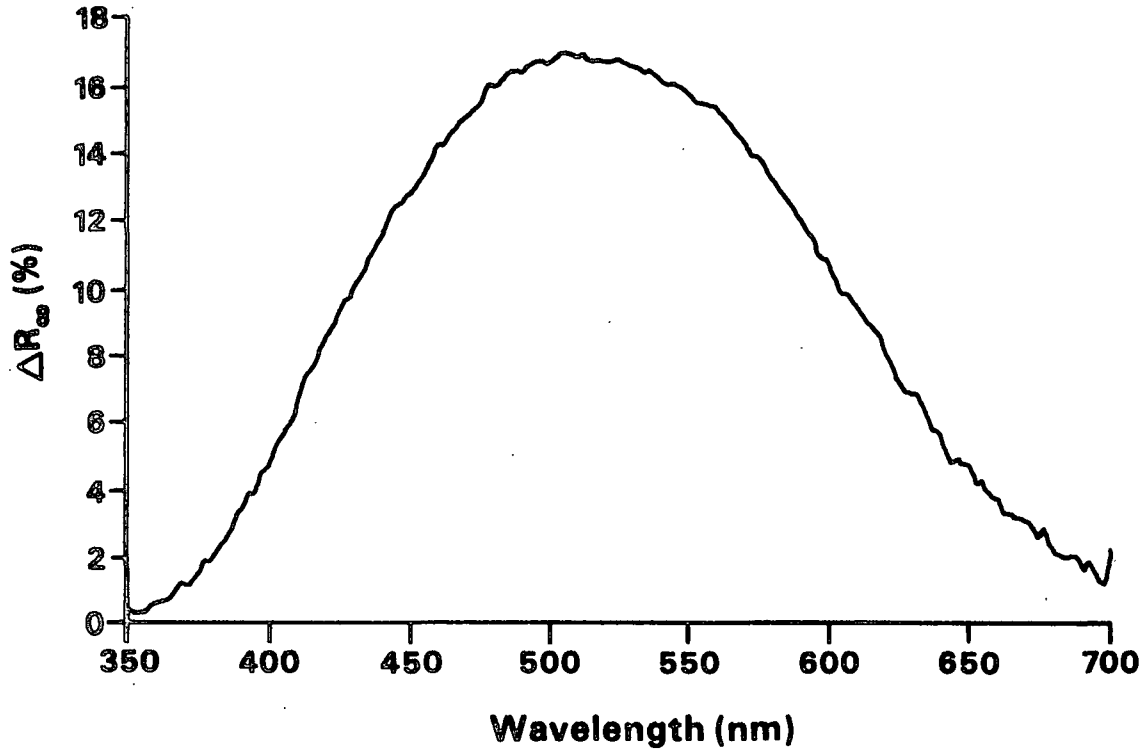

Figure 54. ΔR_∞ spectrum obtained upon reaction of a sheet sample formed from pulp oxidized with Fremy's salt with trimethyl phosphite.

The $\Delta(k/s)_\lambda$ spectrum obtained from the reaction of this pulp was found to be qualitatively similar to the $\Delta(k/s)_\lambda$ spectra obtained from the oxidation of white spruce pulp with Fremy's salt and from impregnation of white spruce pulp with 3-methoxy-ortho-benzoquinone in the visible region of the spectrum (Fig. 55). In the UV region, however, the $\Delta(k/s)_\lambda$ spectrum obtained from the reaction of this pulp had a second absorption band at approximately 370 nm. This second band was attributed to the reaction of trimethyl phosphite with an unknown structure, possibly of a coniferaldehyde type, which has an absorption maximum at this wavelength.

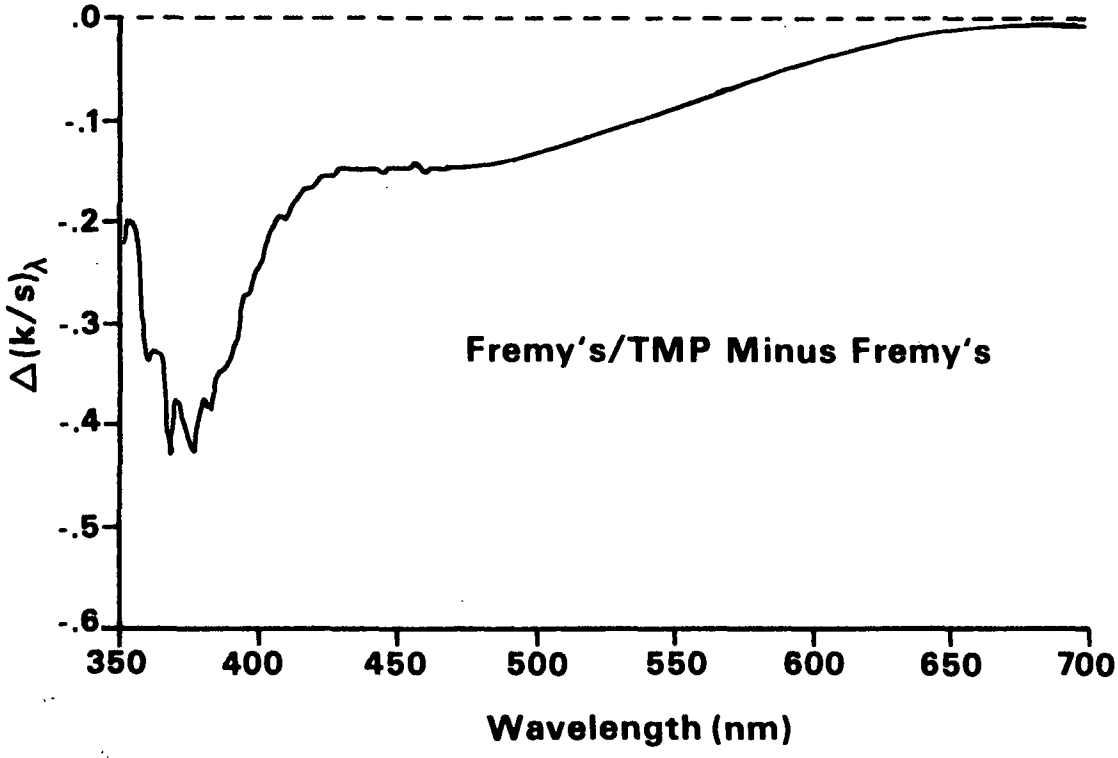

Figure 55. $\Delta(k/s)_\lambda$ spectrum obtained upon reaction of a sheet sample formed from pulp oxidized with Fremy's salt with trimethyl phosphite.

On the basis of the results described above, it was concluded that trimethyl phosphite reacts with the quinonoid groups present in the Fremy's salt pulp. Verification of this conclusion was attempted using diffuse reflectance FTIR spectroscopy. Earlier results suggested that if this conclusion is correct, then the area under the 1665 cm^{-1} absorption band of the lignin present in this pulp should decrease upon reaction with Fremy's salt. Table 8 shows that, as expected, the area under the 1665 cm^{-1} band of the lignin present in this sample was significantly reduced by reaction with trimethyl phosphite.

Table 8. Normalized area under the 1665 cm^{-1} band of a sample of pulp oxidized with Fremy's salt and then reacted with trimethyl phosphite.

Pulp Sample Analyzed	Area Under 1665 cm^{-1} Band (cm^{-1})[a]
Unirradiated pulp	5.73
Fremy's salt oxidized pulp	7.06
Fremy's salt oxidized/TMPh reacted pulp	5.53

[a]Normalized using 1510 cm^{-1} band of lignin.

When compared to the results obtained with sulfur dioxide and sodium dithionite, the magnitude of the reduction of this area was a little less than that achieved with aqueous sulfur dioxide or aqueous sodium dithionite and approximately the same as the reduction achieved with gaseous sulfur dioxide.

Keeping the limitations discussed earlier in mind, an analysis of the functional groups involved in this reaction was attempted using infrared difference spectroscopy. Consistent with the observed decrease in the area under the 1665 cm^{-1} band, the difference spectrum obtained from the reaction of this sample showed a decrease in absorbance in the 1665 cm^{-1} region of the spectrum (Fig. 56).

This decrease was attributed to a reduction in the number of C=O lignin groups (i.e., ortho-quinonoid lignin structures) in the pulp. The difference spectrum presented in Fig. 56 also showed that there were strong increases in the absorbance of the sample in the 2995, 2870, 1760, 1600, 1515, 1470, 1245, 1070, and 1020 cm^{-1} regions of the spectrum. On the basis of the results obtained in model studies,[78,81-83,113] vibrational assignments were postulated for some of these bands (Table 9). On the basis of the last two postulated assignments, it appeared that the product formed in the reaction of trimethyl phosphite with this pulp may not have been the expected 1:1 adduct, but instead may have been a cyclic phosphite triester.

Table 9. Postulated vibrational assignments for the absorption bands observed in the difference spectra shown in Fig. 56.

Absorption Band (cm^{-1})	Postulated Vibrational Assignment
2995 and 2870	CH_3 stretch of OCH_3
1600, 1515, and 1470	C=C aromatic ring stretch
1245	Possible P=O stretch
1070 and 1020	P-O-C stretch

Based on the literature,[98] a reaction sequence such as is shown below would be quite possible for these quinones.

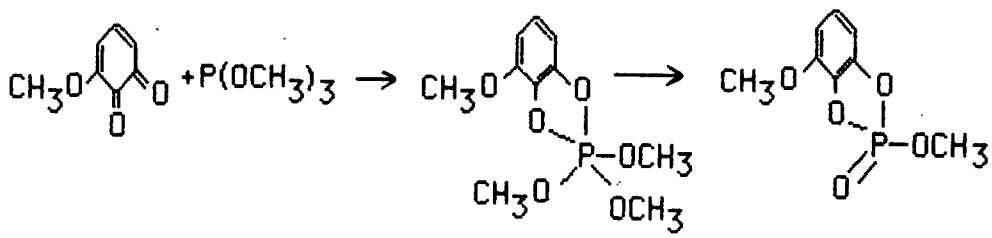

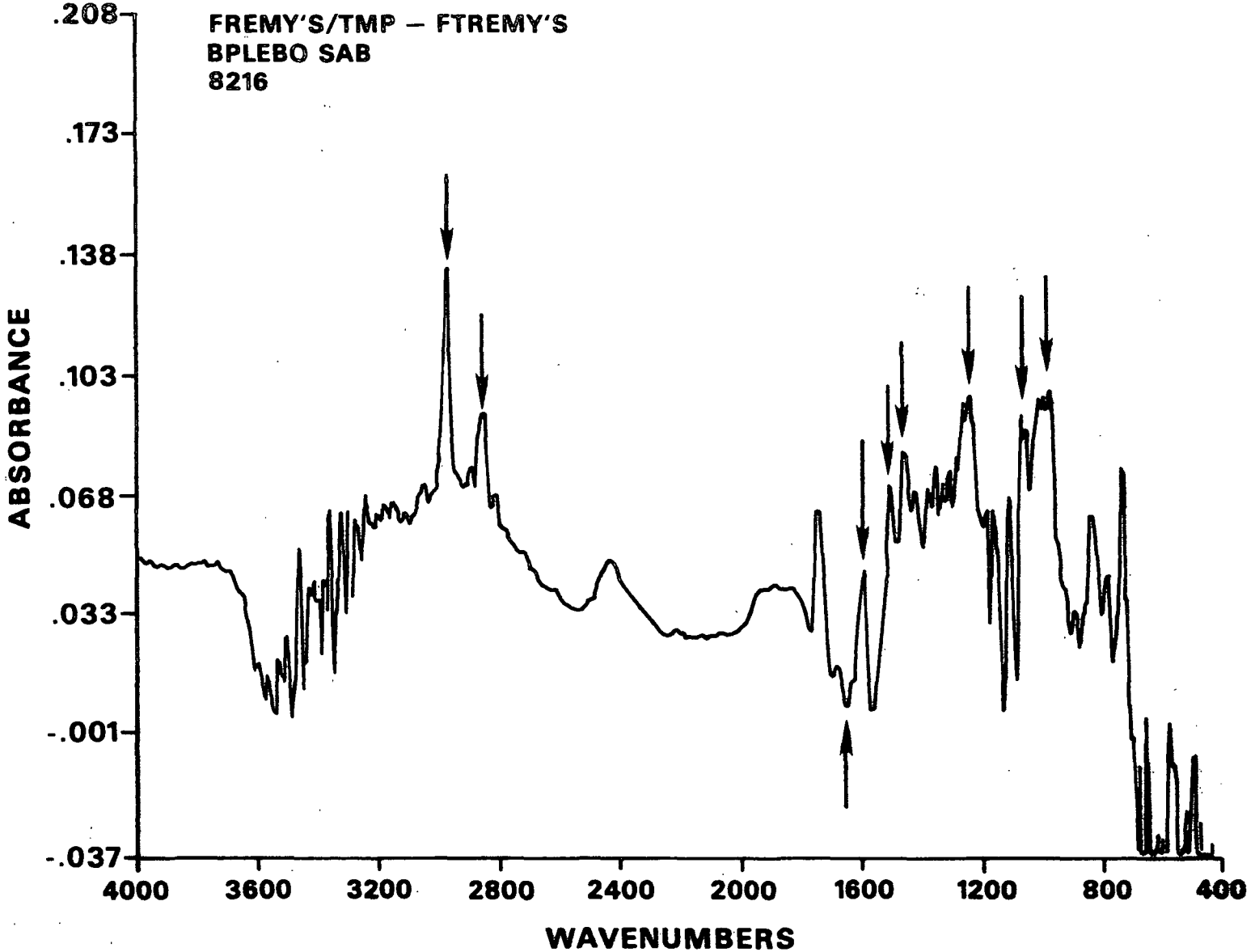

Figure 56. Difference spectrum obtained by subtracting the diffuse reflectance FTIR spectrum of white spruce pulp oxidized with Fremy's salt from the diffuse reflectance FTIR spectrum of white spruce pulp oxidized with Fremy's salt and reacted with trimethyl phosphite (original spectra shown in Appendix VII).

More conclusive evidence for the formation of cyclic phosphate triesters in the reaction of trimethyl phosphite with the above pulp was obtained using solid state ^{31}P NMR analysis. As was mentioned earlier, the expected reaction products [i.e., the 1:1 (ortho-quinone:trimethyl phosphite) adducts] give ^{31}P NMR signals, relative to 85% H_3PO_4, in the -(40-60) ppm range of the spectrum.[133,134] If, however, traces of water or oxygen are present during this reaction (as is likely to be the case with pulp), then the expected product would be a cyclic phosphate triester as shown above. The ^{31}P NMR signals of these types of structures occur in the 10-15 ppm range of the spectrum.[133,134] Any para-quinonoid structures present in these pulps should react to give 1:1 adducts which give ^{31}P NMR signals in the + 1-(-6) ppm range of the spectrum.[133,134]

When pulp oxidized with Fremy's salt and reacted with trimethyl phosphite was analyzed by this method, the resulting ^{31}P NMR spectrum had a single, strong signal (Fig. 57). The chemical shift of this signal (relative to 85% H_3PO_4) was 13.2 ppm. This chemical shift, as expected, was highly indicative of a cyclic phosphate triester. Thus, this result, like the FTIR results, are evidence that a cyclic phosphate triester was the final product obtained when trimethyl phosphite was reacted with the ortho-quinonoid structures present in this pulp. These results also show that this pulp either did not contain any para-quinonoid structures or, if it did, they did not react with the trimethyl phosphite.

Results Obtained from the Analysis of Unirradiated Pulp Samples

As noted above, the 1665 cm^{-1} absorption band observed in the diffuse reflectance FTIR spectrum of the untreated pulp suggested that it contained a small number of quinonoid lignin structures. Thus, before attempting an analysis of "yellowed" pulp, an analysis of the unirradiated pulp was conducted. The methods used in this analysis were essentially the same methods used in the

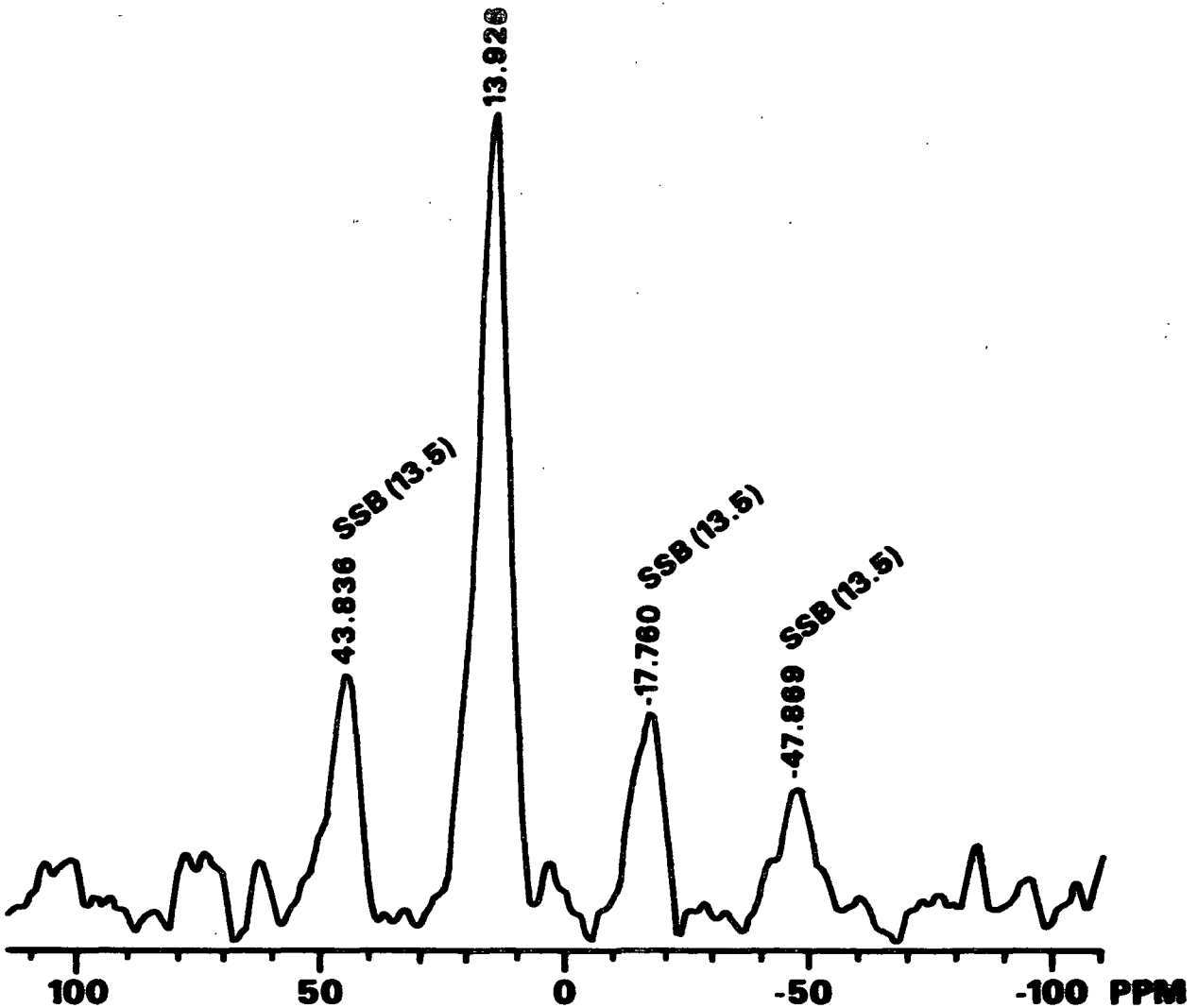

Figure 57. Solid state ^{31}P NMR spectrum of white spruce pulp oxidized with Fremy's salt and reacted with trimethyl phosphite.

above analysis of model systems (i.e., reaction with sulfur dioxide, sodium dithionite, and trimethyl phosphite).

Reaction of Unirradiated Pulp with Sulfur Dioxide and Sodium Dithionite

A slight brightening of the unirradiated pulp was observed when it was reacted with sulfur dioxide or sodium dithionite. With the exception of having slightly broader bands, the ΔR_∞ spectra obtained upon reaction of the unirradiated pulp were similar to the ΔR_∞ spectra obtained upon reaction of the pulp oxidized with Fremy's salt pulp (Fig. 58). These spectra qualitatively showed that there were structures in the unirradiated pulp which react with these reagents. On the basis of their qualitative similarity to the spectra of the Fremy's salt pulp and pulp impregnated with 3-methoxy-ortho-quinone shown earlier, it appears that at least some of these structures were of the ortho-quinonoid lignin type.

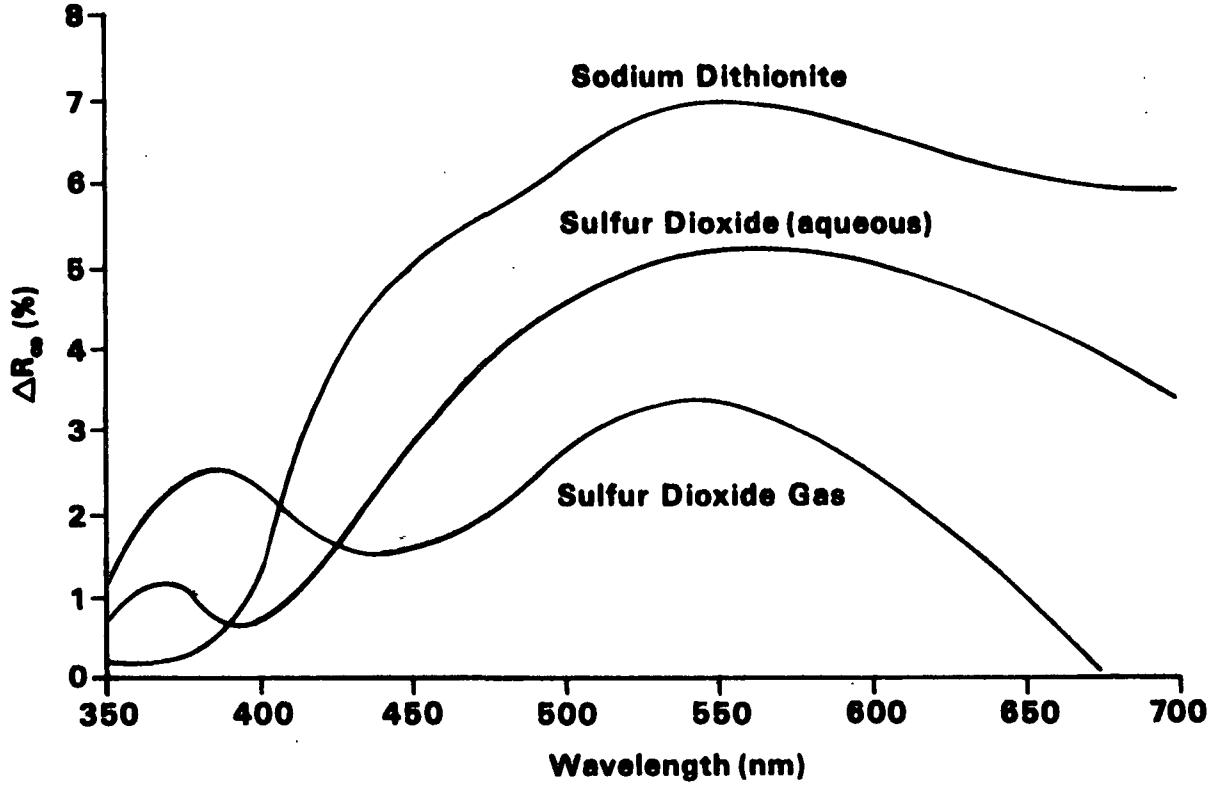

Figure 58. ΔR_∞ spectra obtained upon reaction of white spruce pulp with sulfur dioxide and sodium dithionite.

Except for a slight blue shift, the $\Delta(k/s)_\lambda$ spectrum obtained upon reaction of the unirradiated pulp with sodium dithionite was similar to those obtained upon oxidation of this pulp with Fremy's salt and upon impregnation of this pulp with 3-methoxy-ortho-benzoquinone in the visible region. In the far UV region of the spectrum, however, the absorbance of this sample increased rather than decreased (Fig. 59 and 60). The $\Delta(k/s)_\lambda$ spectra obtained upon reaction of the unirradiated pulp with sulfur dioxide were similar in the entire range to those obtained in the corresponding analysis of this pulp after oxidation with Fremy's salt. The magnitude of the changes observed in these spectra, while less than those in the Fremy's salt samples, followed the same order as these samples followed [i.e., $SO_{2(g)} < SO_{2(aq)} \leq Na_2SO_{4(aq)}$]. Thus, overall, these results show that the control pulp does contain a small number of preexisting ortho-quinonoid lignin structures which react with these reagents.

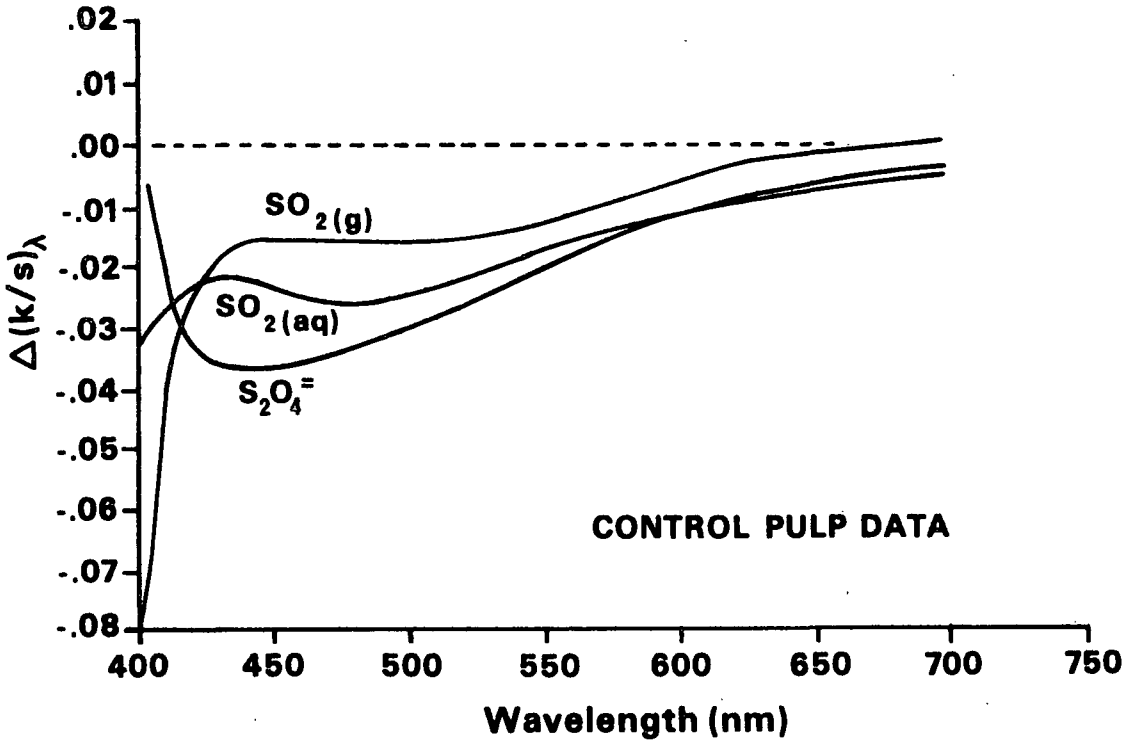

Figure 59. $\Delta(k/s)_\lambda$ spectra obtained upon reaction of white spruce pulp with sulfur dioxide and sodium dithionite (visible region).

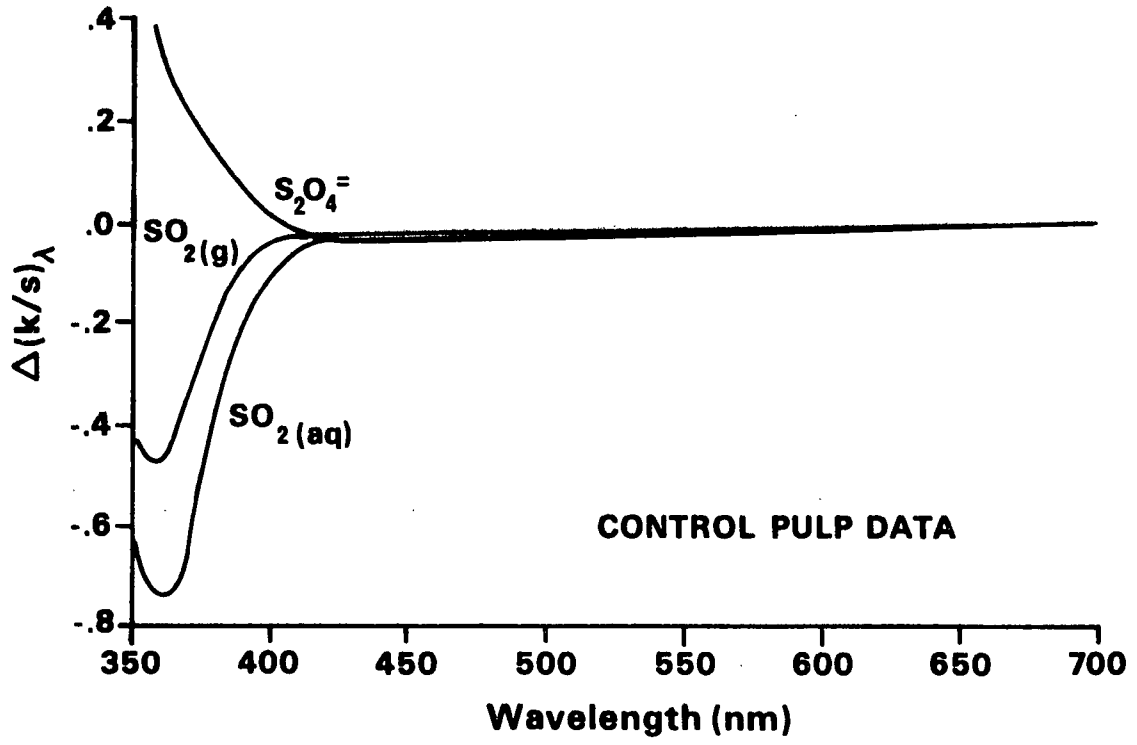

Figure 60. $\Delta(k/s)_\lambda$ spectra obtained upon reaction of white spruce pulp with sulfur dioxide and sodium dithionite (far UV-visible region).

The results of subsequent diffuse reflectance FTIR analysis further supported this conclusion. As was the case when the Fremy's salt treated pulp was treated with sulfur dioxide and sodium dithionite, the normalized area under the 1665 cm^{-1} absorption band of the unirradiated pulp decreased upon exposure to these reagents (Table 10). It was interesting to note that the areas remaining under this band in the unirradiated and reduced pulp samples were approximately the same as those of the pulp oxidized with Fremy's salt and reduced with the same reagents. Thus, the results obtained in this analysis again indicated that the untreated pulp contained reactive quinonoid lignin structures.

Table 10. Effect of reducing agents on the area under the 1665 cm^{-1} band of unirradiated pulp.

Pulp Sample Analyzed	Area Under 1665 cm^{-1} Band (cm^{-1})[a]
Unirradiated	5.73 ± 0.12[b]
Unirradiated/aqueous SO_2 reduced	5.32
Unirradiated/gaseous SO_2 reduced	5.48
Unirradiated/aqueous sodium dithionite reduced (20°C)	5.15
Unirradiated/aqueous sodium dithionite reduced (60°C)	4.99

[a]Normalized using 1510 cm^{-1} band of lignin.
[b]Mean value ± 90% confidence interval.

Reaction of Unirradiated Pulp with Trimethyl Phosphite

A slight increase in brightness was observed when the unirradiated pulp was reacted with trimethyl phosphite. The ΔR_∞ spectrum obtained upon reaction of the unirradiated pulp with this reagent had one broad, asymetric band, and the wavelength maximum of this band was about 450 nm (Fig. 61). There also appeared to be a shoulder on this band in the far UV region of the spectrum (i.e., 350-400 nm). The $\Delta(k/s)_\lambda$ spectrum obtained upon reaction of this pulp had a single absorption band in the UV region of the spectrum [λ(max) approximately 360 nm] which tailed into the visible region (Fig. 62). When compared to the $\Delta(k/s)_\lambda$ spectrum obtained upon reaction of the pulp oxidized with Fremy's salt, this spectrum showed approximately equal change in the UV region of the spectrum. In the visible region of the spectrum, however, the change observed in the spectrum of the unirradiated and reacted sample was considerably less. While these results strongly indicated that a reaction had occurred between the trimethyl phosphite and structures present in the unirradiated pulp, they did not give any

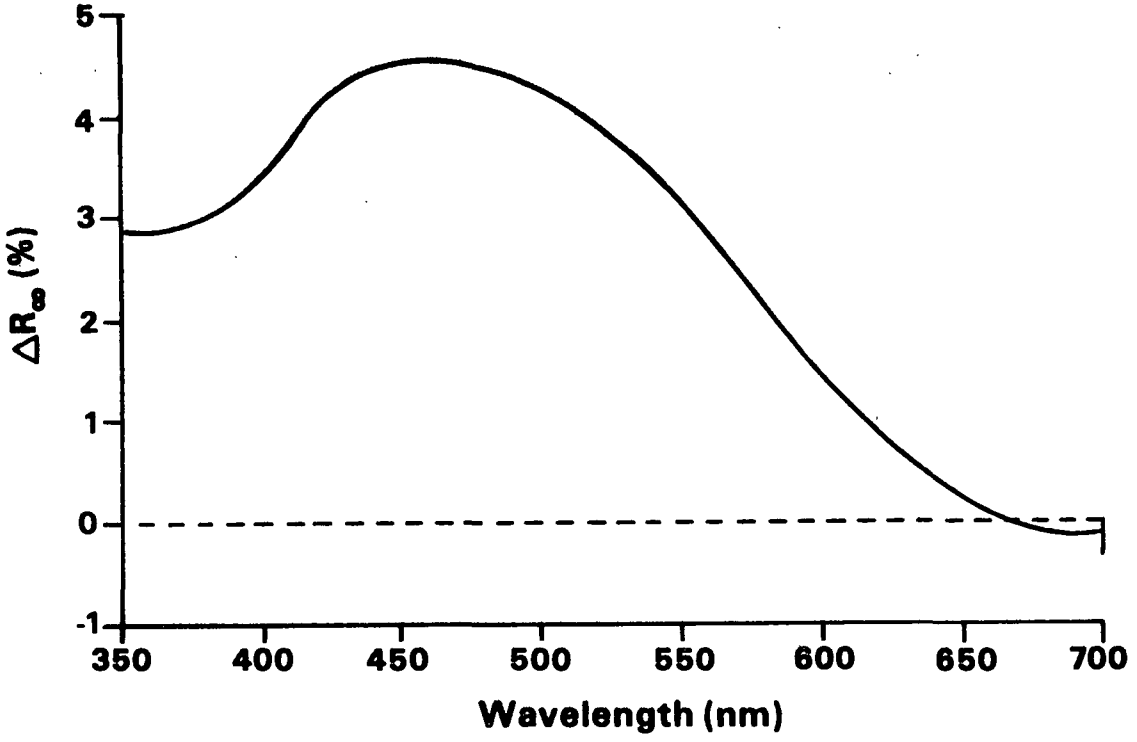

Figure 61. ΔR_∞ spectrum obtained upon reaction of white spruce pulp with trimethyl phosphite.

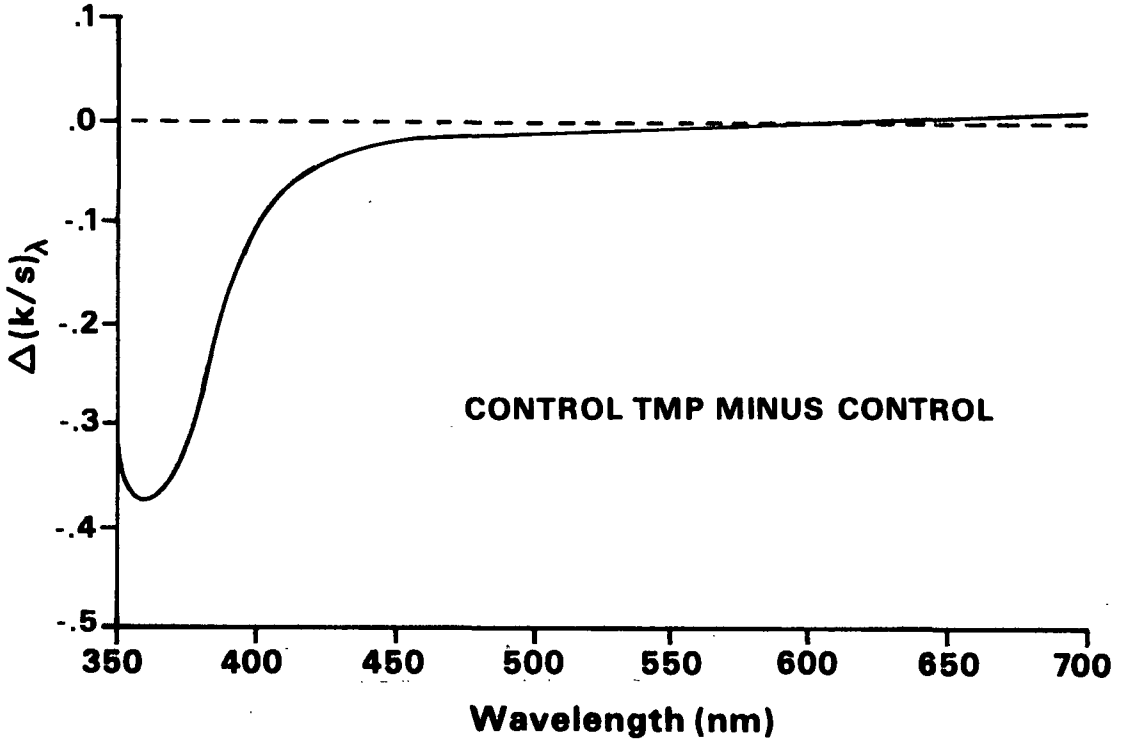

Figure 62. $\Delta(k/s)_\lambda$ spectrum obtained upon reaction of white spruce pulp with trimethyl phosphite.

clear indication as to what these structures were. Thus, the possibility of these structures being quinonoid in nature, while not apparent, could not be eliminated.

In an attempt to further investigate the nature of the reactive structures present in the unirradiated pulp, the reaction of trimethyl phosphite with this pulp was examined using diffuse reflectance FTIR spectroscopy. The results obtained when the areas under the 1665 cm^{-1} band of the unirradiated pulp were determined before and after reaction with trimethyl phosphite showed that, as was expected, a significant reduction in the area under the 1665 cm^{-1} band occurred upon reaction (Table 11). When compared to earlier results, the magnitude of the reduction in the 1665 cm^{-1} band of this pulp was a little less than that achieved with aqueous sulfur dioxide or aqueous sodium dithionite and approximately equal to the reduction achieved with gaseous sulfur dioxide. The reason for this difference was not entirely clear, but one factor which may have contributed to this observation was differences in the reaction conditions (i.e., aqueous versus nonaqueous solvent systems).

Table 11. Normalized area under the 1665 cm^{-1} band of trimethyl phosphite reacted samples of unirradiated pulp.

Pulp Sample Analyzed	Area Under 1665 cm^{-1} FTIR Band (cm^{-1})[a]
Unirradiated pulp	5.73
Unirradiated/trimethyl phosphite reacted	5.52
Pulp oxidized with Fremy's salt	7.06
Pulp oxidized with Fremy's salt/ trimethyl phosphite reacted	5.53

[a]Normalized using 1510 cm^{-1} band of lignin.

A further investigation of the structure of the reactive groups present in these samples was attempted using difference spectroscopy. Consistent with the results presented in Table 11, the difference spectrum obtained showed a decrease in absorbance in the 1665 cm^{-1} region (Fig. 63). The difference spectrum obtained for this sample was somewhat similar to the spectrum obtained in the reaction of the pulp oxidized with Fremy's salt.

The chemical shifts of the signals observed in the ^{31}P NMR spectra of three different phosphite reacted samples of the unirradiated pulp are summarized in Table 12. The actual spectra are shown in Appendix VII. As Table 12 shows, the spectra obtained from these samples were quite similar. Each of these spectra had two signals. The average chemical shifts and relative areas of these signals were 12.4 ppm (71.5%) and 4.2 ppm (28.5%). The chemical shift of this first signal was the same as that of the signal observed in the spectrum of pulp oxidized with Fremy's salt and reacted with TMPh and was attributed to a cyclic phosphate type reaction product. Thus, as was suggested by the above results, the unirradiated pulp did contain reactive ortho-quinonoid lignin structures.

The nature of the reaction product giving rise to the second signal observed in these spectra, a signal which was not observed in the pulp oxidized with Fremy's salt and reacted with TMPh, was not known. One possibility is that this product was simply oxidized trimethyl phosphite [i.e., trimethyl phosphate, $OP(OCH_3)_3$]. The chemical shift of the signal produced by this compound, both neat and absorbed onto pulp, occurred at approximately 2.5 ppm. Thus, the chemical shift of the second reaction product was consistent with it being trimethyl phosphate. One point which spoke against this assignment, however, was that this product, if formed, should have been removed from the pulp during the washing process. Two other related points which spoke against this assignment

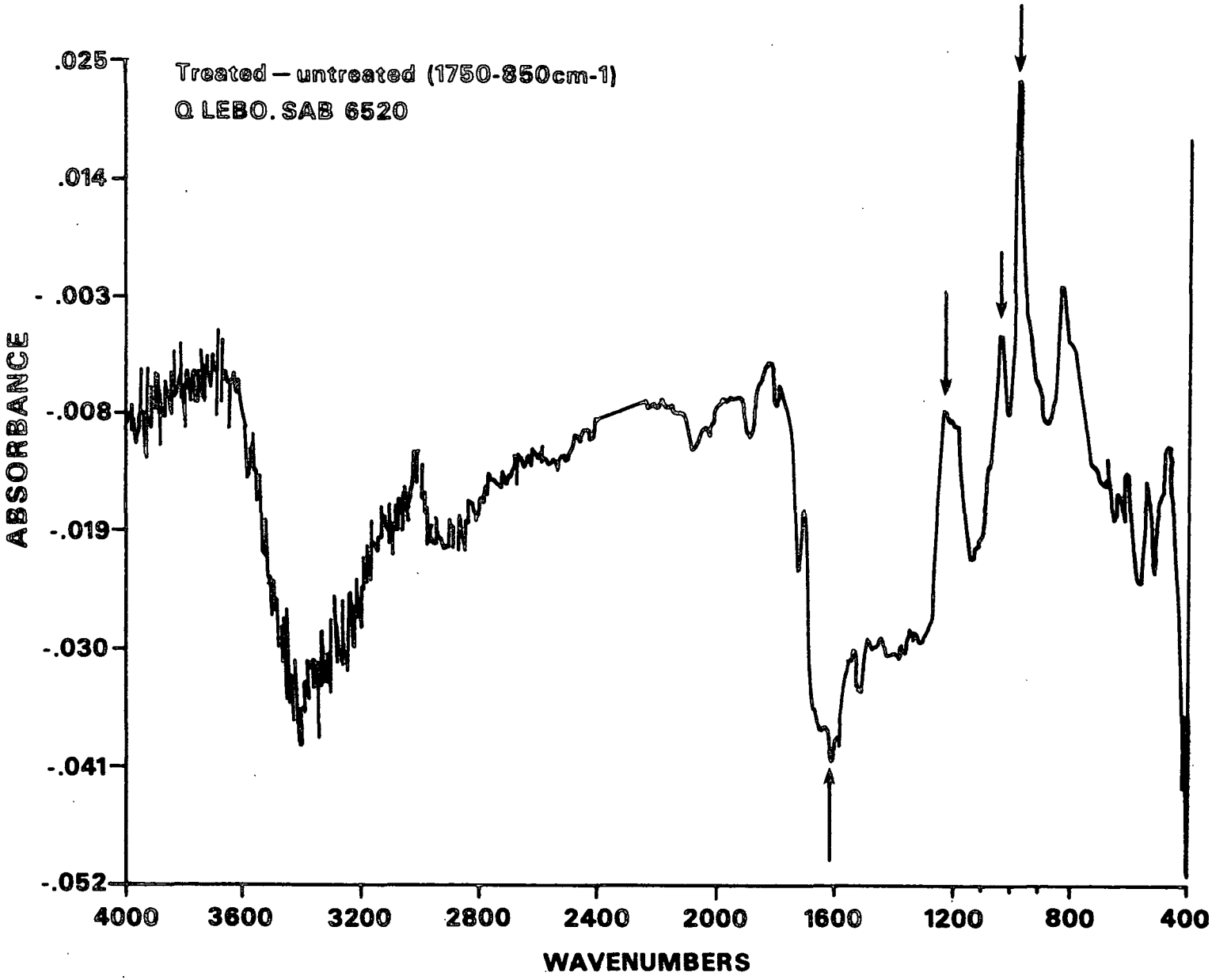

Figure 63. Difference spectrum obtained by subtracting the diffuse reflectance FTIR spectrum of white spruce pulp from the diffuse reflectance FTIR spectrum of white spruce pulp reacted with trimethyl phosphite (original spectra shown in Appendix VII).

were the uniformity in the amount of the product formed in these pulps and the lack of formation of this product in the Fremy's salt oxidized pulp.

Table 12. Summary of the chemical shifts of the signals observed in the ^{31}P NMR spectra of three different reacted samples of unirradiated pulp.

Sample	Chemical Shifts of Observed Signals (ppm)[a,b]	Relative Area of Signal (% of total signal)[b]
Unirradiated-1	13.5	70
	2.5	30
Unirradiated-2	11.9	66
	4.4	34
Unirradiated-3	11.9	78
	5.6	22

[a]Relative to 85% H_3PO_4.
[b]Obtained from deconvolutions of spectra shown in Appendix VII.

Results Obtained in the Analysis of "Yellowed" Pulp Sheets

Diffuse Reflectance UV-Visible Spectroscopic Analysis of Sheets "Yellowed" by Sunlight

The ΔR_∞ spectrum obtained upon exposure to a white spruce sheet to 20 hours of simulated sunlight had a single broad band (Fig. 64). The wavelength minimum of this band occurred at approximately 430 nm. For comparison purposes the ΔR_∞ spectra obtained upon impregnation of white spruce sheets with the quinone models I and II are also presented in Fig. 64. As this figure shows, the ΔR_∞ spectrum obtained upon impregnation of the para-quinone model, II, into a white spruce sheet was similar to the ΔR_∞ spectrum obtained upon exposure of a white spruce sheet to sunlight. The primary difference between these spectra was that in the range from approximately 450-700 nm the apparent absorbance of the sheet impregnated with the para-quinone model was significantly less than that of the sheet "yellowed" by exposure to sunlight. Interestingly, this range was the

same range in which the pulp sheet impregnated with the ortho-quinone model, I, absorbed most strongly.

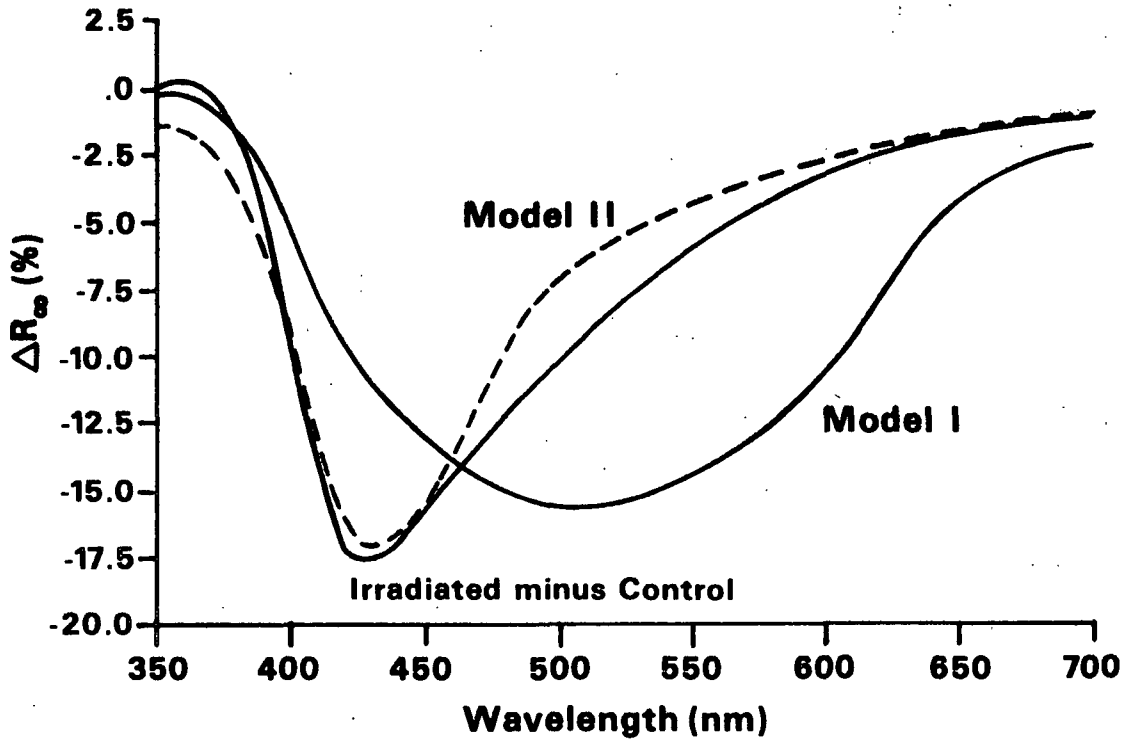

Figure 64. ΔR_∞ spectrum obtained upon irradiation of a white spruce RMP sheet for 20 hours with simulated sunlight.

The $\Delta(k/s)_\lambda$ spectrum obtained upon exposure of a white spruce sheet to 20 hours of simulated sunlight was also prepared (Fig. 65). In order to obtain additional information, an expanded version of this spectrum was also prepared (Fig. 66). As these figures show, the qualitative match between the $\Delta(k/s)_\lambda$ spectra obtained upon exposure of a sheet and upon impregnation of a sheet with the para-quinone model, II, was not as close as the match between their corresponding ΔR_∞ spectra. The wavelength maximum of the absorption band observed in the spectrum obtained upon exposure to sunlight occurred at approximately 400 nm, while the wavelength maximum of the band observed in the spectrum

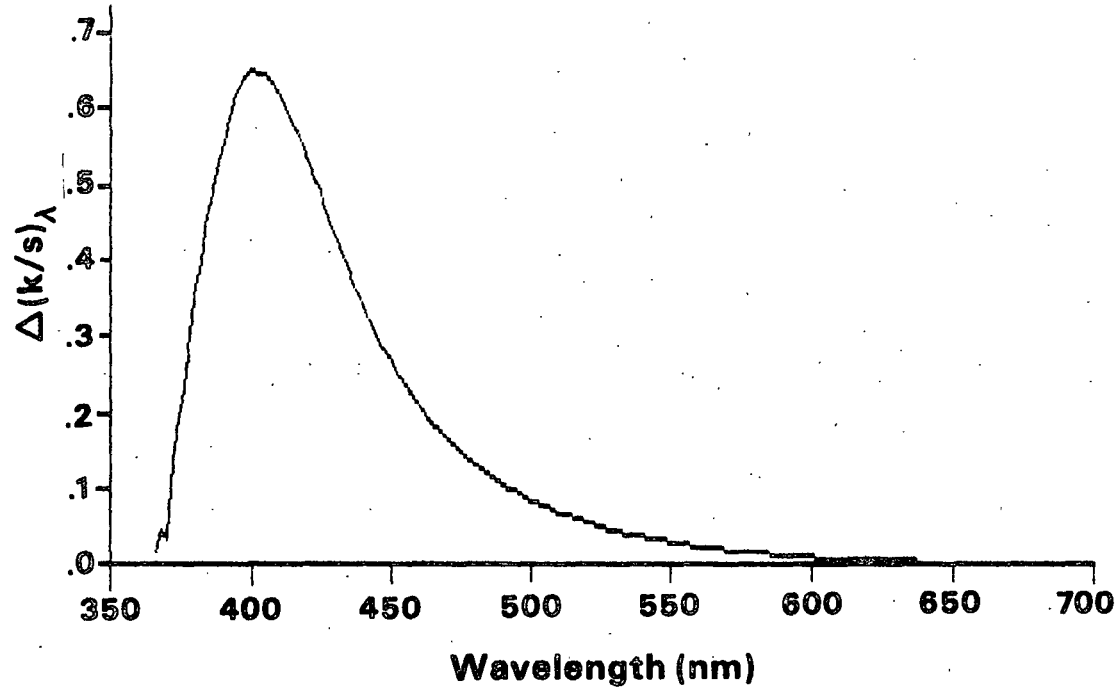

Figure 65. $\Delta(k/s)_\lambda$ spectrum obtained upon irradiation of a white spruce RMP sheet for 20 hours with simulated sunlight.

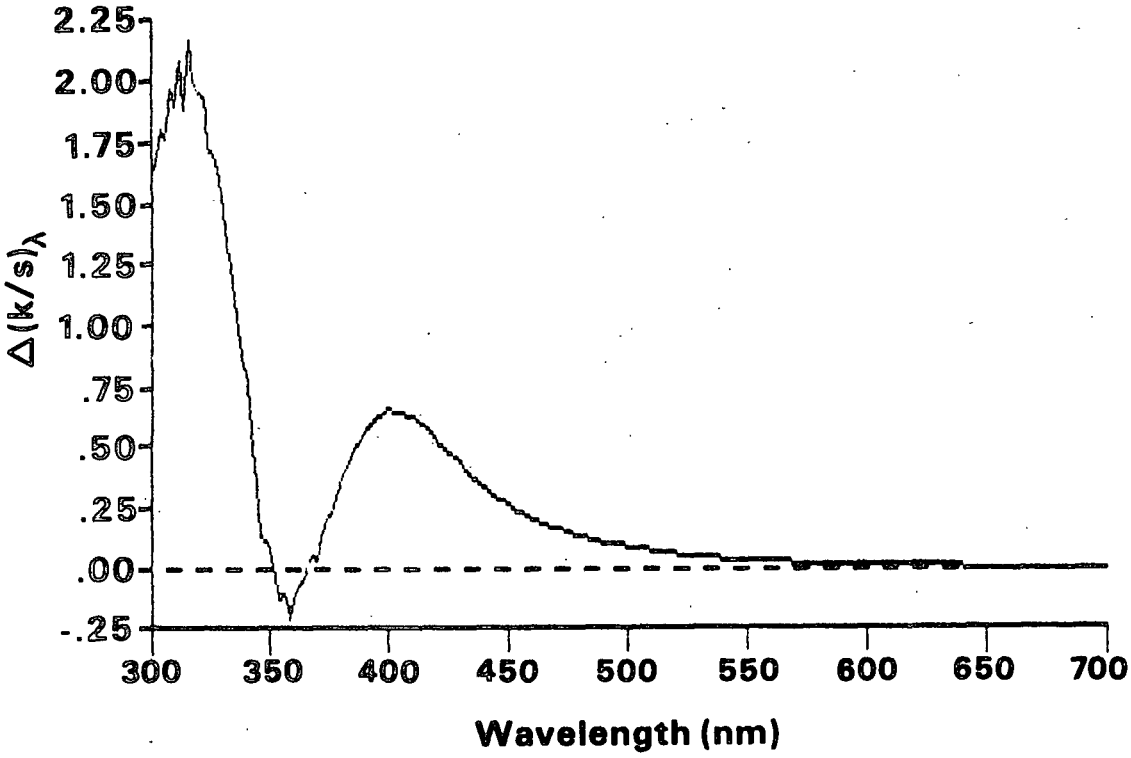

Figure 66. Expanded $\Delta(k/s)_\lambda$ spectrum obtained upon irradiation of a white spruce RMP sheet for 20 hours with simulated sunlight.

obtained upon impregnation of the model occurred at approximately 360 nm. One reason for this observed shift may be that in the wavelength range from 350-700 nm, the $\Delta(k/s)_\lambda$ spectrum obtained upon exposure of this sheet had a weak negative band. The wavelength minimum of this band was around 360 nm. The appearance of this band indicated that some structures in this pulp (i.e., structures which absorb in this region of the spectrum) were photochemically degraded during the yellowing process. Assuming that the absorption band of this degraded product, which has been observed by others,[135] overlaps the absorption band of the colored products formed upon irradiation of this pulp, then this overlap could theoretically account for the observed differences in wavelength maxima. Another possibility would be that the products formed during exposure of the pulp is similar to, but not identical to, the simple quinone models examined here.

In the visible region of the spectrum, the yellowed sheet sample had considerably higher absorbance than the sheet sample impregnated with the para-quinone model. On the basis of Fig. 64 and 65 it appears that this increased absorbance of the "yellowed" sheet in the longer wavelength range may be due to the formation of ortho-quinonoid lignin structures. Thus, while these results do not conclusively show that quinonoid lignin structures are formed during the yellowing process, they are at least consistent with it.

Diffuse Reflectance FTIR and Raman Spectroscopic Analysis of "Yellowed" Pulp

In the diffuse reflectance FTIR spectroscopic analysis of the pulp oxidized with Fremy's salt, an increase in the area under the 1665 cm^{-1} band was observed. For reasons stated earlier, this increase was attributed to the formation of ortho-quinonoid lignin structures. On the basis of this result, it was hypothesized that if quinonoid lignin structures are formed during the yellowing

process, then the area under the 1665 cm^{-1} absorption band of the lignin present in the "yellowed" pulp should increase.

When three "yellow" pulp samples prepared by irradiation with simulated sunlight were analyzed, the results shown in Table 13 were obtained. As expected, the area under the 1665 cm^{-1} band increased from an average of 5.73 to an average of 6.36 cm^{-1}. As before, this increase was attributed to the formation of quinonoid lignin structures.

Table 13. Normalized area under the 1665 cm^{-1} band of unirradiated and sunlight irradiated[a] pulps.

Pulp Sample Analyzed	Area Under 1665 cm^{-1} Band (cm^{-1})[b]
Unirradiated	5.73 ± 0.12[c]
Sunlight irradiated-1	6.20
Sunlight irradiated-2	6.30
Sunlight irradiated-3	6.64

[a]Irradiated for 20 hours in a solar simulator.
[b]Normalized using 1510 cm^{-1} aromatic absorption band of lignin.
[c]Mean value ± 90% confidence interval.

In an attempt to determine the types of quinonoid lignin structures formed in "yellowed" sheets, Raman spectroscopic analysis was conducted. The Raman spectra obtained in this analysis are shown in Fig. 67. As this figure shows, the Raman spectrum obtained from a yellowed pulp sheet had a reproducible shoulder in the 1550-1570 cm^{-1} region of the spectrum. This shoulder was similar to the shoulder observed in the Raman spectra of a sheet formed from the pulp oxidized with Fremy's salt and of a sheet impregnated with the model, 3-methoxy-ortho-benzoquinone. As in these earlier spectra, the location of this shoulder was also consistent with the location of the Raman bands of the two ortho-quinone models, I and III. A second shoulder was also observed in the

1660-1690 cm^{-1} region (i.e., the region where the C=O stretching bands of the models were observed). Together with the results of the FTIR analysis of this pulp, this result supports the conclusion that ortho-quinonoid lignin structures are formed during the yellowing process.

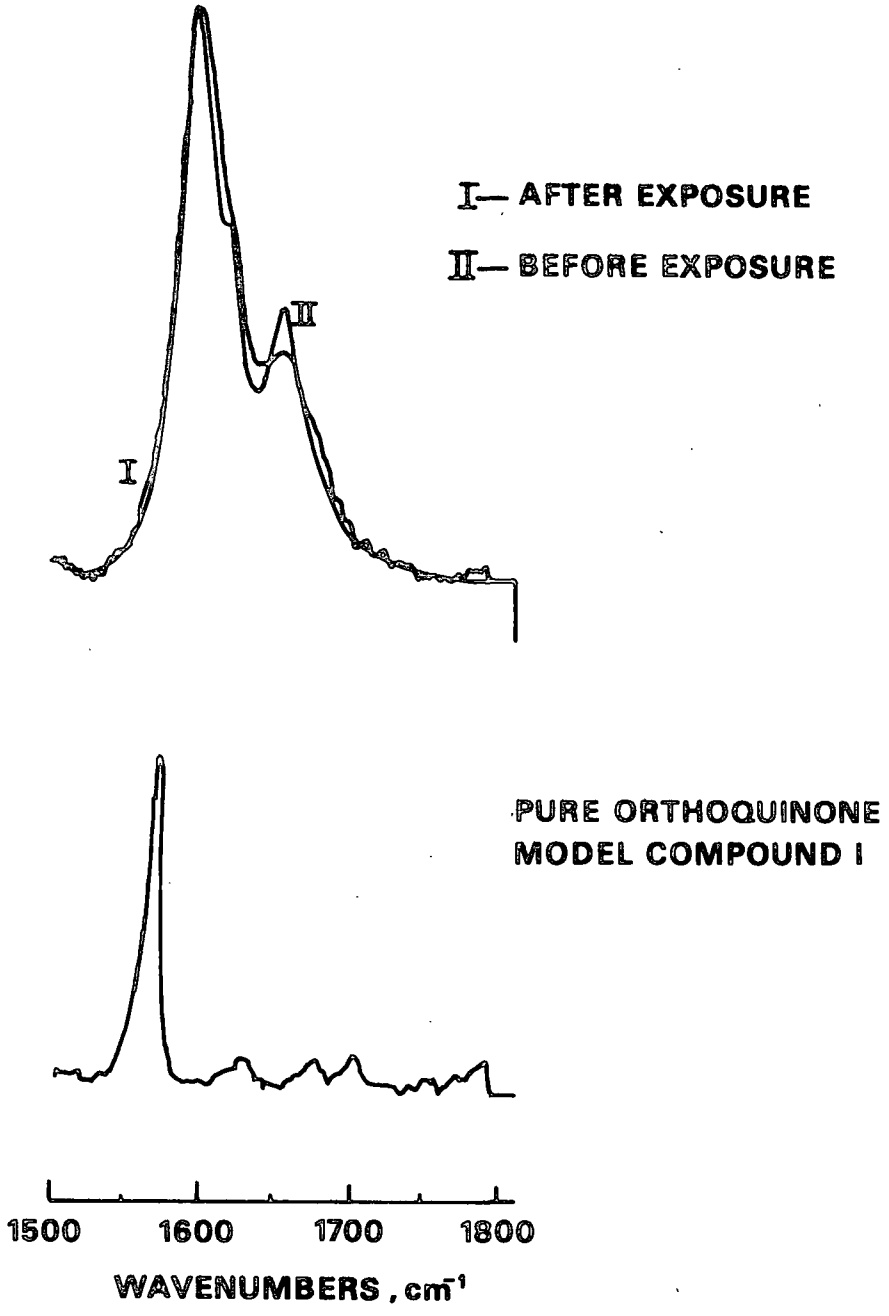

Figure 67. Raman spectra of white spruce RMP sheet before and after exposure to 20 hours of simulated sunlight.

Another point which supported this conclusion was that in the Raman analysis of the "yellowed" pulp sheet, a visible light induced bleaching was observed. As noted earlier, this light induced bleaching was also observed in the analyses of the pulp sheets oxidized with Fremy's salt and impregnated with the model, 3-methoxy-ortho-benzoquinone. Since this observation was considered interesting, it was examined in more detail using diffuse reflectance UV-visible analysis. In this analysis, the "bleaching" effects of two wavelengths of visible light were examined, 514.5 and 457 nm. This light was provided by an argon ion laser and was strictly monochromatic and of relatively high intensity.

The ΔR_∞ spectra obtained upon exposure of pulp sheets irradiated for 20 hours with simulated sunlight and formed from pulp oxidized with Fremy's salt to 514.5 and 457 nm light are shown in Fig. 68 and 69, respectively. As these figures show, both the "yellowed" pulp sheet and the Fremy's salt oxidized pulp sheet were bleached by 514.5 and 457 nm light. In both experiments, the total amount of bleaching obtained for the Fremy's salt pulp was slightly greater than for the "yellow" pulp. Also, while the ΔR_∞ spectra obtained upon irradiation of the sheets formed from the oxidized pulp with 514.5 and 457 nm light were fairly similar, the ΔR_∞ spectra obtained upon irradiation of the "yellowed" pulp sheets were not. For instance, the positive band observed in the spectrum obtained from the 514.5 nm irradiation had a wavelength maximum at approximately 495 nm, and the negative band observed in this spectrum had a wavelength minimum at about 390 nm. In the spectrum of the 457 nm irradiated sample, the positive band had a wavelength maximum at approximately 455 nm, and the negative band had a wavelength minimum at about 375 nm.

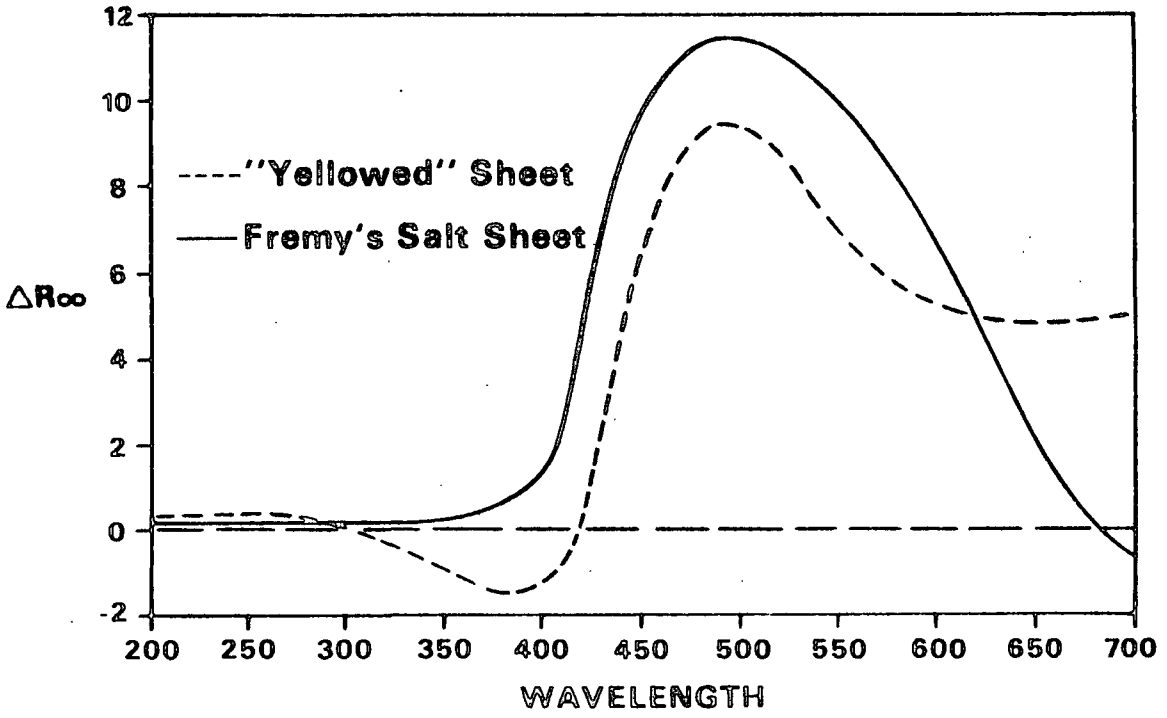

Figure 68. ΔR_∞ spectra obtained upon irradiation of sunlight irradiated and Fremy's salt oxidized white spruce RMP sheets with 514.5 nm laser light.

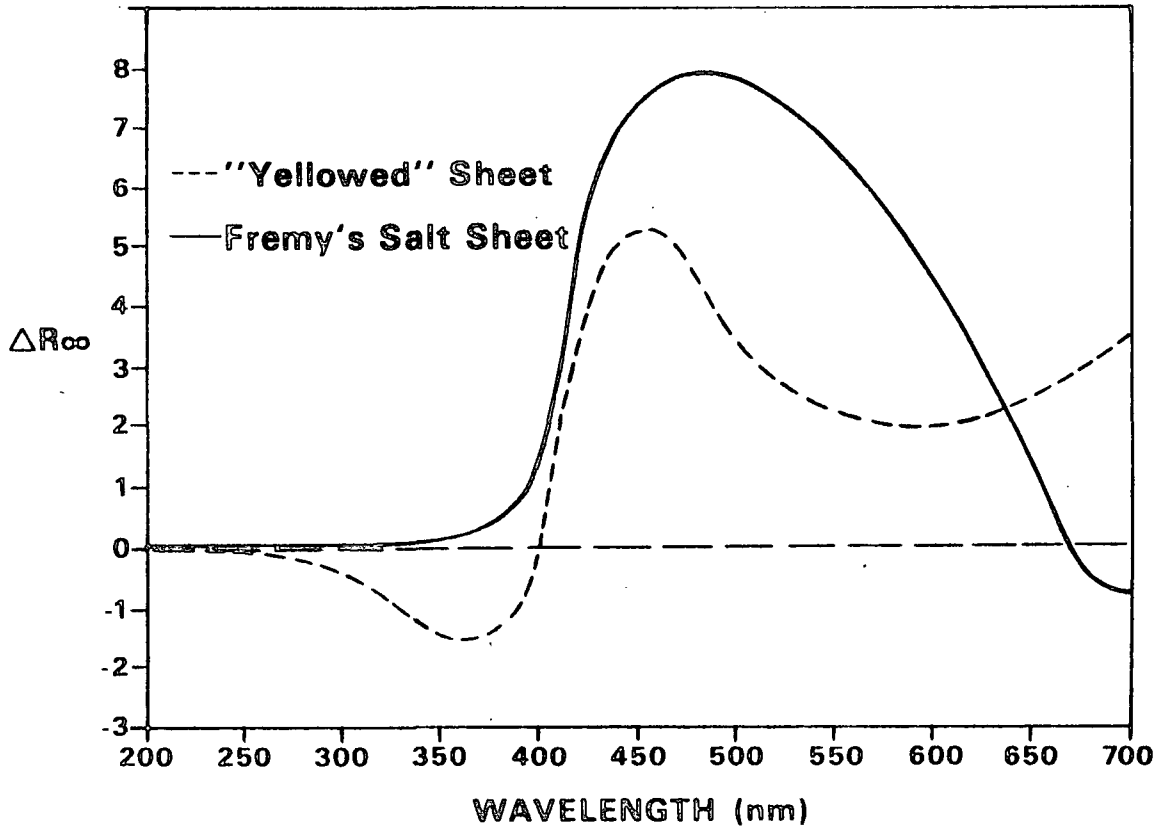

Figure 69. ΔR_∞ spectra obtained upon irradiation of sunlight irradiated and Fremy's salt oxidized white spruce RMP sheets with 457 nm laser light.

The $\Delta(k/s)_\lambda$ spectra obtained upon irradiation of these samples were also similar (Fig. 70 and 71). For instance, Fig. 70 shows that the $\Delta(k/s)_\lambda$ spectra obtained upon irradiation of the oxidized sheets with 514.5 nm light were qualitatively quite similar, and the $\Delta(k/s)_\lambda$ spectra obtained upon irradiation of the sunlight irradiated sheets with 514.5 and 457 nm light displayed a similar shift in wavelength maxima (Fig. 71). While the results obtained here are somewhat limited, they do demonstrate quite clearly that the ortho-quinonoid lignin structures present in the Fremy's salt pulp react photochemically. They also indicated that the "yellowed" (i.e., sunlight irradiated) pulp contains at least some photochemically reactive ortho-quinonoid lignin structures. On the basis of the intensity of the light used in these experiments and the overall magnitudes of the spectra obtained, it appears, however, that the rate of this reaction is relatively slow.

It should be noted at this point that the findings described above were consistent with those of similar work conducted with an aspen thermomechanical pulp.[127] In this work it was shown that aspen thermomechanical pulp contained chromophoric structures which were, in the presence of oxygen, degraded to colorless substances by blue-green light. It was also shown that more of these chromophoric structures were formed when this pulp was irradiated in the presence of oxygen with UV light. These structures, which were postulated to be quinonoid in nature, were also degraded to colorless substances by blue-green light.

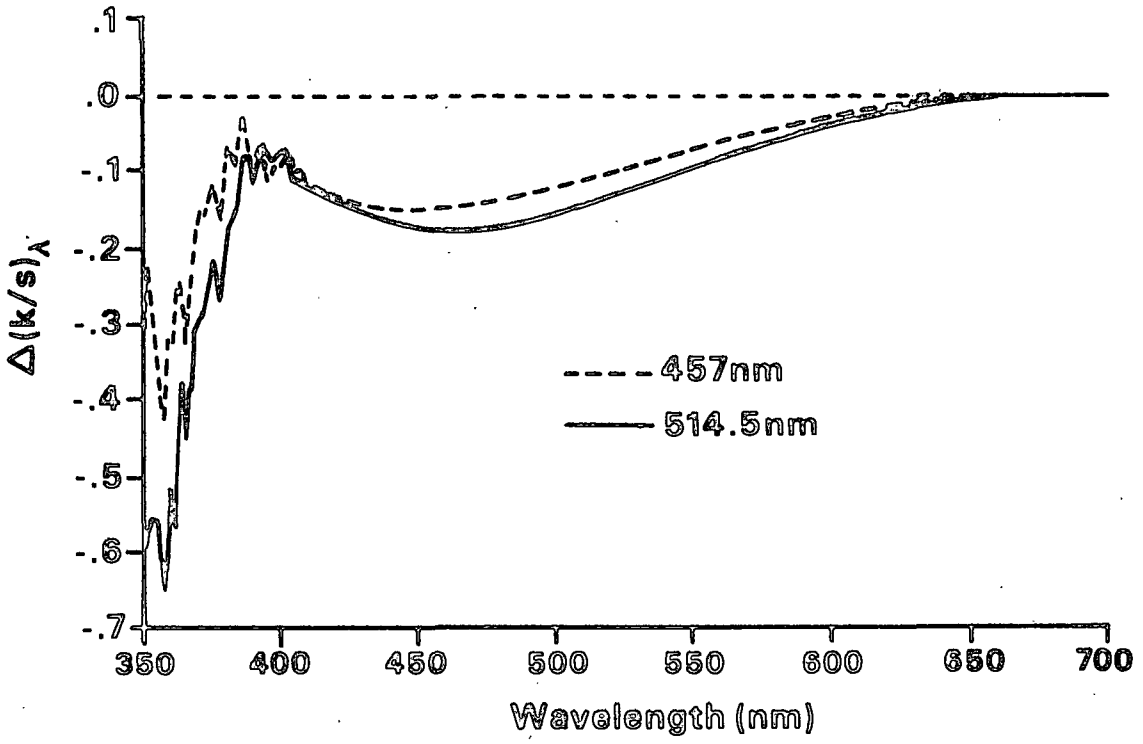

Figure 70. $\Delta k/s)_\lambda$ spectra obtained upon irradiation of Fremy's salt oxidized white spruce RMP sheets with 457 and 514.5 nm laser light.

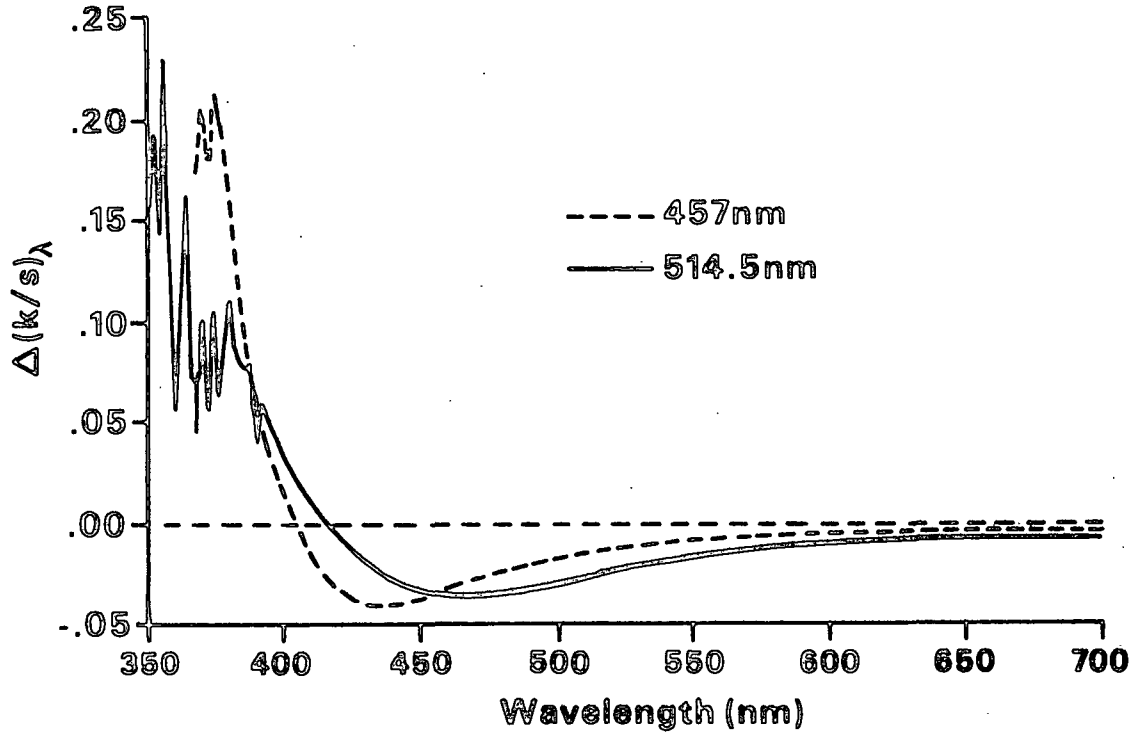

Figure 71. $\Delta(k/s)_\lambda$ spectra obtained upon irradiation of sunlight irradiated white spruce RMP sheets with 457 and 514.5 nm laser light.

Reactions of "Yellowed" Pulp Sheets with Sulfur Dioxide and Sodium Dithionite

When exposed to simulated sunlight, handsheets formed from unirradiated white spruce mechanical pulp "yellowed." If, as the above results suggest, this yellowing results from the formation of quinonoid lignin structures, then pulp sheets "yellowed" by sunlight should react with sulfur dioxide and sodium dithionite. This reaction should, in turn, affect the UV-visible spectra of these samples and reduce the area under their 1665 cm^{-1} FTIR absorption bands.

When "yellowed" sheet samples were reacted with sulfur dioxide or sodium dithionite, the brightness of the pulp increased slightly, but, visually, these sheets still appeared yellow in color. The ΔR_∞ spectra obtained upon reaction of these sample sheets were found to be similar to the corresponding ΔR_∞ spectra obtained upon reaction of the unirradiated and Fremy's salt oxidized pulp sheets indicating, at least qualitatively, that the "yellowed" pulp contained reactive ortho-quinonoid lignin structures (Fig. 72).

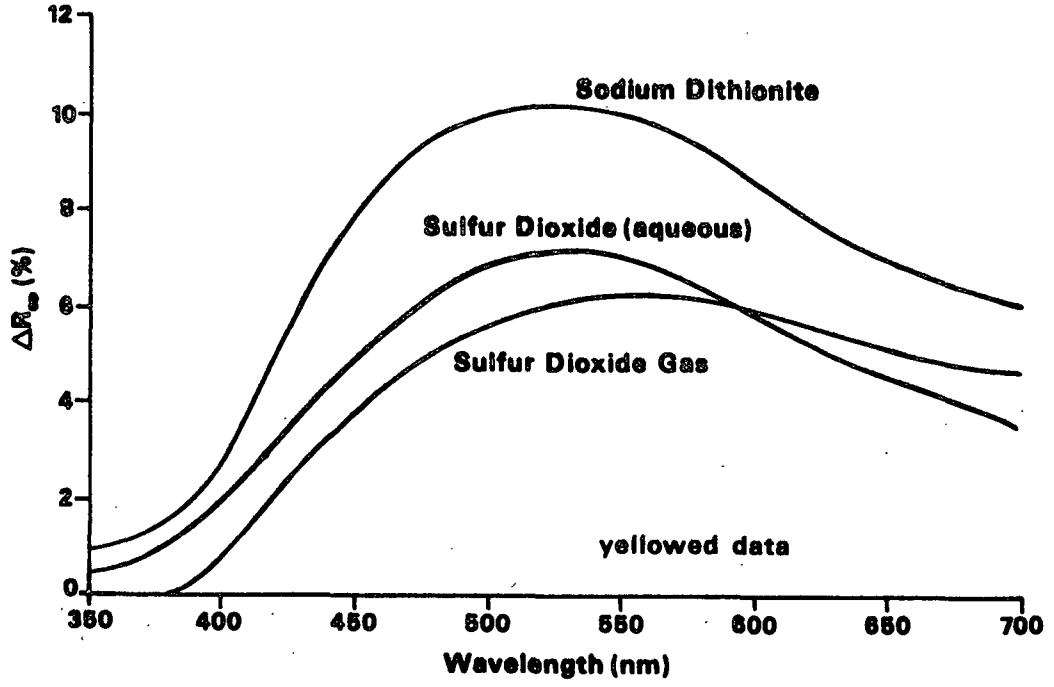

Figure 72. ΔR_∞ spectrum obtained upon reaction of sunlight irradiated white spruce RMP sheets with sulfur dioxide or sodium dithionite.

The $\Delta(k/s)_\lambda$ spectra obtained upon reaction of these samples did not show any clear band in the visible region of the spectrum (Fig. 73). However, all three of the reagents examined here did significantly decrease the absorbance of these "yellowed" sheets in this region. All three of these reagents also decreased the absorbance of the yellowed sheets in the UV region of the spectrum (Fig. 74). Because the magnitudes of these nonquinone related decreases were quite significant, it was difficult to make any firm conclusions about quinone formation. The ΔR_∞ spectra obtained upon reaction of these sheet samples, however, did suggest that ortho-quinonoid structures were formed during the yellowing process.

In order to investigate this point further, "yellowed" pulp and "yellowed" pulp reacted with these reagents were analyzed by diffuse reflectance FTIR spectroscopy. Table 14 gives the areas under the 1665 cm^{-1} band of nonyellowed and yellowed (20 hours of simulated sunlight) white spruce pulp samples. Table 14 also gives the areas under the 1665 cm^{-1} band of yellowed samples treated with sulfur dioxide and with sodium dithionite.

The results presented in Table 14 show that, upon exposure to sunlight, the area under this band increased. The results presented in Table 14 also show that the area under this band decreased when the yellowed pulp was treated with SO_2 or $Na_2S_2O_4$. As in the two earlier cases (i.e., white spruce and Fremy's salt pulps), the magnitudes of these decreases followed the order $SO_{2(g)} < SO_{2(aq)} \leq Na_2S_2O_{4(aq)}$, and the areas remaining under these bands after reduction were approximately the same as was observed earlier. Thus, the results presented in Table 14 clearly show that reactive lignin structures were formed during the yellowing process. As witnessed by the increased absorbance of

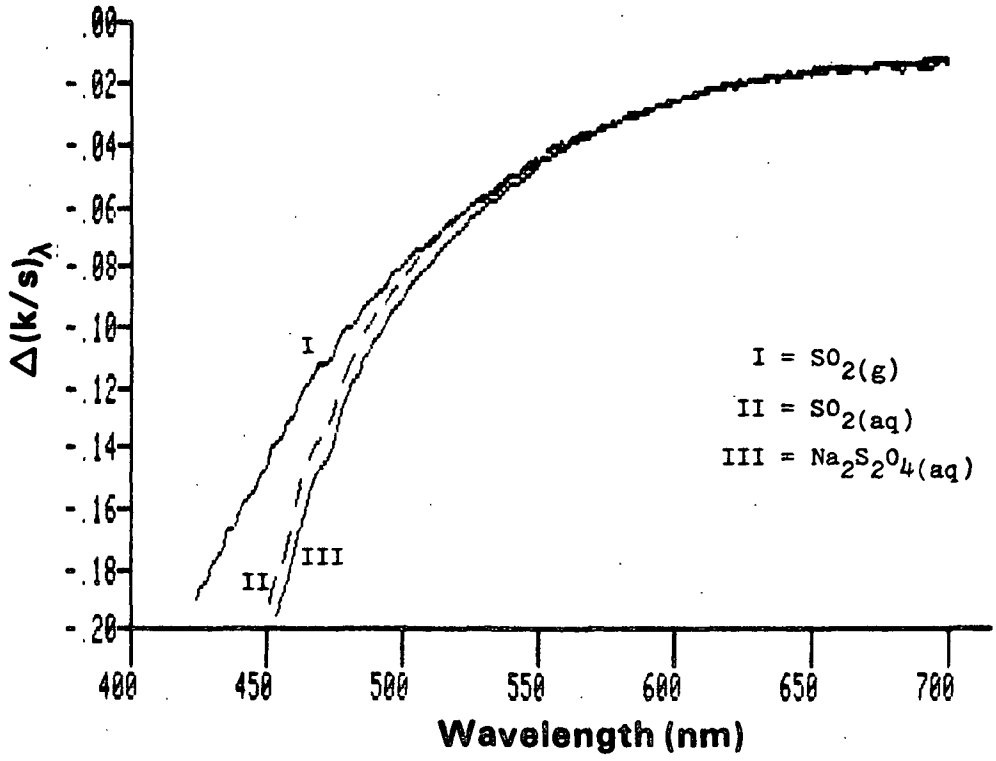

Figure 73. $\Delta(k/s)_\lambda$ spectrum obtained upon reaction of sunlight irradiated white spruce RMP sheets with sulfur dioxide or sodium dithionite (visible region).

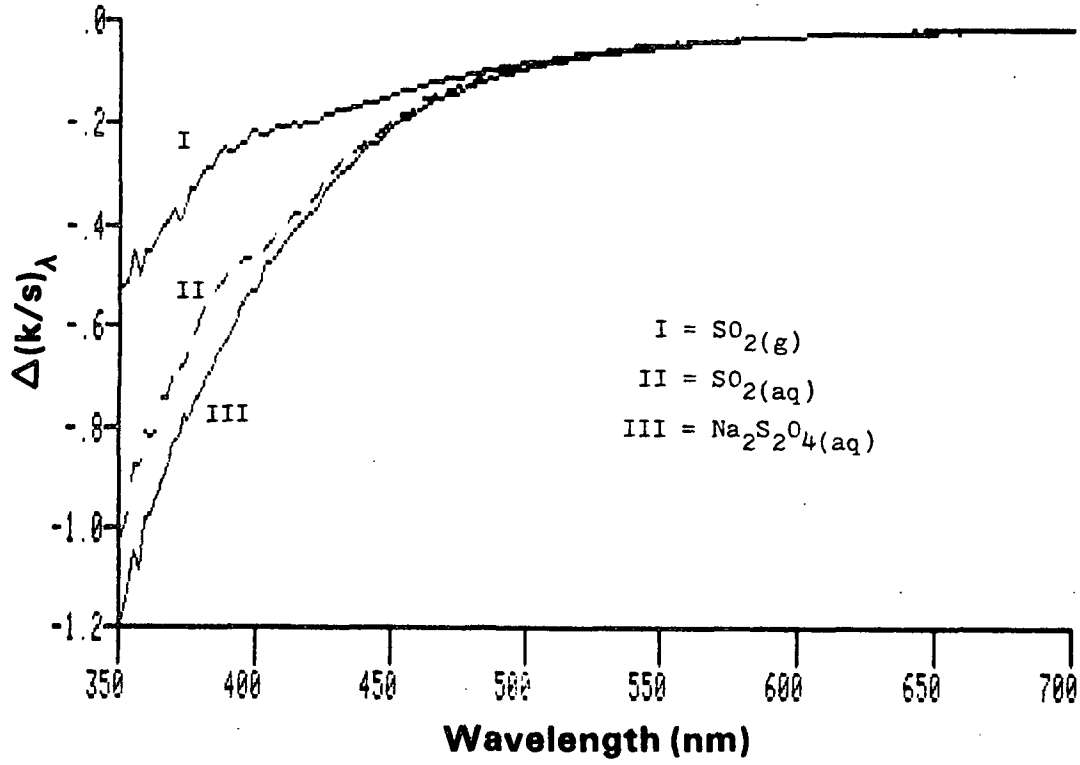

Figure 74. $\Delta(k/s)_\lambda$ spectrum obtained upon reaction of sunlight irradiated white spruce RMP sheets with sulfur dioxide or sodium dithionite (far UV-visible region).

"yellowed" pulp in the 1665 cm^{-1} region of the spectrum, these structures contain C=O functional groups. Thus, together with the results described above, these results show that at least a portion of these reactive structures are ortho-quinonoid lignin structures. These structures, as expected, were easily reduced by sulfur dioxide and sodium dithionite.

Table 14. Normalized area under the 1665 cm^{-1} band of unirradiated pulp, irradiated pulp,[a] and irradiated pulp[a] reduced with the three reagents studied here.

Pulp Sample Analyzed	Area Under 1665 cm^{-1} Band (cm^{-1})[b]
Unirradiated	5.73 ± 0.12[c]
Irradiated	6.38
Irradiated/aqueous SO_2 reduced	5.34
Unirradiated/gaseous SO_2 reduced	5.50
Unirradiated/aqueous sodium dithionite reduced (20°C)	4.96
Unirradiated/aqueous sodium dithionite reduced (60°C)	5.00

[a]Irradiated for 20 hours with simulated sunlight.
[b]Normalized using 1510 cm^{-1} aromatic absorption band of lignin.
[c]Mean value ± 90% confidence interval.

Reaction of "Yellowed" Pulp Sheets with Trimethyl Phosphite

A significant increase in brightness was observed when "yellowed" (4 hours in a solar simulator) pulp sheets were reacted with trimethyl phosphite. The color of these sheets was not, however, completely eliminated. As in the above cases, the ΔR_∞ spectrum obtained upon reaction of a sheet sample had one broad band (Fig. 75). The shape of this band was qualitatively similar to the shape of the bands observed in the ΔR_∞ spectra obtained upon reaction of white spruce

and Fremy's salt oxidized pulp sheets with this same reagent. The wavelength maximum of this band, however, was slightly blue shifted from those observed in the spectra obtained upon reaction of the white spruce and Fremy's salt oxidized pulp sheets. As in the studies described above, the ΔR_∞ spectrum shown in Fig. 75 was not similar to the ΔR_∞ spectrum obtained upon irradiation of a white spruce sheet (Fig. 76).

The $\Delta(k/s)_\lambda$ spectrum obtained upon reaction of this sample, while quite noisy, was somewhat similar to the $\Delta(k/s)_\lambda$ spectrum obtained upon reaction of the pulp oxidized with Fremy's salt (Fig. 77). It was even more similar, in both shape and magnitude, to the $\Delta(k/s)_\lambda$ spectrum obtained upon irradiation of the pulp sheet (Fig. 78). When compared to the reacted control pulp, this sample had considerably more absorbance in the visible region of the spectrum but considerably less absorbance in the UV region. In fact, in the UV portion of the spectrum, the change in absorbance of the reacted yellow pulp appeared to be less than the change in absorbance observed in the Fremy's salt and control samples described earlier. While the reason for this was not clear, one possible explanation may have been a difference in reaction time (see below). Overall, however, it did appear that this "yellowed" pulp sheet contained some reactive ortho-quinonoid lignin structures.

When the above experiment was conducted at long reaction times with a sample sheet yellowed by exposure to 24 hours of simulated sunlight instead of four, the results presented in Appendix VIII were obtained. As the figures in Appendix VIII show, the spectra obtained under these conditions were qualitatively similar to those presented above. There were, however, some significant differences in these two sets of spectra. First, the magnitudes of the absorption bands observed in these spectra, as expected, were much greater than those

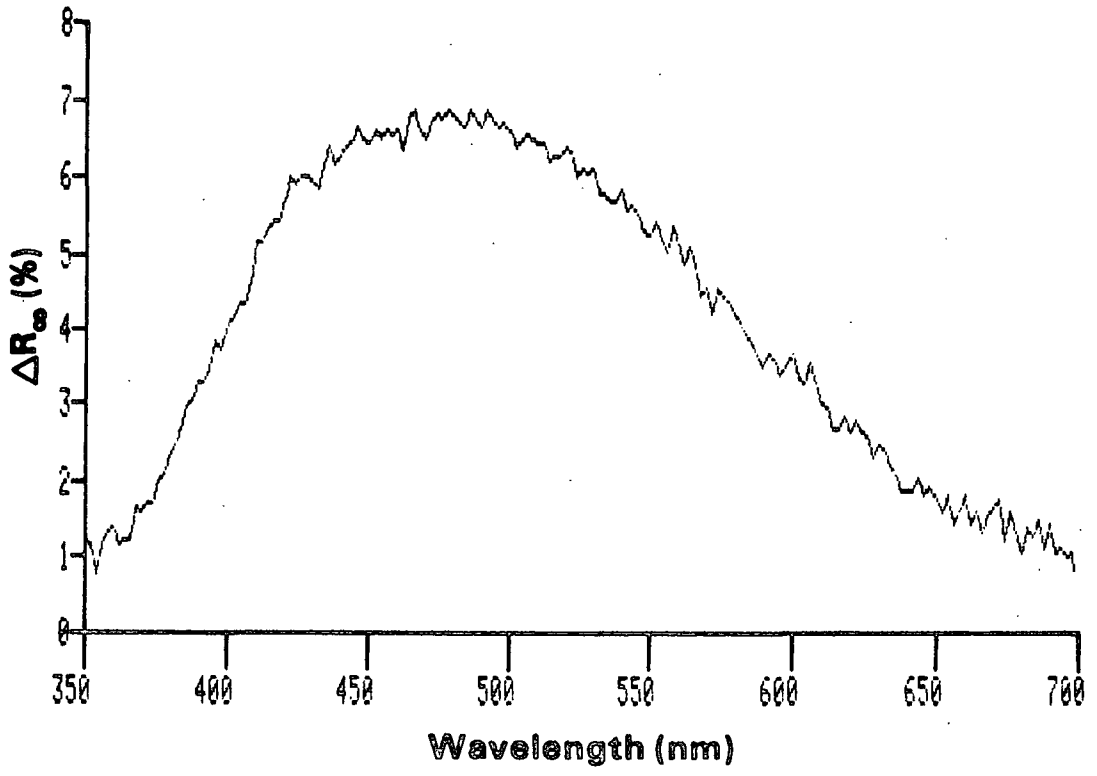

Figure 75. ΔR_∞ spectrum obtained upon reaction of a 4-hour sunlight irradiated white spruce RMP sheet with trimethyl phosphite.

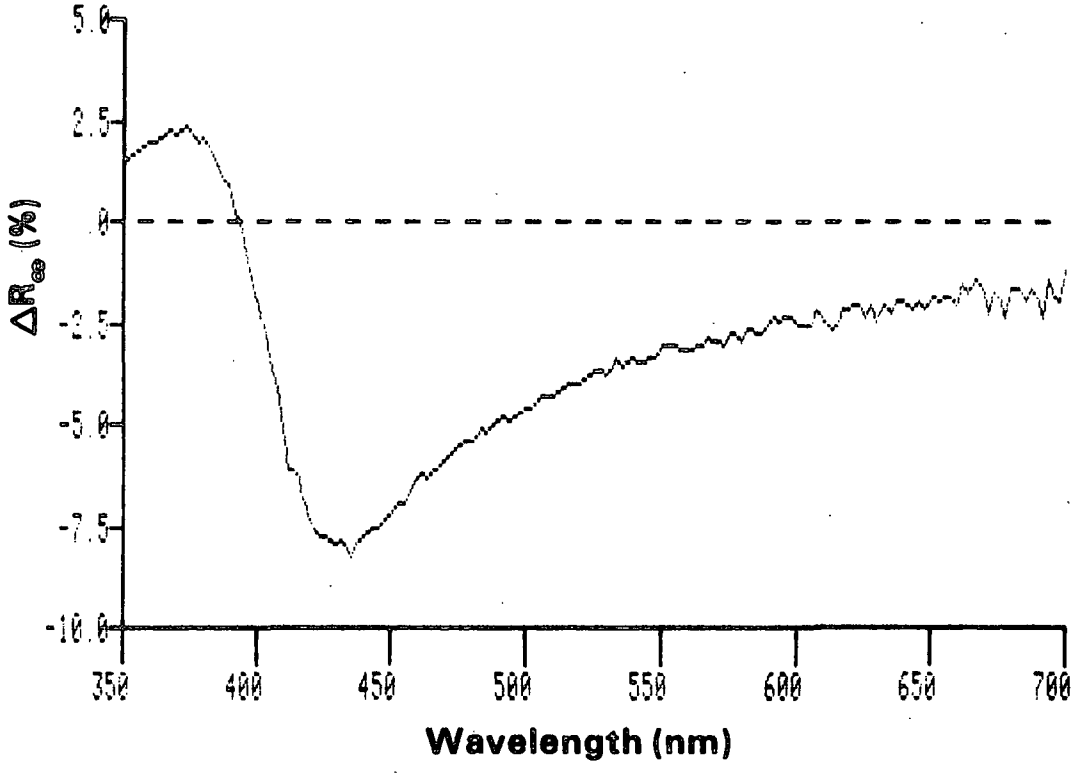

Figure 76. ΔR_∞ spectrum obtained upon irradiation of a white spruce RMP sheet for 4 hours with simulated sunlight.

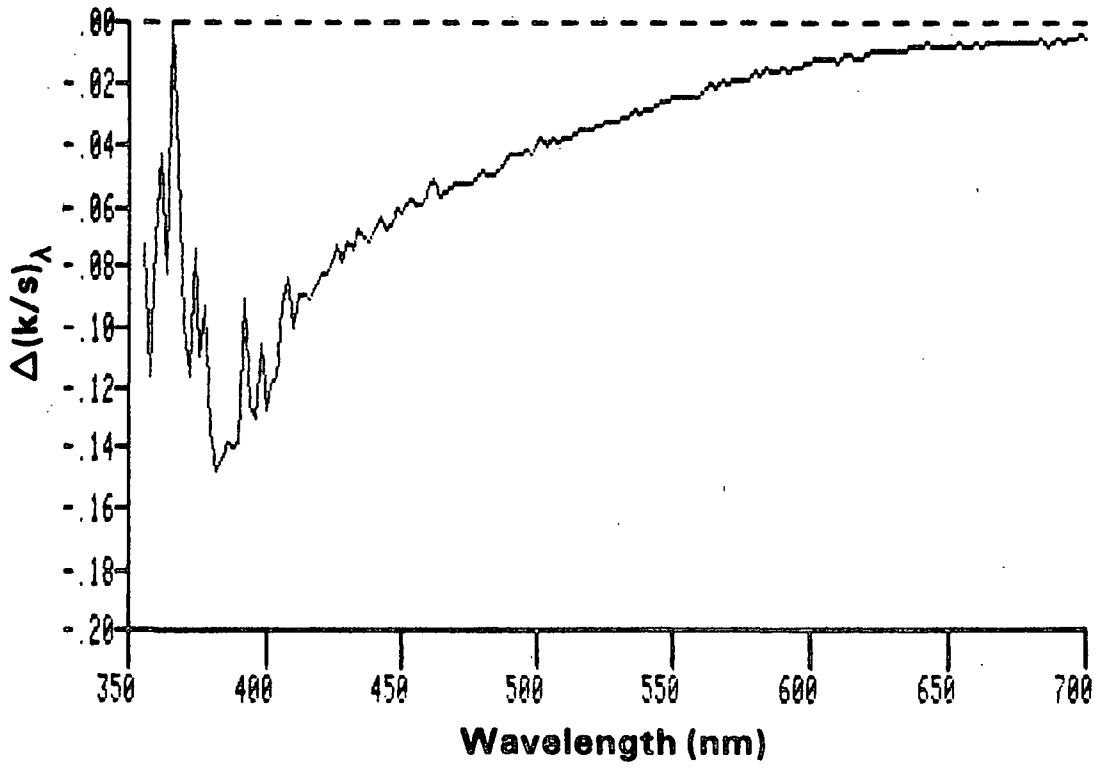

Figure 77. $\Delta(k/s)_\lambda$ spectrum obtained upon reaction of a 4-hour sunlight irradiated white spruce RMP sheet with trimethyl phosphite.

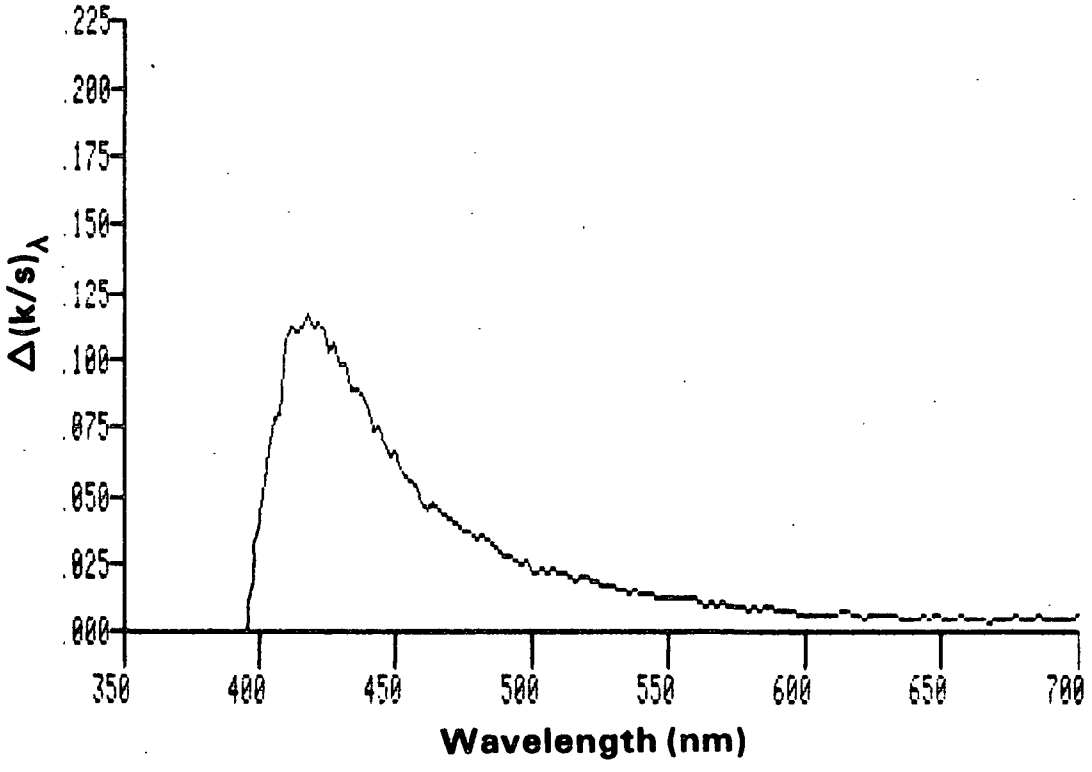

Figure 78. $\Delta(k/s)_\lambda$ spectrum obtained upon irradiation of a white spruce RMP sheet for 4 hours with simulated sunlight.

of the bands observed in the above spectra. A second difference was that the final absorbances of the reacted Fremy's salt and yellowed pulps were significantly less, in both the visible and UV regions, than the absorbance of the reacted control pulp. Thus, at longer reaction times it appeared that these pulps contained more reactive structures than the control pulp.

In an attempt to assess the contributions of the nonlignin components of the above pulp to the spectral changes observed when it was reacted with trimethyl phosphite, unirradiated and irradiated holocellulose and cellulose sheets were studied. The holocellulose used was an acid-chlorite holocellulose prepared from unirradiated pulp. The Klason lignin content of this holocellulose was 1.5% (o.d. basis). The cellulose used in this study was sheets of Whatman No. 1 filter paper.

When a cellulose sheet which had been irradiated for four hours in the solar simulator was analyzed, no significant changes were observed in either the ΔR_∞ or $\Delta(k/s)_\lambda$ spectrum (Fig. 79 and 80). Similar results were obtained when this irradiated sheet was reacted with trimethyl phosphite (Fig. 81 and 82). An unirradiated cellulose sheet did not react with trimethyl phosphite, either. On the basis of these results, two conclusions were made. First, it was concluded that the cellulosic components of the above pulp, on its own, does not yellow, and second, it was concluded that, under the conditions employed here, trimethyl phosphite does not react with cellulose or irradiated cellulose. Thus, the yellowing of the above pulp sheet and its subsequent reactions with trimethyl phosphite must be related to its lignin and/or hemicellulosic components.

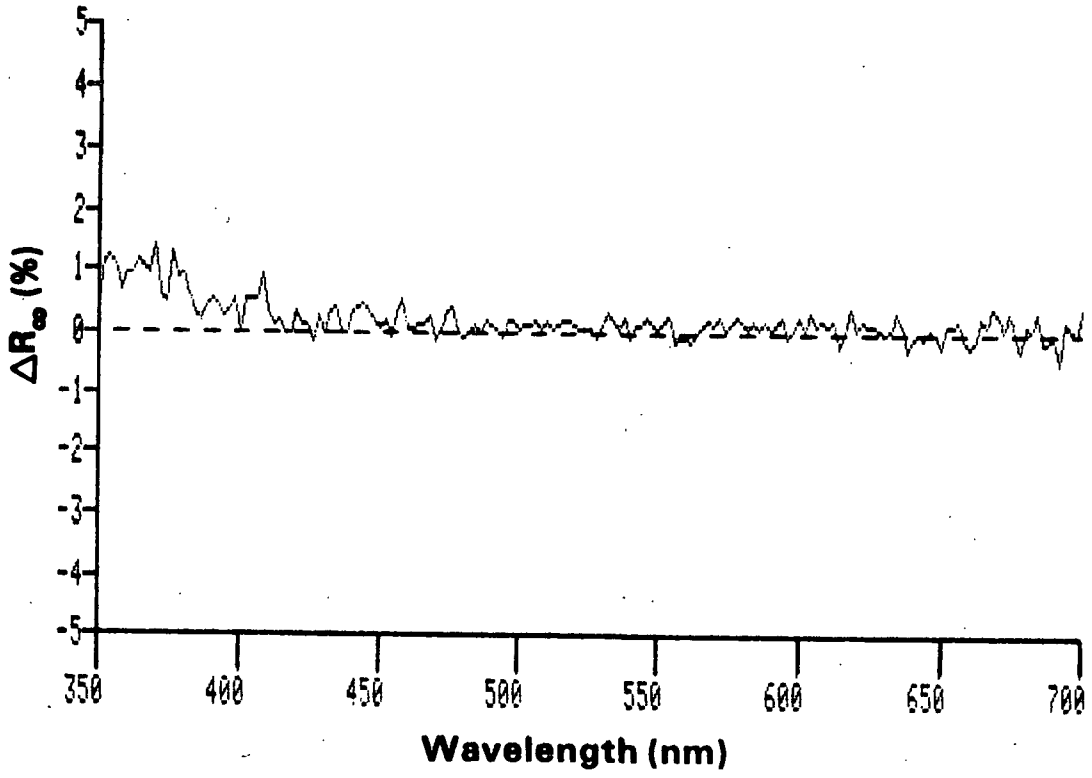

Figure 79. ΔR_∞ spectrum obtained upon irradiation of a cellulose sheet for 4 hours with simulated sunlight.

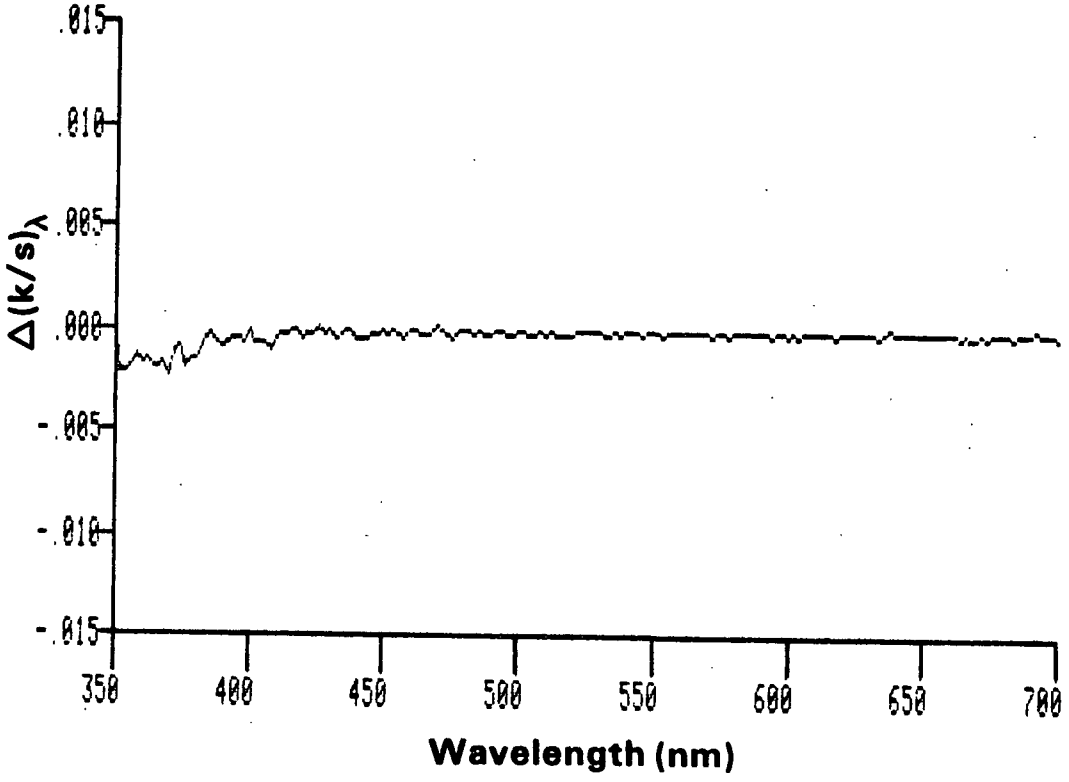

Figure 80. $\Delta(k/s)_\lambda$ spectrum obtained upon irradiation of a cellulose sheet for 4 hours with simulated sunlight.

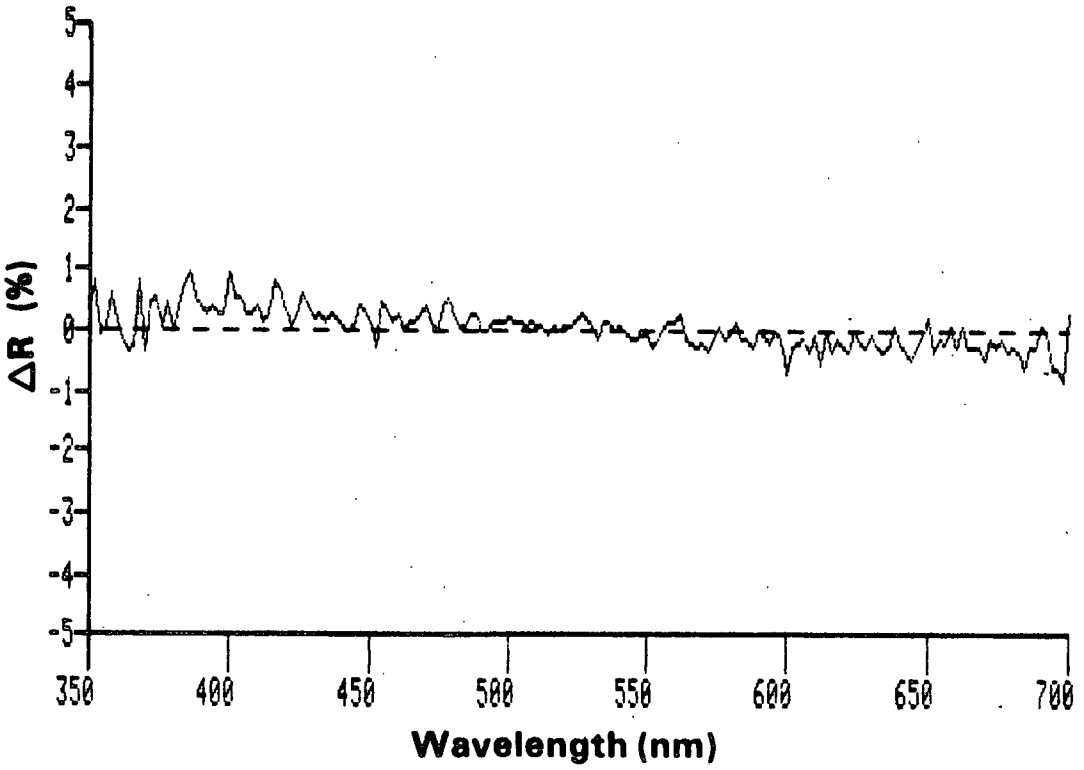

Figure 81. ΔR_∞ spectrum obtained upon reaction of a 4-hour sunlight irradiated cellulose sheet with trimethyl phosphite.

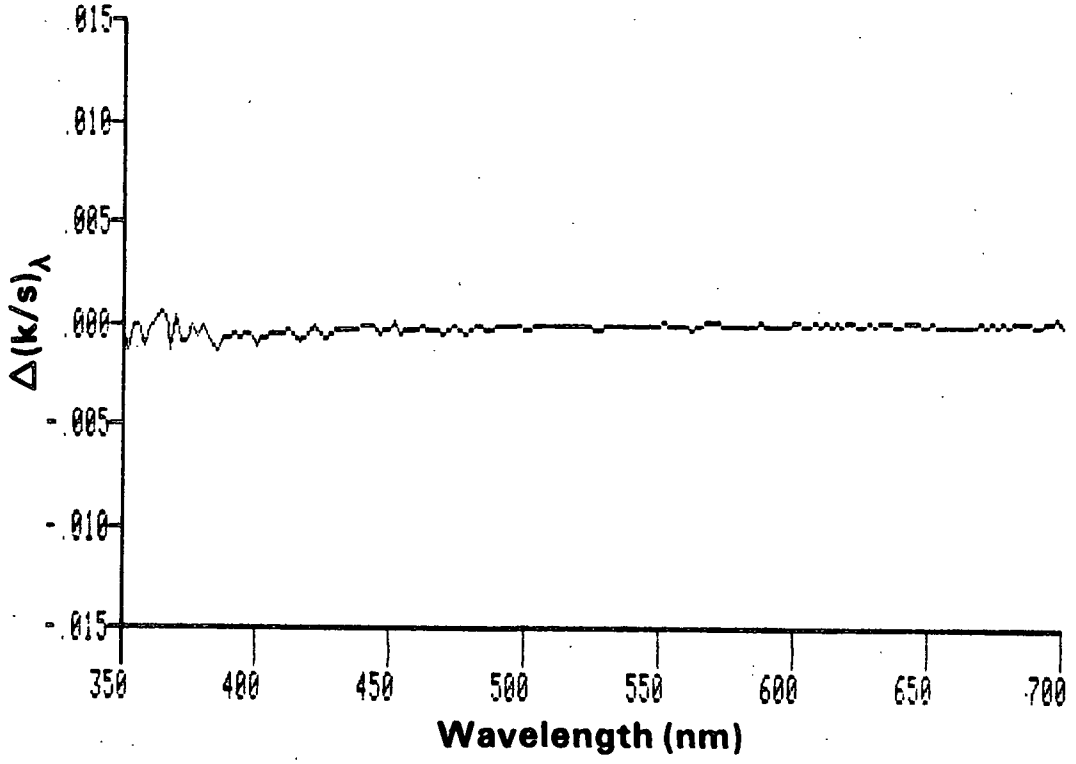

Figure 82. $\Delta(k/s)_\lambda$ spectrum obtained upon reaction of a 4-hour sunlight irradiated cellulose sheet with trimethyl phosphite.

The ΔR_∞ spectrum obtained by subtracting the R_∞ spectrum of an unirradiated white spruce sheet from the R_∞ spectrum of a sheet prepared from the acid-chlorite holocellulose used in this study had two absorption bands; one in the visible and one in the UV region of the spectrum (Fig. 83). The band in the visible region was broad and weak and had a wavelength maximum at 525 nm. The band in the UV region was strong and had a wavelength maximum at 380 nm. The $\Delta(k/s)_\lambda$ spectrum had a very weak band in the visible and a very strong band in the UV (Fig. 84). The wavelength minimum of the UV band was 365 nm. Because the scattering properties of this holocellulose were not independently examined, the difference spectra presented above must be regarded as approximations of the "real" spectra of this sample.

The ΔR_∞ spectrum obtained upon reaction of this holocellulose sheet with trimethyl phosphite showed little change (Fig. 85). The $\Delta(k/s)_\lambda$ spectrum had a broad band with a wavelength minimum at 360 nm, but this band was very weak (Fig. 86). Thus, it appears that trimethyl phosphite does not react to any great extent with the holocellulosic component of the unirradiated pulp.

Surprisingly, when this holocellulose sample was exposed to four hours of simulated sunlight, it turned quite yellow. The ΔR_∞ spectrum obtained upon exposure of this holocellulose sheet to sunlight had a very broad band, and the wavelength minimum of this band occurred at approximately 390 nm (Fig. 87). This band also had a strong shoulder in the visible region of the spectra. Except for an increased absorbance in the visible region of the spectrum, the $\Delta(k/s)_\lambda$ spectrum obtained upon exposure of this sample was similar to the $\Delta(k/s)_\lambda$ spectra obtained from the initial holocellulose analysis (Fig. 88). This result suggested that the same structures removed or degraded by the acid chlorite treatment were somehow reformed when the holocellulose was irradiated with sunlight.

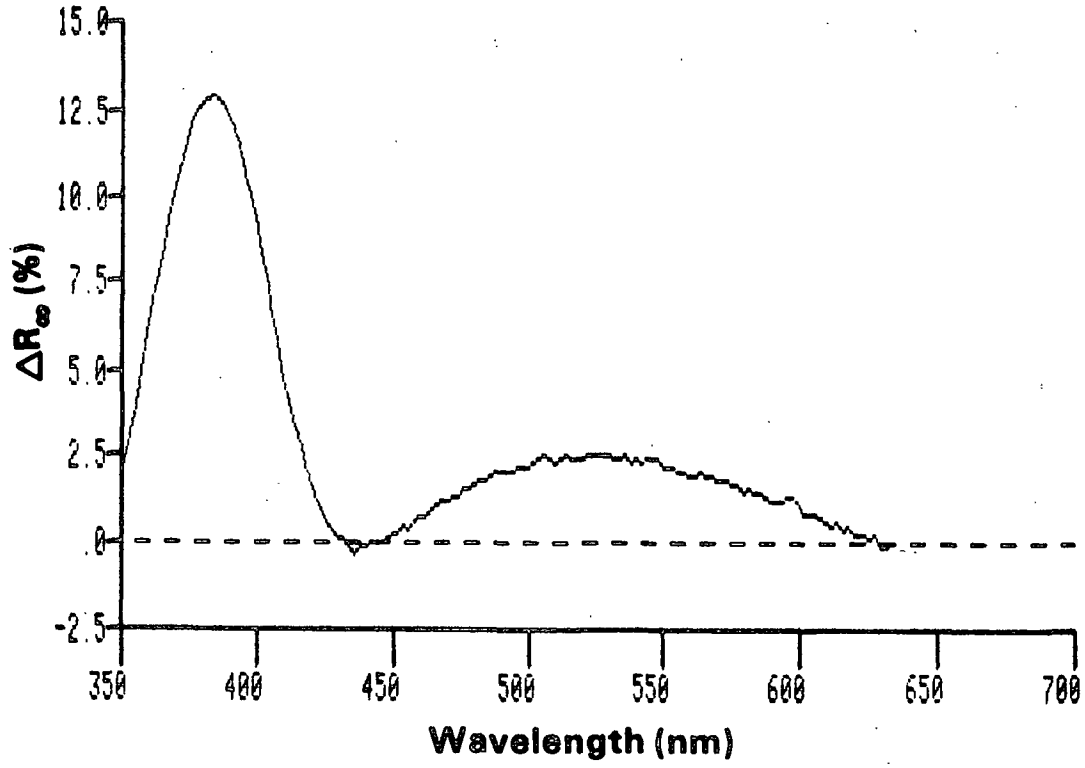

Figure 83. ΔR_∞ spectrum obtained using sheets formed from a white spruce pulp and a white spruce holocellulose.

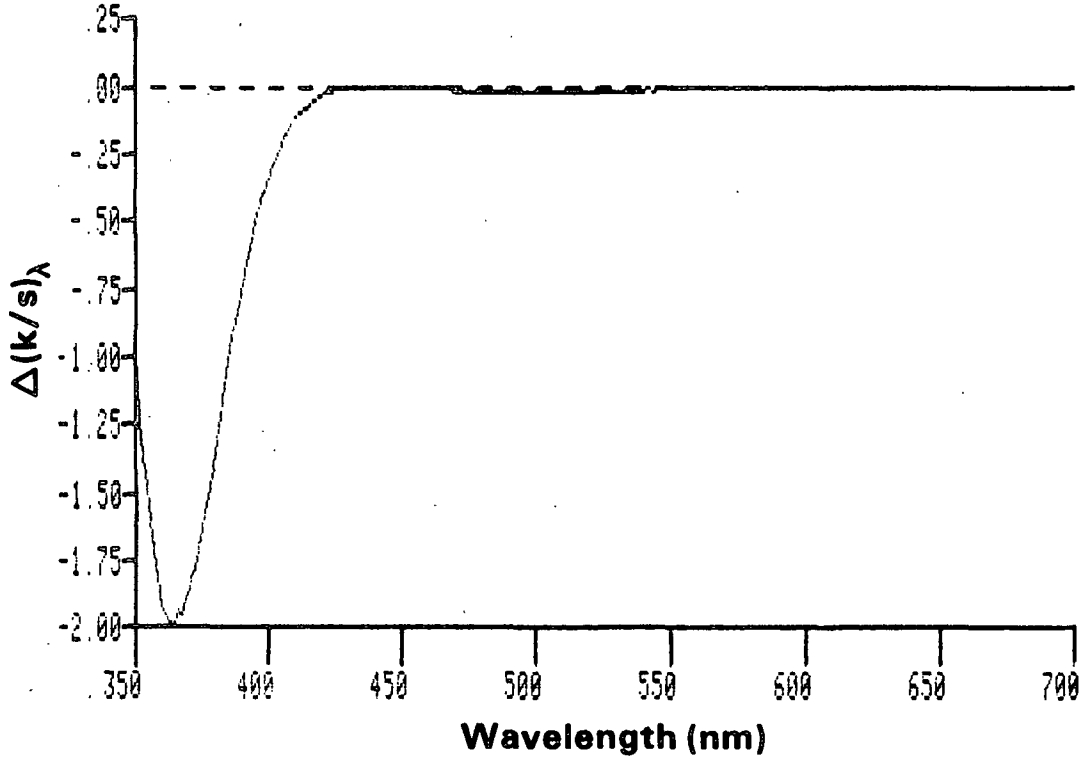

Figure 84. $\Delta(k/s)_\lambda$ spectrum obtained using sheets formed from a white spruce pulp and a white spruce holocellulose.

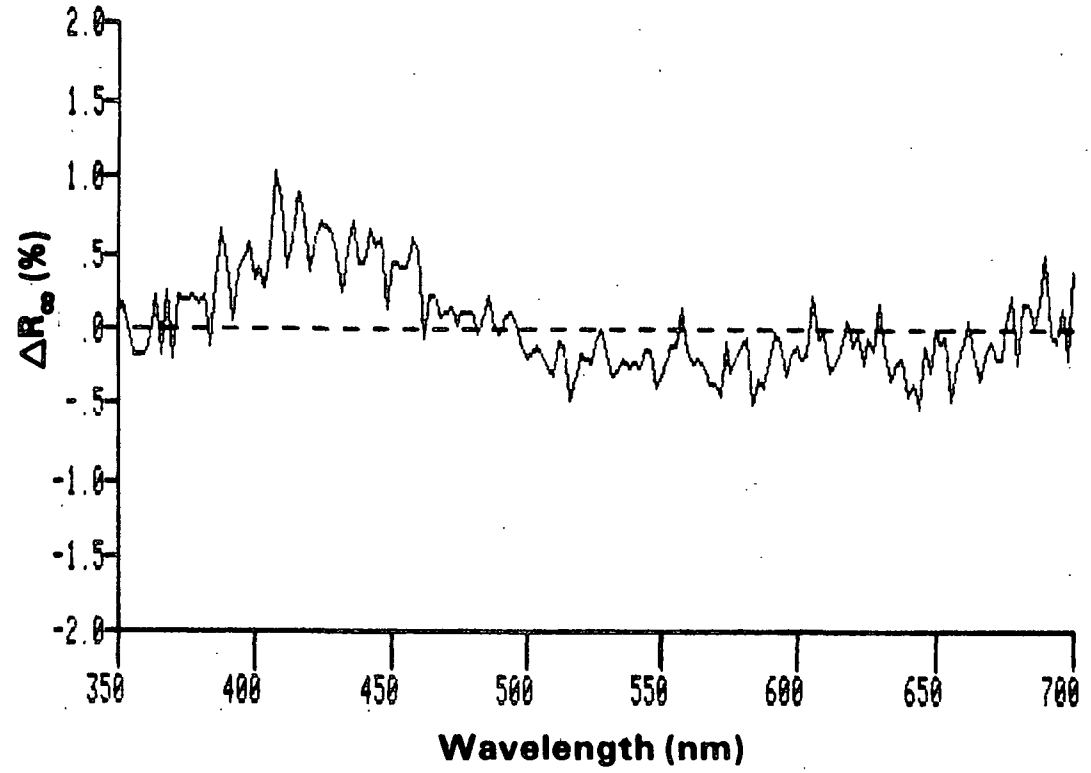

Figure 85. ΔR_∞ spectrum obtained upon reaction of a white spruce holocellulose sheet with trimethyl phosphite.

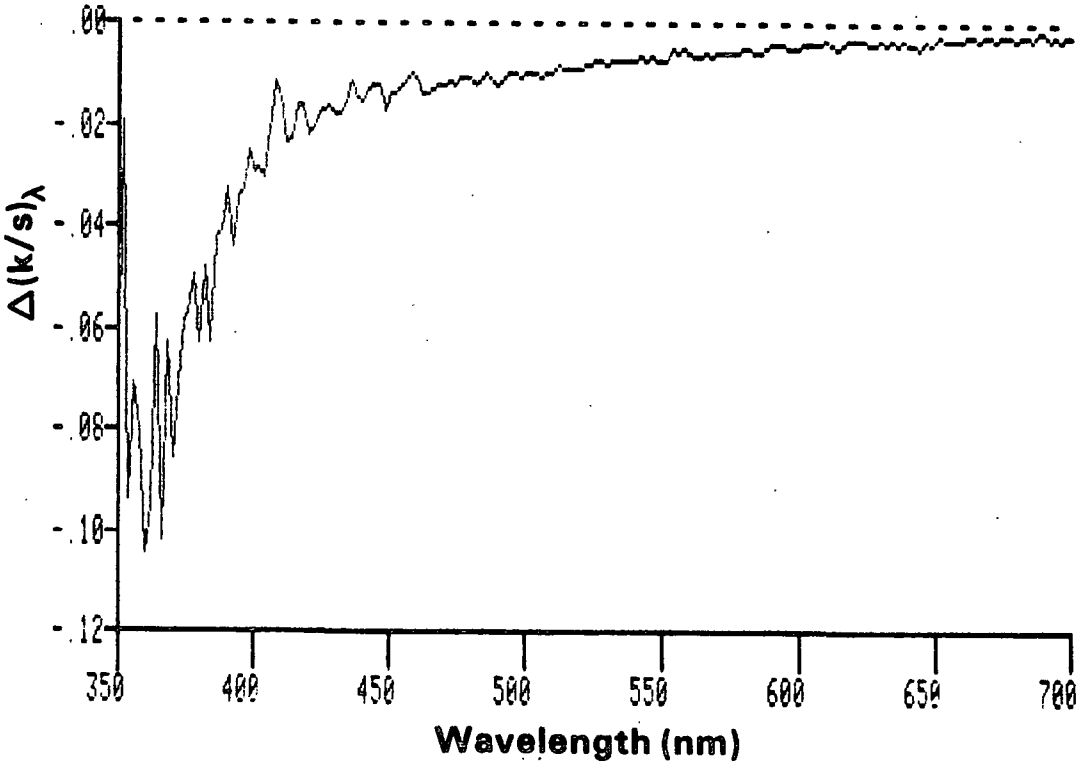

Figure 86. $\Delta(k/s)_\lambda$ spectrum obtained upon reaction of a white spruce holocellulose sheet with trimethyl phosphite.

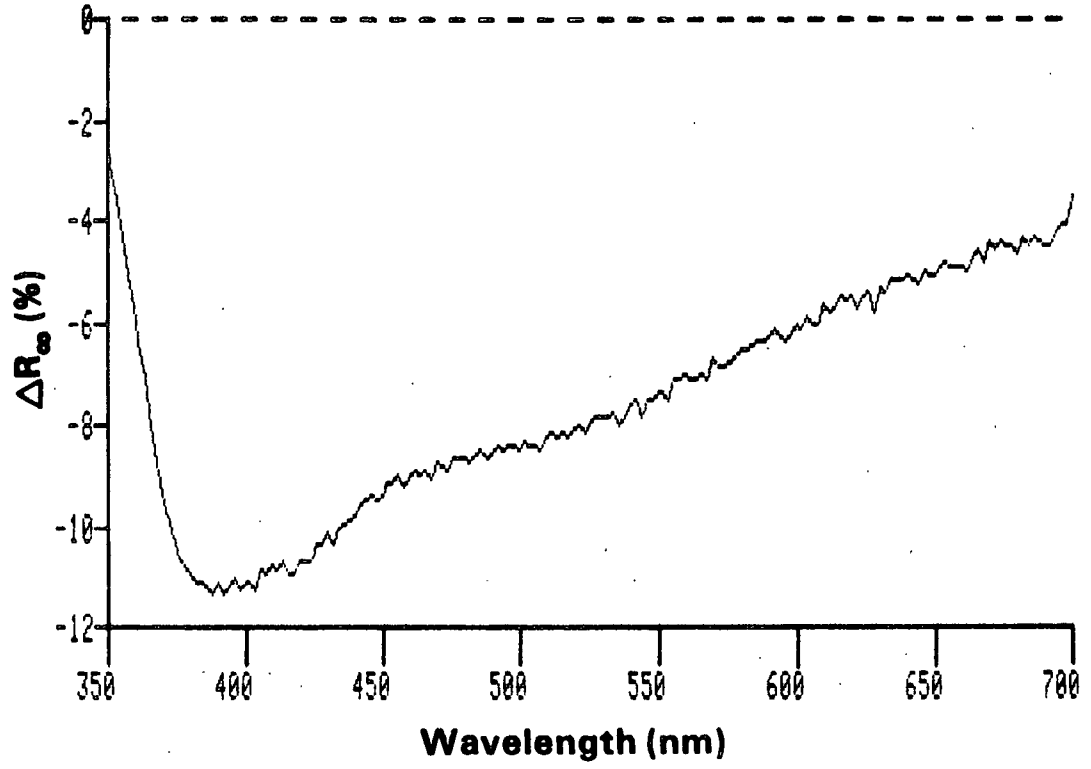

Figure 87. ΔR_∞ spectrum obtained upon irradiation of a sheet formed from a white spruce holocellulose for 4 hours with simulated sunlight.

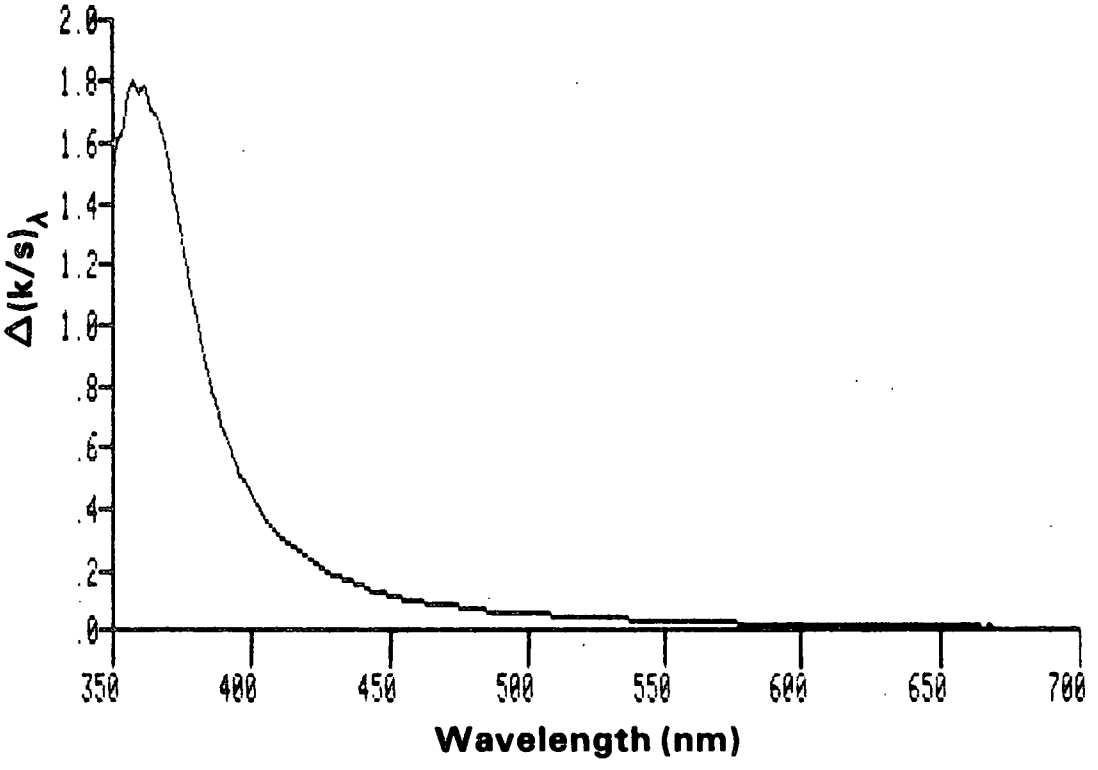

Figure 88. $\Delta(k/s)_\lambda$ spectrum obtained upon irradiation of a sheet formed from a white spruce holocellulose for 4 hours with simulated sunlight.

Overall, the results obtained in this diffuse reflectance UV-visible analysis described above were quite unexpected. Up until now, the photoyellowing of such pulps has been attributed to light induced lignin reactions. In this study, the possible involvement of a nonlignin pulp component was suggested by the fact that the ΔR_∞ and $\Delta(k/s)_\lambda$ spectra obtained in the irradiation of this holocellulose were found to be similar to the spectra obtained in the analysis of the irradiated pulp. Another alternative explanation for the observed yellowing of the holocellulose may be that it resulted from the reactions of the 1.5% lignin which was still present in the holocellulose. If this is the case, then this remaining lignin must be more reactive toward light than was the original lignin.

When the "yellowed" holocellulose sheet described above was reacted with trimethyl phosphite, the color of the sheet was very slightly reduced. The ΔR_∞ spectrum obtained upon reaction of this sample had one broad band (Fig. 89). The wavelength maximum of this band, which was rather weak, occurred at 520 nm. The $\Delta(k/s)_\lambda$ spectrum obtained upon reaction of this sample showed that the absorbance of this sample decreased slightly in the visible region of the spectrum but increased in the UV region of the spectrum (Fig. 90). On the basis of these results and the results described above, it appears that while the acid-chlorite holocellulose sample "yellowed" upon exposure to sunlight, the products responsible for this yellow color did not react with trimethyl phosphite. Thus, the colored structures responsible for the "yellow" color of the irradiated holocellulose were probably not quinonoid type structures formed in the residual 1.5% lignin present in this sample.

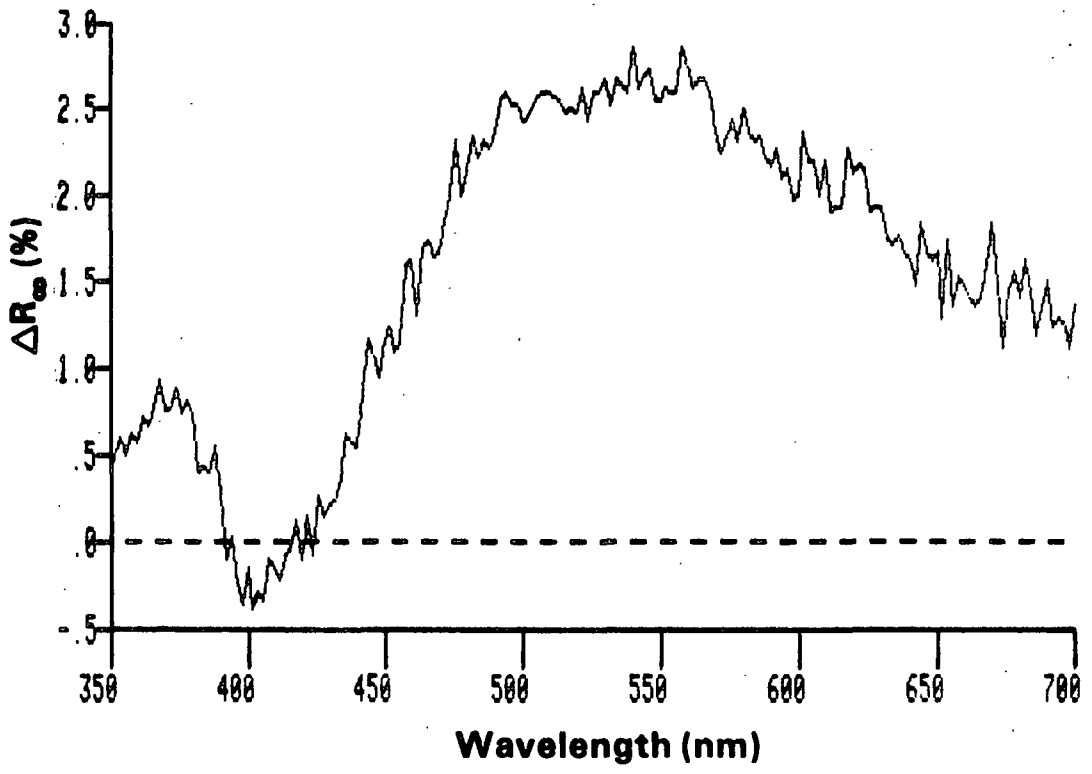

Figure 89. ΔR_∞ spectrum obtained upon reaction of a 4-hour sunlight irradiated holocellulose sheet with trimethyl phosphite.

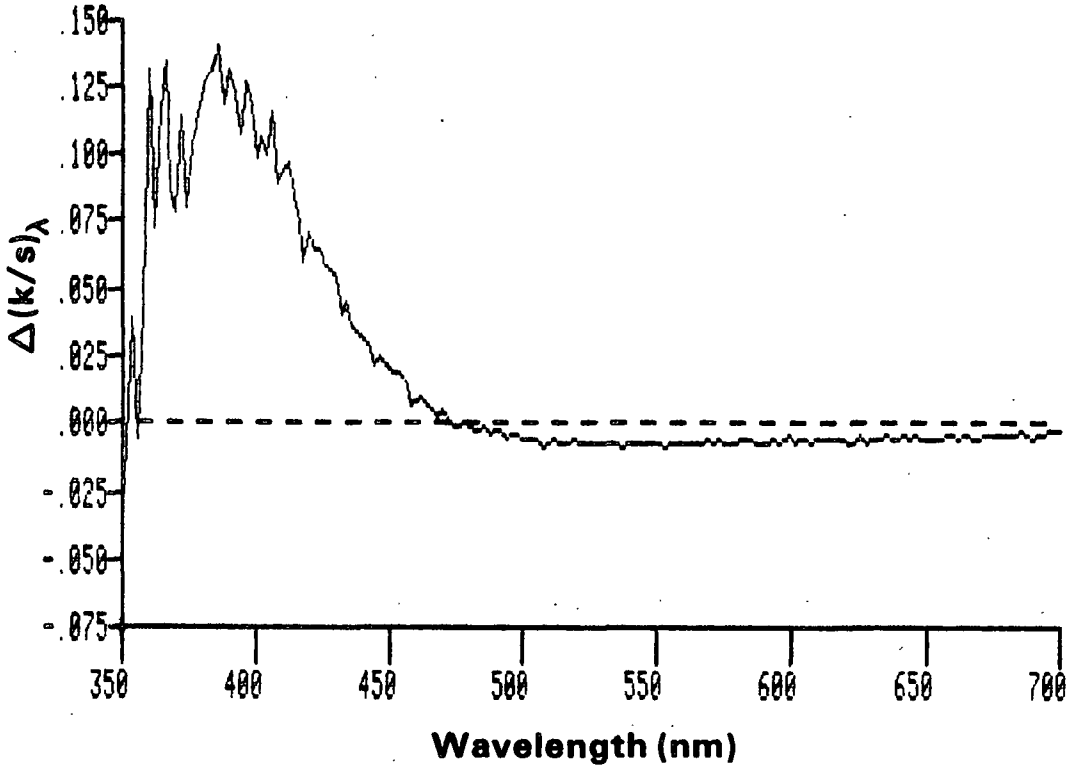

Figure 90. $\Delta(k/s)_\lambda$ spectrum obtained upon reaction of a 4-hour sunlight irradiated holocellulose sheet with trimethyl phosphite.

In an attempt to further investigate the nature of the reactive structures present in the unirradiated and irradiated pulp and in the irradiated holocellulose, the reactions of trimethyl phosphite with the above samples were examined using diffuse reflectance FTIR spectroscopy. For comparison purposes, the reaction of this reagent with cellulose was also examined using this method of analysis. The results obtained in this FTIR analysis are summarized in Table 15. As expected, significant reductions in the area under the 1665 cm^{-1} band of the unirradiated and irradiated pulp samples were observed when they were reacted with trimethyl phosphite. The magnitude of the reduction in the case of the irradiated pulp was a little more than in the case of the unirradiated pulp. In the case of the irradiated pulp, the area remaining under this band after reaction with trimethyl phosphite was about the same as that remaining after reaction with sulfur dioxide or sodium dithionite. The results presented in Table 15 also show that the 1665 cm^{-1} absorption band observed in the pulp samples was not observed in any of the holocellulose or cellulose spectra. On the basis of these results it was concluded that the 1665 cm^{-1} absorption band observed in the pulp spectra resulted exclusively from C=O lignin vibrations. Also, the absence of this band in the spectrum of the irradiated holocellulose indicated that the yellow color of this sample was not due to the formation of quinonoid lignin structures or that such structures were not detectable.

In a further attempt to investigate the structure of the reactive groups present in the irradiated pulp and holocellulose samples, these samples were analyzed by difference spectroscopy. The difference spectrum obtained from the irradiated holocellulose showed very little change (Fig. 91). This was a bit surprising in view of its relatively intense color. Apparently, the concentration of these colored structures was below the detection limit of this method. As

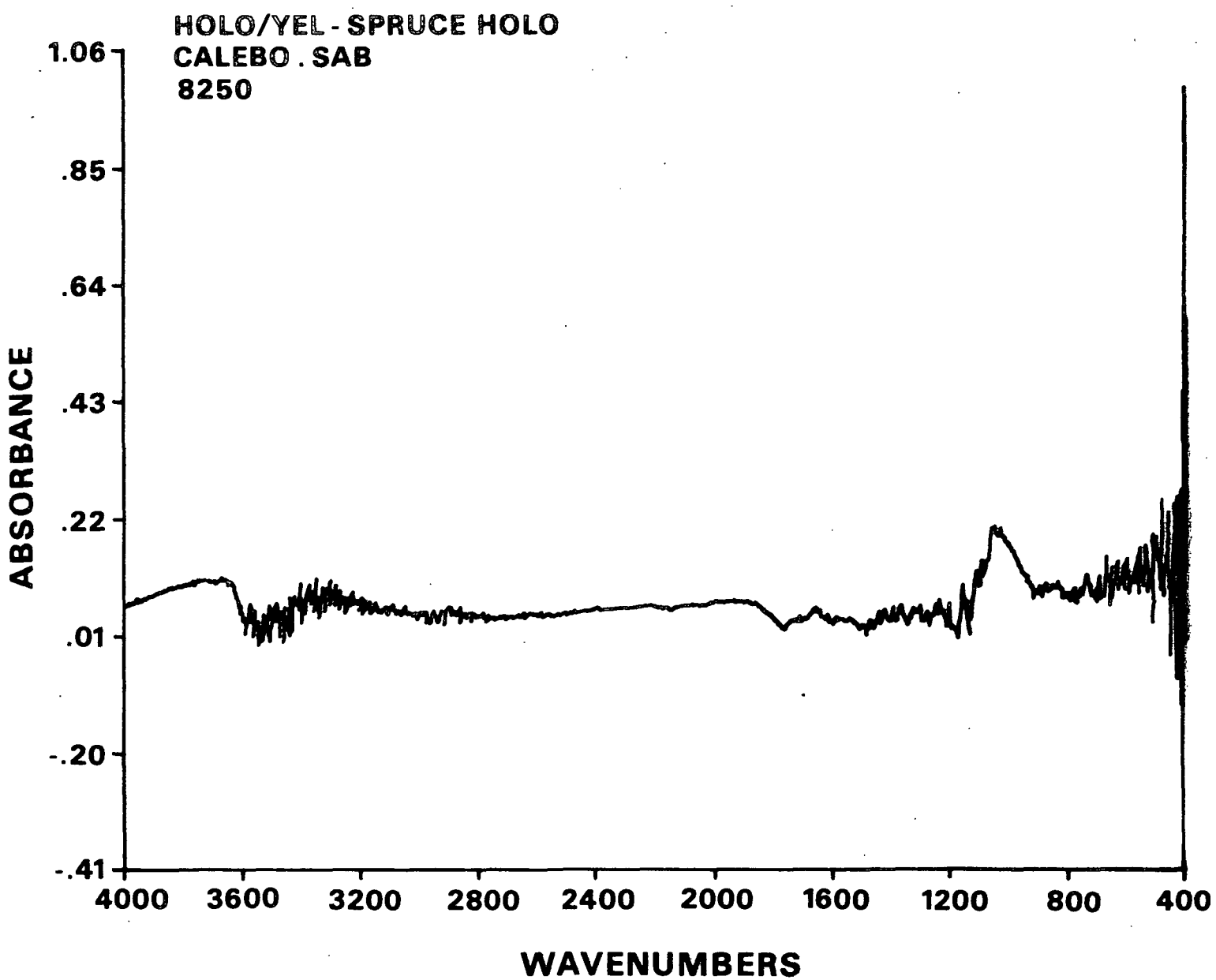

Figure 91. Difference spectrum obtained by subtracting the diffuse reflectance FTIR spectrum of a white spruce holocellulose sheet from the diffuse reflectance FTIR spectrum of the same white spruce holocellulose sheet irradiated for 4 hours with simulated sunlight (original spectra shown in Appendix VII).

noted above, another possibility may have been that the colored structures present in the holocellulose were located in the interior of the fibers and were inaccessible to the infrared light used in the analysis. The difference spectrum obtained upon irradiation of the pulp sample, as expected, showed an increase in absorbance in the 1665 cm^{-1} region of the spectrum (Fig. 92). Consistent with the results presented in Table 15, the difference spectra obtained from this sample after reaction with trimethyl phosphite showed a decrease in absorbance in the same region of the spectrum (Fig. 93). As was observed in the difference spectra of the unirradiated and Fremy's salt oxidized pulps, strong increases in absorbance were observed in this spectrum at 2990, 1780, and 1245 cm^{-1}, indicating the formation of a cyclic phosphate triester.

Table 15. Normalized area under the 1665 cm^{-1} band of trimethyl phosphite (TMPh) reacted samples of unirradiated and sunlight irradiated[a] pulp, holocellulose, and cellulose.

Sample Analyzed	Area Under 1665 cm^{-1} Band (cm^{-1})[a]
Unirradiated pulp	5.73 ± 0.12[c]
Unirradiated/TMPh reacted pulp	5.52
Irradiated pulp	6.38
Irradiated/TMPh reacted pulp	none detected
Unirradiated/TMPh reacted holocellulose	none detected
Irradiated holocellulose	none detected
Irradiated/TMPh reacted holocellulose	none detected
Unirradiated cellulose	none detected
Unirradiated/TMPh reacted cellulose	none detected
Irradiated cellulose	none detected
Irradiated/TMPh reacted cellulose	none detected

[a]Pulp sample irradiated 20 hours in solar simulator; holocellulose and cellulose samples irradiated 4 hours in solar simulator.
[b]Normalized using 1510 cm^{-1} band of lignin.
[c]Mean value ± 90% confidence interval.

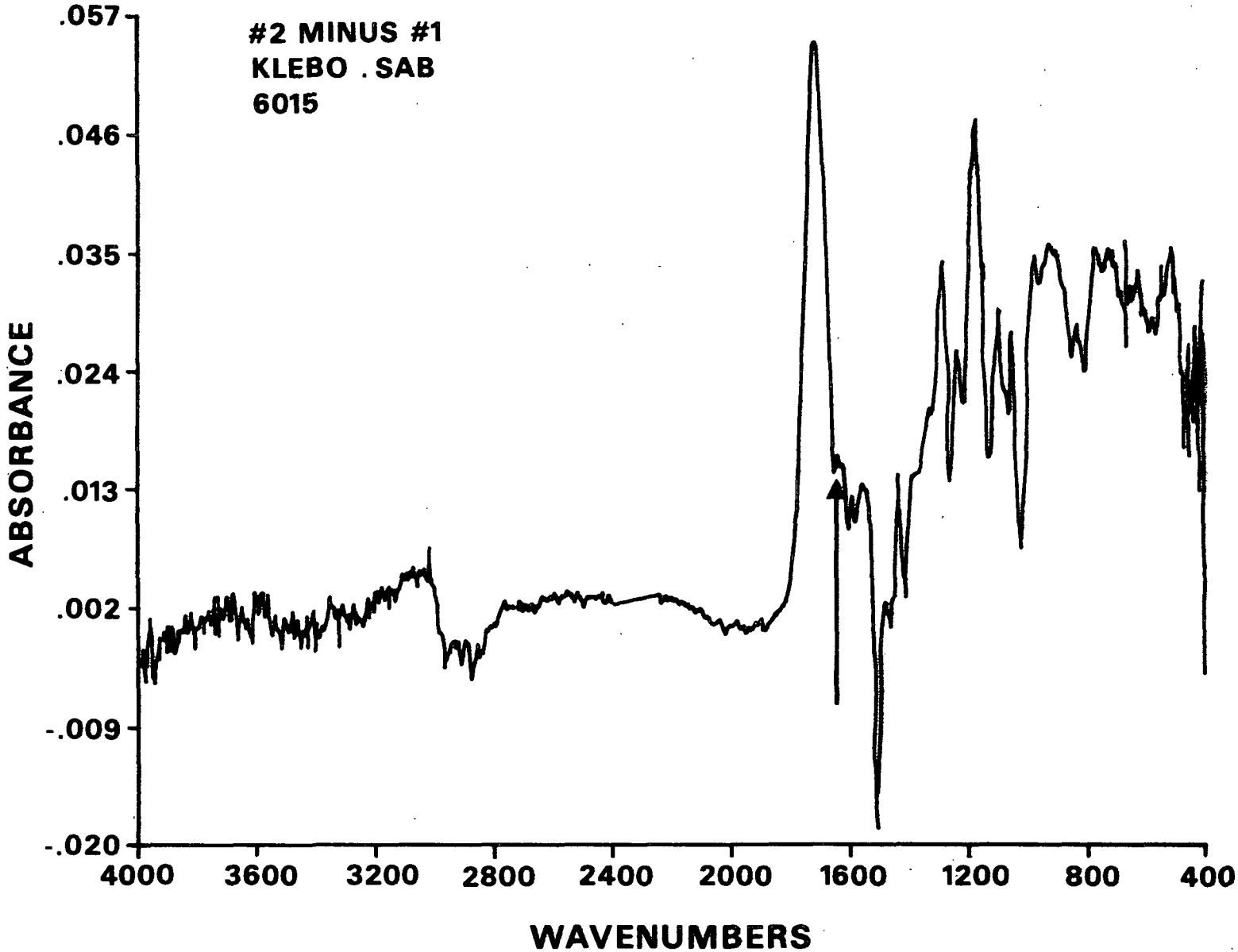

Figure 92. Difference spectrum obtained by subtracting the diffuse reflectance FTIR spectrum of a white spruce sheet from the diffuse reflectance FTIR spectrum of the same white spruce sheet irradiated for 20 hours with simulated sunlight (original spectra shown in Appendix VII).

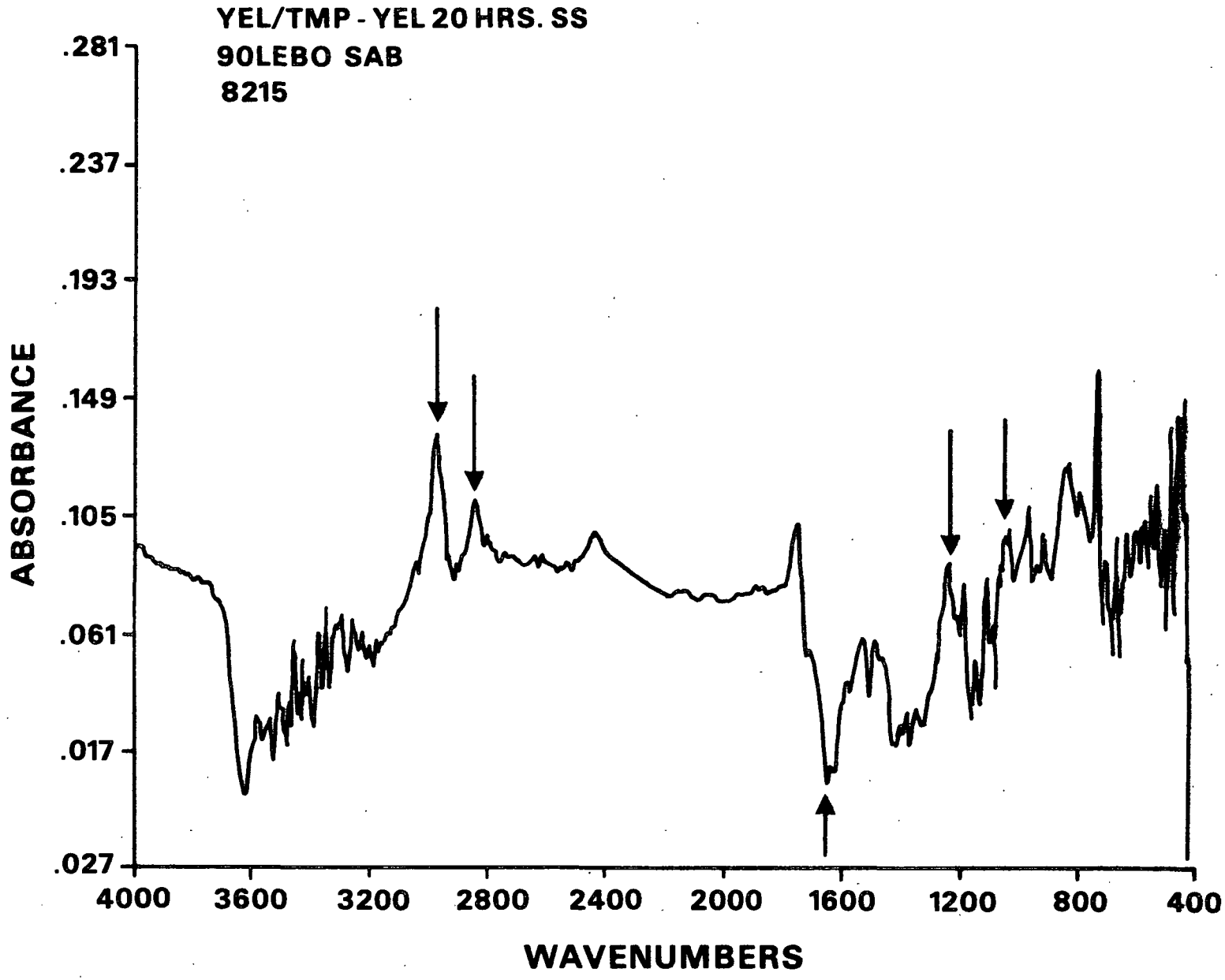

Figure 93. Difference spectrum obtained by subtracting the diffuse reflectance FTIR spectrum of a white spruce pulp sheet irradiated for 20 hours with simulated sunlight from the diffuse reflectance FTIR spectrum of a white spruce pulp sheet irradiated for 20 hours with simulated sunlight and reacted with trimethyl phosphite (original spectra shown in Appendix VII).

On the basis of the above results, it was decided that solid state ^{31}P NMR analysis of the yellowed and trimethyl phosphite reacted pulp sheets should be conducted. For comparison purposes, trimethyl phosphite reacted cellulose and holocellulose samples were also analyzed. The chemical shifts of the signals observed in the ^{31}P NMR spectra of these samples are summarized in Table 16. As the results presented in this table show, the spectrum of the yellowed and trimethyl phosphite treated pulp had two signals. The chemical shifts and relative areas of these signals were 12.6 ppm (95%) and 2.1 ppm (5%). The spectrum of the reacted holocellulose sample also had a signal at 13.9 ppm, but this signal was very weak. No clear signals were observed in the spectrum of the reacted cellulose sample. Assuming that the signal observed in the spectrum of the reacted holocellulose sample results from a product formed from structures associated with the residual lignin present in this sample, then the reaction product giving rise to the signal at 12.6 ppm in the exposed pulp sample must be of a lignin:phosphite nature. As in the unirradiated and Fremy's salt pulps, the chemical shift of the signal generated by this product was consistent with it being a colorless cyclic phosphate. The nature of the product or products giving rise to the second signal observed in the spectrum of the irradiated and trimethyl phosphite treated and yellowed and trimethyl phosphite treated pulps was not known. It appears that this may be the same product observed in the unirradiated pulp.

When the phosphorus contents of all of the above described ^{31}P NMR samples were determined, the results shown in Table 17 were obtained. Considering the percentage of the total phosphorus present in these samples associated with the cyclic phosphate triester product, these results were as expected.

Table 16. Chemical shifts of signals observed in the ^{31}P NMR spectra of trimethyl phosphite reacted samples of irradiated pulp[a] and unirradiated holocellulose and cellulose.

Sample Analyzed	Chemical Shifts of Observed Signals (ppm)[b,c]	Relative Area (% of total signal)[c]
Irradiated pulp	12.6	95
	2.1	5
Holocellulose	13.9	very weak
Cellulose	no clear signal observed	--

[a]Irradiated for 20 hours in a solar simulator.
[b]Relative to 85% H_3PO_4.
[c]Obtained from deconvolution of spectra shown in Appendix VII.

Table 17. Phosphorus contents of the above described ^{31}P NMR samples.

Sample Analyzed	% Total Phosphorus
Unirradiated/TMPh reacted pulp	0.39 ± 0.056[a]
Irradiated/TMPh reacted pulp	0.47[b]
Fremy's salt oxidized/TMPh reacted pulp	0.50[b]
Unirradiated/TMPh reacted holocellulose	0.050[b]
Unirradiated/TMPh reacted cellulose	> 0.050[b]

[a]Average of three samples (two determinations each) ± 90% confidence interval.
[b]Average of two determinations.

Determination of Z-Direction Phosphorus Distribution in Sunlight Irradiated Sheets

In an effort to determine the z-direction distribution of the phosphorus present in irradiated pulp handsheets, these handsheets were reacted with

trimethyl phosphite and then the z-direction distribution of the phosphorus present in samples was analyzed using scanning electron microscopy-energy dispersive spectrometry (SEM-EDS). For comparison purposes, an effort to determine the z-direction of the phosphorus present in irradiated cellulose and holocellulose samples was also made. The results obtained from the irradiated pulp sheets showed that there was a definite gradient of phosphorus, and hence quinonoid lignin structures, in the z-direction of the sheet (Fig. 94). As expected, the phosphorus content of this sheet was highest at the exposed surface and decreased exponentially toward the interior of the sheet. At a distance into the sheet of approximately 0.16-0.20 mm, the phosphorus distribution leveled off at a nonzero value. On the basis of the results presented above, this leveling off was attributed to the reaction of trimethyl phosphite with the quinonoid lignin structures present in the unirradiated pulp. Consistent with the results presented in Table 17, the amount of phosphorus present in the irradiated cellulose and holocellulose sheets was too low to be detected by this method. Thus, information about the z-direction distribution of the small amount of phosphorus present in these sheets was not available.

Reaction of Trimethyl Phosphite with White Spruce Pulp Sheets Irradiated with 312.5 nm UV Light

In addition to studying the reactions of trimethyl phosphite with sunlight irradiated pulp, the reactions of this reagent with pulp samples irradiated with essentially monochromatic UV light was also studied. For the same reasons stated earlier, the wavelength of light used in these studies was 312.5 nm (5 nm band width), and the flux of the light incident on each sample was known. As shown in Table 18, two combinations of incident light flux and irradiation time was studied. These combinations of incident light fluxes and irradiation times generated two sets of samples. The total number of photons absorbed by the

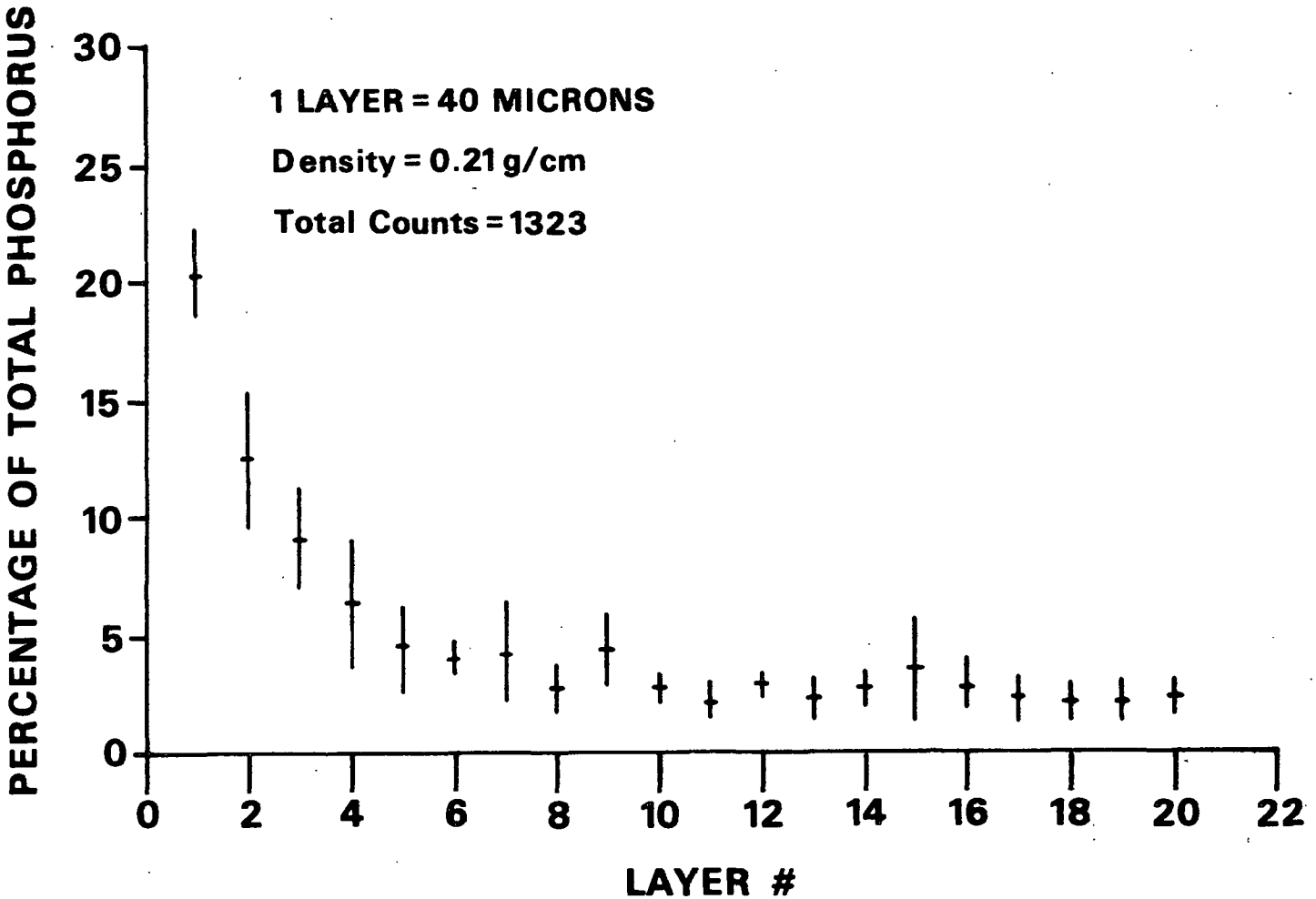

Figure 94. Z-direction phosphorus distribution obtained when a 160 g/m^2 handsheet irradiated for 20 hours with simulated sunlight was reacted with trimethyl phosphite and then analyzed by SEM-EDS.

first set of samples (i.e., 0.380-1 and 0.380-2) was approximately 7.27×10^{18} photons, and the total number of photons absorbed by the second set of samples (i.e., 0.420-1 and 0.420-2) was approximately 1.07×10^{19} photons.

Table 18. Experimental combinations used in preparing 312.5 nm UV light irradiated pulp samples.

Sample	Irradiation Time (hours)	Incident Light Flux (photons/cm^2 sec)	Absorbance $(1-e^{kw})^a$	Absorbed Light Flux (photons/cm^2 sec)
0.380-1	36.0	2.03×10^{13}	0.98	1.99×10^{13}
0.380-2	36.0	2.03×10^{13}	0.98	1.99×10^{13}
0.420-1	48.0	2.24×10^{13}	0.98	2.20×10^{13}
0.420-2	48.0	2.24×10^{13}	0.98	2.20×10^{13}

[a]Based on a sheet basis weight of 160.0 g/m^2.

The ΔR_∞ and $\Delta(k/s)_\lambda$ spectra obtained upon irradiation of the sample sheets described upon irradiation of these sample sheets above are shown in Fig. 95-98. As Figures 95 and 96 show, the ΔR_∞ spectra obtained were, in the visible range of the spectrum, similar to the ΔR_∞ spectra of the sunlight irradiated sheets described earlier. In the UV region of the spectrum, however, there was an observable difference between these spectra. The positive band observed in the 350-380 nm region of the sunlight irradiated sample spectra was not present in the spectra of the 312.5 nm irradiated samples. A similar comparison of the $\Delta(k/s)_\lambda$ spectra obtained upon irradiation of white spruce sheets with sunlight and with 312.5 nm light also showed that the absorbances of the latter samples were higher in the 350-380 nm region. It was also noted that the wavelength maxima of the absorption bands observed in the spectra obtained in the 312.5 nm irradiation occurred at a slightly shorter wavelength than those observed in the spectra obtained in the sunlight irradiation; approximately 390 and 400 nm, respectively (Fig. 99).

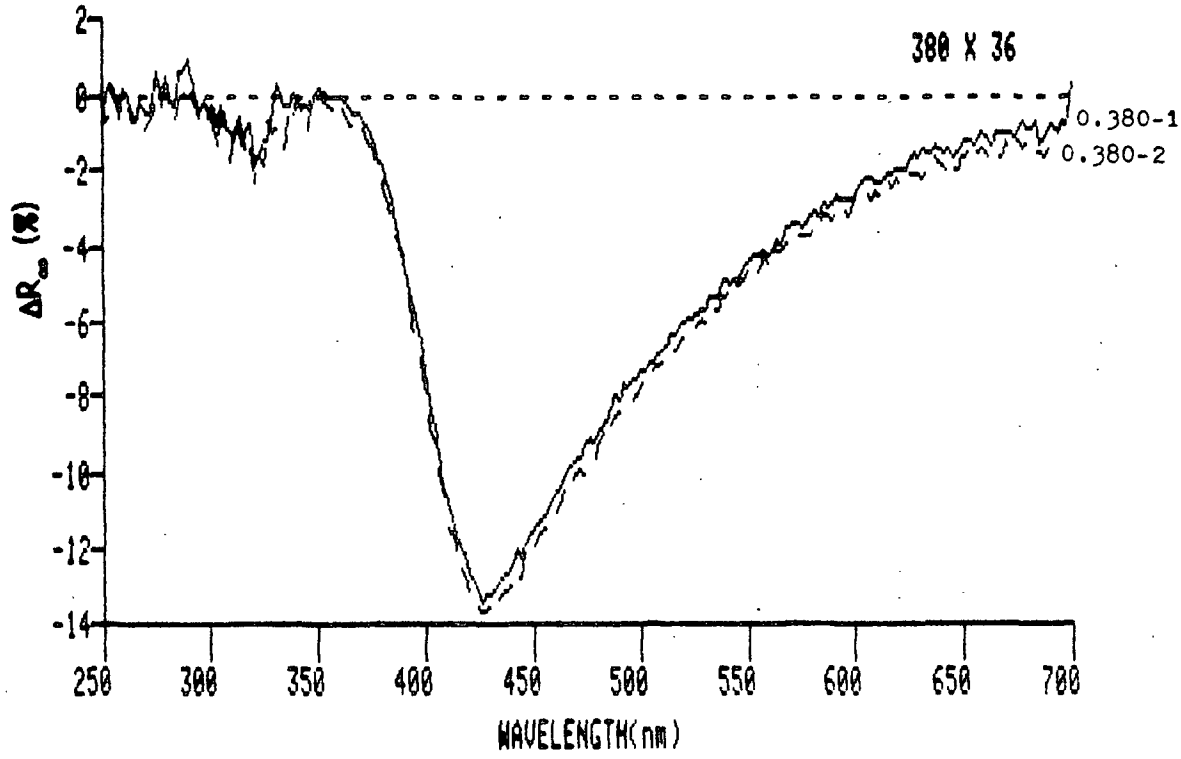

Figure 95. ΔR_∞ spectra obtained upon irradiation of white spruce RMP sheets with 312.5 nm UV light; samples 0.380-1 and 0.420-2.

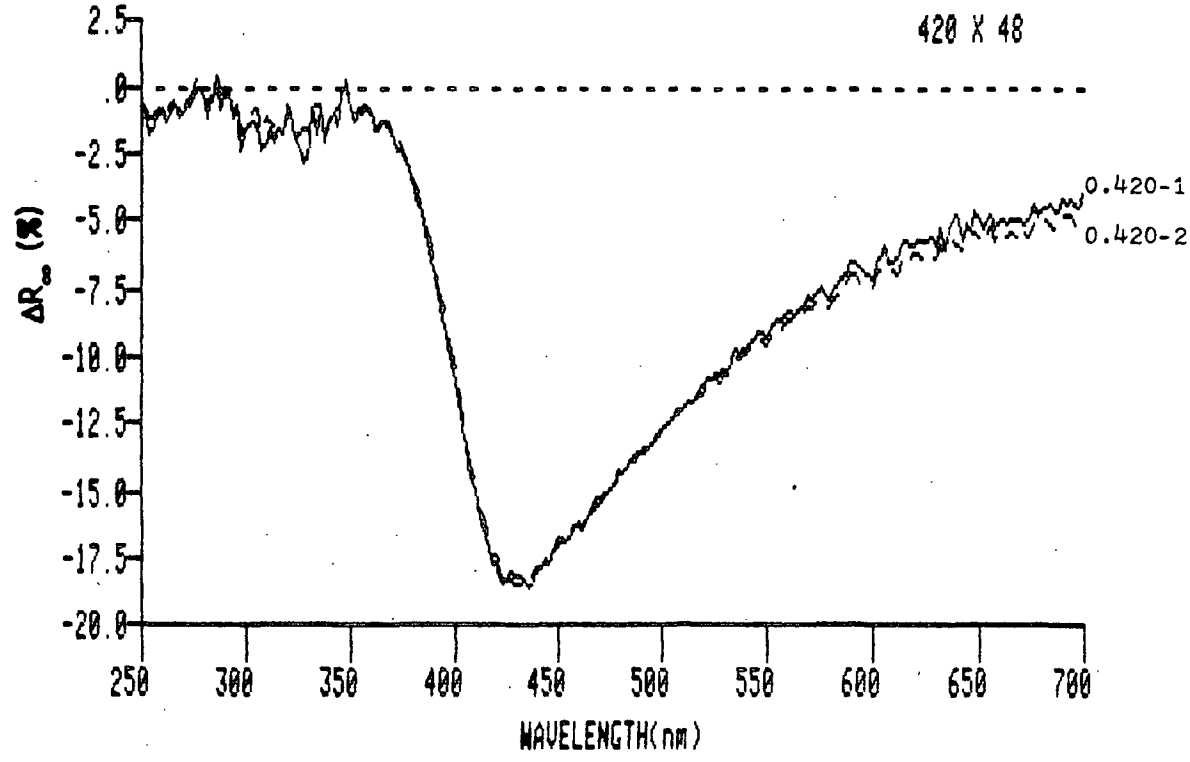

Figure 96. ΔR_∞ spectra obtained upon irradiation of white spruce RMP sheets with 312.5 nm UV light; samples 0.420-1 and 0.420-2.

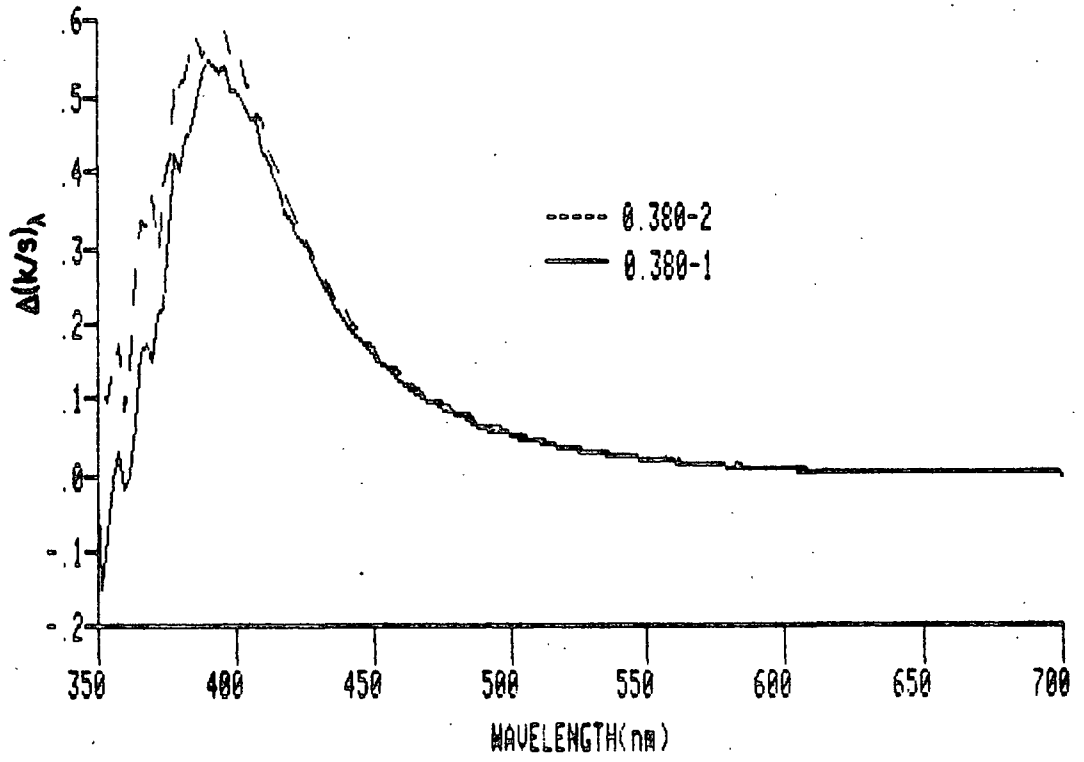

Figure 97. $\Delta(k/s)_\lambda$ spectra obtained upon irradiation of white spruce RMP sheets with 312.5 nm UV light; samples 0.380-1 and 0.380-2.

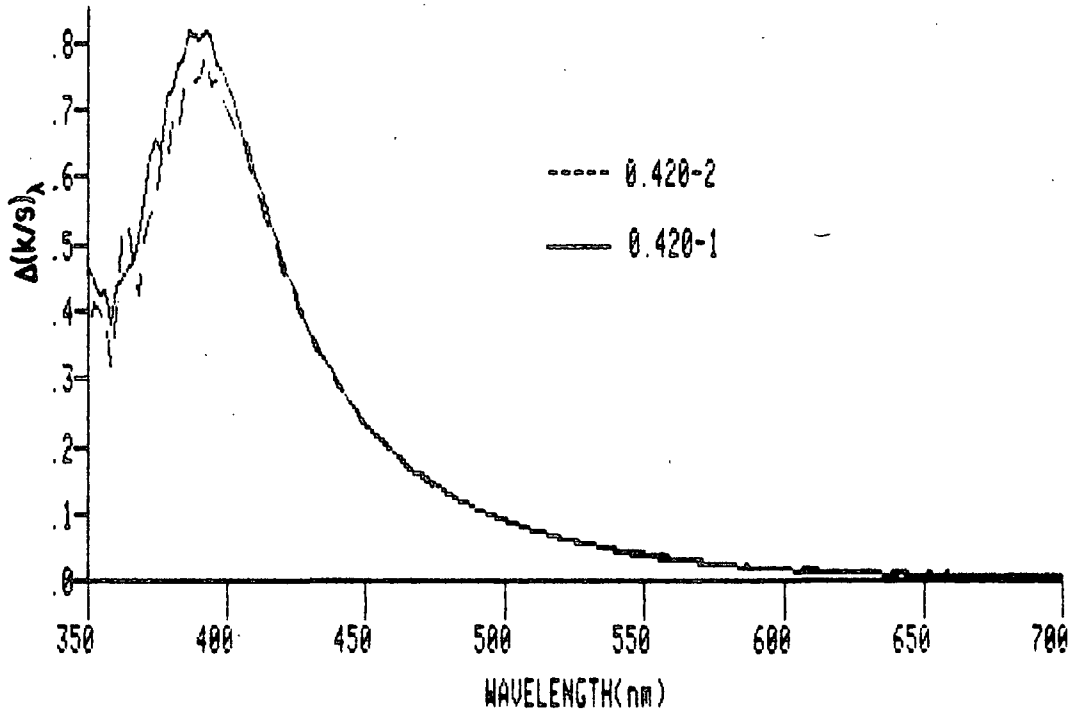

Figure 98. $\Delta(k/s)_\lambda$ spectra obtained upon irradiation of white spruce RMP sheets with 312.5 nm UV light; samples 0.420-1 and 0.420-2.

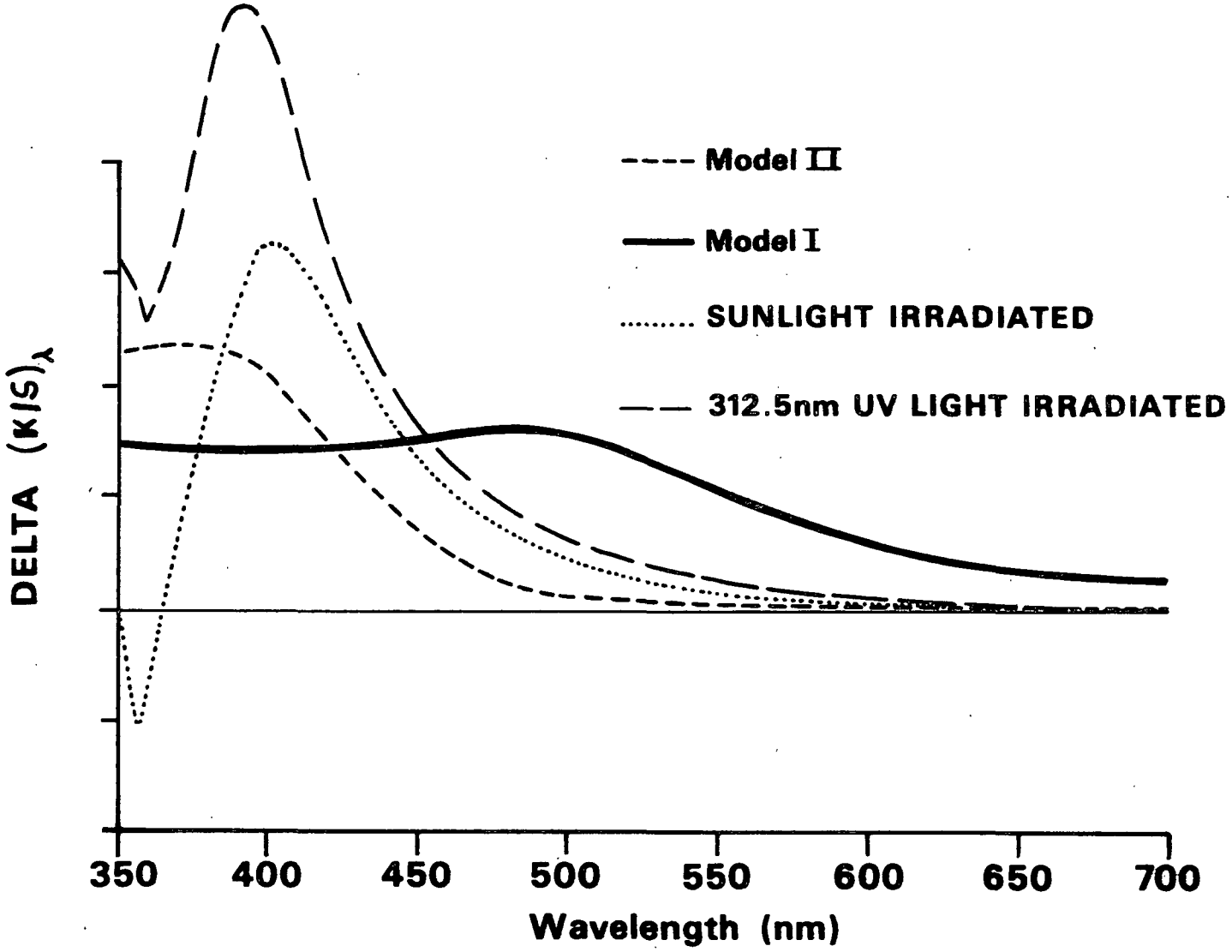

Figure 99. $\Delta(k/s)_\lambda$ spectra obtained upon impregnation of white spruce RMP sheets with models I and II and upon irradiation of white spruce RMP sheets with sunlight and 312.5 nm UV light.

When the two sets of 312.5 nm UV light irradiated samples were reacted with trimethyl phosphite, they appeared, visually, to be brighter. Like the sunlight irradiated samples, however, they still looked yellow. The results obtained in subsequent ^{31}P NMR analysis and phosphorus microanalysis of these samples are summarized in Table 19. This table shows that, like the sunlight irradiated samples, the ^{31}P NMR spectra of these samples all had signals at a chemical shift of approximately 13 ppm. Thus, like the sunlight irradiated samples, these samples contained reactive ortho-quinonoid lignin structures. No signals were seen in the region where para-quinone:TMPh adducts would be expected to be seen. Thus, as in the case of the sunlight irradiated pulp samples, the ^{31}P NMR results obtained here indicated that para-quinonoid lignin structures were either not formed in these pulp samples or, if they were, they did not react with trimethyl phosphite. The nature of the structures giving rise to the signals at 37.9 and 20.7 ppm was not clear, although one possibility was that these structures were present in the aged trimethyl phosphite used in these experiments. On the basis of the results presented above, the number of ortho-quinonoid lignin structures present in these samples was estimated, and the results of these estimations are described in the following section.

Semiquantitative Estimation of the Number of ortho-Quinonoid Lignin Structures Present in Unirradiated and Irradiated Pulp Sheets

By combining the results of ^{31}P NMR analysis and phosphorus microanalysis, the number of quinonoid lignin structures present in unirradiated, the 312.5 nm UV light irradiated and the sunlight irradiated pulp samples was estimated. The equations used in these estimations are described in the following section. After this, the results obtained for these various samples are described.

Table 19. Summary of the results obtained in the ^{31}P NMR analysis and phosphorus microanalysis of 312.5 nm UV light irradiated and trimethyl phosphite reacted pulp samples.

Sample	Signal	^{31}P NMR Analysis[a,b] Chemical Shift (ppm)	Relative Area (%)[b]	Microanalysis (%) Run 1	Run 2
38 hours irradiated and TMPh reacted-1	1	3.1	37.1	0.69	0.74
	2	12.5	62.9		
38 hours irradiated and TMPh reacted-2	1	4.2	22.4	0.73	0.78
	2	13.6	56.3		
	3	38.8	21.4		
42 hours irradiated and TMPh reacted-1	1	13.9	86.3	0.72	0.69
	2	20.7	13.7		
42 hours irradiated and TMPh reacted-2	1	2.5	31.0	0.70	0.71
	2	12.6	69.0		

[a]All chemical shifts relative to 85% H_3PO_4.
[b]Obtained from deconvolutions of spectra shown in Appendix VII.

Equations Used in Calculations

The following equations were used in estimating the number of ortho-quinonoid lignin structures. First the amount of phosphorus associated with these structures was calculated;

$$\%\ P_q = \%\ \text{phosphorus associated with ortho-quinonoid structures} = \%\ P_{total} \times (\%\ \text{area})$$

where $\%\ P_{total}$ = g phosphorus/g pulp determined through microanalysis

$\%$ area = % area associated with 13 ppm ^{31}P NMR signal.

Assuming that there is one mole of ortho-quinonoid lignin structures per mole of phosphorus, then the moles of ortho-quinonoid lignin structures per gram of

lignin is:

$$m_q = \text{moles of } \underline{\text{ortho}}\text{-quinonoid lignin structures/g lignin} = \frac{\%\ P_q}{(\%\ \text{Klason lignin})\ (\text{MW phosphorus})}$$

Using a unit weight for spruce lignin of 185 g lignin/mole of C_9 units,[137] the number of ortho-quinonoid lignin structures per 100 C_9 units is

$$\text{no. ortho-quinonoid lignin structures/100 } C_9 \text{ units} = [m_q \times 185] \times 100.$$

Sample Sheets Irradiated with 312.5 nm UV Light

Using the equations described above, the number of moles of ortho-quinonoid lignin structures and the number of ortho-quinonoid lignin structures per 100 C_9 lignin units present in the 312.5 nm UV light irradiated and unirradiated samples were calculated. The results of these calculations are presented in Table 20.

Table 20. Calculated ortho-quinonoid lignin contents of unirradiated and 312.5 nm irradiated samples

Sample	Approximate Number of Photons Absorbed	Moles of Quinone Present[a]	Average No. of ortho-Quinonoid Structures per 100 C_9 Units
Unirradiated	--	1.5×10^{-6}	6.18
0.380 (average)	7.27×10^{18}	2.1×10^{-6}	9.70
0.420 (average)	1.07×10^{19}	3.1×10^{-6}	12.16

[a]Calculated as follows: average number of moles present = m_q x wt. of lignin in sample.

From the results presented in Table 20, plots of the average number of moles of ortho-quinonoid lignin structures versus the total number of moles of photons absorbed and of the average number of ortho-quinonoid lignin structures per 100

C_9 lignin units versus the total number of photons absorbed were prepared (Fig. 100 and 101). Theoretically, these plots should be linear with slopes equal to the quantum yield of ortho-quinonoid lignin structure formation at 312.5 nm and intercepts equal to the initial amount of ortho-quinonoid lignin structure. Regression analyses of the two sets of data yielded slopes of 8.0×10^{-2} moles of ortho-quinonoid lignin structures per mole of photons absorbed and 5.5×10^{-19} ortho-quinonoid lignin structures per 100 C_9 lignin units per photon absorbed and intercepts of 1.5×10^{-6} moles of ortho-quinonoid lignin structures and 6.1 ortho-quinonoid lignin structures per 100 C_9 lignin units, at a sheet basis weight of 160 g/m^2.

Sample Sheets Irradiated with Simulated Sunlight

As was noted above, the number of ortho-quinonoid lignin structures estimated to be present in the unirradiated pulp was about 6 per 100 C_9 lignin units. On the basis of other estimates presented in the literature,[11,12,57,116] this number seems reasonable. The number of ortho-quinonoid lignin structures estimated to be present in the 20 hour sunlight irradiated pulp was around 10.5 per 100 C_9 lignin units. Thus, approximately 4.5 ortho-quinonoid lignin structures were formed per 100 C_9 lignin units when this pulp was exposed to 20 hours of simulated sunlight and, as witnessed by the z-direction distribution results, most of these structures were formed on the surface of the sheets.

Estimation of the Contribution of ortho-Quinonoid Lignin Structures to the Absorbance of Unirradiated and Sunlight Irradiated Pulp Sheets

Using the Kubelka-Munk absorption coefficients of unirradiated and irradiated (24 hours in the solar simulator) pulp sheets before and after reaction with trimethyl phosphite, the contribution of the ortho-quinonoid lignin structures present in these sheets to the absorbance or increase in absorbance of these

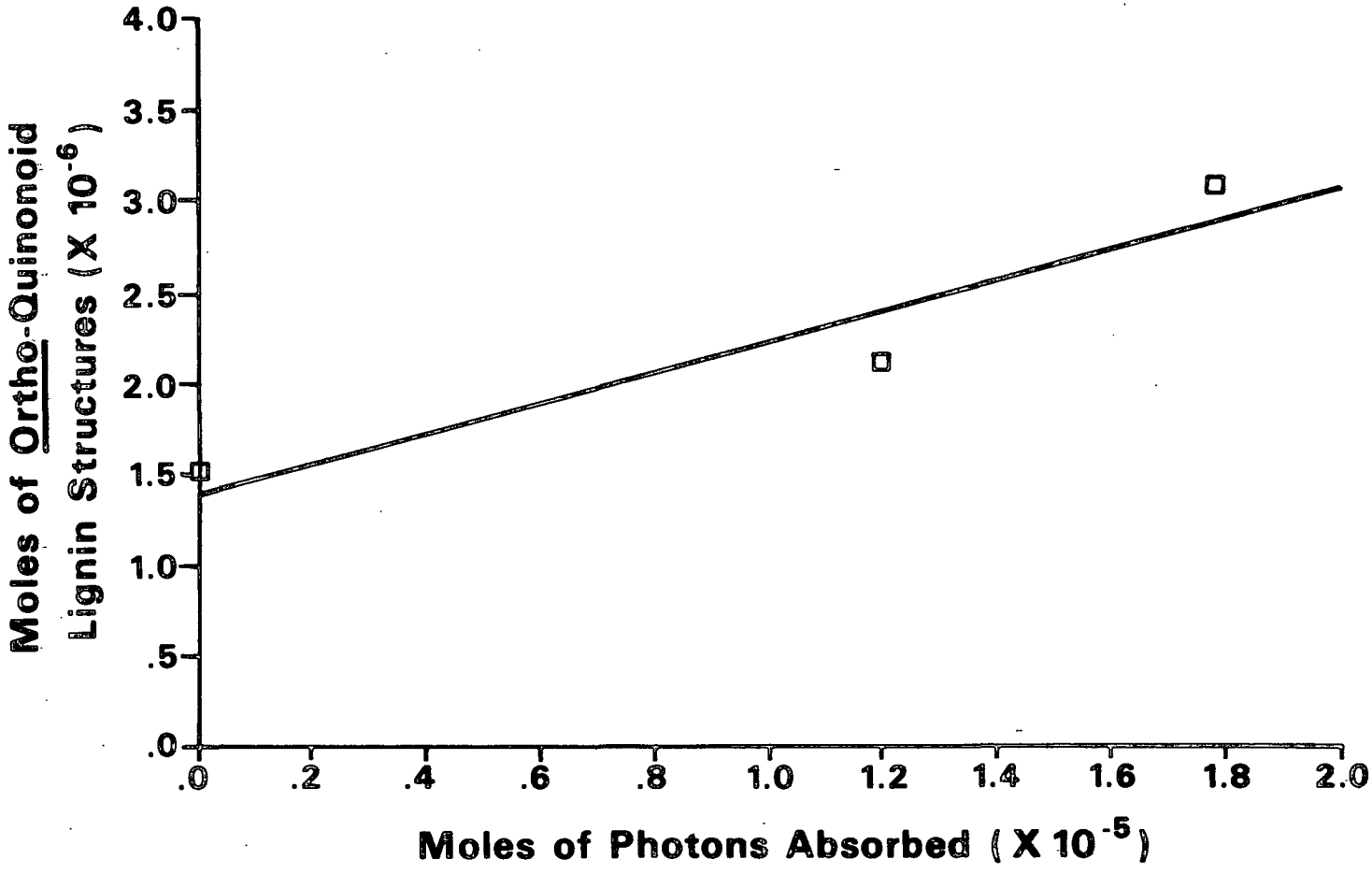

Figure 100. Plots of the number of moles of ortho-quinonoid lignin structures formed versus the number of moles of photons absorbed (obtained using white spruce sheets of 160 g/m^2 basis weight).

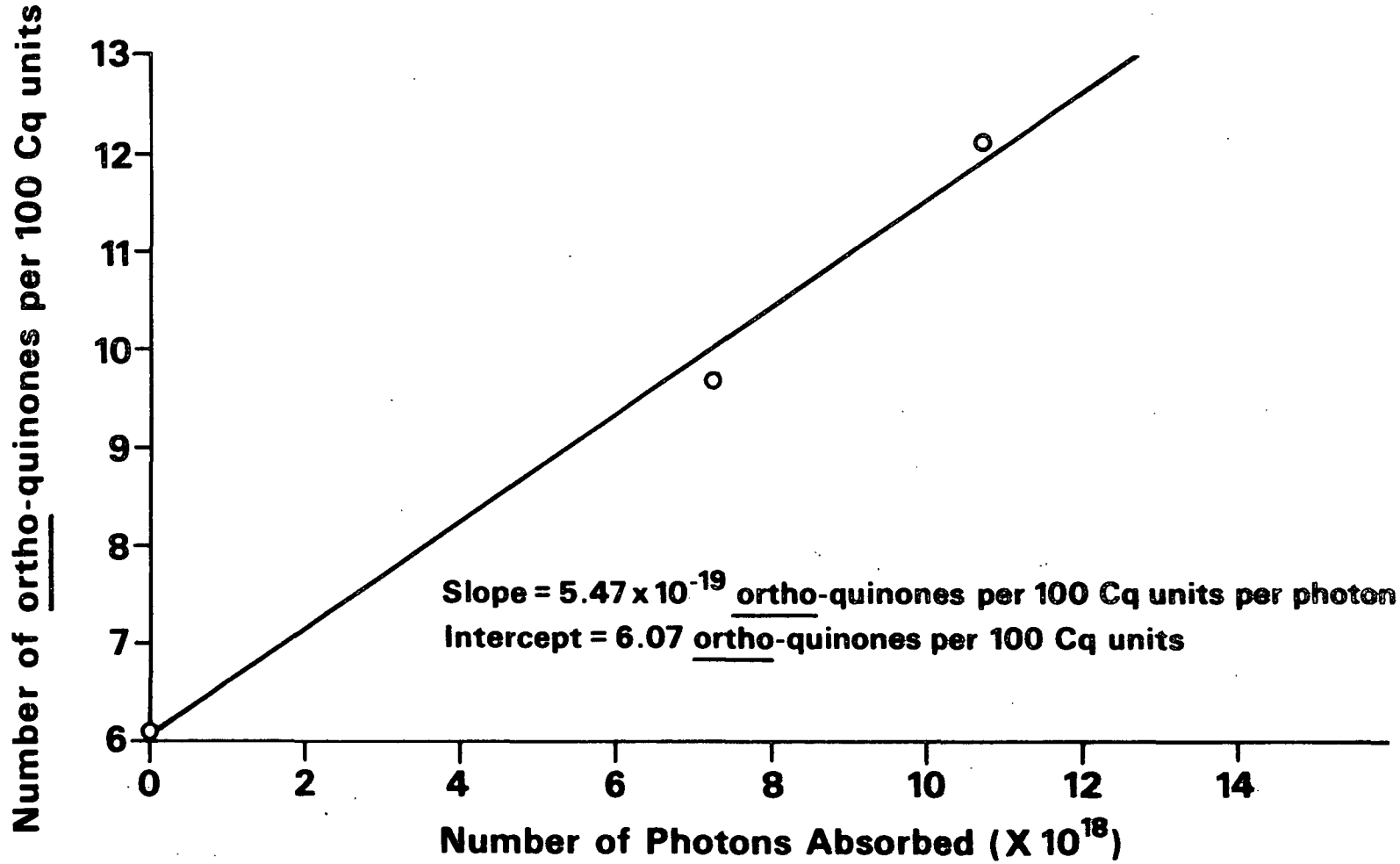

Figure 101. Plot of number of ortho-quinonoid lignin structures formed per 100 C_9 lignin units versus total number of photons absorbed (obtained using white spruce sheets of 160 g/m^2 basis weight).

sheets was estimated. These estimations were made at 415, 457, and 520 nm (i.e., at the same wavelengths used in the kinetics studies described earlier), and in these estimations it was assumed that the scattering properties of these sheets were not significantly changed by irradiation or reaction with trimethyl phosphite. It was also assumed that trimethyl phosphite reacts selectively with the ortho-quinonoid lignin structures present in these sheets. It appears, based on the spectra presented in Appendix VIII, that the latter of these two assumptions is not strictly valid for the 415 nm estimation, and thus, the estimation of the contribution of these structures to the absorbance of these samples at this wavelength is probably on the high side. None the less, this estimation should still provide a rough idea of the extent of the contribution of such structures to the overall absorbance of these samples.

Table 21 shows the k_λ coefficients of unirradiated and irradiated white spruce sheets before and after reaction with trimethyl phosphite (TMPh). Based on these values the contribution of the ortho-quinonoid lignin structures present in these sheets to the absorbance (unirradiated) or increase in absorbance (irradiated) was calculated as follows:

$$\text{Contribution of ortho-quinonoid lignin structures to the absorbance of unirradiated pulp sheet} = \frac{k(\text{unirradiated sheet}) - k(\text{unirradiated/reacted sheet})}{k(\text{unirradiated sheet})}$$

$$\text{Contribution of ortho-quinonoid lignin structures to the increase in absorbance of irradiated pulp sheet} = \frac{k(\text{irradiated sheet}) - k(\text{irradiated/reacted sheet}) - C_p}{k(\text{irradiated sheet}) - k(\text{unirradiated sheet})}$$

where $C_p = [k(\text{unirradiated sheet}) - k(\text{unirradiated/reacted sheet})]$.

Table 21. k_λ Coefficients of unirradiated and irradiated white spruce sheets before and after reaction[a] with trimethyl phosphite (TMPh).

Sample Sheet	k_λ (cm^2/g) 415 nm	457 nm	520 nm
Unirradiated sheet	141.36	48.86	20.24
Unirradiated/TMPh reacted sheet	74.67	13.15	5.01
Irradiated sheet	442.45	185.63	68.42
Irradiated/TMPh reacted sheet	170.52	46.26	14.97

[a]Reaction time = 7 days in dichloromethane.

The results obtained from these calculations are shown in Table 22. As these results show, in the case of the unirradiated sheet the contribution of the ortho-quinonoid lignin structures present in this sheet to the absorbance at 415, 457, and 520 nm was approximately 47, 73, and 75%, respectively. In the case of the sunlight irradiated sheet, the contribution of such structures to the increase in absorbance at 415, 457, and 520 nm was approximately 68, 75, and 79%, respectively. Thus, it can be concluded that ortho-quinonoid lignin structures contribute significantly, but not totally, to the absorbance of both unirradiated and irradiated pulp sheets.

Table 22. Results obtained in the estimations of the contributions of ortho-quinonoid lignin structures to the absorbance of unirradiated white spruce pulp sheets and increase in absorbance of irradiated white spruce pulp sheets.

Sample	Contribution to Absorbance or Increase in Absorbance (%) 415 nm	457 nm	520 nm
Unirradiated pulp sheet	47	73	75
Irradiated pulp sheet	68	75	79

CONCLUSIONS

White spruce refiner mechanical pulp was found to contain approximately six ortho-quinonoid lignin structures per 100 C_9 units. Reaction of this pulp with sulfur dioxide, sodium dithionite, and trimethyl phosphite indicated that the contribution of these structures to the absorbance of this pulp was approximately 47% at 415 nm, 73% at 457 nm, and 75% at 520 nm. Upon exposure to sunlight or UV light, additional ortho-quinonoid lignin structures were formed in this pulp. The quantum yield for the 312.5 nm light induced formation of these structures was estimated to be 8.0×10^{-2} moles of ortho-quinonoid lignin structures per mole of photons absorbed. Reaction of sunlight irradiated pulp with sulfur dioxide, sodium dithionite, and trimethyl phosphite indicated that the contribution of these structures to the absorbance of this pulp was approximately 68% at 415 nm, 75% at 457 nm, and 79% at 520 nm.

The results obtained for the sunlight irradiated pulp also indicated that ortho-quinonoid lignin structures were not the only colored structures formed when white spruce refiner mechanical pulp was exposed to sunlight. The other contributor to the absorbance of this irradiated pulp was not identified, but it was shown that this structure had an absorption maximum in the 395-400 nm range. Unlike the ortho-quinonoid lignin structures described above, this contributor was not readily reduced by sulfur dioxide, sodium dithionite or trimethyl phosphite.

Photochemically, the overall rate of 290-390 nm UV light induced yellowing was found to be a function of the wavelength of incident light. While all wavelengths in this range induced yellowing, the overall rate of this yellowing was greatest at an incident wavelength of 312.5 nm. The rate of light induced

yellowing at this wavelength was not directly proportional to the incident light flux indicating that the products generated in this process were formed in secondary photochemical reactions.

RECOMMENDATIONS

The results of this work demonstrated that ortho-quinonoid lignin structures are present in high yield pulps and are formed when such pulps are exposed to light. They also demonstrated that such structures are the major contributor to the absorbance of such pulps. They are not, however, the only colored product present in these pulps.

Thus, a major area of recommended further work is that of determining the nature of the other color causing chromophore. Some preliminary work with various "lignin-free" holocellulosic materials has indicated that the yellowing of such pulps may not be entirely due to lignin (Appendix IX). Further work along these lines would be of great interest to the high yield pulp manufacturer. Another related area of interest would be the possible occurrence of charge-transfer effects in high yield pulps. These types of interactions have been shown to occur in closely related materials and their occurrence results in enhanced color.

Trimethyl phosphite was shown to be a good reagent for detecting ortho-quinonoid lignin structures in high yield pulp systems. Thus, this reagent may be useful in studying quinones in other polymeric systems.

ACKNOWLEDGMENTS

The author wishes to acknowledge the assistance and guidance provided by his thesis advisory committee: Dr. W. F. W. Lonsky and Dr. T. J. McDonough. The author is especially grateful to these gentlemen for their encouragement, support, and friendship throughout the course of this work. The author is also grateful to Drs. E. W. Malcolm and R. Atalla for their comments and assistance.

Financial support from the member companies of The Institute of Paper Chemistry is gratefully acknowledged. The assistance of Dr. G. Turner of Spectral Data Services, Dr. P. Mathiaparanam of Appleton Papers, and S. Berben, E. Foxgrover, C. Woitkovich, and J. Biasca of The Institute of Paper Chemistry is sincerely appreciated.

The author would also like to thank members of the Institute faculty and staff, too numerous to mention individually here, for their efforts in support of this thesis. Thanks, also, to my fellow students, past and present, whose friendship made the last few years good ones.

I would like to thank my family for their love and encouragement, especially my mother and father, whose inspiration and pride brought me to this point. Finally, I would like to express my sincere gratitude to my wife, Sandy, for her love, understanding, and sacrifice during this time. Without them, this work would have never been possible.

LITERATURE CITED

1. Aario, M., Paper 194(2):15-16, 21(1980).

2. Breck, D. H.; Styan, G. E., Pulp Paper Can. 86(3):109-12, 114-16(1985).

3. Freudenberg, K., Angew Chem. 68:84-92(1956).

4. Freudenberg, K., Holzforschung 18(6):166-8(1964).

5. Luner, P., Tappi 43(10):819-26(1960).

6. Chudachov, M. I.; Samsanova, A. P., Sbornik Trudov Gos. Nauch-Issled. Inst. Gidroliz Sulfit-no-Spirt Prom. 15:285-90(1966).

7. Pew, J. C.; Connors, W. J., Tappi 54(2):245-51(1971).

8. Connors, W. J.; Ayers, J. S.; Sarkanen, K. V.; Gratzl, J. S., Tappi 54(8): 1284-8(1971).

9. Polcin, J.; Rapson, W. H., Pulp Paper Mag. Can. 72(3):69-80(1971).

10. Polcin, J.; Rapson, W. H., Pulp Paper Mag. Can. 72(3):80-91(1971).

11. Falkehag, S. I.; Marton, J.; Adler, E. Chromophores in kraft lignin. In Lignin Structure and Reactions. Adv. Chem. Ser. 59:75-89, Am. Chem. Soc., Washington, DC, 1966.

12. Imsgard, F.; Falkehag, S. I.; Kringstad, K. P., Tappi 54(10):1680-4(1971).

13. Gierer, J., Papier 27(10A):469-74(1973).

14. Hon, D. S.; Glasser, W., Polymer Plast. Technol. Eng. 12(2):159-79(1979).

15. Cole, J. W.; Sarkanen, K. V.; Hooper, J. E. Preprints of Fourth International Symposium on Wood and Pulping Chemistry, Paris, Vol. 1:321-6(April 27-30, 1987).

16. Leary, G. J., Tappi 50(1):17-19(1967).

17. Leary, G. J., Tappi 51(6):257-60(1968).

18. Leary, G. J., Nature 217:672-3(Feb. 17, 1969).

19. Andrews, D. A.; DesRosiers, P., Pulp Paper Mag. Can. 67:T119-28(1966).

20. Singh, R. P., Tappi 49(7):281-6(1966).

21. Teüber, H. J.; Stäiger, G., Chem. Ber. 88:802-27(1955).

22. Adler, E., Paperi Puu 11:826(1957).

23. Adler, E.; Lundquist, K., Acta Chem. Scand. 15:223-4(1961).

24. Kringstad, K., Tappi 52(6):1070-4(1969).

25. Lin, S. Y.; Kringstad, K. P., Tappi 53(4):658-63(1970).

26. Lin, S. Y.; Kringstad, K. P., Tappi 53(9):1175-7(1970).

27. Kringstad, K. P.; Lin, S. Y., Tappi 53(12):2296-301(1970).

28. Lin, S. Y.; Kringstad, K. P., Norsk Skogind. 25(9):252-6(1971).

29. Gierer, J.; Lin, S. Y., Svensk Papperstid. 75(7):233-9(1972).

30. Gellerstedt, G.; Pettersson, E., Acta Chem. Scand. B29:1005-10(1975).

31. Gellerstedt, G.; Pettersson, E., Svensk Papperstid. 80(1):15-21(1977).

32. Gellerstedt, G.; Pettersson, I.; Sundin, S., Svensk Papperstid. 89:R157-63(1983).

33. Gratzl, J. S., Papier 39(10A):V14-23(1985).

34. Hirashima, H.; Sumimoto, M., J. Japan Wood Res. Soc. 32(9):705-12(1986).

35. Lonsky, W. F. W., unpublished work, The Institute of Paper Chemistry, Appleton, WI, 1985.

36. Heitner, C.; Min, T., Preprints of Fourth International Symposium on Wood and Pulping Chemistry, Paris, Vol. 1:327-32(April 27-30, 1987).

37. Forsskåhl, I. Photosensitized reactions of lignin model compounds and the role of singlet oxygen in lignin photochemistry. Societas Scientiarum Fennica, Commentationes Physico Mathematicae 61/1985, Dissert. No. 5, Helsinki, 1985. 127 p.

38. Launer, H. F.; Wilson, W. J., J. Res. NBS 30:55-74(1943).

39. Nolan, P.; Van den Akker, J. A.; Wink, W. A., Paper Trade J. 121:33-7 (1945).

40. Sinclair, R. M.; Vincent, T. A., New Zealand J. Sci. 7:196(1964).

41. Forman, L. V., Paper Trade J. 111(21):34(1940).

42. Manchester, D. F.; McKinney, J. W.; Pataky, A. A., Svensk Papperstid. 63 (20):699-706(1960).

43. Brunow, G.; Sivonen, M., Papper och Trä 4a:215-20(1975).

44. Matsuura, T.; Yoshimura, N.; Nishinage, A.; Saito, I., Tetrahedron Letters 21:1669-71(1969).

45. Brunow, G.; Eriksson, B., Acta Chem. Scand. 25(7):2779-81(1971).

46. Dence, C., personal communication, 1987.

47. Lonsky, W. F. W.; Ogryzlo, E., unpublished work, The Institute of Paper Chemistry, Appleton, WI, 1986.

48. Castellan, A.; Vanucci, C.; Girard, P.; De Violet, P. F.; Bouas-Laurent, H., Preprints of Fourth International Symposium on Wood and Pulping Chemistry, Paris, Vol. 2:239-44(April 27-30, 1987).

49. Rubin, M. B., Fortschr. Chem. Forsch. 13(2):251-306(1969).

50. Wilson, R. M.; Wunderly, S. W., Annals, New York Acad. Sci. 267:201-15 (1976).

51. Laird, T. Comprehensive organic chemistry: the synthesis and reactions of organic compounds. Oxford, England, Pergamon, Vol. 1:1213-27(1979).

52. Horspool, W. M., Photochemistry 6:348-99(1975).

53. Otting, W.; Stäiger, G., Chem. Ber. 88:828-33(1955).

54. Ternay, A. L., Jr., In Contemporary Organic Chemistry, W. B. Saunders Co., Philadelphia, 1979. p. 993.

55. Williams, D. H.; Fleming, I., In Spectroscopic Methods in Organic Chemistry. 2nd ed., Chapter 2, McGraw Hill, London, 1973.

56. Adler, E.; Hernestam, S., Acta Chem. Scand. 9(2):319-34(1955).

57. Furman, G. S., Jr. The contribution of charge-transfer complexes to the color of kraft lignin. Doctoral Dissertation, Appleton, WI, The Institute of Paper Chemistry, 1986. 170 p.

58. Heitner, C., personal communication, 1987.

59. Mitchell, G. R. Introduction to Raman spectroscopy. Class Notes, Purdue University Calumet, 1983.

60. Dollish, F. R.; Fateley, W. G.; Bentley, F. F. Characteristic Raman frequencies of organic compounds. New York, NY, John Wiley and Sons, 1974:97-104.

61. Hosoya, S.; Hatakeyama, H.; Nakano, J., J. Japan Wood Res. Soc. 16:140-4 (1970).

62. Hosoya, S.; Seike, K.; Nakano, J., J. Japan Wood Res. Soc. 22:314-19 (1976).

63. Marton, J.; Adler, E., U.S. pat. 3,071,570(Jan. 1, 1963).

64. Nadein, A. F.; Prokshin, G. F.; Bogomolov, B. D., Izv. VUZ, Lesnoi Zh. (6):114-16(1984).

65. Kukhtin, V. A.; Kirillova, K. M., CA 58:546h, 4543a, 8489d, 1105b(1962).

66. Birum, G. H.; Dever, J. L., U.S. pat. 2,961,455(1960).

67. Birum, G. H.; Dever, J. L., Fr. pat. 1,238,015(1960).

68. Birum, G. H.; Dever, J. L., U.S. pat. 3,014,949(1961).

69. Ramirez, F.; Mitra, R. B.; Desai, N. B., J. Am. Chem. Soc. 82:2651-2(1960).

70. Ramirez, F.; Desai, N. B., J. Am. Chem. Soc. 82:2652-3(1960).

71. Ramirez, F.; Mitra, R. B.; Desai, N. B., J. Am. Chem. Soc. 82:5763-4(1960).

72. Ramirez, F.; Ramanathan, N., J. Org. Chem. 26:3041-2(1961).

73. Ramirez, F.; Yamanaka, H.; Basedow, O. H., J. Am. Chem. Soc. 83:173-8(1961).

74. Ramirez, F.; Mitra, R. B.; Desai, N. B., J. Am. Chem. Soc. 84:1317-18(1962).

75. Ramirez, F.; Desai, N. B.; Ramanathan, N., J. Am. Chem. Soc. 85:1874-6(1963).

76. Ramirez, F.; Patwardham, A. V.; Desai, N. B.; Ramanathan, N.; Greco, C. V., J. Am. Chem. Soc. 85:3056-7(1963).

77. Ramirez, F.; Desai, N. B., J. Am. Chem. Soc. 85:3252-8(1963).

78. Ramirez, F.; Ramanathan, N.; Desai, N. B., J. Am. Chem. Soc. 85:3465-72 (1963).

79. Ramirez, F., Pure Appl. Chem. 9:337-69(1964).

80. Ramirez, F.; Patwardham, A. V.; Ramanathan, N.; Desai, N. B.; Greco, C. V.; Heller, S. R., J. Am. Chem. Soc. 87(3):543-8(1965).

81. Ramirez, F.; Patwardham, A. V.; Desai, N. B.; Heller, S. R., J. Am. Chem. Soc. 87(3):549-53(1965).

82. Ramirez, F.; Madan, O. P.; Desai, N. B.; Meyerson, S.; Banas, E. M., J. Am. Chem. Soc. 85:2681-2(1963).

83. Ramirez, F., Acc. Chem. Res. 1(6):168-74(1968).

84. Ramirez, F.; Kugler, H. J.; Smith, C. P., Tetrahedron 24:1931-44(1968).

85. Ramirez, F.; Tasaka, K.; Desai, N. B.; Smith, C. P., J. Am. Chem. Soc. 90(3):751-5(1968).

86. Ramirez, F.; Bigler, A. J.; Smith, C. P., J. Am. Chem. Soc. 90(3):3507-11 (1968).

87. Ramirez, F.; Glaser, S. L.; Bigler, A. J.; Pilot, J. F., J. Am. Chem. Soc. 91(2):496-500(1969).

88. Ramirez, F., Bull. Chim. Soc. Fr. 90:3491-519(1970).

89. Ramirez, F.; Loewengart, G. L.; Tsolis, E. A.; Tasaka, K., J. Am. Chem. Soc. 94(10):3531-6(1972).

90. Ramirez, F.; Chaw, Y. F.; Marecek, J. F.; Ugi, I., J. Am. Chem. Soc. 96(8):2429-33(1974).

91. Ramirez, F.; Marecek, J. F.; Tsuboi, H.; Okazaki, H.; Nowakowski, M., Phosphorous 6:215-18(1976).

92. Ramirez, F.; Nowakowski, M.; Marecek, J. F., J. Am. Chem. Soc. 99(13): 4515-17(1977).

93. Ramirez, F.; Dershowitz, S., J. Org. Chem. 22:856-7(1957).

94. Ramirez, F.; Dershowitz, S., J. Org. Chem. 22:1282-3(1957).

95. Ramirez, F.; Dershowitz, S., J. Org. Chem. 23:778-9(1958).

96. Ramirez, F.; Dershowitz, S., J. Am. Chem. Soc. 81:587-90(1959).

97. Ramirez, F.; Chen, E. H.; Dershowitz, S., J. Am. Chem. Soc. 81:4338-42 (1959).

98. Medvecz, P. J., Independent Study, The Institute of Paper Chemistry, Appleton, WI, 1987.

99. Van den Akker, J. A., TAPPI Monograph Series No. 27, New York, TAPPI, 1963:19.

100. Kubelka, P.; Munk, F., Z. Tech. Physik 12:593(1931).

101. Kubelka, P., J. Opt. Soc. Am. 33:448(1948).

102. Kubelka, P., J. Opt. Soc. Am. 44:330(1954).

103. Steele, F. A., Paper Trade J. 100(12):37-42(1935).

104. Judd, D. B., Res. Paper Nat. Bur. Stds. 19:287-305(1937).

105. Judd, D. B.; Shaw, M. B., Res. Paper Nat. Bur. Stds. 19:287-305(1937).

106. Judd, D. B., Paper Trade J. 106(1):39(1938).

107. Campbell, W. B.; Benny, J., Pulp Paper Mag. Can. 47(7):74-8(1946).

108. Van den Akker, J. A., Tappi 32(11):498-501(1949).

109. Shepard, W.; Schneider, S.; Andrews, I., Paper for A257 Class (G. A. Baum, ed.), The Institute of Paper Chemistry, 1980.

110. Polcin, J.; Rapson, W. H., Tappi 52(10):1970-4(1969).

111. Foote, W. J., Tech. Assoc. Papers 22:397(1937).

112. Van den Akker, J. A. In Modern Aspects of Reflectance Spectroscopy (W. W. Wendlandt, ed.), New York, Plenum Press, 1968:27-46.

113. Schreyer, G., Z. Phys. Chem. 12:39(1957).

114. Kortüm, G.; Vogel, J., Z. Phys. Chem. 18:110(1958).

115. Stenius, A. S., J. Opt. Soc. Am. 44:330(1954).

116. Berben, S. A.; Rademacher, J. P.; Sell, L. O.; Easty, D. B., Tappi J., in press.

117. Uhlin, I., A490 Progress Report III, The Institute of Paper Chemistry, May 1, 1986.

118. Polcin, J.; Rapson, W. H., Tappi 52(10):1965-70(1969).

119. Foote, W. J., Jr. An investigation of the optical scattering and absorption coefficients of dyed handsheets and the application of the ICI system of color specification to these handsheets. Doctoral Dissertation, Appleton, WI, The Institute of Paper Chemistry, 1938.

120. Calvert, J. G.; Pitts, J. N., Jr., Photochemistry, New York, NY, John Wiley and Sons, 1966:659-60.

121. Abadie-Maumert, F. A.; Loras, V., Papeterie 100(6):257-62, 267(1978).

122. Adler, E.; Marton, J., Acta Chem. Scand. 13(1):75-96(1959).

123. Marton, J.; Adler, E., Acta Chem. Scand. 15(2):357-83(1961).

124. Goldschmid, O. Ultraviolet spectra. In Sarkanen and Ludwig's Lignins Occurrence, Formation, Structure, and Reactions. New York, NY, Wiley-Interscience, 1971:241-66.

125. Whiting, P., personal communication, 1987.

126. Johnson, R., personal communication, 1987.

127. Lebo, S. E., Jr., Independent study, The Institute of Paper Chemistry, Appleton, WI. 1983.

128. Dallos, D., Independent study, The Institute of Paper Chemistry, Appleton, WI. 1985.

129. Adler, E.; Marton, J., Acta Chem. Scand. 13(1):75-96(1959).

130. Gellerstedt, G., Svensk Papperstid. 79(16):537-43(1976).

131. Hergert, H. L. O. Infrared spectra. In Sarkanen and Ludwig's Lignins Occurrence, Formation, Structure, and Reactions. New York, NY, Wiley-Interscience, 1971:267-97.

132. Schultz, T. P.; Glasser, W. G., Holzforsch. 40:37-44(1986).

133. Ramirez, F.; Kugler, H. J.; Parwardham, A. V.; Smith, C. P., J. Org. Chem. 33(3):1185-92(1968).

134. Crutchfield, M. M.; Dungan, C. H.; Letcher, J. H.; Mark, V.; Van Wazer, J. R. P31 Nuclear magnetic resonance. New York, NY, Interscience Publishers, 1968:227-448.

135. Claesson, S.; Olson, E.; Wennerblom, A., Svensk Papperstid. 71(8):335-40 (1968).

136. Iiyama, K.; Nakano, J., Japan Tappi 27(11):530-42(1973).

137. Björkman, A.; Person, B., Svensk Papperstid. 60(5):158-69(1957).

APPENDIX I

APPLE III PASCAL PROGRAM USED TO CALCULATE KUBELKA-MUNK ABSORPTION AND SCATTERING COEFFICIENTS FROM R_∞ AND R_o DATA

by Jim Biasca, IPC (1985)

```
{$LIST .printer}
{*$I-*}
{*$R-*}
{*$V-*}
PROGRAM SPECT(SAMPLE, INTLABEL, RESULTS);
USES REALMODES, TRANSCEND;

{*************************************************************}
{*                                                           *}
{*                  JAMES E. BIASCA                          *}
{*          THE INSTITUTE OF PAPER CHEMISTRY                 *}
{*               APPLETON, WISCONSIN                         *}
{*                                                           *}
{*  WRITTEN:  MARCH 21, 1985                                 *}
{*  REVISED:                                                 *}
{*                                                           *}
{*************************************************************}
{*                                                           *}
{*  KTRANS CALCULATE ABSORPTION COEFFICIENT ACCORDING        *}
{*  TO THE KUBELKA-MUNK THEORY. THE PROGRAM EXPECTS          *}
{*  REFLECTANCE DATA IN FILE ONE AND LIGHT SCATTERING        *}
{*  DATA IN FILE TWO. KTRANS PERFORMS THE CAL-               *}
{*  CULATIONS. THE RESULTS ARE STORED IN FILE THREE.         *}
{*  STRANS CALCULATE SCATTERING COEFFICIENT FROM             *}
{*  REFLECTANCE DATA. THE PROGRAM EXPECTS R INFINITY         *}
{*  DATA IN FILE ON AND R ZERO DATA IN FILE TWO.             *}
{*  DTRANS SUBTRACT THE SECOND FILE FROM THE FIRST.          *}
{*  MOST VARIABLES ARE GLOBAL AND CARE SHOULD BE TAKEN       *}
{*  IN MODIFYING THE PROGRAM. THE RECORD STRUCTURE           *}
{*  HAS BEEN DEFINED IDENTICAL TO THE RECORD STRUCTURE       *}
{*  OF APPLE BUSINESS GRAPHICS POINT OR LABEL FILES.         *}
{*  ADDITIONAL MODULES CAN BE ADDED TO PERFORM OTHER         *}
{*  CALCULATION OUT ABS FILES.                               *}
{*                                                           *}
{*************************************************************}

{*  PROGRAM CONSTANT AND VARIABLE DEFINITIONS                *}

CONST
  TLEN=60;
  LLEN=11;
  FLEN=15;


TYPE
  CRTCOMMAND=(ERASEOS,ERASEOL,UP,DOWN,RIGHT,LEFT,LEADIN);
  SETOFCHAR=SET OF CHAR;
  SPECTRA=RECORD
    CASE RECTYPE: INTEGER OF
      0: (R0: RECORD
                XLNUM:   INTEGER;
                YLNUM:   INTEGER;
                XYNUM:   INTEGER;
                SXTITLE: STRING[TLEN];
                SYTITLE: STRING[TLEN];
              END);
      1: (R1: ARRAY[1..FLEN] OF RECORD
                WAVELENGTH:   REAL;
                REFLECTANCE:  REAL;
                NLABEL:       STRING[LLEN];
                SLABEL:       STRING[LLEN];
```

```
                FILLER:         INTEGER;

                END;
    END;
  SPECTRUM = FILE OF SPECTRA;


VAR
  CH:          CHAR;
  FILENUMBER:CHAR;
  POINTS:      INTEGER;
  PTNUM:       INTEGER;
  LABNUM:      INTEGER;
  MAXLAB:      INTEGER;
  MINLAB:      INTEGER;
  RECNUM:      INTEGER;
  RECOFF:      INTEGER;
  REC:         SPECTRA;
  SAMPLE:      SPECTRUM;
  INTLABEL:    SPECTRUM;
  RESULTS:     SPECTRUM;
  SUCESSFUL:   BOOLEAN;
  TRANS:       BOOLEAN;
  CRTINFO:     PACKED ARRAY[CRTCOMMAND] OF CHAR;
  PREFIXED:    ARRAY[CRTCOMMAND] OF BOOLEAN;

(* END PROGRAM CONSTANT AND VARIABLE DEFINTIONS                    *)


PROCEDURE GETCRTINFO;
(*****************************************************************)
(*                                                               *)
(*  READ SYSTEM.MISCINFO AND GET CRT CONTROL CHARACTER INFO      *)
(*                                                               *)
(*****************************************************************)

VAR
  BUFFER: PACKED ARRAY[0..511] OF CHAR;
  I,BYTE: INTEGER;
  F: FILE;

BEGIN
  RESET(F,'*SYSTEM.MISCINFO');
  I:=BLOCKREAD(F,BUFFER,1);
  CLOSE(F);
  BYTE:=ORD(BUFFER[72]); (* PREFIX INFORMATION BYTE *)
  CRTINFO[LEADIN]:=BUFFER[62];  PREFIXED[LEADIN]:=FALSE;
  CRTINFO[ERASEOS]:=BUFFER[64]; PREFIXED[ERASEOS]:=ODD(BYTE DIV 8);
  CRTINFO[ERASEOL]:=BUFFER[65]; PREFIXED[ERASEOL]:=ODD(BYTE DIV 4);
  CRTINFO[RIGHT]:=BUFFER[66];   PREFIXED[RIGHT]:=ODD(BYTE DIV 2);
  CRTINFO[UP]:=BUFFER[67];      PREFIXED[UP]:=ODD(BYTE);
  CRTINFO[LEFT]:=BUFFER[68];    PREFIXED[LEFT]:=ODD(BYTE DIV 32);
  CRTINFO[DOWN]:=CHR(10);       PREFIXED[DOWN]:=FALSE;
END (* GETCRTINFO *);


PROCEDURE CRT(C: CRTCOMMAND);
(*****************************************************************)
(*                                                               *)
(*  CRT COMMANDS ARE: ERASEOS,ERASEOL,UP,DOWN,RIGHT,LEFT.        *)
(*                                                               *)
(*****************************************************************)

BEGIN
  IF PREFIXED[C] THEN UNITWRITE(1,CRTINFO[LEADIN],1,0,12);
  UNITWRITE(1,CRTINFO[C],1,0,12);
END (* CRT *);
```

```
PROCEDURE PROMPTAT(Y: INTEGER; S: STRING);
(*************************************************************************)
(*                                                                       *)
(*  PROMPTAT DISPLAYS THE PROMPT DEFINED IN S, Y ROWS DOWN THE           *)
(*  SCREEN.                                                              *)
(*                                                                       *)
(*************************************************************************)

BEGIN
  GOTOXY(0,Y);
  WRITE(S);
  CRT(ERASEOL);
END (* PROMPAT *);


FUNCTION GETCHAR(OKSET: SETOFCHAR): CHAR;
(*************************************************************************)
(*                                                                       *)
(*  GET A CHARACTER, BEEP IF NOT IN OKSET, ECHO ONLY IF PRINTING         *)
(*                                                                       *)
(*************************************************************************)

VAR
  CH: CHAR;
  GOOD: BOOLEAN;

BEGIN
  REPEAT
    READ(KEYBOARD,CH);
    IF EOLN(KEYBOARD) THEN CH:=CHR(13);
    GOOD:= CH IN OKSET;
    IF NOT GOOD THEN WRITE(CHR(7))
      ELSE IF CH IN [' '..')'] THEN WRITE(CH);
  UNTIL GOOD;
  GETCHAR:=CH;
END (* GETCHAR *);


PROCEDURE GETSTRING(VAR S: STRING; MAXLEN: INTEGER);
(*************************************************************************)
(*                                                                       *)
(*  GET AND ECHO A STRING UP TO MAXLEN CHARS LONG.                       *)
(*  IF NULL STRING ENTERED, DEFAULT AND PRINT PREVIOUS VALUE.            *)
(*                                                                       *)
(*************************************************************************)

VAR
  S1: STRING[1];
  STEMP: STRING[80];
  OKSET: SET OF CHAR;

BEGIN
  OKSET:=[' '..')'];
  S1:=' ';
  STEMP:='';
  REPEAT
    IF LENGTH(STEMP) = 0 THEN S1[1]:=GETCHAR(OKSET + [CHR(13)])
      ELSE IF LENGTH(STEMP)=MAXLEN THEN S1[1]:=GETCHAR([CHR(13),CHR(8)])
             ELSE S1[1]:=GETCHAR(OKSET + [CHR(13),CHR(8)]);
    IF S1[1] IN OKSET THEN STEMP:=CONCAT(STEMP,S1)
      ELSE IF S1[1]=CHR(8) THEN
        BEGIN
          CRT(LEFT); WRITE(' '); CRT(LEFT);
          DELETE(STEMP,LENGTH(STEMP),1);
```

```
      END;
  UNTIL S1[1] = CHAR(13);
  IF LENGTH(STEMP) <> 0 THEN S:=STEMP
  ELSE WRITE(S);
END (* GETSTRING *);


PROCEDURE GETFILE;
(*************************************************************)
(*                                                           *)
(*  GETFILE PROMPTS FOR THE FILE NUMBER (FILENUMBER).        *)
(*                                                           *)
(*************************************************************)

BEGIN
  REPEAT
    PROMPTAT(2,'Which file:  1) Sample, 2) Label, 3) Results? ');
    FILENUMBER:=GETCHAR(['1','2','3']);
  UNTIL IORESULT=0;
END (* GETFILE *);


PROCEDURE GETLABEL;
(*************************************************************)
(*                                                           *)
(*  GETLABEL PROMPTS FOR THE LABEL NUMBER (LABNUM).          *)
(*                                                           *)
(*************************************************************)

BEGIN
  REPEAT
    PROMPTAT(4,'Which label? ');
    READLN(LABNUM);
  UNTIL IORESULT=0;
END (* GETLABEL *);


PROCEDURE LABTOPT;
(*************************************************************)
(*                                                           *)
(*  LABTOPT TRANSFORMS THE LABEL NUMBER INTO A POINT         *)
(*  NUMBER.                                                  *)
(*                                                           *)
(*************************************************************)

BEGIN
  PTNUM:=(702-LABNUM) DIV 2;
END (* PTTOREC *);


PROCEDURE PTTOREC;
(*************************************************************)
(*                                                           *)
(*  PTTOREC TRANSFORMS THE POINT NUMBER INTO A RECORD        *)
(*  NUMBER AND AN OFFSET INTO THE RECORD.                    *)
(*                                                           *)
(*************************************************************)

BEGIN
  RECNUM:=((PTNUM-1) DIV 15) + 1;
  RECOFF:=PTNUM - ((RECNUM-1) * 15);
END (* PTTOREC *);


PROCEDURE CHANGE;
FORWARD;
```

```
PROCEDURE GETREC(VAR WORKFILE: SPECTRUM);
{*****************************************************************}
{*                                                               *}
{*  GETREC RETRIEVES THE RECNUM RECORD OF FILE FILENUMBER.       *}
{*                                                               *}
{*****************************************************************}

PROCEDURE NORECORD;
BEGIN
  GOTOXY(0,4);CRT(ERASEOL);
  WRITELN('Record ',LABNUM,' not in file ',FILENUMBER,'.');
  GOTOXY(0,6);CRT(ERASEOL);
  PROMPTAT(6,'Press <RETURN> to continue.');
  READLN;
  EXIT(CHANGE);
END;

BEGIN
  WORKFILE^.RECTYPE:=1;
  SEEK(WORKFILE,RECNUM);
  GET(WORKFILE);
  IF EOF(WORKFILE) THEN NORECORD;
  REC:=WORKFILE^;
END {* GETREC *};


PROCEDURE PUTREC(VAR WORKFILE: SPECTRUM);
{*****************************************************************}
{*                                                               *}
{*  PUTREC PLACES REC ON THE RECNUM RECORD OF FILE               *}
{*  FILENUMBER.                                                  *}
{*                                                               *}
{*****************************************************************}

PROCEDURE NOWRITE;
BEGIN
  GOTOXY(0,20);
  WRITELN(CHR(7),'Unable to write to file, no data written.');
  PROMPTAT(22,'Press <RETURN> to continue.');
  READLN;
END;

BEGIN
  WORKFILE^:=REC;
  SEEK(WORKFILE,RECNUM);
{*$I-*}
  PUT(WORKFILE);
{*$I+*}
  IF (IORESULT<>0) THEN NOWRITE;
END {* PUTREC *};


PROCEDURE SHOWREC;
{*****************************************************************}
{*                                                               *}
{*  SHOWREC DISPLAYS A RECORD.                                   *}
{*                                                               *}
{*****************************************************************}

BEGIN
  GOTOXY(0,7); CRT(ERASEOS);
  WRITELN('Point: ',PTNUM); WRITELN;
  REC.RECTYPE:=1;
  WITH REC DO
```

```
    BEGIN
      WRITELN( Label          , LABNUM,':');
      WRITELN('Wavelength  ', R1[RECOFF].WLABEL);
      WRITELN('Reflectance ', R1[RECOFF].REFLECTANCE:8:2);
    END;
END (* SHOWREC *);


PROCEDURE CHANGEREC;
(*****************************************************************)
(*                                                               *)
(*  CHANGEREC CHANGES THE SPECIFIED RECORD IN THE FILE.          *)
(*                                                               *)
(*****************************************************************)

BEGIN
  GOTOXY(0,13); CRT(ERASEOS);
  PROMPTAT(13,'(Press <SPACE> to continue or E)xit.)');
  CH:=GETCHAR([' ','E','e']);
IF CH <> ' ' THEN EXIT(CHANGEREC);
  REC.RECTYPE:=1;
  WITH REC DO
    BEGIN
      GOTOXY(0,13);
      CRT(ERASEOS);
      WRITELN('Point ',PTNUM);
      WRITELN('Label ',LABNUM,':'); WRITELN;
      WRITE  ('Wavelength:  '); READLN(REC.R1[RECOFF].WLABEL);
      WRITE  ('Reflectance: '); READLN(REC.R1[RECOFF].REFLECTANCE);
    END;
END; (* CHANGEREC *)


PROCEDURE CHANGE;
(*****************************************************************)
(*                                                               *)
(*  CHANGE PROMPTS FOR THE RECORD TO CHANGE AND CALLS            *)
(*  CHANGEREC.                                                   *)
(*                                                               *)
(*****************************************************************)

PROCEDURE RESULT;

BEGIN
  IF TRANS <> TRUE THEN
      BEGIN
        WRITELN('No output file to Change until after Transforming.');
        PROMPTAT(6,'Press <RETURN> to continue.');
        READLN;
      END;
  IF TRANS <> TRUE THEN
      EXIT(CHANGE);
  IF TRANS = TRUE THEN
     GETREC(RESULTS);
END (* RESULT *);

BEGIN
  GOTOXY(0,0);
  CRT(ERASEOS);
  WRITELN('                          Change a point ... ');
  GETFILE;
  GETLABEL;
  LABTOPT;
  PTTOREC;
  CASE FILENUMBER OF
    '1':  GETREC(SAMPLE);
```

```
    '2': GETREC(INTLABEL);
    '3': RESULT;
  END;
  SHOWREC;
  CHANGEREC;
  CASE FILENUMBER OF
    '1': PUTREC(SAMPLE);
    '2': PUTREC(INTLABEL);
    '3': PUTREC(RESULTS);
  END;
END (* CHANGE *);


PROCEDURE NEXT;
(*************************************************************)
(*                                                           *)
(*  NEXT INCREMENTS THE RECORD POINTER BY ONE AND CALLS      *)
(*  VIEW TO SHOW THE 'NEXT' RECORD.                          *)
(*                                                           *)
(*************************************************************)

PROCEDURE NOLABEL;
BEGIN
  GOTOXY(0,4);CRT(ERASEOL);
  WRITE('Label ',LABNUM,': not in file.');
  GOTOXY(0,6);CRT(ERASEOL);
  PROMPTAT(6,'Press <RETURN> to continue.');
  READLN;
  EXIT(NEXT);
END;

BEGIN
  IF (CH = 'N') OR (CH = 'n')
    THEN
      BEGIN
        GOTOXY(0,0);
        CRT(ERASEOS);
        WRITELN('                          Next point ... ');
      END;
  REPEAT
      LABNUM:=LABNUM-2;
      IF LABNUM > MAXLAB THEN NOLABEL;
      IF LABNUM < MINLAB THEN NOLABEL;
    (*$I+*)
      LABTOPT;
      PTTOREC;
      CASE FILENUMBER OF
        '1': GETREC(SAMPLE);
        '2': GETREC(INTLABEL);
        '3': GETREC(RESULTS);
      END;
      SHOWREC;
      PROMPTAT(18, 'Press <N> for next label or <SPACE> for command line.'
      CH:=GETCHAR([' ','N','n']);
  UNTIL CH = ' ';
END(* NEXT *);


PROCEDURE VIEW;
(*************************************************************)
(*                                                           *)
(*  VIEW ALLOW THE USER TO BROWSE THROUGH THE FILES.         *)
(*                                                           *)
(*************************************************************)

BEGIN
```

```
(*$I -*)
  GOTOXY(0,0);
  CRT(ERASEOS);
  WRITELN('                          View a point ... ');
  GETFILE;
  IF (FILENUMBER = '3') AND (TRANS <> TRUE) THEN
    BEGIN
      WRITELN;
      WRITELN('No output file to View until after Transforming.');
      WRITELN;
      WRITELN('Press <RETURN> to continue.');
      READLN;
      FILENUMBER:='1';
      EXIT(VIEW);
    END;
  GETLABEL;
  LABNUM:=LABNUM+2;
  NEXT;
END (* VIEW *);


PROCEDURE KTRANS;
(*************************************************************)
(*                                                           *)
(*  KTRANS CREATES THE OUTPUT FILES USING THE TWO            *)
(*  INPUT FILES AND THE FOLLOWING EQUATION.                  *)
(*  K = (1-R)**2 / (2*R) * S                                 *)
(*************************************************************)

VAR
  K1,K2,K3: REAL;

BEGIN
  GOTOXY(0,0);
  CRT(ERASEOS);
  WRITELN('                          Calculating absorption coefficient ... ');
  WRITE  ('                          ');
  TRANS:=TRUE;
  RECNUM:=1;
  SAMPLE^.RECTYPE:=1;
  INTLABEL^.RECTYPE:=1;
  RESULTS^.RECTYPE:=1;
  SEEK(SAMPLE,RECNUM);
  SEEK(INTLABEL,RECNUM);
  SEEK(RESULTS,RECNUM);
  REPEAT
    WRITE('.');
    GET(SAMPLE);
    GET(INTLABEL);
    IF EOF(SAMPLE) OR EOF(INTLABEL) THEN EXIT(KTRANS);
    FOR RECOFF:=1 TO FLEN DO
      BEGIN
        RESULTS^.R1[RECOFF]:=SAMPLE^.R1[RECOFF];
        K1:=SAMPLE^.R1[RECOFF].REFLECTANCE;
        K2:=INTLABEL^.R1[RECOFF].REFLECTANCE;
        K3:=(SQR(1.0 - K1/100)*50/K1)*K2;
        RESULTS^.R1[RECOFF].REFLECTANCE:=K3;
      END;
    PUT(RESULTS);
  UNTIL EOF(SAMPLE);
END (* KTRANS *);


PROCEDURE STRANS;
(*************************************************************)
(*                                                           *)
```

```
(*  STRANS CREATES THE OUTPUT FILE USING THE TWO
 *  INPUT FILES AND THE FOLLOWING EQUATION.
(*  S = (R/(W)/(1-R)**2) * LN ((1-R*R0)*R)/(R-R0)                    *)
(*****************************************************************)

VAR
  S1,S2,S3: REAL;
  BASISWEIGHT: REAL;
  NEGATIVE: STRING[3];

BEGIN
  GOTOXY(0,0);
  CRT(ERASEOS);
  WRITELN('                          Calculate scattering coefficient ... ');
  PROMPTAT(2,'What is the samples basis weight in g/m^2? ');
  READLN(BASISWEIGHT);
  BASISWEIGHT:=BASISWEIGHT/10000;
  WRITELN;
  WRITELN('                                        calculating ... ');
  WRITE  ('                                        ');
  TRANS:=TRUE;
  NEGATIVE:='No';
  RECNUM:=1;
  SAMPLE^.RECTYPE:=1;
  INTLABEL^.RECTYPE:=1;
  RESULTS^.RECTYPE:=1;
  SEEK(SAMPLE,RECNUM);
  SEEK(INTLABEL,RECNUM);
  SEEK(RESULTS,RECNUM);
  REPEAT
    WRITE('.');
    GET(SAMPLE);
    GET(INTLABEL);
    IF EOF(SAMPLE) OR EOF(INTLABEL)
      THEN
        BEGIN
          WRITELN;
          WRITELN('At some point, R infinity was =< R zero - ',NEGATIVE);
          WRITELN;
          WRITELN('Press <RETURN> to continue.');
          READLN;
          EXIT(STRANS);
        END;
    FOR RECOFF:=1 TO FLEN DO
      BEGIN
        RESULTS^.R1[RECOFF]:=SAMPLE^.R1[RECOFF];
        S1:=SAMPLE^.R1[RECOFF].REFLECTANCE/100;
        S2:=INTLABEL^.R1[RECOFF].REFLECTANCE/100;
        IF S2 >= S1 THEN NEGATIVE:='Yes';
        S3:=(S1/BASISWEIGHT/(1-S1*S1))*LN(ABS((1-S1*S2)*S1/(S1-S2)));
        RESULTS^.R1[RECOFF].REFLECTANCE:=S3;
      END;
    PUT(RESULTS);
  UNTIL EOF(SAMPLE);
END (* STRANS *);


PROCEDURE KSTRANS;
(*****************************************************************)
(*                                                               *)
(*  KSTRANS CREATES THE OUTPUT FILES USING ONLY THE FIRST        *)
(*  INPUT FILE AND THE FOLLOWING EQUATION.                       *)
(*  K/S = (1-R)**2 / (2*R)                                       *)
(*****************************************************************)
```

```
  KS1, KS2, KS3: REAL;

BEGIN
  GOTOXY(0,0);
  CRT(ERASEOS);
  WRITELN('                          Calculating K/S ... ');
  WRITE  ('                          ');
  TRANS:=TRUE;
  RECNUM:=1;
  SAMPLE^.RECTYPE:=1;
  INTLABEL^.RECTYPE:=1;
  RESULTS^.RECTYPE:=1;
  SEEK(SAMPLE,RECNUM);
  SEEK(INTLABEL,RECNUM);
  SEEK(RESULTS,RECNUM);
  REPEAT
    WRITE('.');
    GET(SAMPLE);
    GET(INTLABEL);
    IF EOF(SAMPLE) OR EOF(INTLABEL) THEN EXIT(KSTRANS);
    FOR RECOFF:=1 TO FLEN DO
      BEGIN
        RESULTS^.R1[RECOFF]:=SAMPLE^.R1[RECOFF];
        KS1:=SAMPLE^.R1[RECOFF].REFLECTANCE;
        KS2:=INTLABEL^.R1[RECOFF].REFLECTANCE;
        KS3:=(SQR(1.0 - KS1/100)*50/KS1);
        RESULTS^.R1[RECOFF].REFLECTANCE:=KS3;
      END;
    PUT(RESULTS);
  UNTIL EOF(SAMPLE);
END (* KSTRANS *);

PROCEDURE DTRANS;
(*************************************************************)
(*                                                           *)
(*  DTRANS CREATES THE OUTPUT FILES USING THE TWO            *)
(*  INPUT FILES AND THE FOLLOWING EQUATION.                  *)
(*  FILE 1 - FILE 2                                          *)
(*************************************************************)

VAR
  D1,D2,D3: REAL;

BEGIN
  GOTOXY(0,0);
  CRT(ERASEOS);
  WRITELN('                          Calculating difference ... ');
  WRITE  ('                          ');
  TRANS:=TRUE;
  RECNUM:=1;
  SAMPLE^.RECTYPE:=1;
  INTLABEL^.RECTYPE:=1;
  RESULTS^.RECTYPE:=1;
  SEEK(SAMPLE,RECNUM);
  SEEK(INTLABEL,RECNUM);
  SEEK(RESULTS,RECNUM);
  REPEAT
    WRITE('.');
    GET(SAMPLE);
    GET(INTLABEL);
    IF EOF(SAMPLE) OR EOF(INTLABEL) THEN EXIT(DTRANS);
    FOR RECOFF:=1 TO FLEN DO
      BEGIN
        RESULTS^.R1[RECOFF]:=SAMPLE^.R1[RECOFF];
        D1:=SAMPLE^.R1[RECOFF].REFLECTANCE;
        D2:=INTLABEL^.R1[RECOFF].REFLECTANCE;
```

```
        D3:= D1 - D2;
        RESULTS^.RECORD^.REAL1:=D3;
      END;
    PUT(RESULTS);
  UNTIL EOF(SAMPLE);
END (* DTRANS *);


PROCEDURE OPENFILE(VAR WORKFILE: SPECTRUM; FILENUMBER: INTEGER);
(*****************************************************************)
(*                                                               *)
(*  OPENFILE OPENS THE INPUT AND OUTPUT FILES.                   *)
(*                                                               *)
(*****************************************************************)

VAR
  FILENAME: STRING;

(*$I-*)
BEGIN
  REPEAT
      IF FILENUMBER = 1 THEN
          PROMPTAT(2,'First input file name:  ')
        ELSE IF FILENUMBER = 2 THEN
          PROMPTAT(4,'Second input file name:  ')
        ELSE IF FILENUMBER = 3 THEN
          PROMPTAT(6,'Output file name:  ');
      READLN(FILENAME);
      WRITELN;
      IF (FILENUMBER = 1) OR (FILENUMBER = 2) THEN
        BEGIN
          RESET(WORKFILE, FILENAME);
          SUCESSFUL:=(IORESULT=0);
          IF NOT SUCESSFUL THEN
            WRITELN('File does not exist or cannot be opened.');
        END
      ELSE
        BEGIN
          REWRITE(WORKFILE, FILENAME);
          SUCESSFUL:=(IORESULT=0);
          IF NOT SUCESSFUL THEN
            WRITELN('File cannot be opened.');
        END
UNTIL SUCESSFUL;
END (* OPENFILE *);


PROCEDURE FILEINFO(VAR WORKFILE: SPECTRUM; VAR FILEKIND, POINTS: INTEGER);
(*****************************************************************)
(*                                                               *)
(*  FILEINFO READS THE FIRST RECORD OF THE FILE NAMED IN         *)
(*  THE PROCEDURE CALL AND PASSES THE VALUES OF XLNUM            *)
(*  (AS FILEKIND) AND XYNUM (AS POINTS) BACK TO                  *)
(*  COMPAREFILES.                                                *)
(*                                                               *)
(*****************************************************************)

BEGIN
  RECNUM:=0;
  WORKFILE^.RECTYPE:=0;
  SEEK(WORKFILE,RECNUM);
  GET(WORKFILE);
  FILEKIND:=WORKFILE^.R0.XLNUM;
  POINTS:=WORKFILE^.R0.XYNUM;
END (* FILEINFO *);
```

```
PROCEDURE COMPAREFILES;
(*****************************************************)
(*                                                   *)
(*  COMPAREFILES CHECKS TO SEE THAT BOTH INPUT FILES *)
(*  ARE HORIZONTAL LABEL FILES AND CONTAIN EQUAL NUMBER*)
(*  OF POINTS.                                       *)
(*                                                   *)
(*****************************************************)

VAR
  KIND1, KIND2: INTEGER;
  POINTS1, POINTS2: INTEGER;

BEGIN
  FILEINFO(SAMPLE, KIND1, POINTS1);
  FILEINFO(INTLABEL, KIND2, POINTS2);
  IF (KIND1 <> 0) OR (KIND2 <> 0) THEN
    PROMPTAT(14, 'One or both files are not HORIZONTAL LABEL files.');
  IF POINTS1 <> POINTS2 THEN
    PROMPTAT(16, 'The number of points in the files are not equal.');
  PROMPTAT(18, 'Press <SPACE> to continue.');
  CH:=GETCHAR(' ');
  POINTS:=POINTS1;
  MAXLAB:=700;
  MINLAB:=MAXLAB-(POINTS * 2)+2;
END (* COMPAREFILES *);

PROCEDURE DEFINEOUTFILE;
(*****************************************************)
(*                                                   *)
(*  DEFINEOUTFILE WRITES THE HEADER RECORD TO THE RESULTS*)
(*  FILE.                                            *)
(*                                                   *)
(*****************************************************)

BEGIN
  RECNUM:=0;
  SAMPLE^.RECTYPE:=0;
  SEEK(SAMPLE,RECNUM);
  RESULTS^.RECTYPE:=0;
  RESULTS^:=SAMPLE^;
  PUT(RESULTS);
END (* DEFINEOUTFILE *);

(* SPECT *)
(*****************************************************)
(*                                                   *)
(*  THE SPECT OPENS THE FILES AND THEN FOLLOWS THE   *)
(*  USER COMMANDS UNTIL THE QUIT COMMAND. AFTER THAT *)
(*  SPECT CLOSES THE FILES AND RETURNS CONTROL TO    *)
(*  PASCAL SYSTEM.                                   *)
(*                                                   *)
(*****************************************************)

BEGIN
  GETCRTINFO;
  GOTOXY(0,0); CRT(ERASEOS);
  WRITELN('                                    Spectrum ');
  OPENFILE(SAMPLE, 1);
  OPENFILE(INTLABEL, 2);
  OPENFILE(RESULTS, 3);
  COMPAREFILES;
  DEFINEOUTFILE;
  REC.RECTYPE:=1;
  SAMPLE^.RECTYPE:=1;
```

```
  INTLABEL^.RECTYPE = 1;
  RESULTS^.RECTYPE:=1;
  RECNUM:=1;
  RECOFF:=1;
  LABNUM:=700;
  PTNUM:=1;
  TRANS:=FALSE;
  REPEAT
    GOTOXY(0,0); CRT(ERASEOS);
    PROMPTAT(0,' Commands:          C(hange, V(iew, N(ext, Q(uit.');
    PROMPTAT(1,' Transformations:  K( Absorption coefficient');
    PROMPTAT(2,'                   S(cattering coefficient');
    PROMPTAT(3,'                   Z( K/S');
    PROMPTAT(4,'                   D(elta');
    CH:=GETCHAR(['C','c','V','v','N','n','Q','q','K','k','S','s','D','d',
                 'Z','z']);
    CASE CH OF
      'C','c': CHANGE;
      'V','v': VIEW;
      'N','n': NEXT;
      'K','k': KTRANS;
      'S','s': STRANS;
      'Z','z': KSTRANS;
      'D','d': DTRANS
    END;
  UNTIL CH IN ['Q','q'];
  GOTOXY(0,0); CRT(ERASEOS);
  CLOSE(SAMPLE,LOCK);
  CLOSE(INTLABEL,LOCK);
  CLOSE(RESULTS,LOCK);
END.
```

APPENDIX II

DETERMINATION AND COMPARISON OF ATTENUATION FACTORS

The attenuation factors of the various components used in this work were experimentally determined using the procedure described below. The attenuation factors thus determined were then compared to those provided by the manufacturer, ORIEL Corporation.

DETERMINATION OF THE ATTENUATION FACTORS OF THE OPTICAL DEVICES USED IN INCIDENT LIGHT FLUX DETERMINATIONS

Two optical devices were used to attenuate the flux of the light incident upon the photomultiplier. These two devices were a 4.0 nominal density neutral density filter and a UV grade diffuser, both from ORIEL Corporation. The attenuation factors of these devices were determined as follows:

1. The lamp and photomultiplier components of the optical apparatus shown in Fig. 18 and 19 were started and warmed-up for 30 minutes. The bias on the covered photomultiplier head was set at 200 volts. During this time the lamp shutter was closed.

2. An ORIEL multiple filter holder was attached to the output side of the monochromator, and the neutral density filter was placed in this filter holder. The monochromator was set at the desired wavelength and the slits of the monochromator were then set to the desired values. The photomultiplier head was then uncovered. The photomultiplier head was never uncovered with the room light on as this could potentially damage the tube.

3. The lamp shutter assembly was opened and the current generated by

this light was recorded. The shutter was closed and the UV grade diffuser was attached to the photomultiplier head (flange mounted). No other changes were made.

4. The lamp shutter was opened and the current generated by this attenuated beam was recorded.

5. The above procedure was then repeated for each wavelength examined and average attenuation factors were calculated as shown below (Table 22).

$$\text{Attenuation factor (\%)} = \frac{\text{average current generated by attenuated light beam}}{\text{average current generated by unattenuated light beam}} \times 100$$

6. With the diffuser attached to the photomultiplier head, the above procedure was repeated with the neutral density filter and attenuation factors were calculated (Table 23).

7. These factors were then compared with those provided by ORIEL (June, 1979 catalog) and were found to be quite comparable.

DETERMINATION OF THE ATTENUATION FACTORS OF THE OPTICAL DEVICES USED IN THE DETERMINATION OF SHIFT FACTORS

Two additional optical devices were used in the determination of the radiant power sensitivity shift factors described in Appendix II. These devices were a 0.3 and a 2.0 nominal density neutral density filter from ORIEL Corporation. The attenuation factors of these devices were evaluated using the same procedure described above for the 4.0 nominal density neutral density filter, except that the incident wavelengths examined were the wavelengths

produced by the Argon ion laser. Also, strictly monochromatic light, rather than narrow band width light, was used in these determinations. The results obtained in these experiments are shown in Table 24. These factors were also found to be in good agreement with those provided by ORIEL (June, 1979 catalog).

Table 23. Experimentally determined UV grade diffuser and neutral density filter attenuation factors.

Incident Wavelength (nm)	Band Width (nm)	Average Attenuation Factors (%)	
		UV Grade Diffuser	4.0 Neutral Density Filter
295	5	1.506	7.46×10^{-3}
300	5	1.788	7.11×10^{-3}
305	5	2.065	8.00×10^{-3}
310	5	2.194	7.85×10^{-3}
312.5	5	2.152	7.70×10^{-3}
315	5	2.164	7.73×10^{-3}
320	5	2.147	8.18×10^{-3}
325	5	2.166	8.47×10^{-3}
330	5	2.115	8.10×10^{-3}
335	5	2.178	8.08×10^{-3}
340	5	2.185	8.02×10^{-3}
345	5	2.228	8.13×10^{-3}
350	5	2.225	8.39×10^{-3}
355	5	2.225	8.57×10^{-3}
360	5	2.323	8.54×10^{-3}
365	5	2.257	7.74×10^{-3}
370	5	2.337	8.43×10^{-3}
375	5	2.599	8.23×10^{-3}
380	5	2.985	9.15×10^{-3}
385	5	2.681	11.38×10^{-3}
390	5	5.504	12.62×10^{-3}

Table 24. Experimentally determined attenuation factors for the optical devices used in evaluating radiant power sensitivity shift factors.

Incident Wavelength (nm)	Average Attenuation Factors (%)			
	0.3 Filter	2.0 Filter	4.0 Filter	UV Grade Diffuser
458	52.8	10.9	9.21×10^{-3}	2.51
476.5	52.4	10.6	9.41×10^{-3}	2.48
488	52.2	10.7	9.96×10^{-3}	2.63
496.5	52.0	10.6	10.30×10^{-3}	2.54
514.5	51.9	10.5	11.79×10^{-3}	2.60

APPENDIX III

CONVERSION OF PHOTOMULTIPLIER TUBE CURRENTS INTO INCIDENT LIGHT FLUXES

In monochromatic irradiation experiments, the flux of the light incident upon a given sample was determined as follows. The lamp in Fig. 18 was started and, following warm-up, set to the desired total output. Using the monochromator slits, the output from the monochromator was adjusted to produce a beam of light of the desired characteristics (i.e., wavelength maximum, wavelength band, and illumination area). In the experiments described in this study the wavelength band used was 5 nm and the illumination area was 2.82 cm^2. This was the minimum possible area for later diffuse reflectance UV-visible spectroscopic analysis. Using a black sample, the lens on the output side of the monochromator was used to focus the beam onto a practice sample. The shutter assembly of the lamp was closed and the sample mount shown in Fig. 18, was replaced with the photomultiplier head. With the phototube covered, the readout unit was turned on and a bias of 600 volts was set across the tube. After allowing 15 minutes for warm-up, the cover was removed, the shutter of the lamp was opened and the current generated by the incident light was recorded. This current was then converted into incident light flux using the equation shown below

$$\text{Incident light flux (photons/cm}^2\text{ sec per nm)} = \frac{[C]}{[RPS]_\lambda [AF]_f [AF]_d [AI][E_p][B][SF]}$$

where: $[C]$ = measured photomultiplier current (amperes)

$[RPS]_\lambda$ = radiant power sensitivity of tube at incident wavelength λ [ampere/J (sec)]

$[AF]_f$ = attenuation factor of 4.0 neutral density filter (%)

$[AF]_d$ = attenuation factor of UV grade diffuser (%)

[AI] = area of illumination (cm^2)

[E_p] = energy of a photon of wavelength λ (J/photon)

[B] = band width (nm)

[SF] = "shift" factor.

This last factor arises from the fact that the radiant power sensitivity curve of the photomultiplier head given by ORIEL is only a "rough guide to system design." This fact was compensated for by measuring the actual radiant power sensitivity of the head in the visible region of the spectrum and then comparing these values with those provided by ORIEL. Visible light was used in these comparisons because this was the only range of light of accurately known radiant power available. Any differences observed in the UV range of the spectrum should, however, parallel the differences observed in the visible range. The procedure for determining this shift factor is described below.

1. The optical apparatus shown in Fig. 102 was assembled. In brief, the system consisted of a Coherent Radiation model 90-4 Argon ion laser, three ORIEL Corporation neutral density filters (0.3, 2.0, and 4.0 nominal densities), a UV grade optical diffuser (ORIEL Corporation) and the ORIEL Corporation photomultiplier detector system described above. The attenuation factors of these filters and diffuser were measured experimentally and were found to be in good agreement with those provided by ORIEL (Appendix II). Light from an Argon ion laser was used because it was the only available light of accurately known radiant power (wavelengths = 457, 476.5, 488, 496.5, and 514 nm). The radiant power of this light was read from the meter on the laser control panel and measured with a Coherent Model 210 power meter. The neutral density filters and

the UV grade diffuser served to attenuate the laser light to a level which could be measured with the PMT detector system.

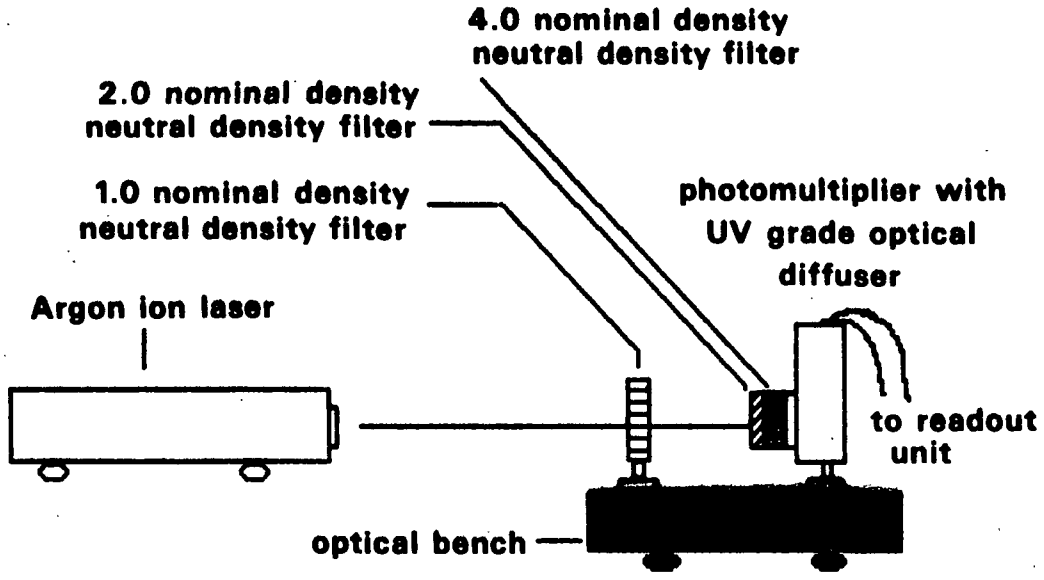

Figure 102. Schematic diagram of the optical apparatus used in the determination of "shift" factors.

2. The radiant power output of the laser at 457 nm was adjusted to 50 milliwatts (as measured using the model 210 power meter and laser control panel).

3. The shutter of the laser was closed and a bias of 600 volts was set across the photomultiplier tube, and the tube was allowed to warm-up for 20 minutes.

4. After zeroing the photomultiplier current, the shutter of the laser was opened and the photomultiplier current generated by the attenuated monochromatic light beam was recorded.

5. The above procedure was repeated using 476.5, 488, 496.5, and 514.5 nm light from the laser.

6. The entire experiment was then repeated and average photomultiplier currents were calculated for each wavelength and incident radiant power examined. From these values, the radiant power sensitivity of the photomultiplier tube was calculated as a function of wavelength as follows:

$$\text{Radiant power sensitivity (amperes/watt)} = \frac{\text{photomultiplier current (amperes)}}{[\text{radiant laser power (watts)}][AF_x]}$$

where AF_x = attenuation factor at wavelength x

7. Attenuation factors (AF_x) as a function of wavelength were calculated by multiplying the attenuation factors of the 1.0 neutral density filter, the 2.0 neutral density filter, the 4.0 neutral density filter and the UV grade optical diffuser components of the system (Table 25).

Table 25. Experimentally determined attenuation factors for the various components used in the determination of the spectral sensitivity of the photomultiplier system.

Wavelength (nm)	Individual Attenuation Factors (%)				
	1.0 Filter	2.0 Filter	4.0 Filter	UV Grade Diffuser	Total Attenuation Factor (%)
457	10.9	0.93	0.0092	2.51	2.34×10^{-7}
476.5	10.6	0.96	0.0094	2.48	2.37×10^{-7}
488	10.7	0.98	0.0100	2.63	2.75×10^{-7}
496.5	10.6	0.99	0.0103	2.54	2.73×10^{-7}
514.5	10.5	0.99	0.0118	2.60	3.19×10^{-7}

8. The calculated radiant power sensitivity values were then compared to those provided by ORIEL Corporation, and "shift" factors for

the radiant power sensitivity curve provided by ORIEL were then calculated as follows:

$$\text{"Shift" factor} = \frac{\text{experimentally determined value}}{\text{value provided by ORIEL Corporation}}$$

9. The results obtained for each wavelength (Table 26) were then averaged into a single shift factor which was used in the above calculations.

Table 26. Comparison of experimentally determined radiant power sensitivities (RPS) with those provided by ORIEL.[a]

Incident Wavelength (nm)	[A] Experimentally Determined RPS (amperes/watt)	[B] RPS from ORIEL (amperes/watt)	Shift Factor [A]/[B]
458	6.11×10^3	2.45×10^3	2.49
476.5	5.87×10^3	2.30×10^3	2.55
488	4.59×10^3	2.00×10^3	2.30
496.5	3.19×10^3	1.60×10^3	2.00
514.5	2.43×10^3	1.20×10^3	2.03
			Average = 2.27 ± (0.28)

[a]See Fig. 103.

Radiant Power Sensitivity

Shown below are typical curves of radiant power sensitivity in Amperes per Radiant Watt vs. wavelength with 600 volts bias. With most of these tubes 600 volts provides the highest signal to noise ratio and therefore the most usable sensitivity. The typical current noise levels at this voltage allow you to calculate the noise in terms of radiant power at any given wavelength. These sensitivity and noise figures may vary substantially from tube to tube; therefore, this data is given only as a rough guide for system design. To determine the overall sensitivity of the measuring system take into account the attenuation factors given for the input accessories on pages F-8 and 9.

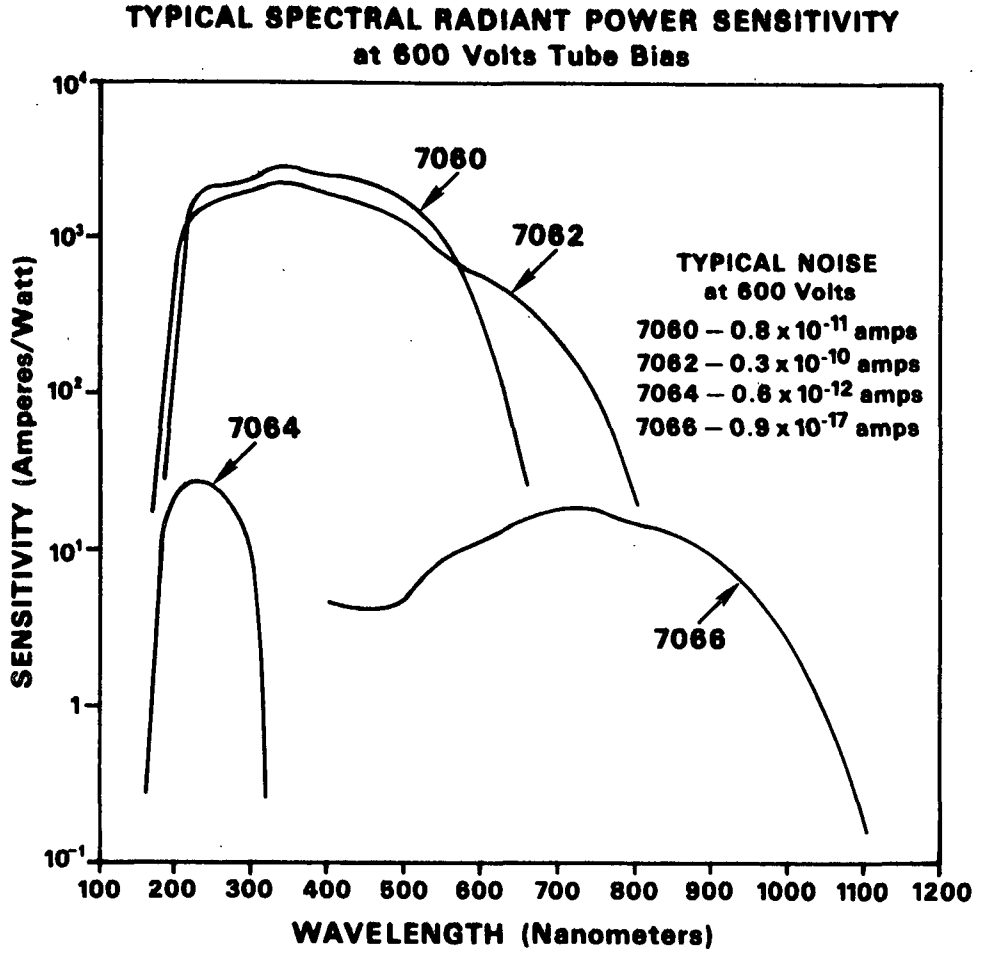

Figure 103. Radiant power sensitivity curve provided by ORIEL (tube no. = 7060).

APPENDIX IV

Δk_λ SPECTRA OBTAINED UPON IRRADIATION OF SAMPLE SHEETS WITH "MONOCHROMATIC" UV LIGHT (FOR DETAILS SEE TEXT)

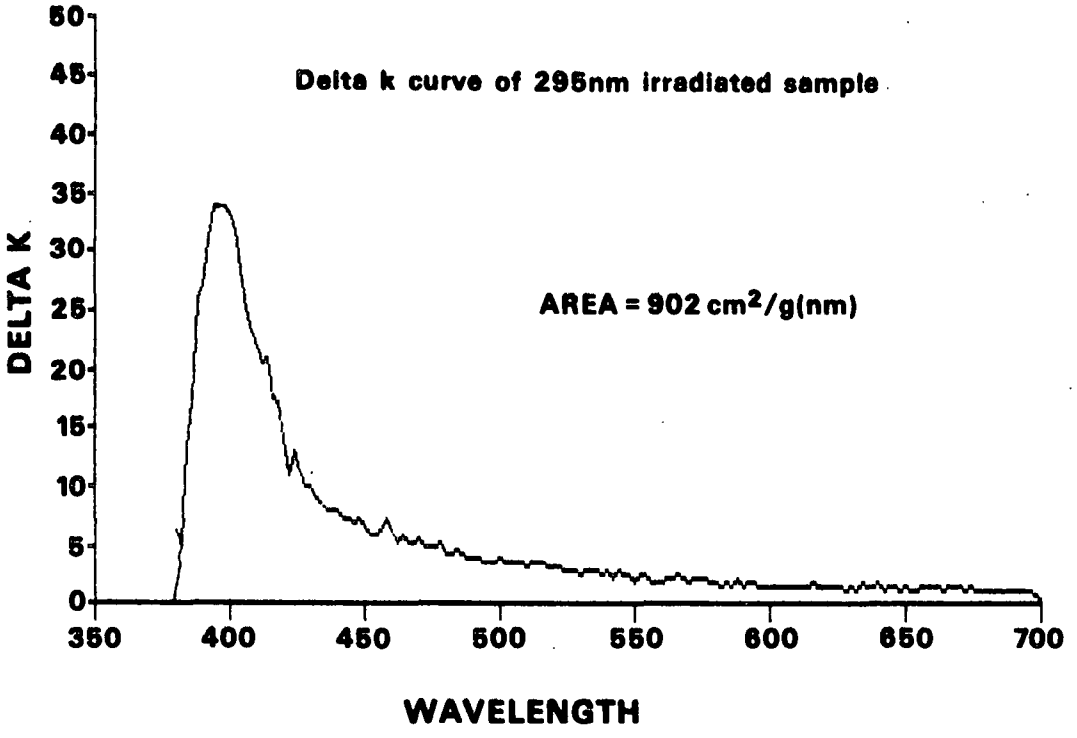

Figure 104. ΔK_λ spectra obtained upon irradiation of a white spruce RMP sheet with 295 nm UV light.

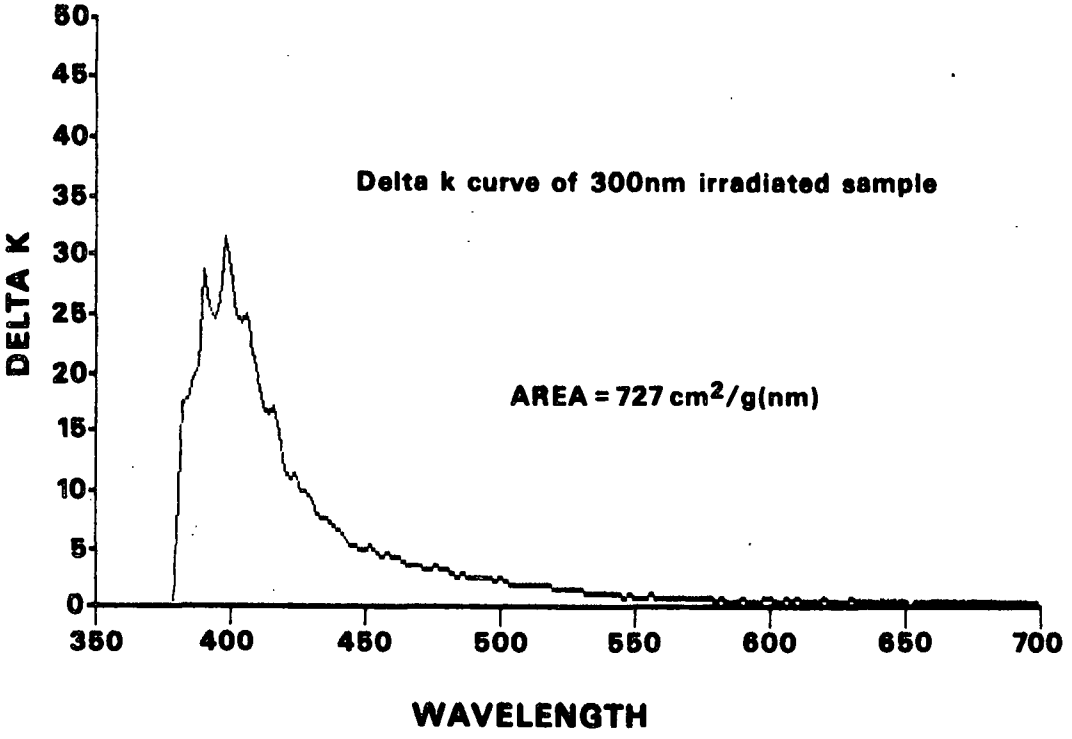

Figure 105. ΔK_λ spectra obtained upon irradiation of a white spruce RMP sheet with 300 nm UV light.

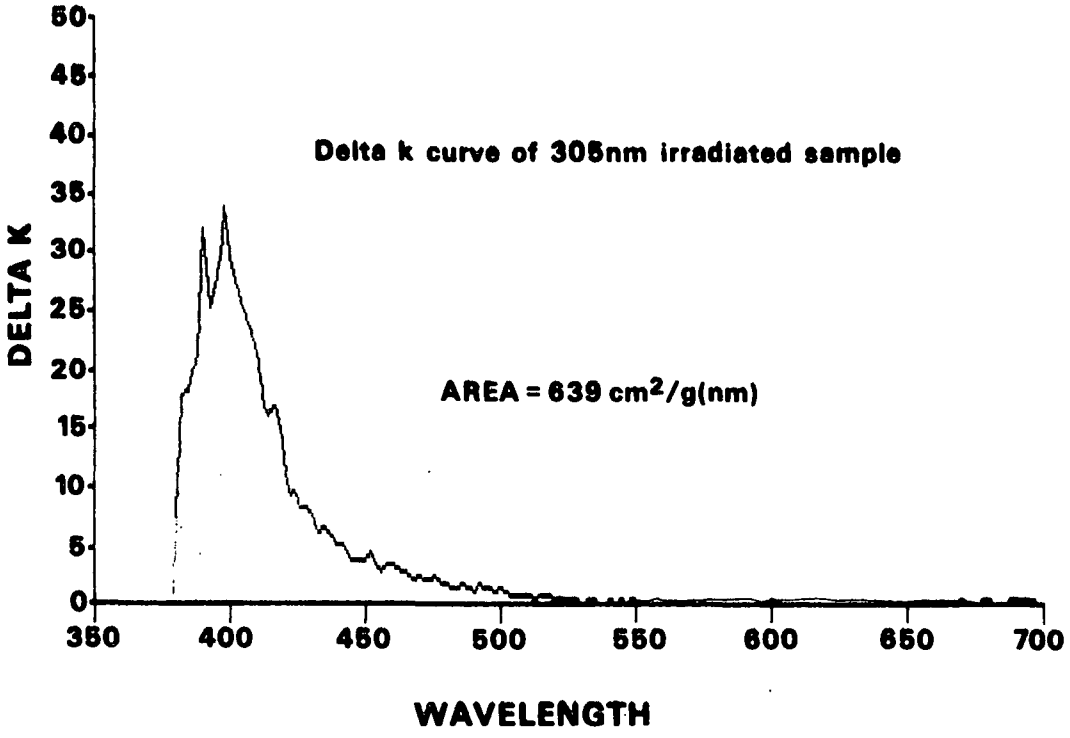

Figure 106. ΔK_λ spectra obtained upon irradiation of a white spruce RMP sheet with 305 nm UV light.

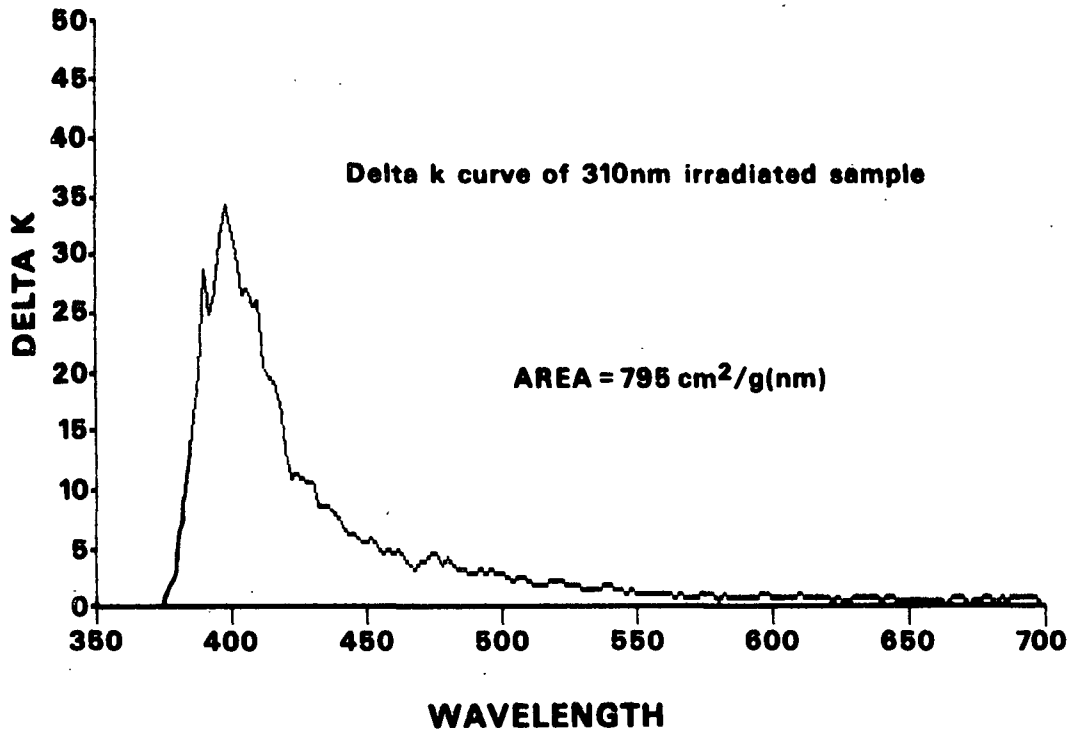

Figure 107. ΔK_λ spectra obtained upon irradiation of a white spruce RMP sheet with 310 nm UV light.

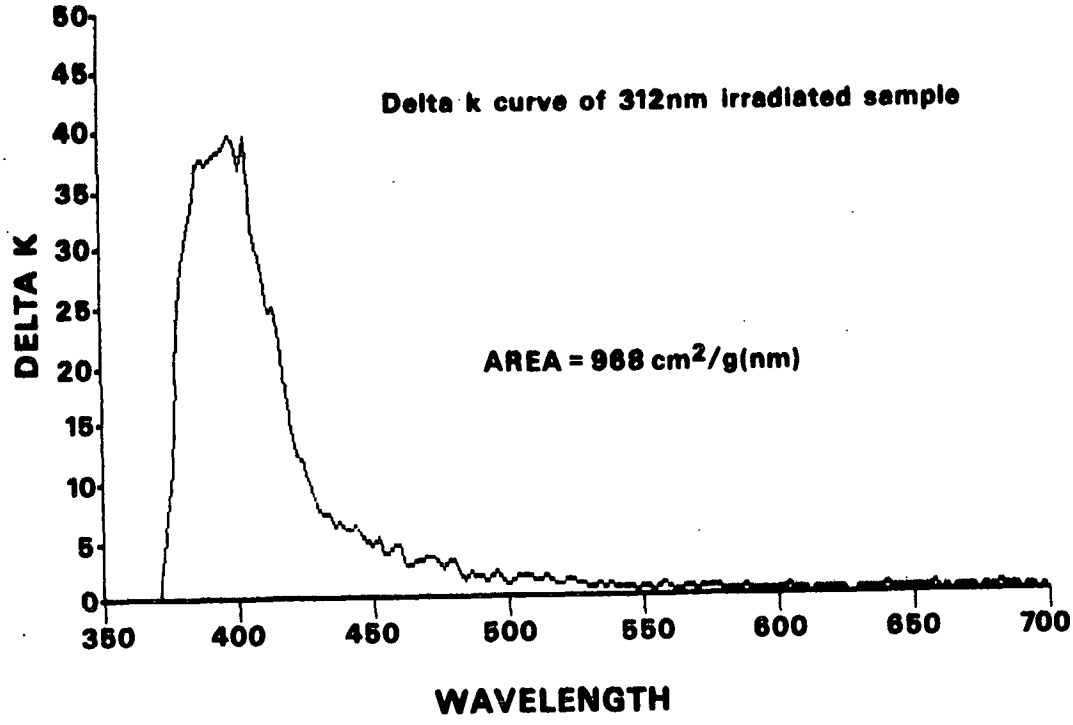

Figure 108. ΔK_λ spectra obtained upon irradiation of a white spruce RMP sheet with 312.5 nm UV light.

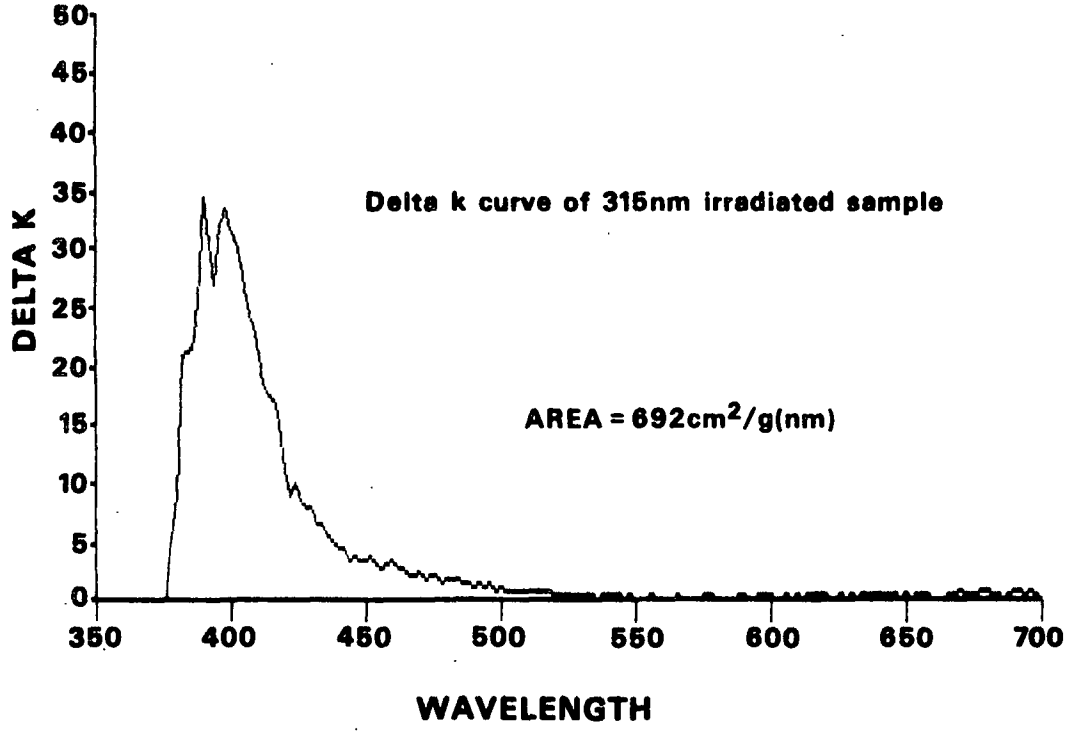

Figure 109. ΔK_λ spectra obtained upon irradiation of a white spruce RMP sheet with 315 nm UV light.

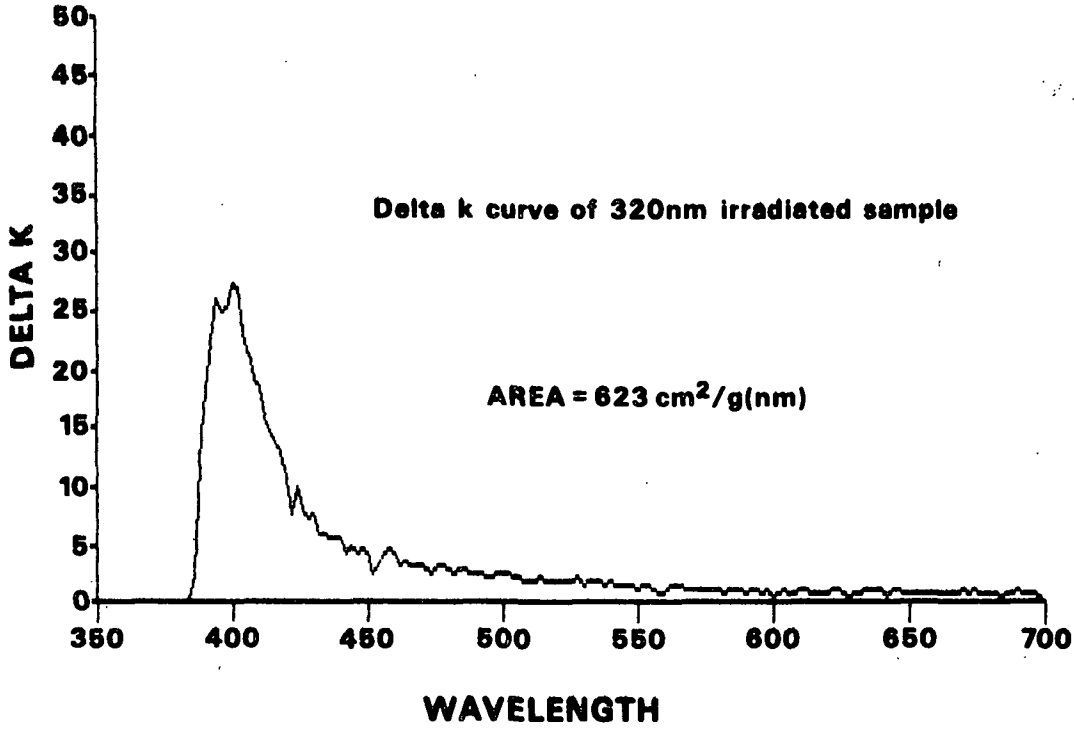

Figure 110. ΔK_λ spectra obtained upon irradiation of a white spruce RMP sheet with 320 nm UV light.

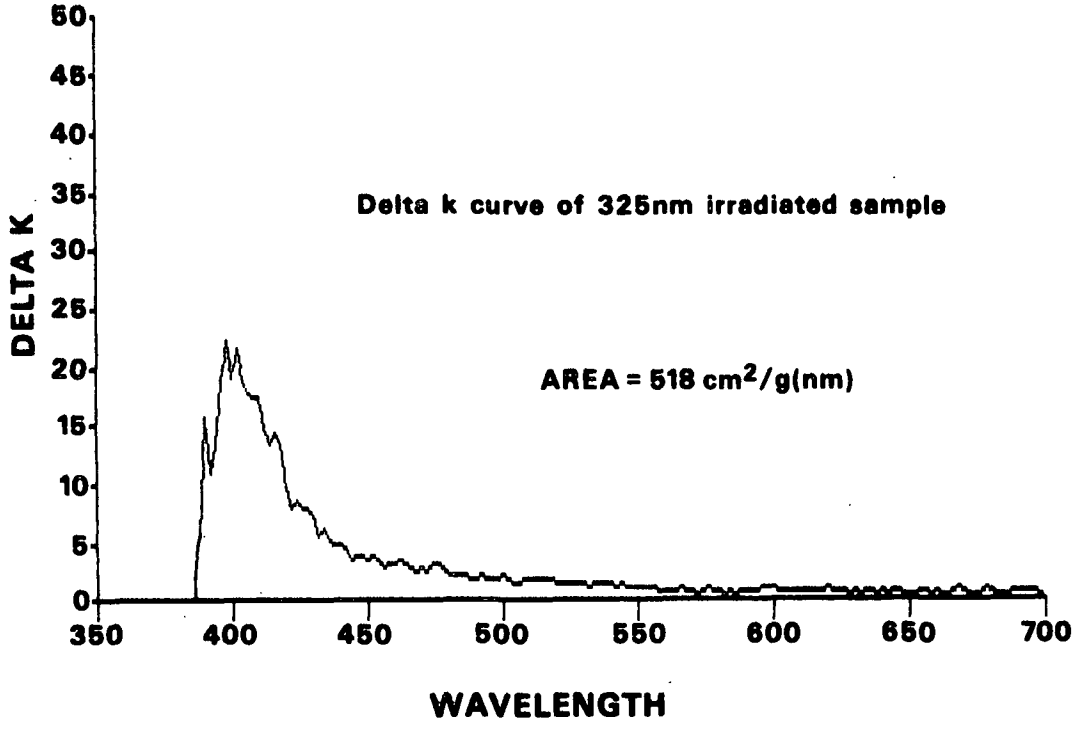

Figure 111. ΔK_λ spectra obtained upon irradiation of a white spruce RMP sheet with 325 nm UV light.

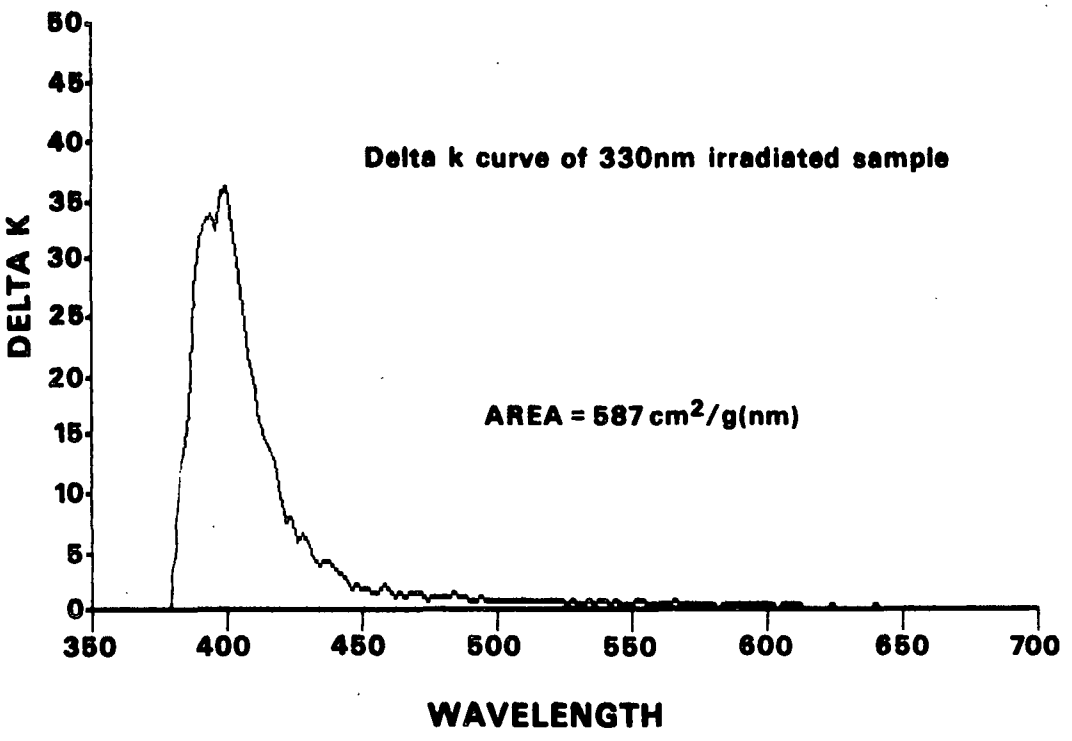

Figure 112. ΔK_λ spectra obtained upon irradiation of a white spruce RMP sheet with 330 nm UV light.

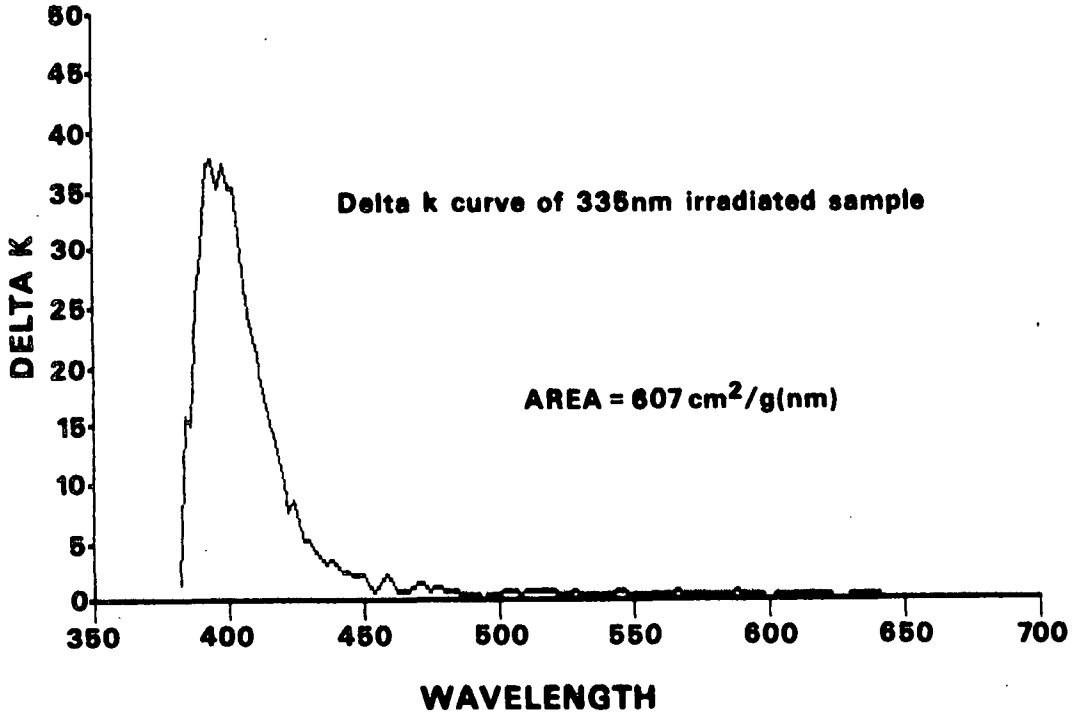

Figure 113. ΔK_λ spectra obtained upon irradiation of a white spruce RMP sheet with 335 nm UV light.

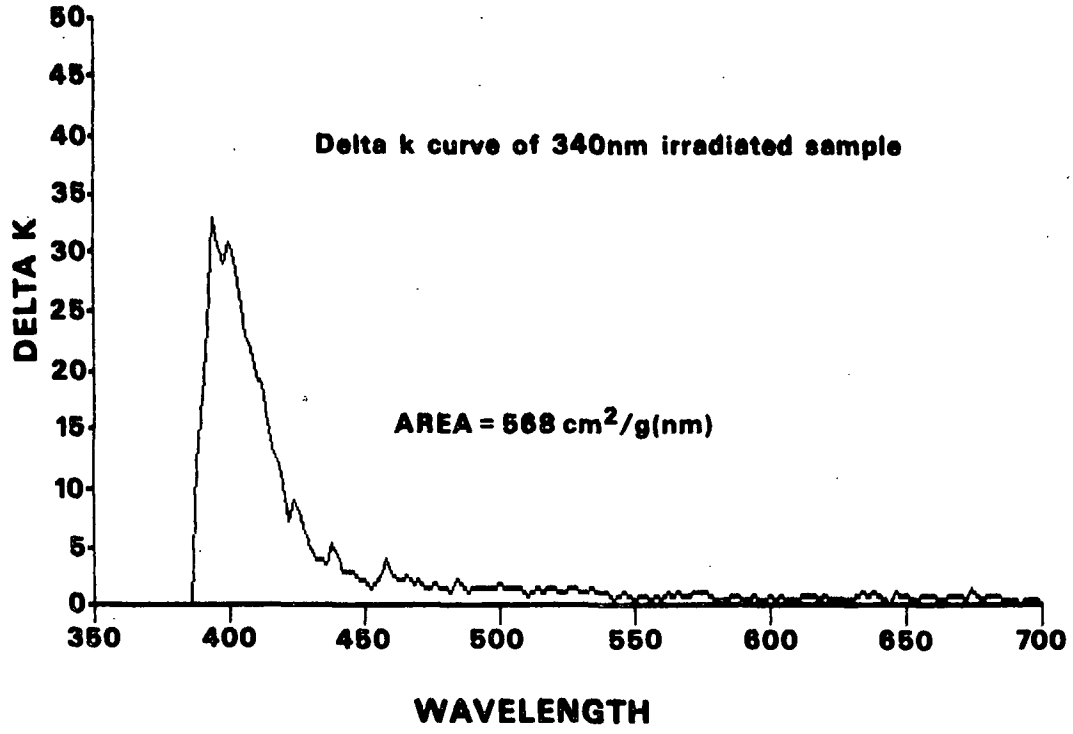

Figure 114. ΔK_λ spectra obtained upon irradiation of a white spruce RMP sheet with 340 nm UV light.

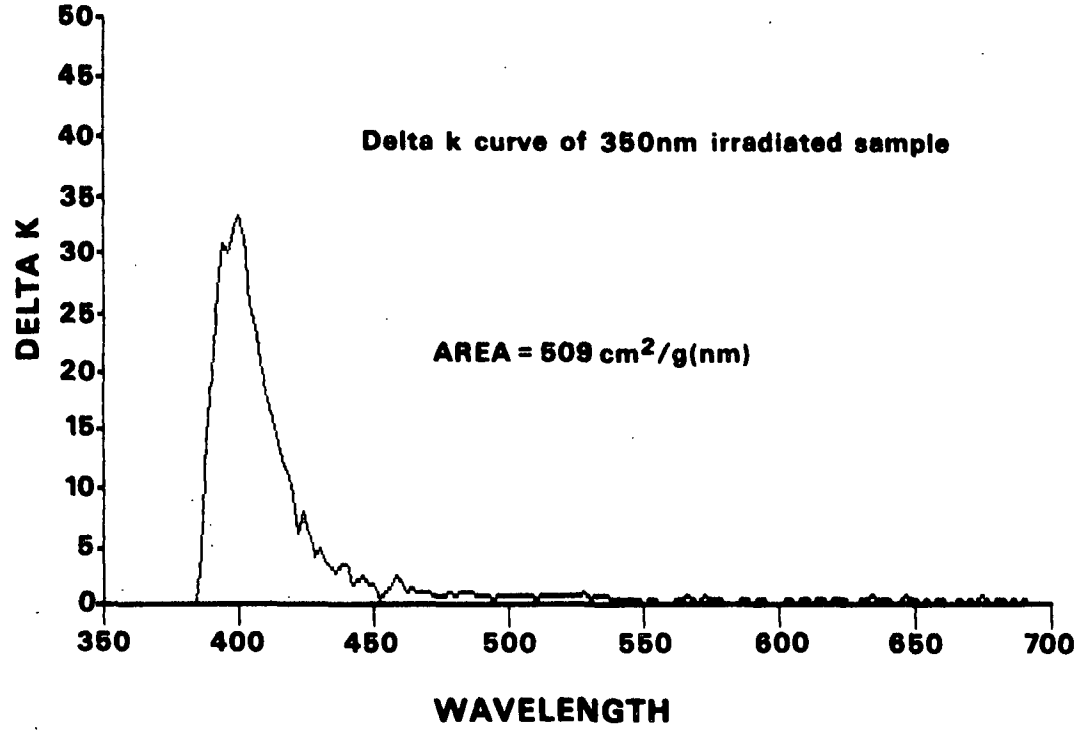

Figure 115. ΔK_λ spectra obtained upon irradiation of a white spruce RMP sheet with 350 nm UV light.

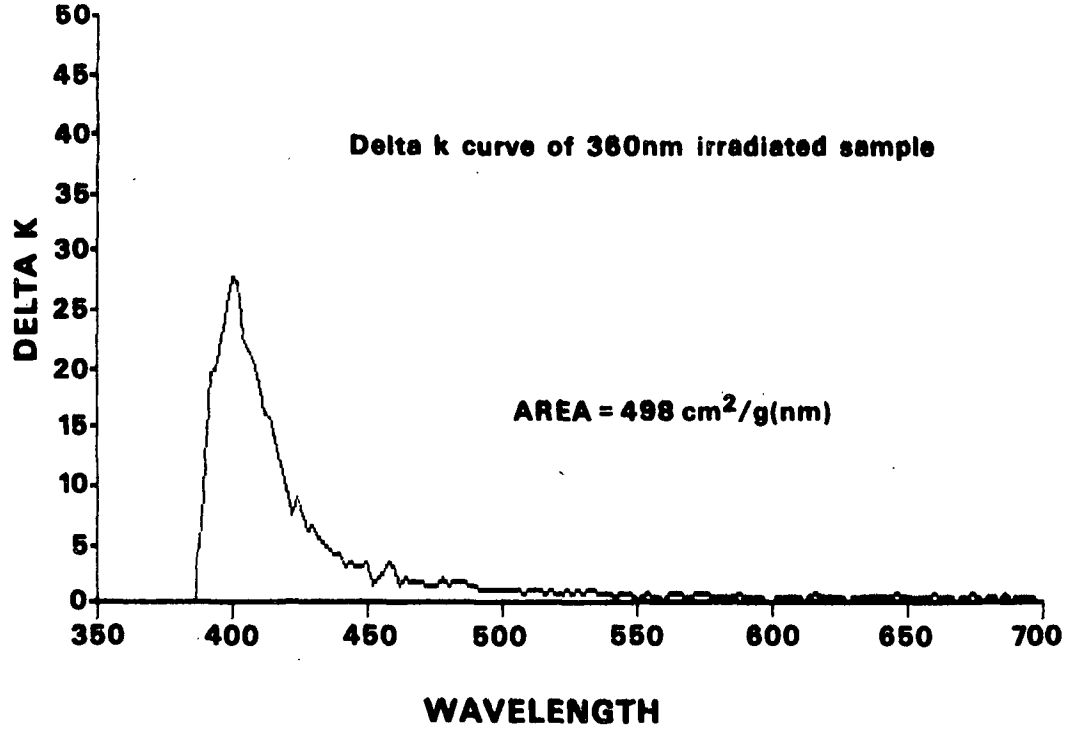

Figure 116. ΔK_λ spectra obtained upon irradiation of a white spruce RMP sheet with 360 nm UV light.

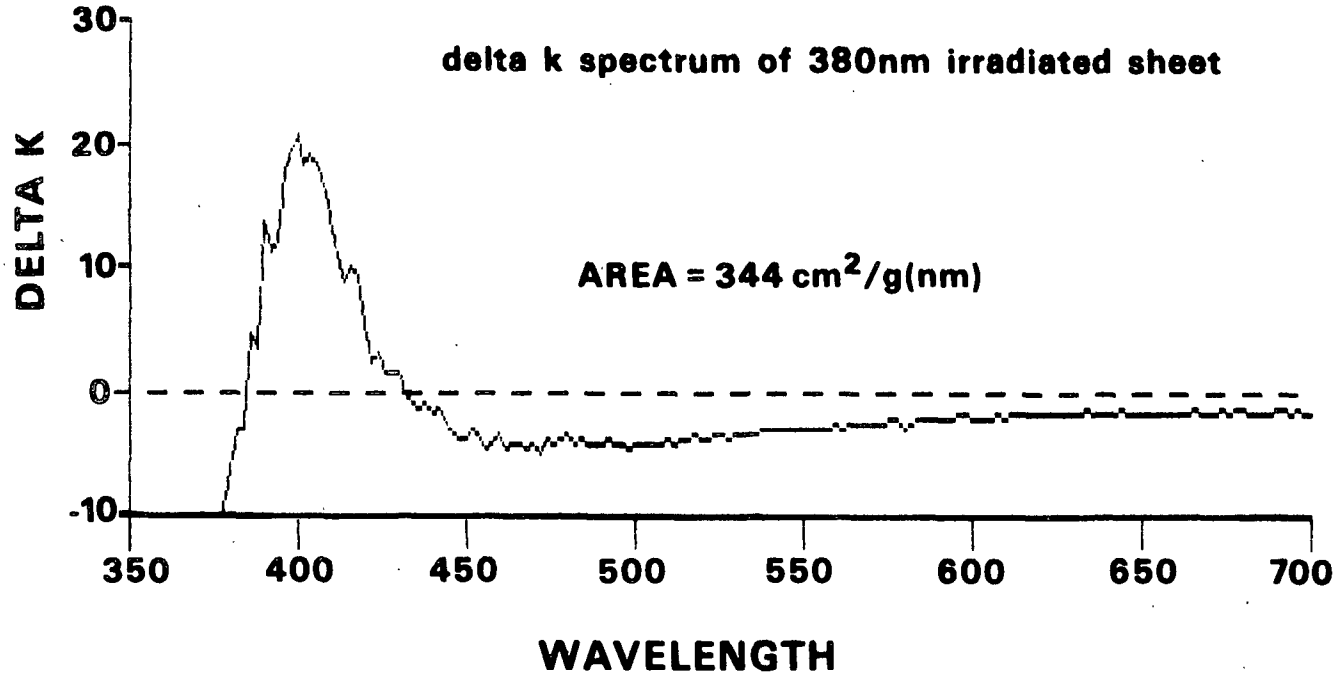

Figure 117. ΔK_λ spectra obtained upon irradiation of a white spruce RMP sheet with 380 nm UV light.

APPENDIX V

UV-VISIBLE SPECTRA OF QUINONE MODELS I-IV IN METHANOL

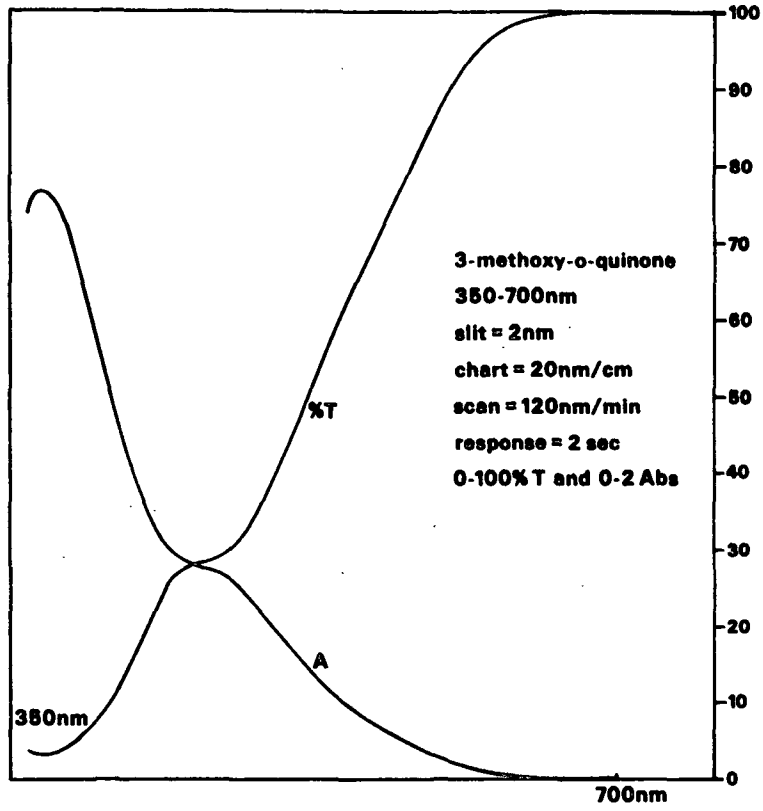

Figure 118. UV-visible spectrum of quinone model I in methanol.

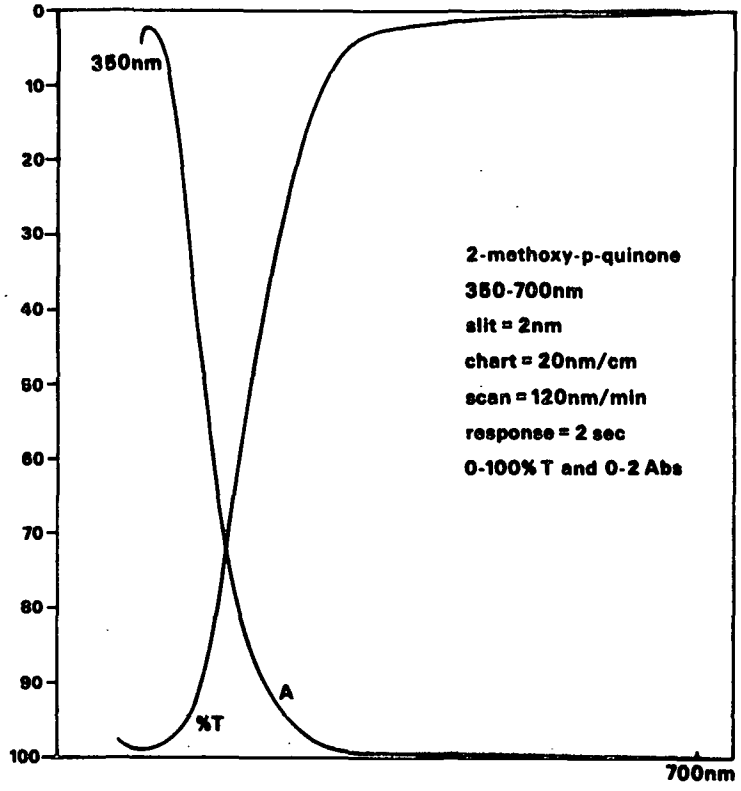

Figure 119. UV-visible spectrum of quinone model II in methanol.

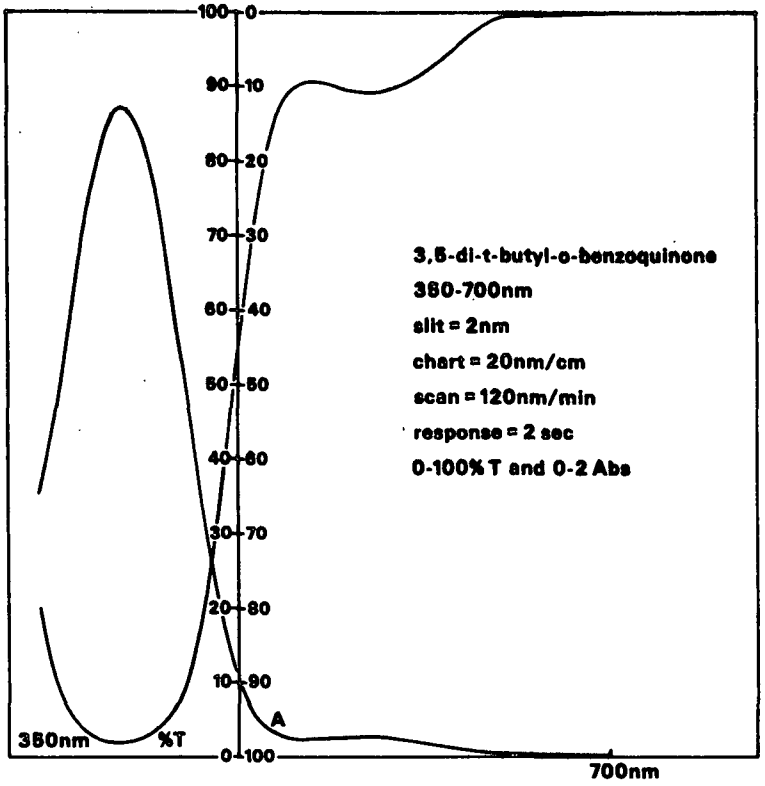

Figure 120. UV-visible spectrum of quinone model III in methanol.

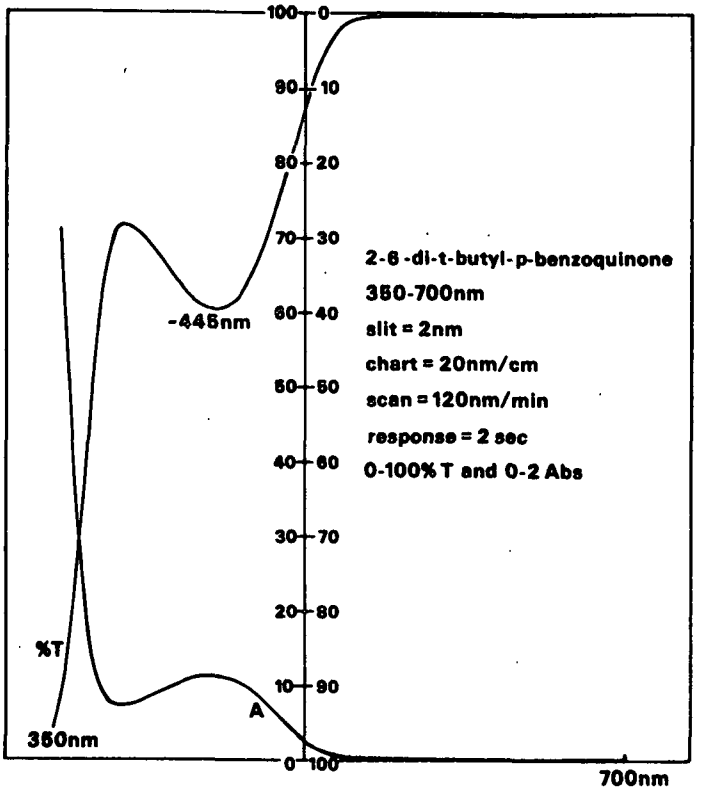

Figure 121. UV-visible spectrum of quinone model IV in methanol.

APPENDIX VI

^{31}P NMR SPECTRA OF THE TRIMETHYL PHOSPHITE TREATED WHITE SPRUCE PULP SAMPLES DESCRIBED IN THIS TEXT

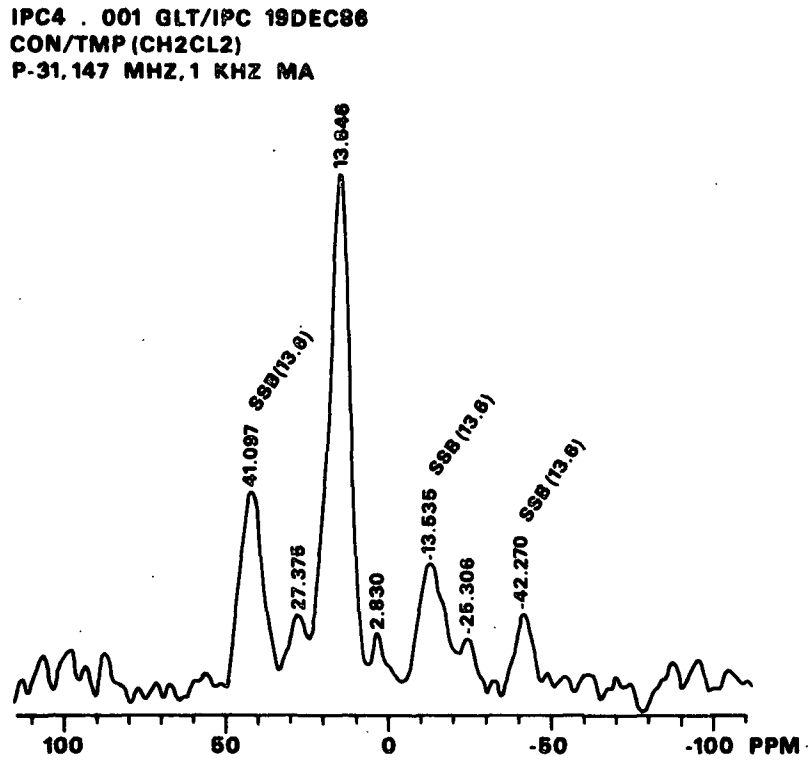

Figure 122. ^{31}P NMR spectrum of trimethyl phosphite treated white spruce pulp-1.

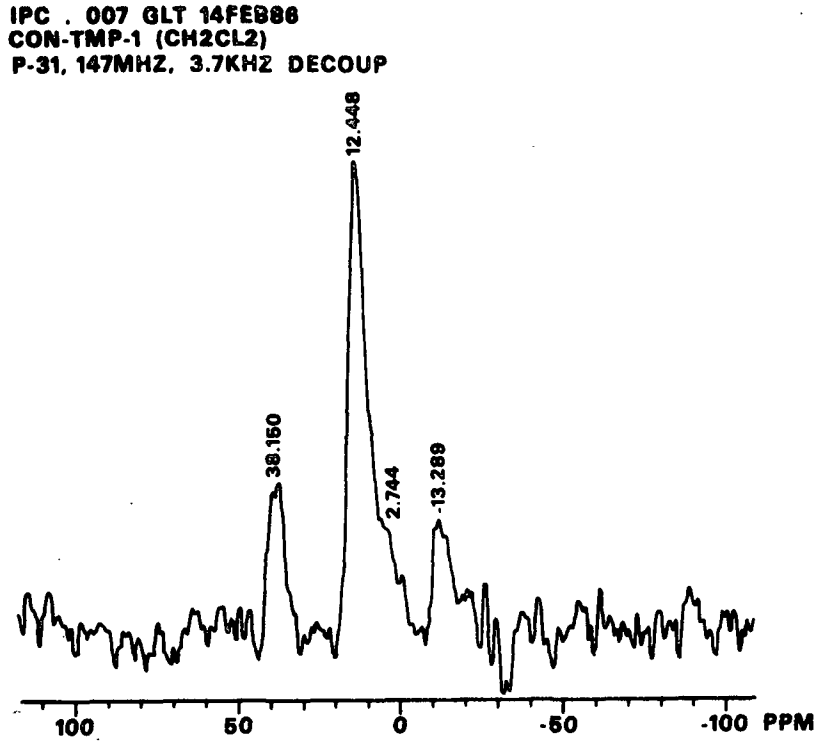

Figure 123. ^{31}P NMR spectrum of trimethyl phosphite treated white spruce pulp-2.

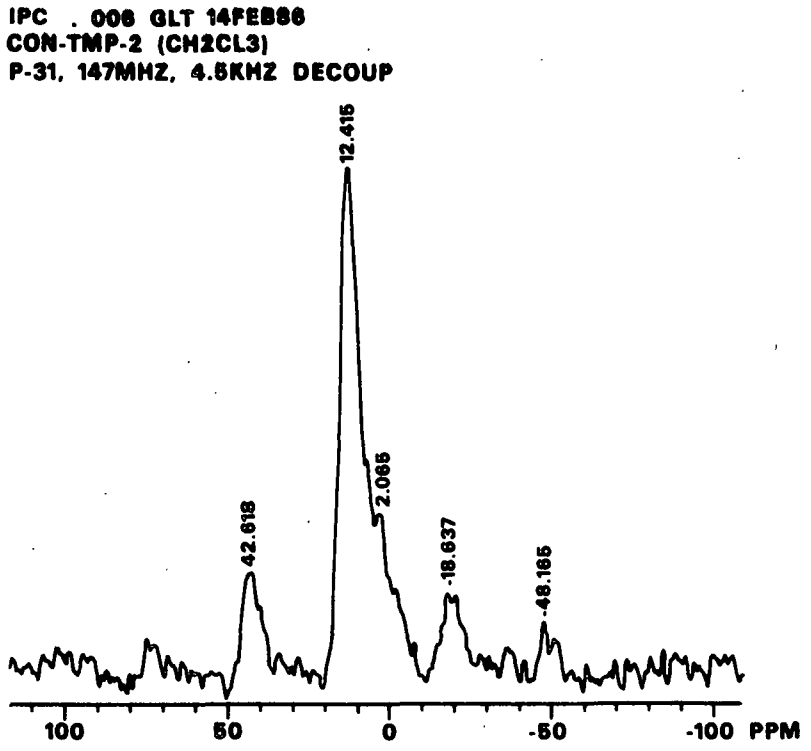

Figure 124. ^{31}P NMR spectrum of trimethyl phosphite treated white spruce pulp-3.

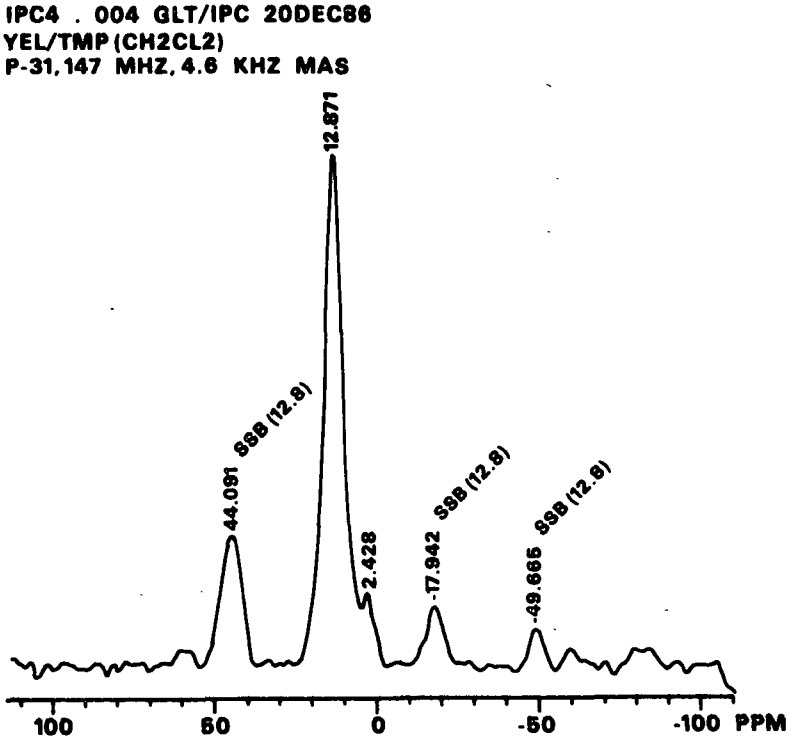

Figure 125. ^{31}P NMR spectrum of white spruce pulp irradiated for 20 hours with simulated sunlight and then reacted with trimethyl phosphite.

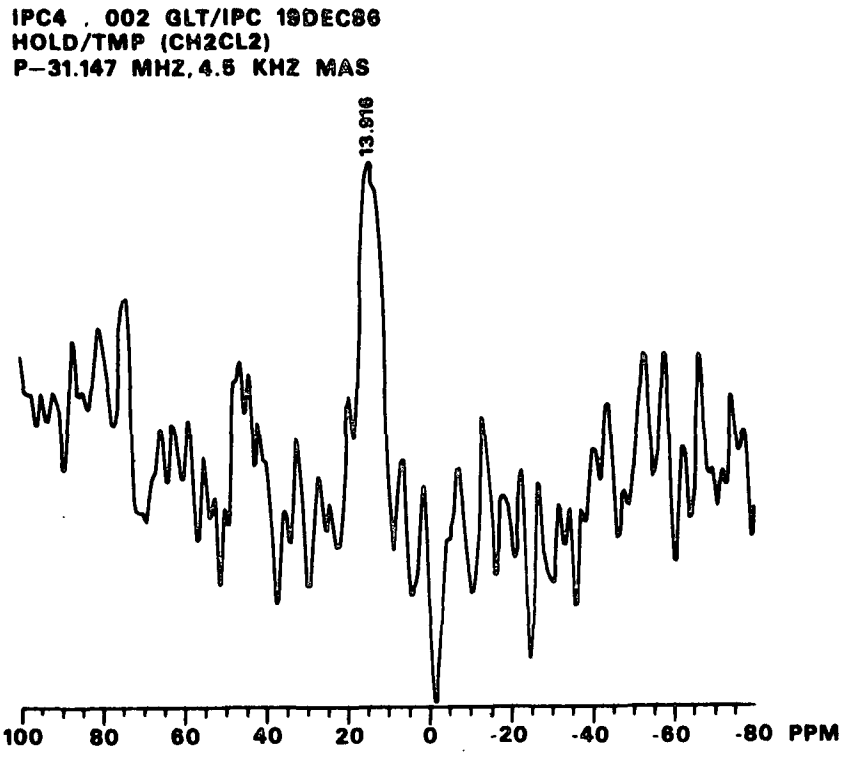

Figure 126. ^{31}P NMR spectrum of trimethyl phosphite treated white spruce holocellulose.

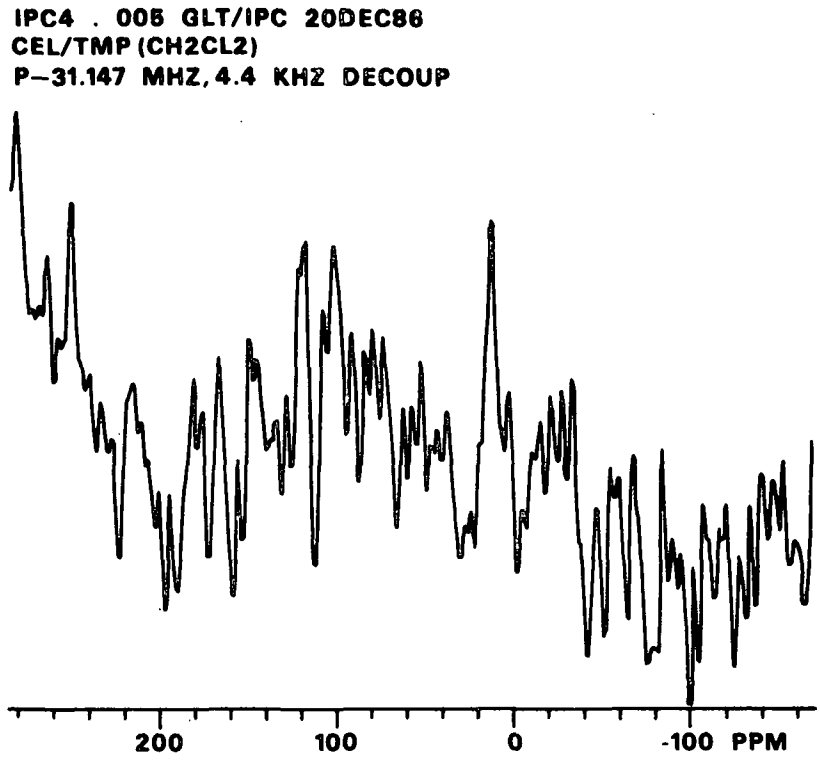

Figure 127. ^{31}P NMR spectrum of trimethyl phosphite treated cellulose.

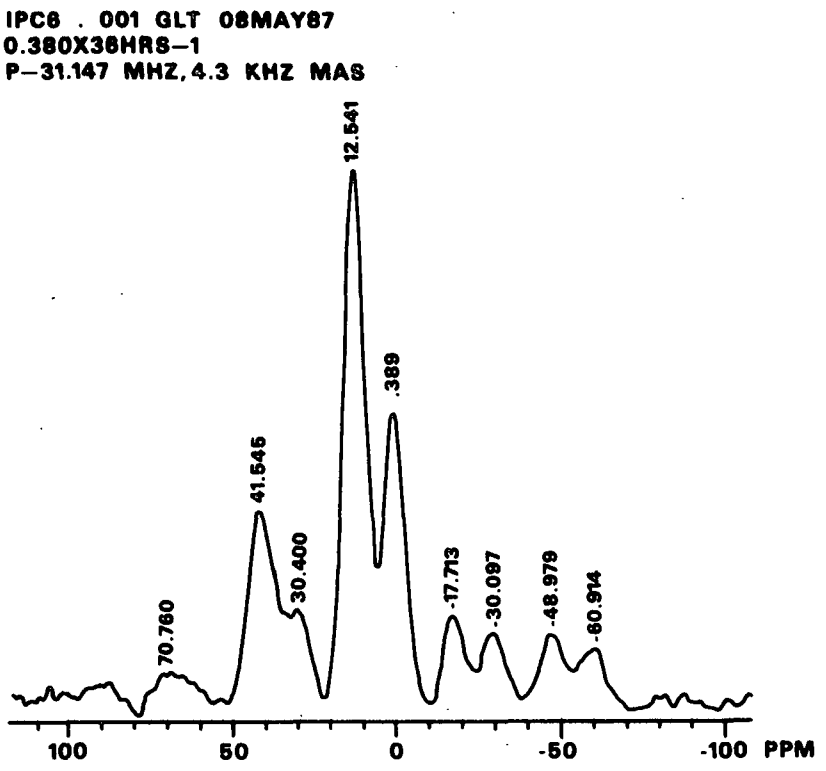

Figure 128. ^{31}P NMR spectrum of irradiated and trimethyl phosphite treated sample 0.380-1.

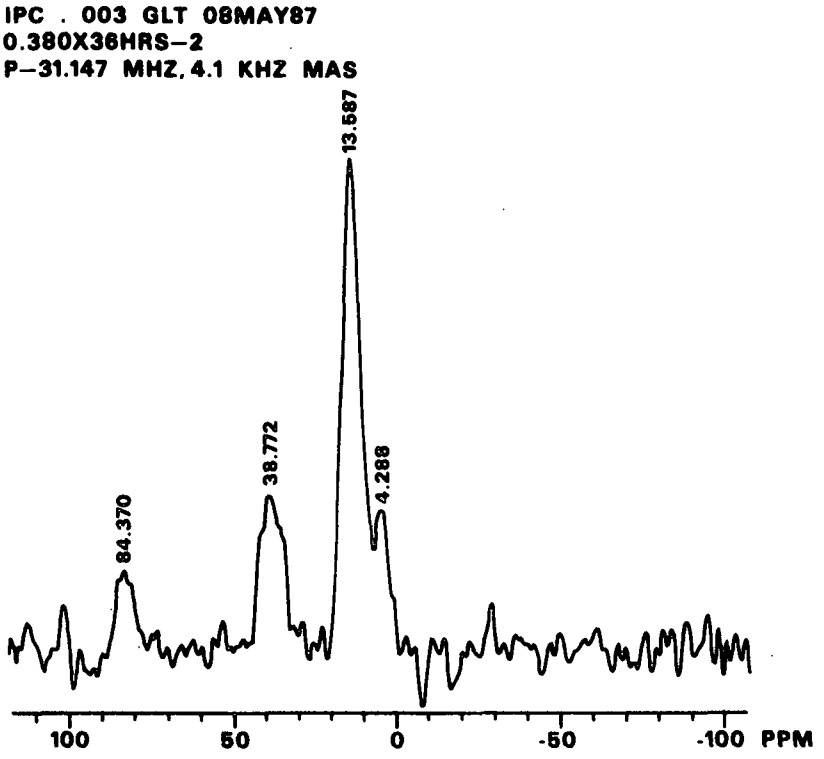

Figure 129. ^{31}P NMR spectrum of irradiated and trimethyl phosphite treated sample 0.380-2.

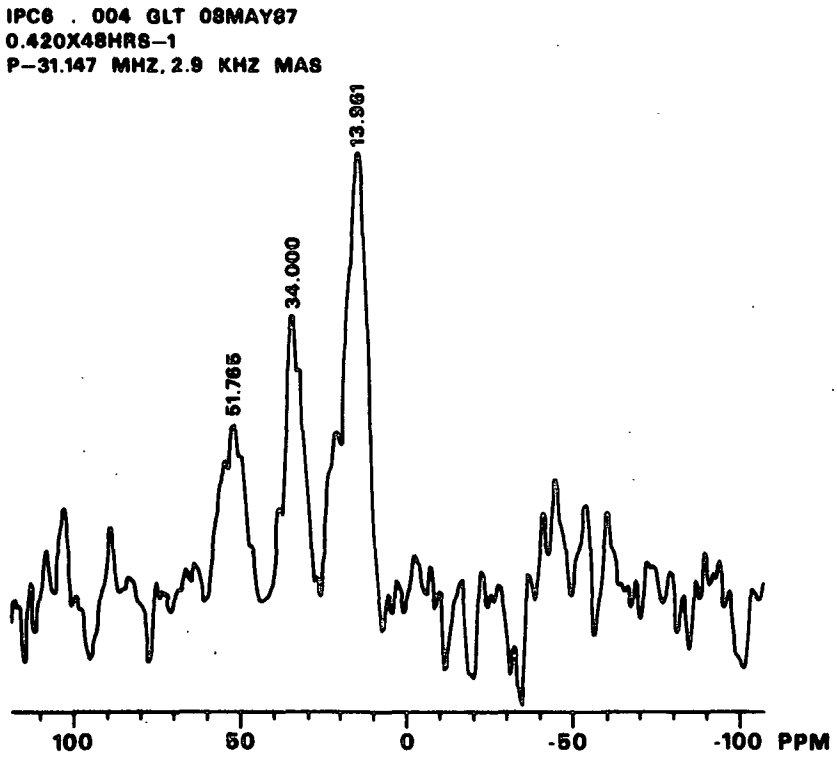

Figure 130. ^{31}P NMR spectrum of irradiated and trimethyl phosphite treated sample 0.420-1.

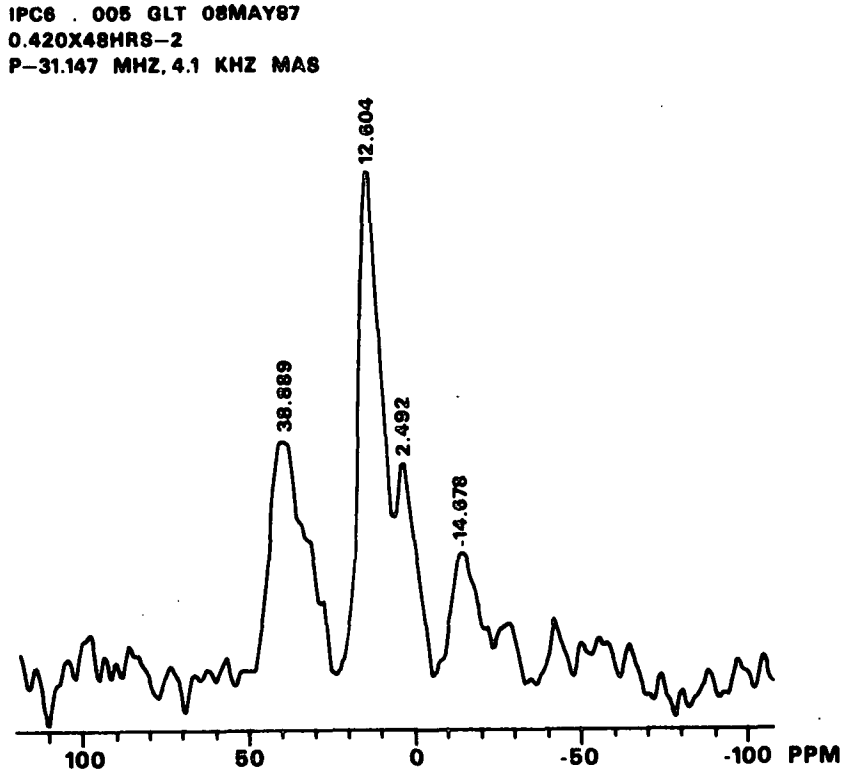

Figure 131. ^{31}P NMR spectrum of irradiated and trimethyl phosphite treated sample 0.420-2.

APPENDIX VII

DIFFUSE REFLECTANCE FTIR SPECTRA OF VARIOUS SAMPLES DESCRIBED IN THIS TEXT

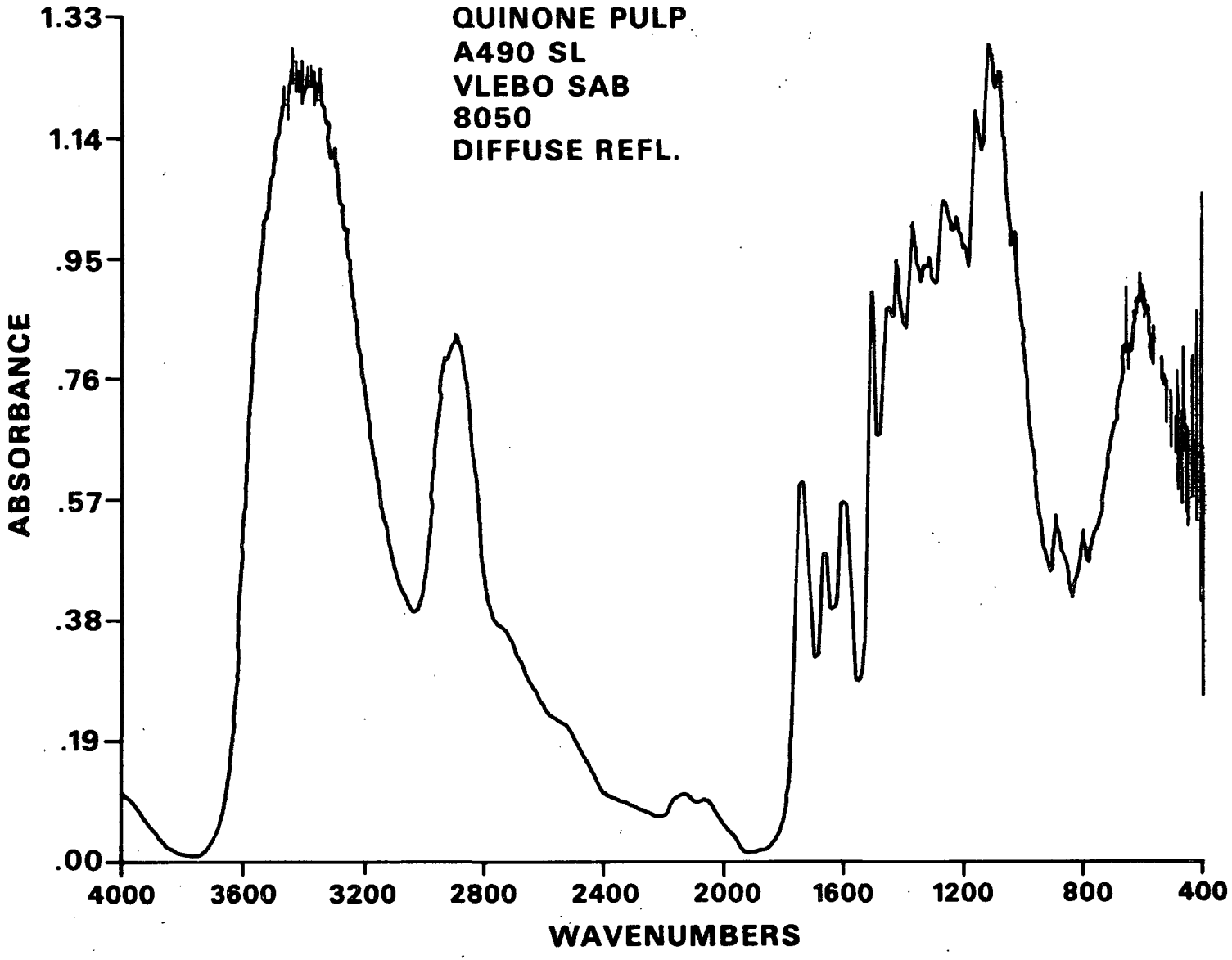

Figure 132. Diffuse reflectance FTIR spectrum of white spruce refiner mechanical pulp oxidized with Fremy's salt.

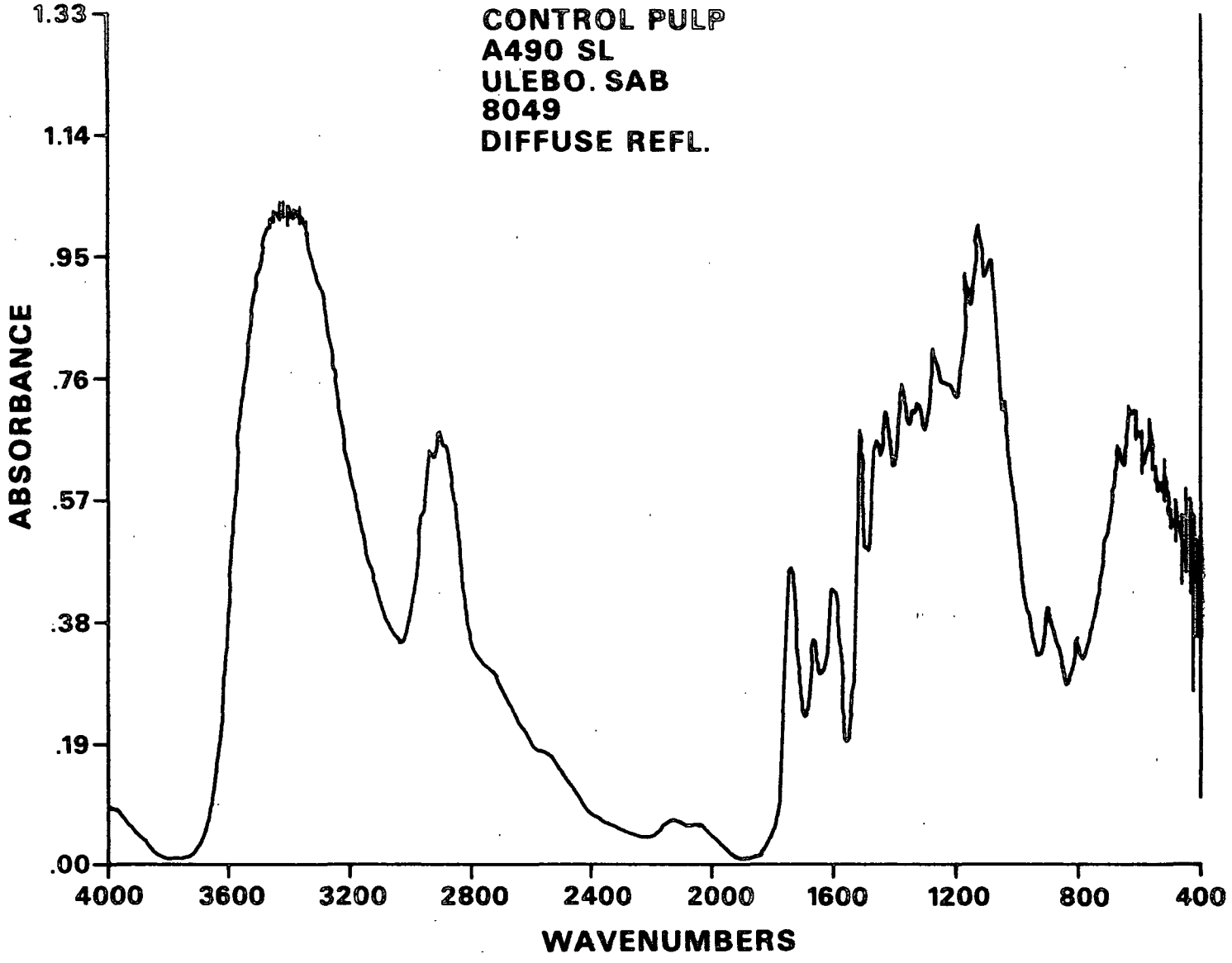

Figure 133. Diffuse reflectance FTIR spectrum of white spruce refiner mechanical pulp.

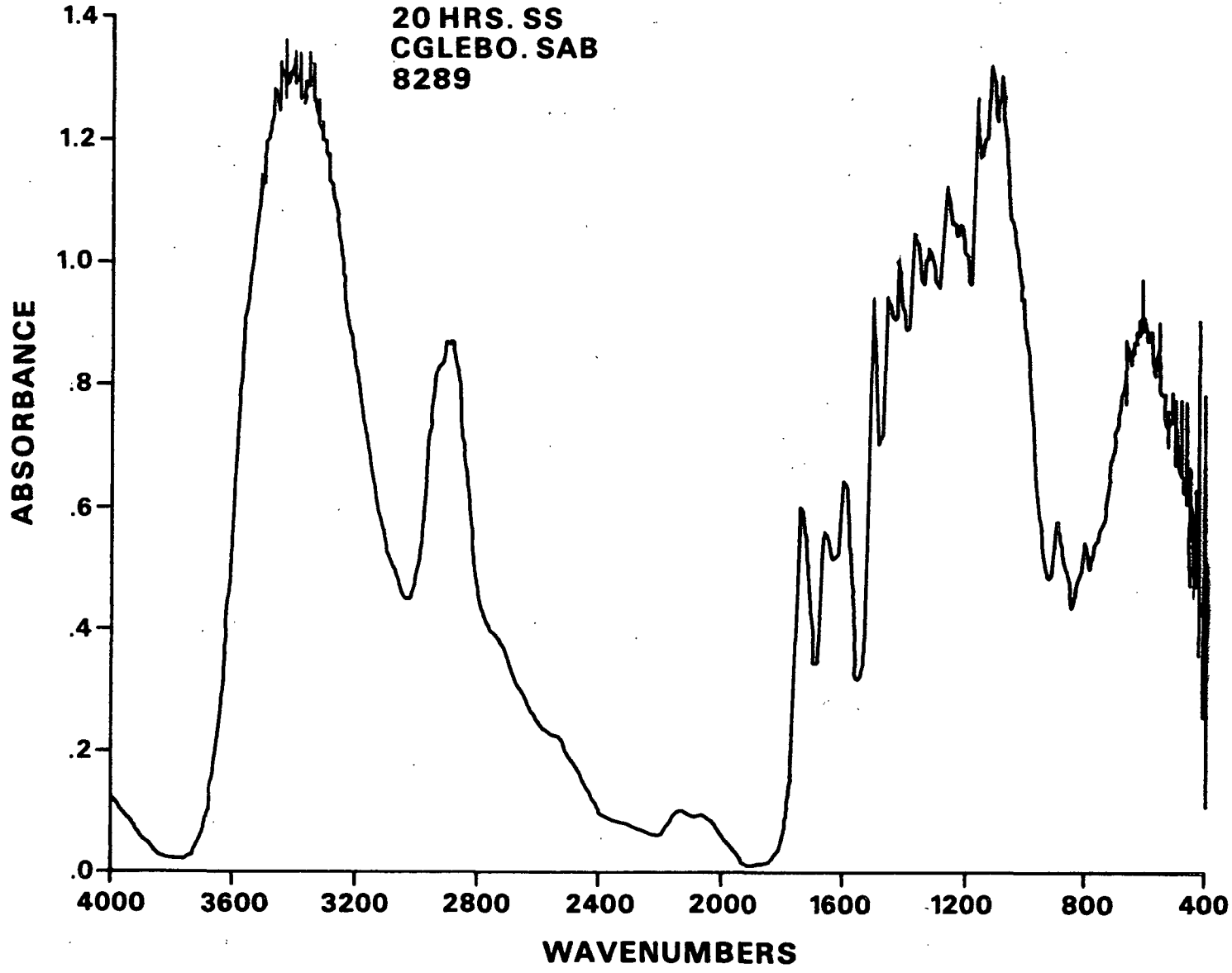

Figure 134. Diffuse reflectance FTIR spectrum of white spruce refiner mechanical pulp irradiated for 20 hours with simulated sunlight.

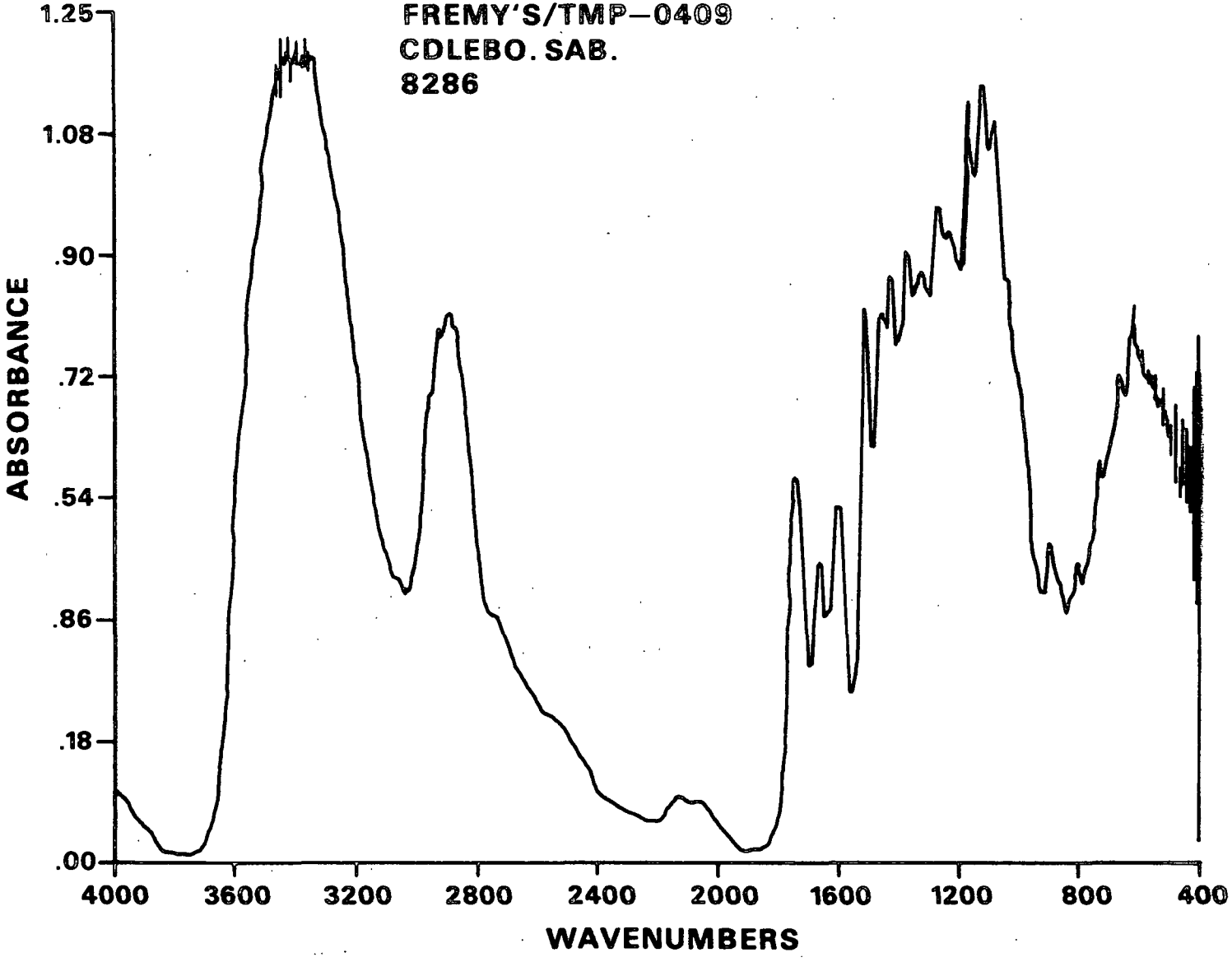

Figure 135. Diffuse reflectance FTIR spectrum of white spruce refiner mechanical pulp oxidized with Fremy's salt and reacted with trimethyl phosphite.

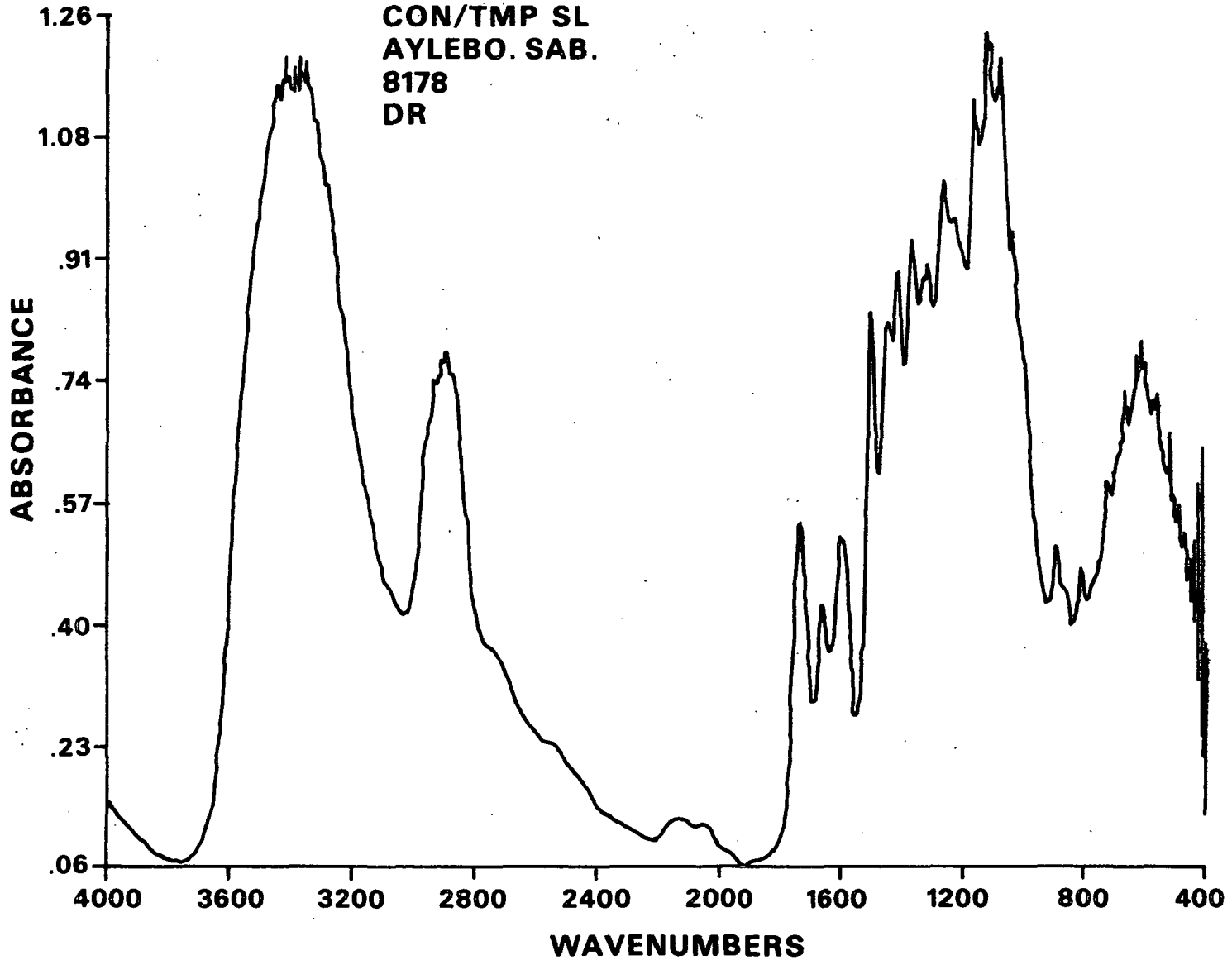

Figure 136. Diffuse reflectance FTIR spectrum of white spruce refiner mechanical pulp reacted with trimethyl phosphite.

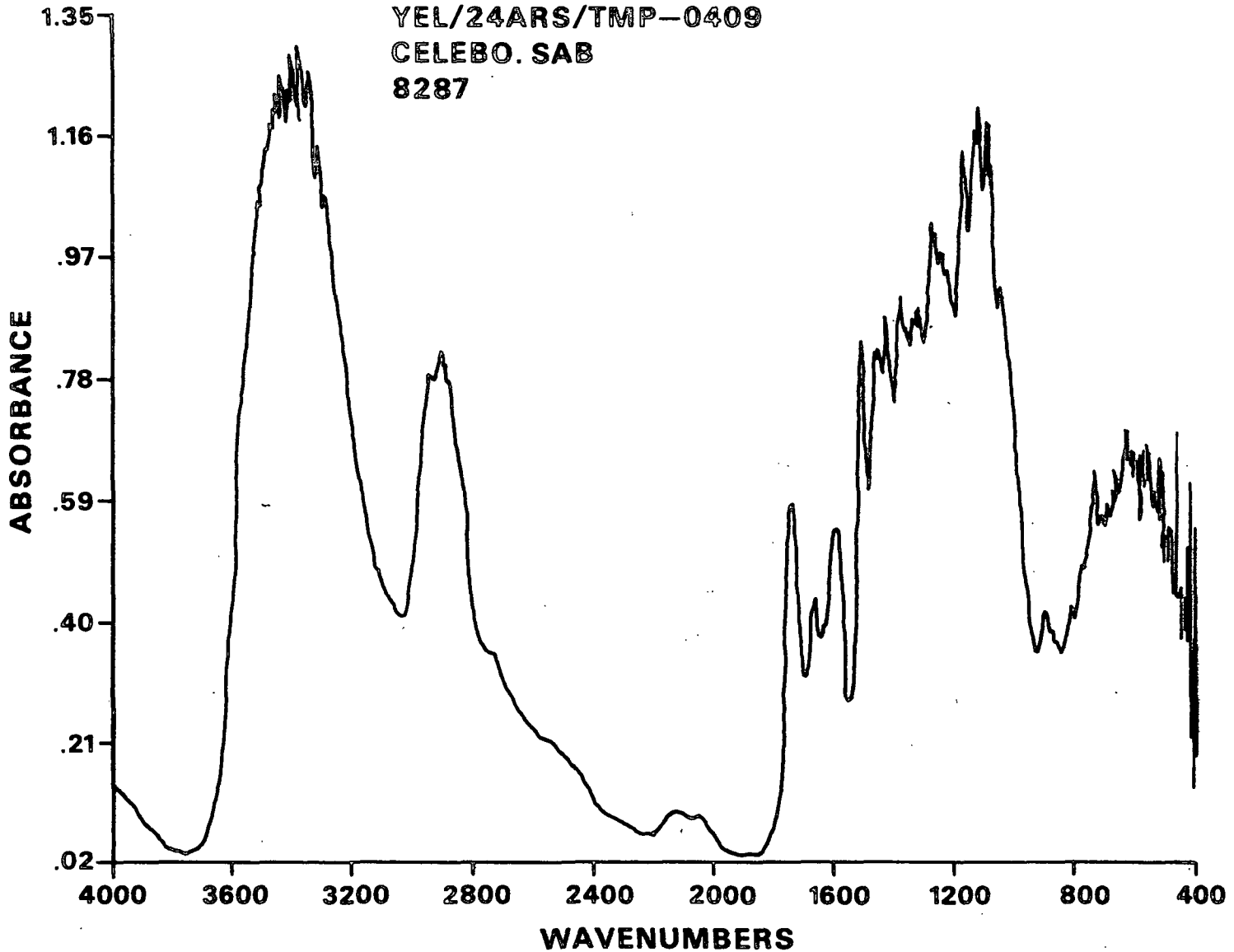

Figure 137. Diffuse reflectance FTIR spectrum of white spruce refiner mechanical pulp irradiated for 20 hours with simulated sunlight and reacted with trimethyl phosphite.

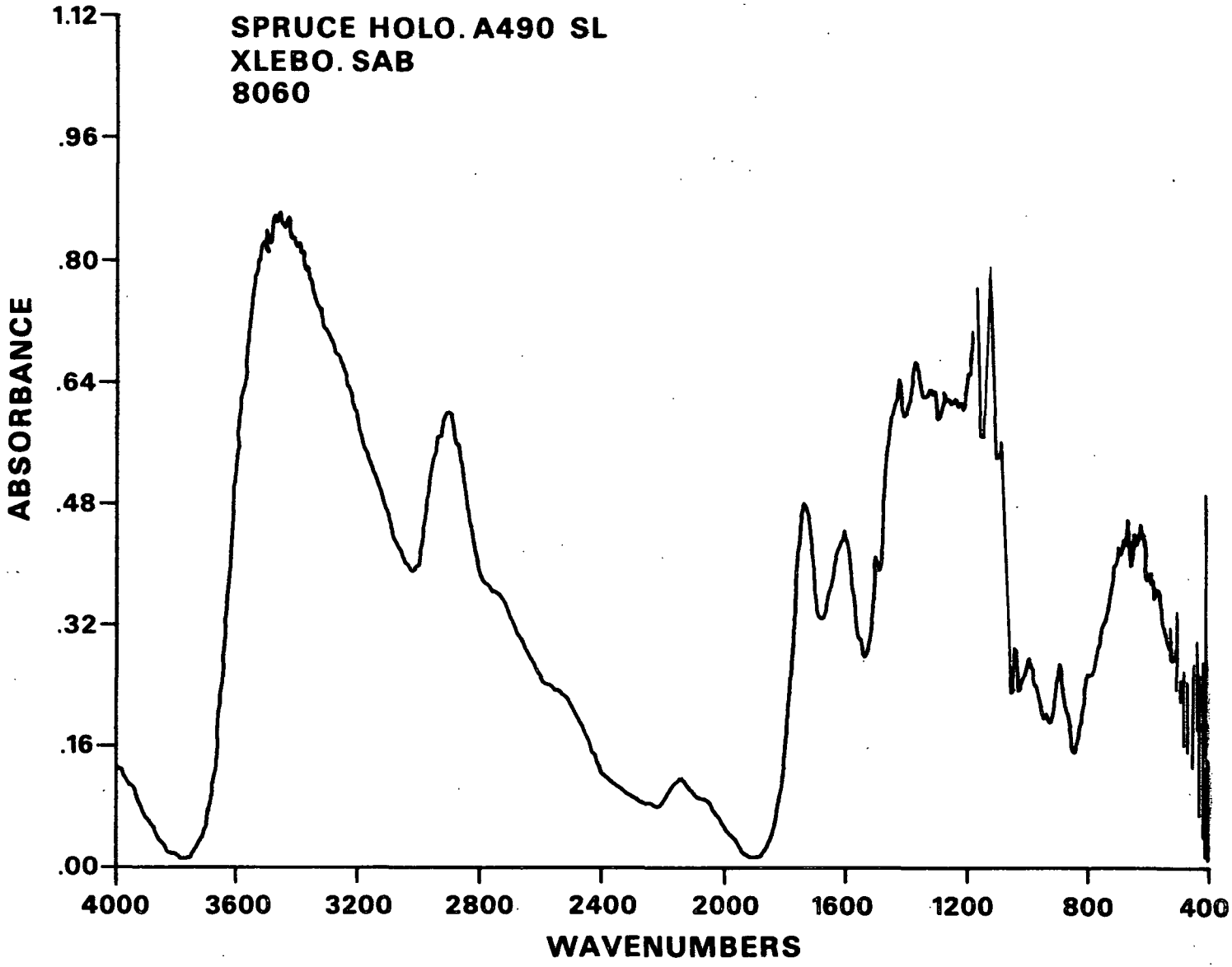

Figure 138. Diffuse reflectance FTIR spectrum of holocellulose prepared from white spruce refiner mechanical pulp.

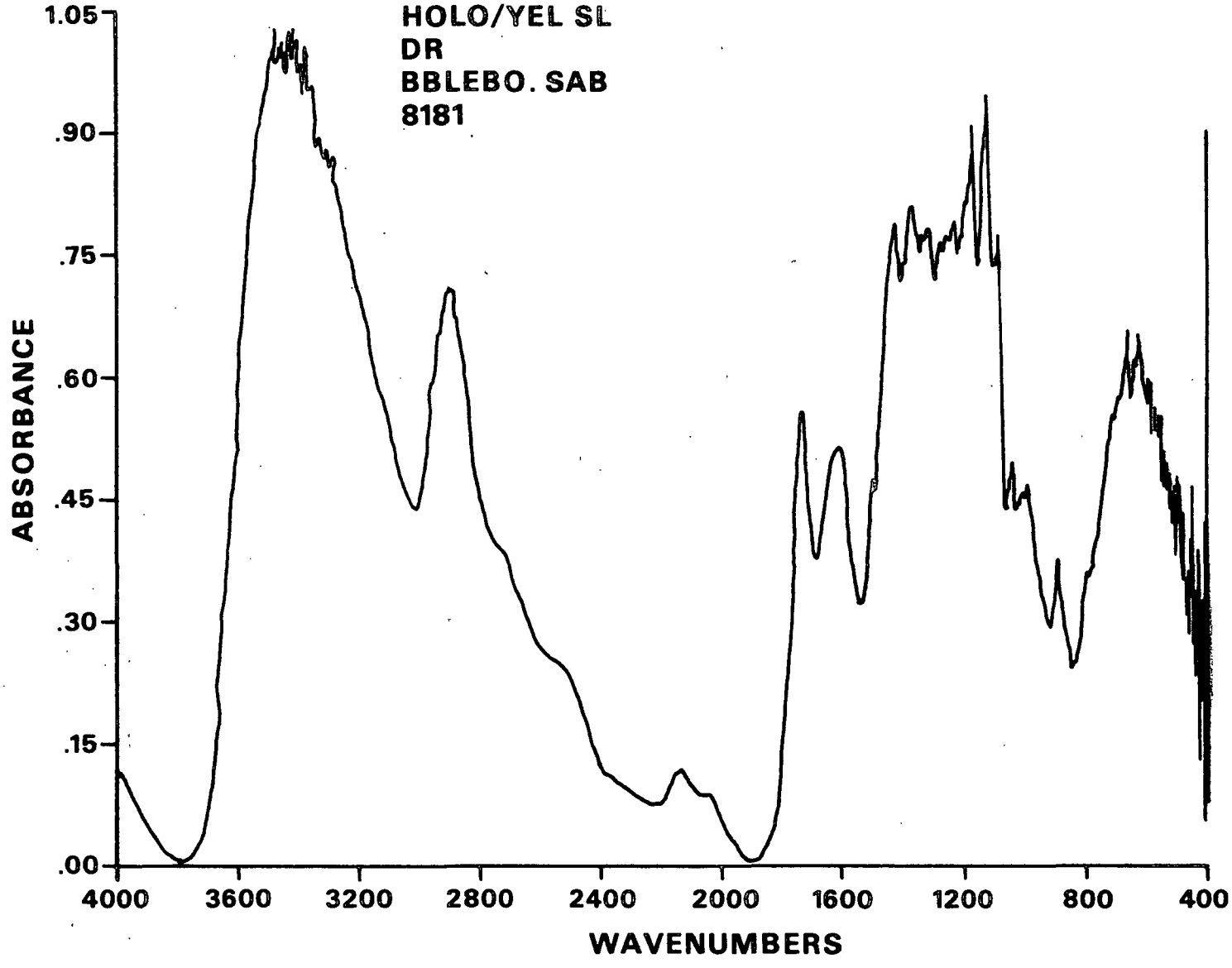

Figure 139. Diffuse reflectance FTIR spectrum of holocellulose (prepared from white spruce refiner mechanical pulp) irradiated for 4 hours with simulated sunlight.

APPENDIX VIII

ΔR_∞ AND $\Delta(k/s)_\lambda$ SPECTRA OBTAINED UPON REACTION OF UNIRRADIATED, IRRADIATED (20 HOURS WITH SIMULATED SUNLIGHT), AND FREMY'S SALT OXIDIZED SHEET SAMPLES WITH TRIMETHYL PHOSPHITE: REACTION TIME = 7 DAYS

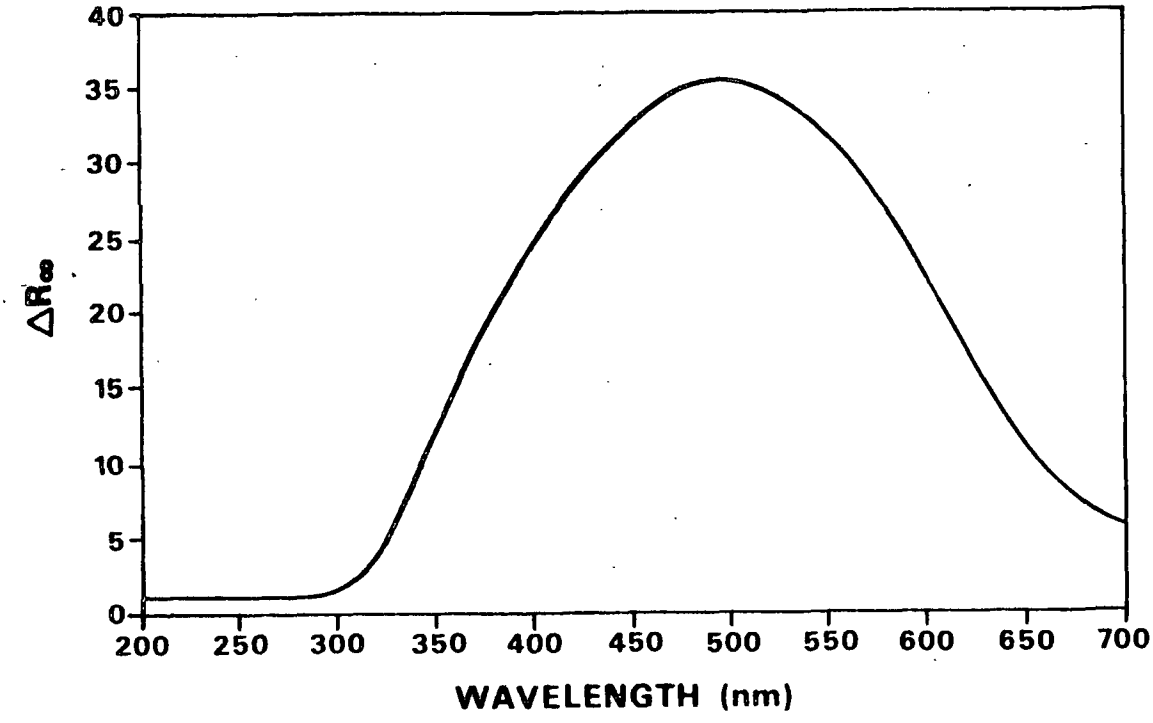

Figure 140. ΔR_∞ spectrum obtained upon reaction of Fremy's salt oxidized sheet sample with trimethyl phosphite (reaction time = 7 days).

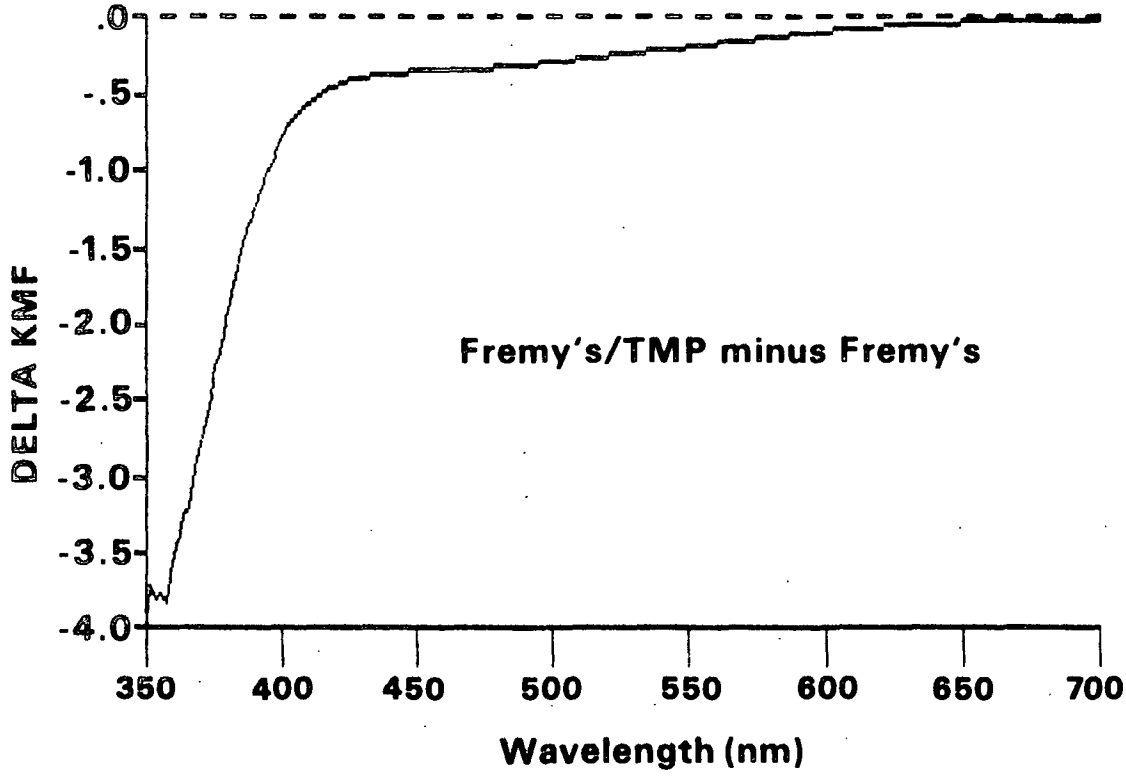

Figure 141. $\Delta(k/s)_\lambda$ spectrum obtained upon reaction of Fremy's salt oxidized sheet sample with trimethyl phosphite (reaction time = 7 days).

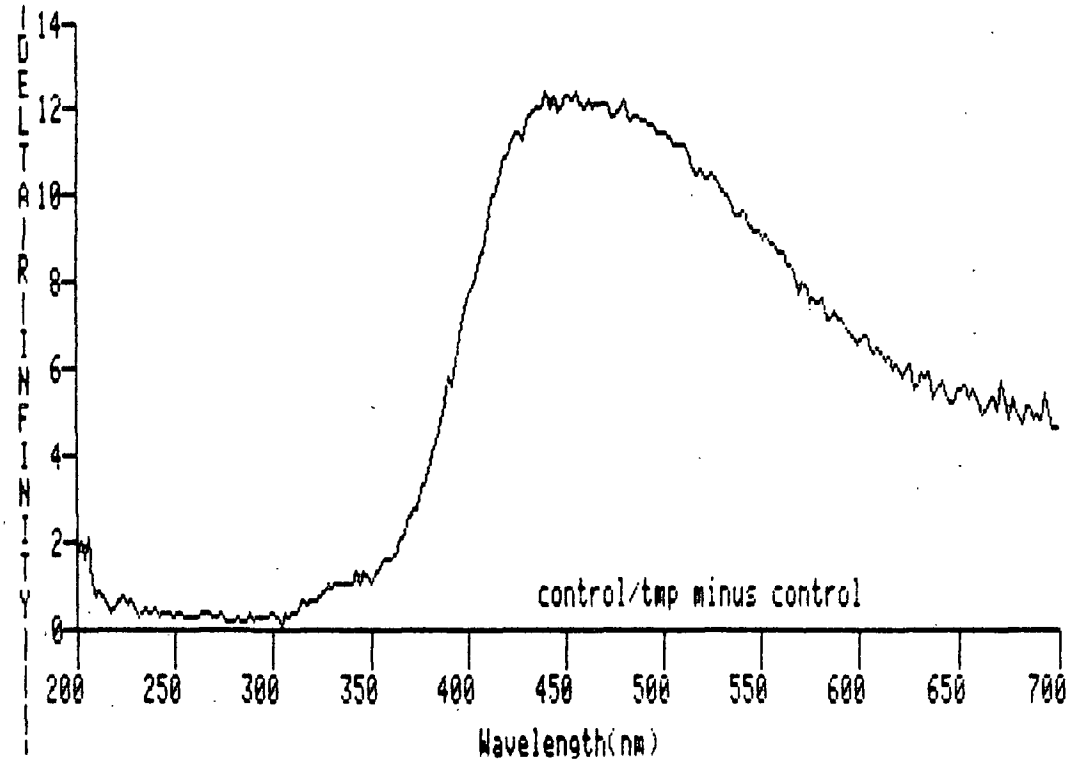

Figure 142. ΔR_∞ spectrum obtained upon reaction of an unirradiated white spruce pulp sheet sample with trimethyl phosphite (reaction time = 7 days).

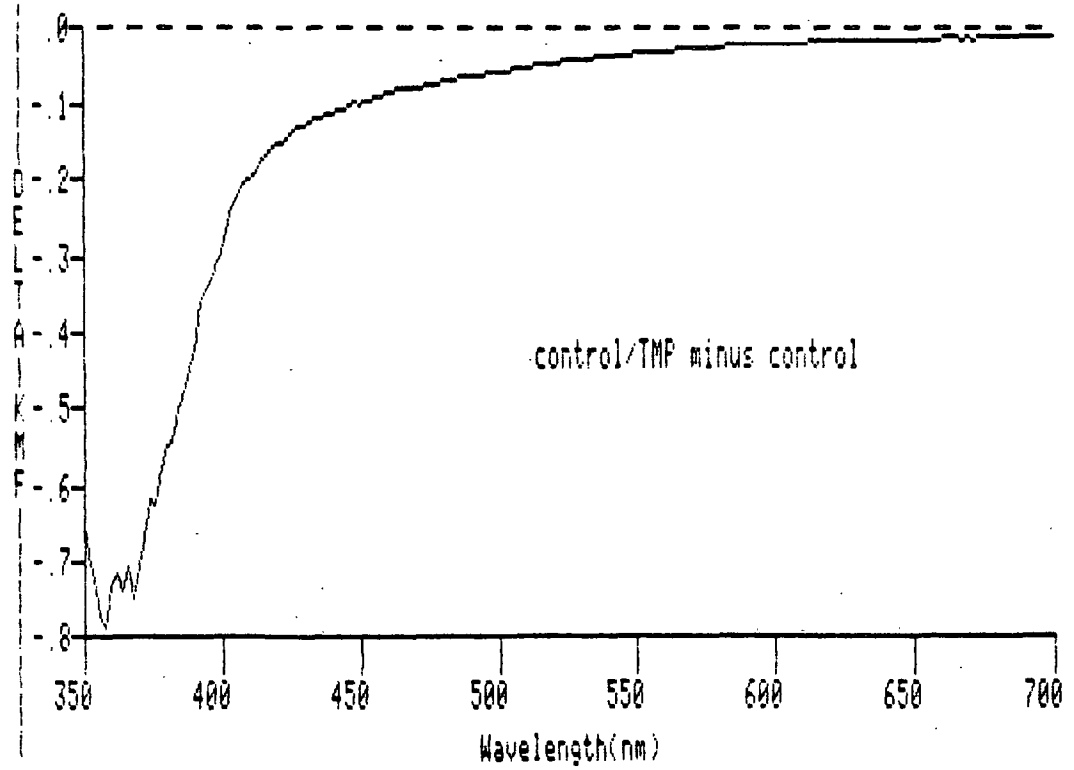

Figure 143. $\Delta(k/s)_\lambda$ obtained upon reaction of an unirradiated white spruce pulp sheet sample with trimethyl phosphite (reaction time = 7 days).

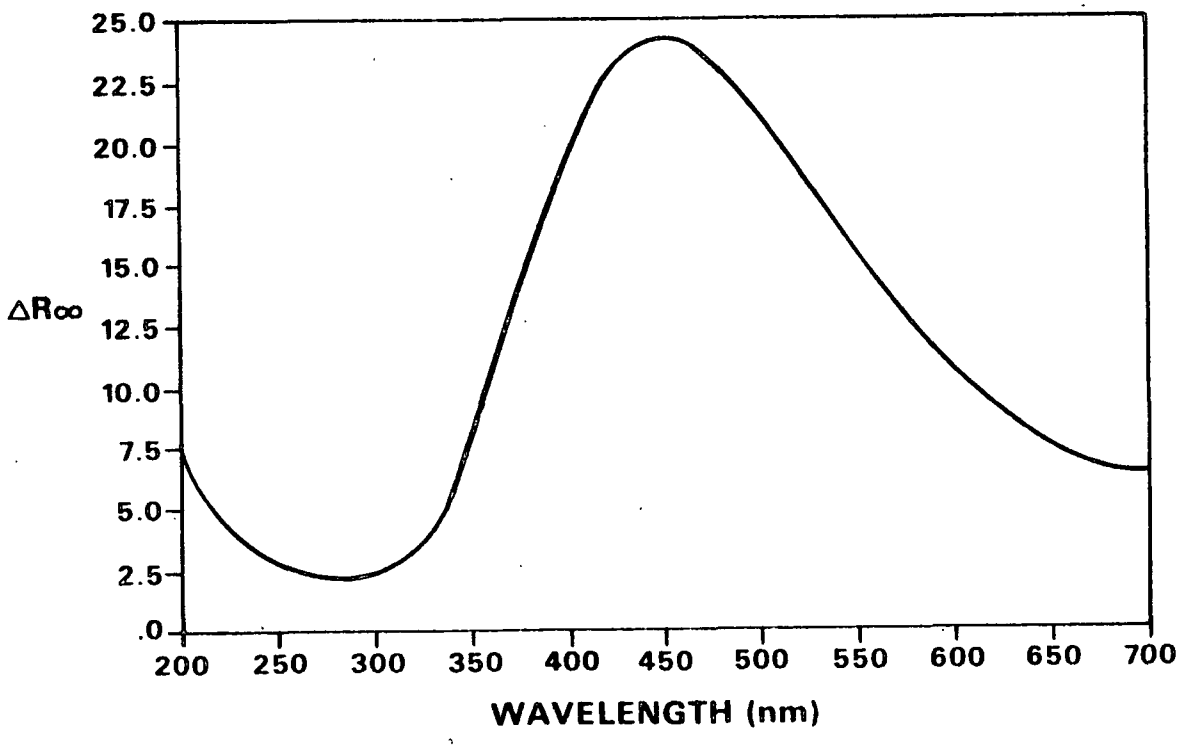

Figure 144. ΔR_∞ spectrum obtained upon reaction of an irradiated (24 hours in the solar simulator) white spruce pulp sheet sample with trimethyl phosphite (reaction time = 7 days).

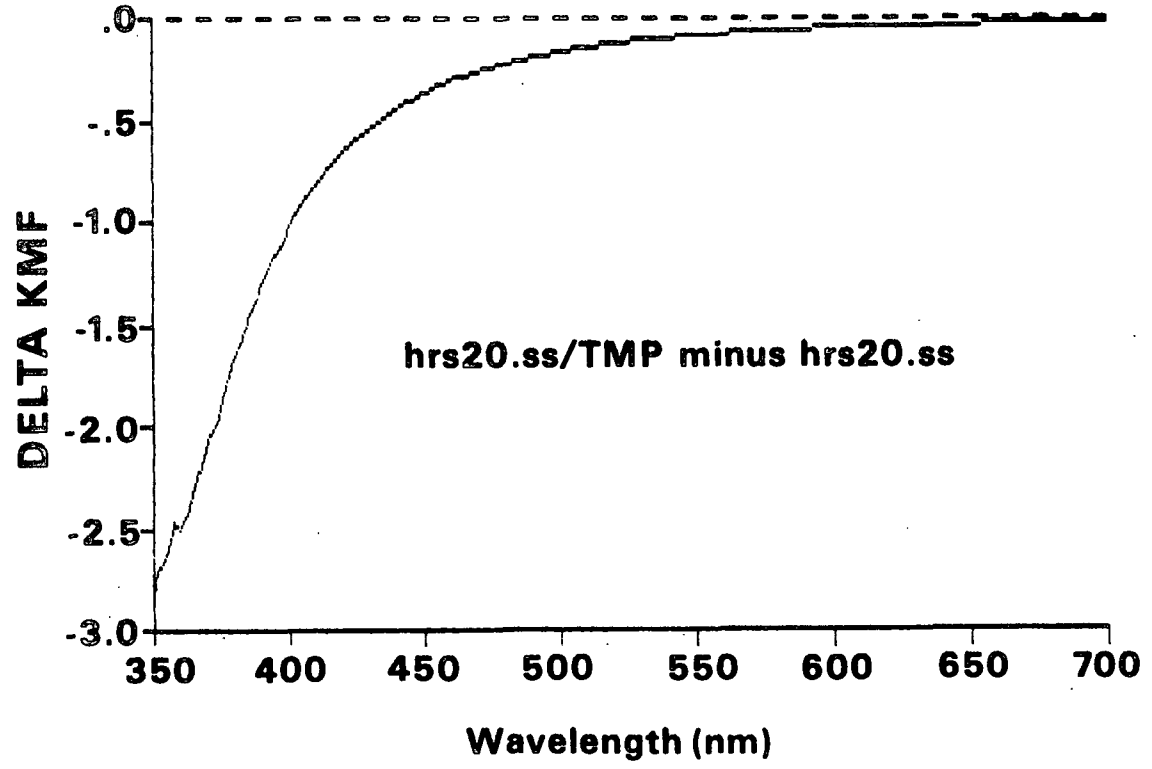

Figure 145. $\Delta(k/s)_\lambda$ spectrum obtained upon reaction of an irradiated (24 hours in the solar simulator) white spruce pulp sheet sample with trimethyl phosphite (reaction time = 7 days).

APPENDIX IX

RESULTS OBTAINED IN THE IRRADIATION OF SOME MATERIALS RELATED TO THE "NONLIGNIN" COMPONENTS OF PULP

This appendix covers some of the results obtained in the irradiation of some materials related to the "nonlignin" components of pulp. These results were not presented in the main body of this text because the effects of irradiation on the nonlignin components of pulp were not the main objective of this study. These results were considered to be quite interesting, however, and thus will be briefly covered here.

RESULTS OBTAINED WHEN AN ISOLATED SPRUCE GLUCOMANNAN WAS IRRADIATED FOR VARIOUS TIMES WITH SIMULATED SUNLIGHT

When a compact formed from an isolated spruce glucomannan (obtained from Dr. Norman Thompson) was irradiated for 15 hours with simulated sunlight, a slight "yellowing" of the material was observed. The ΔR_∞ spectrum obtained upon irradiation of this compact for 15 hours had a single broad band (Fig. 145). The wavelength minimum of this band occurred at approximately 400 nm, and the band tailed into the far visible region of the spectrum. While it was quite noisy, the $\Delta(k/s)_\lambda$ spectrum obtained upon irradiation of this compact also seemed to have a single band, but the wavelength maximum of this band was in the far UV region of the spectrum (Fig. 146). This band also tailed into the far visible region of the spectrum. Similar results were obtained at other irradiation times.

When the $(k/s)_\lambda$ values of a spruce glucomannan compact at 415, 457, and 520 nm were plotted as a function of irradiation time, the results presented in Fig. 147 were obtained. In the time period studied, the rate of change of $(k/s)_{520\ nm}$ was fairly linear. The rates of change of $(k/s)_{457\ nm}$ with irradiation time and

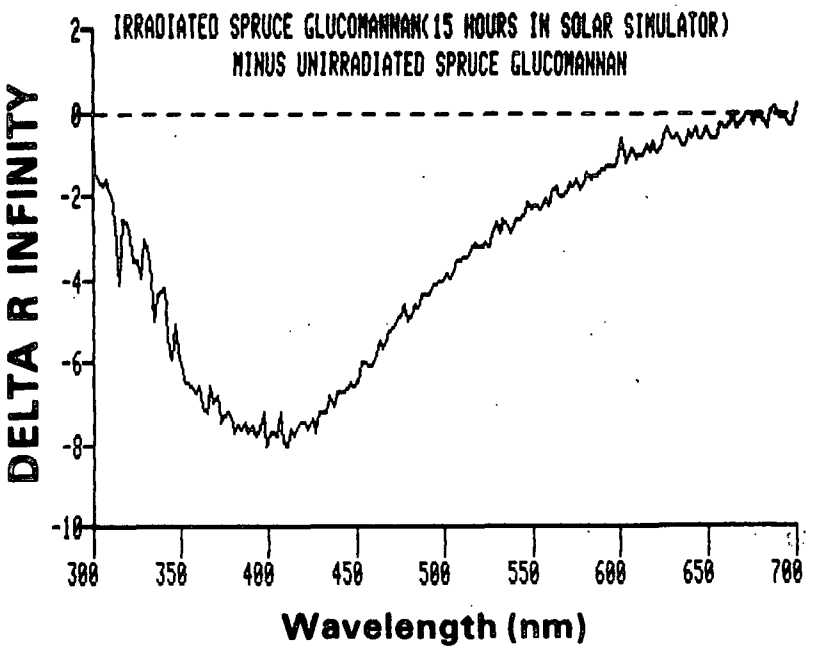

Figure 146. ΔR_∞ spectrum obtained upon irradiation of a spruce glucomannan compact for 20 hours with simulated sunlight.

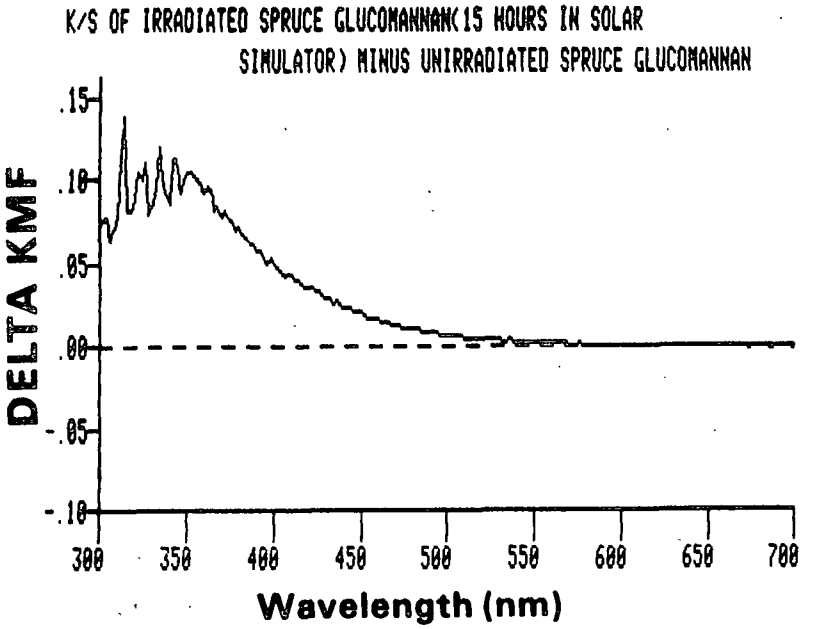

Figure 147. $\Delta(k/s)_\lambda$ spectrum obtained upon irradiation of a spruce glucomannan compact for 20 hours with simulated sunlight.

$(k/s)_{415\ nm}$ with irradiation time were qualitatively similar to those observed for white spruce refiner mechanical pulp (i.e., initially very rapid and, at longer times, fairly linear).

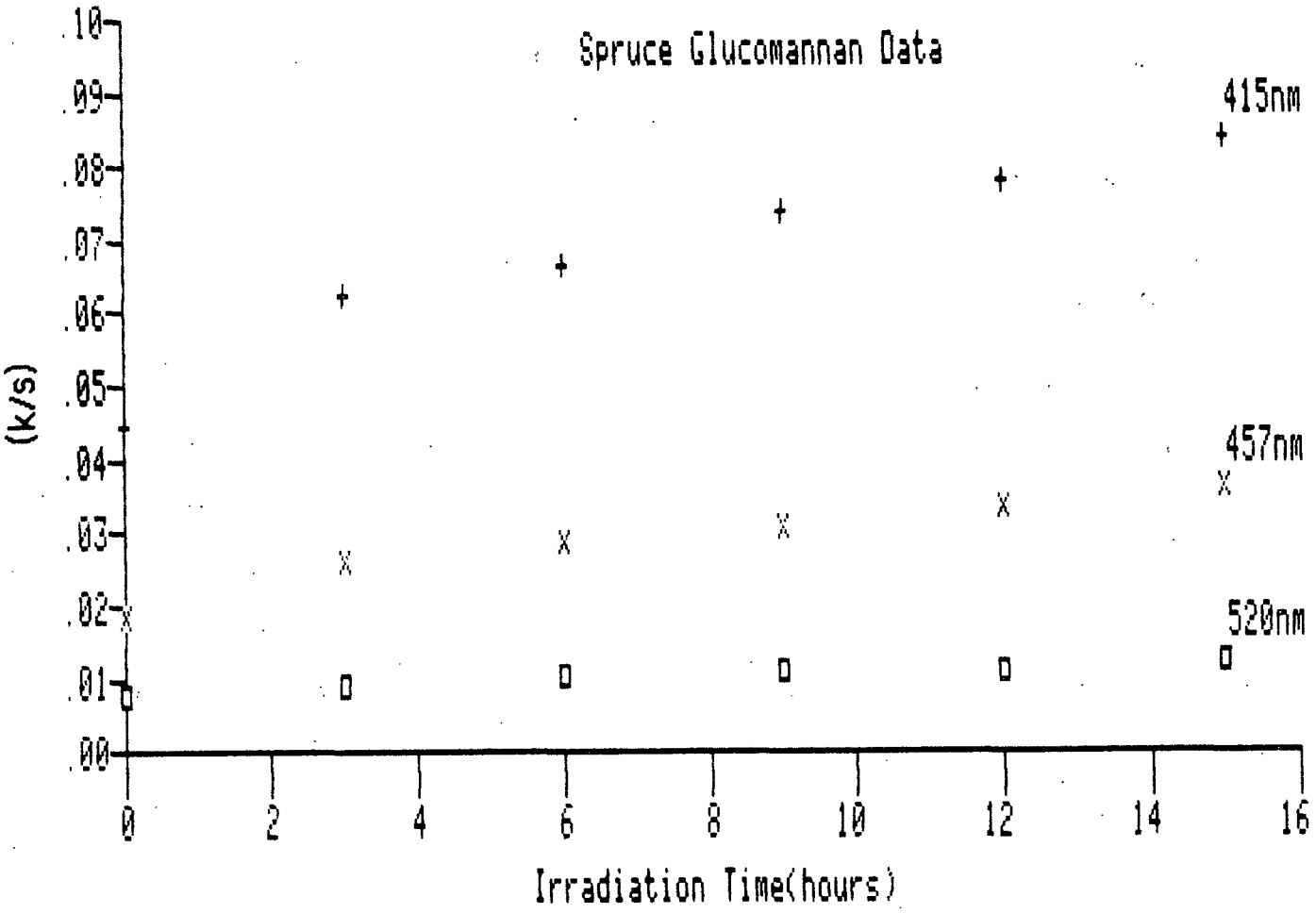

Figure 148. Plots of $(k/s)_{415\ nm}$, $(k/s)_{457\ nm}$, and $(k/s)_{520\ nm}$ versus irradiation time with simulated sunlight for a spruce glucomannan compact.

On the basis of the results presented above, it appeared that the reactions of hemicelluloses in white spruce pulp may account for at least some of the color developed upon irradiation. Since the origin of the glucomannan was unknown, it was decided at this point that the composition of this glucomannan should be investigated. The results obtained from a sugar analysis of the

hydrolyzate obtained from this material were: arabinose, 0.3% (o.d. basis); xylose, 1.7%; mannose, 60.3%; galactose, 2.0%; and glucose, 21%. As these results show, only 85.3% of this material could be accounted for in the analysis. The other 14.7%, which was acid soluble, was of an unidentified nature. Thus, these results indicated that the origins of the observed changes upon irradiation of this material may or may not be glucomannan related. Perhaps this would make an interesting topic for future work.

RESULTS OBTAINED WHEN IVORY NUT WAS IRRADIATED FOR 20 HOURS WITH SIMULATED SUNLIGHT

The ΔR_∞ and $\Delta(k/s)_\lambda$ spectra obtained upon irradiation of a compact formed from ivory nut for 20 hours with simulated sunlight are shown in Fig. 148 and 149. Both of these spectra showed that color producing changes did occur when this material was irradiated. A sugar analysis was performed, and the following results were obtained: arabinose, 0.2%; xylose, 0.3%; mannose, 86.4%; galactose, 2.5%; and glucose, 8.3%. Thus, 97.7% of this material could be accounted for. Since no lignin was present, these results again suggest that the hemicelluloses present in high yield pulps may contribute to the color developed upon irradiation.

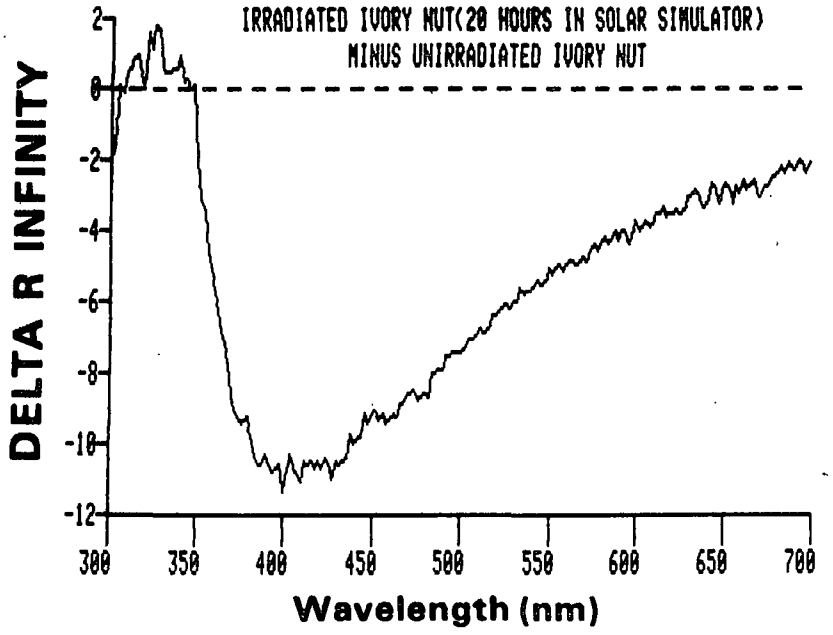

Figure 149. ΔR_∞ spectrum obtained upon irradiation of an ivory nut compact for 20 hours with simulated sunlight.

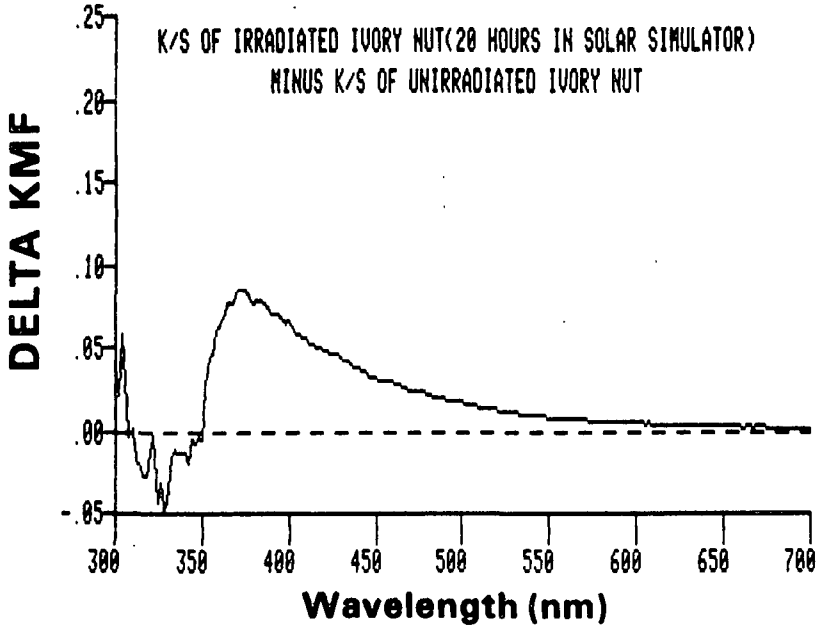

Figure 150. $\Delta(k/s)_\lambda$ spectrum obtained upon irradiation of an ivory nut compact for 20 hours with simulated sunlight.